The separation of waste oily water using carbon adsorption

Mehta, Rupel

Award date:
2007

Awarding institution:
University of Bath

The Separation of Waste Oily Water using Carbon Adsorption

Rupel Mehta

A thesis submitted for the degree of Doctor of Philosophy

University of Bath

Department of Chemical Engineering

May 2007

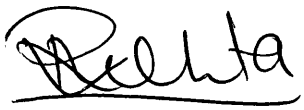

ProQuest LLC
789 East Eisenhower Parkway
P.O. Box 1346
Ann Arbor, MI 48106-1346

Table of Contents

List of Tables

List of Tables

List of Tables

List of Figures

List of Figures

Acknowledgements

Firstly, I would like to express my gratitude to Professor Barry Crittenden for his invaluable input to this thesis. Thank you for your time. Thanks to Dr Semali Perera for her support throughout the course of the research.

I would also like to thank all the technical staff at the University of Bath for all their help, particularly Ann O'Reilly for assisting me with SEM and ASAP studies, as well as Mac Forsyth and Elaine Odgers. My special thanks go to Mervyn Newnes, who not only helped me technically in building my rig but also made me laugh and kept me sane throughout my years at Bath. Thank you for being a friend.

I would like to thank all the Partners involved in the WOWSEP Consortium, each of whom played a role throughout the course of this project, especially Steve Tennison and Andy Blackburn, who manufactured and supplied the activated carbons and also provided me with technical support.

I am grateful to Jo who, even though is not a scientist or an engineer, still took the time to proof read through part of my thesis when my brain just wasn't working anymore. Thank you for your thoughtful comments.

I would like to express my deepest gratitude and appreciation to all my family and friends; in particular Bina, Deepti, Ruth and Sukie, to name a few, but without whose encouragement, motivation and wise words, I would never have lasted the course of this thesis.

I am indebted to my fiancée, Ashraf, for his continuous encouragement, motivation, understanding and utmost patience, I love you.

Last but definitely not least, I would like to express thanks to my parents and brother for all their love and support over the years.

Abstract

This thesis addresses the widespread concern of aquatic pollution, in particular wastewater derived from the use of cutting (metalworking) fluids. This waste generally contains particulates, free, emulsified and soluble oils. The treatment of particulates, free and emulsified oils is well documented, and was carried out using gravity separation, coalescence and ultrafiltration or chemical splitting, respectively. However, that of soluble oils is not so well understood. Hence, the main focus of this project was to study the separation and recovery of the soluble oils, such that the separated 'oil' and 'water' may be reused or recycled and the waste minimised.

Many experimental factors and operating conditions (such as type of adsorbent, pre-treatment of adsorbate, flowrate, pH, temperatures *etc.*) were considered on a laboratory scale rig to find the optimal conditions for this process such that it could be scaled up in to a prototype, which was later to be tested in the motor industry.

Due to commercial confidentiality the exact contents of the cutting fluids were unknown. It was therefore initially assumed that the pre-treated cutting fluid was a homogenous single component solution, although it was later proved that the solution was not single component, but moreover a binary mixture containing an "amine" and "organic" fraction. Therefore the treatment of this cutting fluid waste was carried out using carbon adsorption, ion exchange and steam regeneration. Whilst these technologies are established, the novelty of this research was moreover in the use of a novel phenolic resin carbon (PRC), manufactured by MAST Carbons Ltd. and in the *in-situ* steam regeneration process which used relatively low temperature superheated steam (approximately 200°C).

Overall it was found that a combination of carbon adsorption and ion exchange reduced the TOC concentration of the pre-treated cutting fluid drastically. It was found that the waste volume could be reduced by 90% and 95% of the resultant 'water' could be reused in factory washing, reformulation *etc.* However, the recovered 'oil' fraction could not be used in reformulation of the cutting fluid as its exact composition was unknown.

Keywords: waste minimisation, cutting (metalworking) fluids, carbon adsorption, ion exchange, low temperature superheated steam regeneration.

Nomenclature

θ	Fractional coverage of adsorbent by adsorbate
λ	Wavelength of the x-ray radiation,
ν or μ/ρ	Momentum diffusivity of solute, $m^2 s^{-1}$
φ	Angle, radians
ρ or ρ_f	Fluid density, kg m^{-3}
ρ_b	Bulk density, kg m^{-3}
ρ_c	Crystalline density, kg m^{-3}
ρ_p	Particle or apparent density, kg m^{-3}
ρ_w	Wet density, kg m^{-3}
μ	Fluid viscosity, kg $m^{-1} s^{-1}$
$\in$	Fraction of external voids
χ	Internal porosity of particles
σ	Pore surface area of dry solid, $cm^2 g^{-1}$
$\partial c/\partial x$	Concentration gradient, m^{-1}
ΔH	Heat of adsorption, kJ $kmol^{-1}$
π_i^o	Spreading pressures, N m^{-2}
ε_p	Porosity of adsorbent particles
$1/n$	Freundlich parameter, relating to strength of adsorbate-adsorbent interaction
A	surface area of the adsorbent, m^2
A_p	External surface area, m^2
B	Cost of biological oxidation treatment of settled sewage, cost m^{-3}
b	Langmuir equilibrium constant, dimensionless
Bi	Biot number
b_o	Nature of frequency factor, dimensionless
B_v	Cost of additional biological treatment used, cost m^{-3}
c, c_i, c_f	concentration, mg l^{-1} ,subscripts i and f refer to the initial and final concentrations respectively
C_e	Total charge for trade effluent, cost m^{-3}
c_i^o,	Single solute liquid concentration, g m^{-3}

C_o, c_{oi}	Initial concentration, mg l^{-1} or g m^{-3}
c_s	Concentration of the adsorbate in the solid phase, g m^{-3}
D	Diffusivity in a cylindrical pore, kmol m^{-1} s^{-1}
dc/dt	Concentration gradient, mg l^{-1} s^{-1}
$(dc/dt)_r$	Rate of regeneration, mg l^{-1} $mins^{-1}$
D_{eff}	Effective particle diffusivity, m^2 s^{-1}
D_i	Molecular diffusivity of solute I, m^2 s^{-1}
d_p	Particle diameter, m
D_p	Pore diffusivity
f	Friction factor
f_s	Activity coefficients on the adsorbent surface, dimensionless
I	Scattering intensity
I_φ	Intensity of scattering at angle φ
I_e	Intensity of scattering for one electron
J	Flux, kmol m^{-2} s^{-1}
K_f	Freundlich parameter, relating to adsorption capacity
K	Henry's coefficient (equilibrium constant), m^3 g^{-1}
k	Rate constant, $mins^{-1}$
k_a and k_d	Equilibrium constants for adsorption and desorption respectively (as functions of temperature)
k_f	External mass transfer coefficient, m s^{-1}
k_o	Arrhenius constant or the frequency factor, $mins^{-1}$
LUB	Length of Unused Bed
M	Mass of adsorbent, mg
n	(n>1) empirical constant, dimensionless
N	Mass transfer or difusional flux, g s^{-1}
N_m	Number of molecular layers
O_s	COD of average strength settled sewage, mg l^{-1} (ppm)
O_t	Chemical oxygen demand (COD) of the trade effluent after 1 hour quiescent settlement, mg l^{-1} (ppm)
p	Pressure, N m^{-2}
p^o	Saturated vapour pressure
q	Loading (mass adsorbate per mass adsorbent), $g_{adsorbate}$ $g_{adsorbent}^{-1}$ or g g^{-1}

q_{cs}	Total loading of the chemically split cutting fluid, mg mg^{-1}
q_i	Initial loading, mg mg^{-1}
q_i^o	Single solute surface loading, g g^{-1}
q_s	Maximum monolayer loading, g g^{-1}
q_T	Total surface loading, g g^{-1}
R	Molar universal gas constant, (8.314 kJ $kmol^{-1}$ K^{-1})
r	Particle radius, m
R_c	Cost of reception and conveyance of trade effluent in the public foul water sewer, cost m^{-3}
Re	Reynolds number, dimensionless
s	Cost per cubic metre of treatment, cost m^{-3}
Sc	Schmidt number, dimensionless
Sh	Sherwood number, dimensionless
S_s	The suspended solids of average strength crude sewage, mg l^{-1} (ppm)
S_t	The total suspended solids of the trade effluent at pH 7 of the mixed sewage, mg l^{-1} (ppm)
T	Absolute temperature, K
t	Time, mins
T_b	Breakthrough time, mins
T_e	Equilibrium time (time at end of breakthrough), mins
u	Fluid velocity, m s^{-1}
V	Volume of adsorbate, l
V_c	Cost of preliminary and primary treatment of sewage treated and disposed of in waste water treatment works, cost m^{-3}
W_s	Mass of adsorbent, g
x	Silica to alumina ratio (≥1)
y	Molar water hydration
z_i,	Mole fraction of component i, dimensionless
ΔH	Activation energy, kJ $kmol^{-1}$

Abbreviations

ACF	Activated Carbon Fibres
$Al_2O_3 \cdot nH_2O$	Activated aluminas (hydrated aluminium)
Al_2SO_4	Aluminium Sulphate
AlO_4	Alumina
ASAP	Accelerated Surface Area and Porosimetry
BC	Before Christ
BET	Brunauer Emmett and Teller
Bi	Biot Number
BIDS	Bath Information Database System
BJH	Barrett, Joyner and Halenda
BOD	Biological Oxygen Demand
c.	Around, about, approximately
Ca^{2+}	Calcium ions
CATEM	Controlled Atmosphere Transmission Electron Microscopy
Cl^-	Chloride ions
CN	Cyanide
Co.	Company
CO_2	Carbon dioxide
COD	Chemical Oxygen Demand
COSHH	Control Of Substances Hazardous to Health
DFT	Density Functional Theory
D-R	Dubinin-Radushkevich
D-S	Dubinin-Stoeckli
DTI	Department of Trade and Industry
EA	Environmental Agency
EBCT	Empty Bed Contact Time
EPA	Environmental Protection Act
EPSRC	Engineering and Physical Sciences Research Council
ESR	Electron Spin Resonance
ETBPP	Environmental Technology Best Practice Programme
FTIR	Fourier Transform Infra Red
GAC	Granular Activated Carbon

H^+	Hydrogen ions
H_2SO_4	Sulphuric acid
HCl	Hydrochloric acid
HPLC	High Performance Liquid Chromatography
HRTEM	High Resolution Transmission Electron Microscopy
HRTES	High Resolution Transmission Electron Spectroscopy
HSDM	Homogeneous Surface Diffusion Model
HT	High Transmission
IAST	Ideal Adsorbed Solution Theory
IC	Inorganic Carbon
IPC	Integrated Pollution Control
IPPC	Integration Pollution Prevention and Control
IUPAC	International Union of Pure and Applied Chemistry
LA	Local Authorities
Ltd.	Limited
$M_{2/n}{\cdot}Al_2O_3{\cdot}xSiO_2{\cdot}yH_2O$	Alumino-Silicates
MEA	Monoethanolamine
mtf	Mass Transfer Front
mtz	Mass Transfer Zone
Na^+	Sodium ions
NaCl	Sodium Chloride
NaOH	Sodium Hydroxide
NDIR	Non-Dispersive Infrared
NMR	Nuclear Magnetic Resonance
NO_x	Nitrogen Oxide
NPOC	Non-Purgeable Organic Carbon
OC	Organic Carbon
OPEC	Oil Pollution Environmental Control
PAC	Powdered Activated Carbon
PERA	Production Engineering Research Association
POC	Purgeable Organic Carbon
POTW	Privately Owned Treatment Works
ppm	Parts per million
PRC	Phenolic Resin Carbon

psd	Pore Size Distribution
PSDM	Pore Surface Diffusion Model
PVDC	Polyvinyldene Chloride
R5/026/03	D. A. Stuart Oil's semi-synthetic cutting fluid
R_c^-	Cationic resin
Re	Reynolds Number
SAXS	Small Angle X-ray Scattering
Sc	Schmidt Number
SEM	Scanning Electron Microscopy
Sh	Sherwood Number
SiO_2	Silica (Silicon Oxide)
SiO_4	Tetrahedral silica
SME	Small to Medium sized Enterprise
SO_x	Sulphur Oxide
SPE	Subtracting Pore Effect
SS	Sutcliffe Speakman
STP	Standard Temperature and Pressure
TC	Total Carbon
TEM	Transmission Electron Microscopy
TOC	Total Organic Carbon
TSS	Total Suspended Solids
UK	United Kingdom
US	United Satates
USA	United States of America
UV	Ultraviolet
WMR3	Waste Minimisation through Recycling, Re-use and Recovery in Industry
WOWSEP	Waste Oily Water SEParation process
XRD	X-ray Diffraction

1.0 Introduction

"Water, water, everywhere,
And all the boards did shrink,
Water, water, everywhere,
Nor any drop to drink."

Samuel Taylor Coleridge (1772 - 1834)
The Rime of the Ancient Mariner, II, 1798

This verse from the 'Rime of Ancient Mariner II' (Coleridge, 1798) portrays the Ancient Mariner and his shipmates on a boat in the midst of the ocean with the still air and hot sun beaming down on them. However, the irony is that even with all this water around them the ship dried out and the men were parched with thirst. The simile of this quotation and the incentive for the proposed research is that even though there are oceans, seas, rivers *etc.* surrounding the world, a large portion of these waters is hazardous and harmful to humans, animals, fish and plants alike, making it directly unavailable. This provides the requirement for pollution reduction policies and water treatment.

There are many aspects of life from which water pollution originates, such as sewers, run off water, waste disposal *etc.* However, to demonstrate the extent of aquatic pollution from just one aspect, it is estimated that the 40,000 engineering workshops in the UK produce and dispose of approximately 400,000 tonnes of factory wastewater per annum (Envirowise, 2001). This waste mainly contains large quantities of spent metalworking fluids (cutting fluids) though it may also include lubricating oils and cleaning solvents.

Metalworking fluids are multifunctional. They are used in operations such as metal cutting, drilling, tapping and turning, for the purposes of lubrication, cooling, prevention of surface corrosion, heat and swarf removal, friction reduction and to extend machinery life (Sales *et al.*, 2001). The extensive use of these fluids creates harmful wastewater, a major pollution hazard to river systems. Research into the reduction and treatment of such wastewater is valuable in order to protect the environment. However, pollution reduction and disposal creates substantial costs for industry, so it is imperative that an approach to the problem is economically attractive.

Oily wastewater typically contains free and emulsified oils, soluble organic chemical contaminants and a small percentage of particulates and suspended solids. There are a variety of processes to treat wastewaters containing these contaminants. Membrane or chemical technologies primarily treat wastewaters to separate the non-aqueous phase from the aqueous phase before being discharged to sewers and river systems (Alther, 2001; Chang *et al.*, 2001; Cheryan and Rajagopalan, 1998). Further treatment is dependent on the physical and chemical character of the water. Well-established processes such as oleophilic mops and coalescers are generally used to remove the free oils (Lucas, 1975), whilst processes such as ultrafiltration or chemical separation are used to break down the emulsified oils (Alper, 2000; Kilbourne and Hodson, 1996; Reed *et al.*, 1998), and filtration is commonly used to remove the particulates (Lin and Miller, 2000; Clasen, 1998; Mouri and Niwa, 1993). Significantly, the organic chemical fraction of the wastewater consists of a cocktail of water-soluble toxic compounds which are unaffected by these processes. These are usually disposed of via a sewer or transported by tankers to Privately Owned Treatment Works (POTW).

Due to the large volume of metalworking fluid waste produced by industry, off-site disposal costs are high. Additionally, ever-increasing demands for water from industry have made the need for research into water recycling essential. This thesis focuses on the viability of on-site treatment, removal and recycling of these fluid remnants.

1.1 Aims and objectives

The overall aim of this project was to develop a low cost, on-site oily wastewater treatment system capable of achieving a high quality polished water and recovering the adsorbed aqueous organic fraction of the feed, for reuse. In addition, it was necessary to develop the technology such that it possessed the potential for wider industrial applications.

In support of these aims the research objectives were:

1. To design and build an integrated system consisting of:
    - Pre-treatment stages for the removal of particulates, free and emulsified oils,
    - A purification stage for the removal of soluble organic contaminants, and
    - A final innovative stage for the recovery of soluble contaminants.
2. To develop a novel synthetic carbon capable of:

- Adsorbing soluble oils and organic chemicals from pre-treated wastewater,
- Being regenerated *in-situ*.

1.2 Funding and consortium

This research was a Waste Minimisation through Recycling, Re-use and Recovery in Industry (WMR3) LINK project, also known as the Waste Oily Water SEParation (WOWSEP) process. It was supported and funded by the Department of Trade and Industry (DTI), the Engineering and Physical Sciences Research Council (EPSRC) and the Environmental Technology Best Practice Programme (ETBPP, now known as Envirowise).

Specifically, this research involved a study of the adsorption and regeneration steps of a cyclic process, using a novel polymer resin carbon (PRC) manufactured by MAST Carbon Ltd. The project consortium comprised the University of Bath and the following industrial partners: PERA, Ford Motor Co. Ltd., MAST Carbon Ltd., D. A. Stuart Oil Co. Ltd., BTR Environmental Ltd., OPEC Ltd. and Alpha Construction Ltd. The principal role for the University was to research the use of synthetic carbons intended for the removal and recovery of the soluble constituents from cutting fluids. Stuart Oils provided specialist information on the complex formulations of cutting fluids, whilst OPEC provided knowledge and equipment required for the removal of free oils from the feed stream. BTR Environmental provided filtration equipment and design advice, Alpha Construction provided expertise concerning the design and construction of the prototype and Ford Motor Co. was a representative of the end-users of the new technology. The overall project was managed by PERA, who also provided expertise in the choice of pre-treatment technologies, as well as constructing and testing the developed prototype system. The background and role of each participating partner is summarised in Table 1.0.

Table 1.0 Background and Role of Each Partner in the WOWSEP Consortium

Partner	Background	Role
The University of Bath, Department of Chemical Engineering, Bath	An academic institution, which teaches undergraduate degrees, but also specialises in research.	To study the performance of the novel carbon in the removal of soluble oils from factory waste and the *in-situ* regeneration of carbon.
Production Engineering Research Association (PERA), Melton Mowbray	An independent research organisation, whose policy is to provide expertise in research.	To manage and lead the consortium. To develop the pre-treatment stage and manufacture the prototype.
MAST Carbon Ltd., Guildford	A small to medium sized enterprise (SME), which researches into and manufactures novel carbons.	To develop and provide carbons capable of removing soluble oils and organic chemicals from pre-treated wastewater with the capability of being steam regenerated, *in –situ.*
D. A. Stuart Oil Co. Ltd., Wolverhampton	A company that supplies many industries (including motor industries) with metal working fluids for use in their machinery.	To provide technical information regarding the formulation and chemistry of cutting fluids as well as to supply the cutting fluids.
Oil Pollution Environmental Control Ltd. (OPEC), Batley	A company that specialises in equipment required for the removal of free oils.	To provide expertise in equipment for the removal of free oils, such as roll mops and oil traps.
BTR Environmental Ltd. (formerly known as Vokes), Guildford	A company that manufactures filters, specialising in oil separation and cleaning hydraulic oil filters.	To provide expertise and supply filters for the prototype system.
Alpha Construction Ltd., Derby	A company that provides a civil engineering and building service to all sections of industry.	To provide information on waste treatment systems, process design and civil construction.
Ford Motor Company Ltd., Bridgend	A company that manufactures vehicles and are an example of an industrial end user that would benefit from this improved wastewater treatment system.	To provide waste for the prototype trials.

1.3 Environmental issues

A general awareness of worldwide environmental issues has led to the increasing implementation of pollution reduction policies within industry. In the mid 1970s, after the establishment of the Environmental Protection Agency in the USA, strict legislation was introduced to protect the environment by controlling the disposal of pollutants. Enforcement became the duty of Local Authorities (LA) who had the power to fine companies breaching regulations. However, these charges soon became commonplace (Burke, 1991) and were accepted as an additional 'running cost'. Indeed, companies found it more worthwhile to concentrate on their production rates, rather than researching and introducing treatment processes to reduce their waste output.

In addition to UK legislation, UK industries have had to respond to requirements originating from European Law (Archibald and Bowes, 1993). Most notably, the areas of health and safety at work and environmental pollution increased pressure on companies to become more environmentally aware (Mosley, 1994). Therefore it became progressively more difficult to continue the practice of releasing trade effluent contaminants into the environment (Breach, 1996), whether this was through landfill, aquatic or atmospheric discharge (Lee, 1989).

In order to comply with regulations industries could adopt more environmentally friendly production processes, improve and/or add to existing waste treatment processes (Anon, 1994). Overwhelmingly the latter prevailed. Waste treatment processes were frequently only employed to comply with regulations, and were viewed as 'end-of-pipe' or 'add-ons', that is, they were not always considered as an integral part of the production process, but something extra. In fact they did not always eliminate the waste, but often merely diluted it or transferred it from one environmental medium (air, water, land) to another (Crittenden and Kolaczkowski, 1995; Mizsey, 1994; Vigneswaran and Dharmappa, 1992).

However, diluting or transferring waste puts industrial companies at risk of being penalised. For example, if consent limits were broken, local water companies could fine the industries concerned based on the Mogden Formula (Croner's, 1991) as described in the following section (1.3.1). However, using this formula, many industries calculated that it was cheaper to use large volumes of water to dilute and consequently reduce the

Chemical Oxygen Demand (COD) concentration of the pollutants in order to meet the terms of the consent limits than to pay the fines (where the COD is a measure of the oxygen equivalent of the organic matter content of a sample that is susceptible to oxidation by a strong chemical oxidant).

To ensure legal compliance, companies must undertake regular assessments and make sure they control hazardous or potentially harmful materials, which includes those arising from the use of metalworking fluids.

Relevant UK legislation and EU Directives include:

- Environmental Protection Act (EPA), 1990

  Part I of the EPA (1990) refers to prescribed processes and substances, which are considered to be particularly harmful if released into the environment. They are controlled through the regulation of the processes, which use or generate them.
- Integrated Pollution Control (IPC), 1991

  The EPA 1990 introduced the IPC regime to control pollution from industry. The IPC applies an integrated approach to the environmental regulation of certain industrial activities, which are concerned with the release of polluting substances to air, land and water.
- Integration Pollution Prevention and Control (IPPC) Directive, 96/61/EEC

  The IPC regime is in the process of being replaced in England, Wales and Scotland by the IPPC regime. IPPC is a system following the European Community Directive (96/61/EEC) which will introduce a more integrated approach to controlling pollution from industrial sources, across England and Wales. The purpose of this Directive is to achieve integrated prevention and control of pollution arising from the activities listed in Annex I of the IPC. It lays down measures designed to prevent or reduce emissions in the air, water or land in order to achieve a high level of protection of the environment as a whole.
- Control Of Substances Hazardous to Health (COSHH) regulations, 1999

  COSHH ensures adequate health and safety practices to protect employees in any industry or workplace. The "substances hazardous to health" are virtually all substances including preparations, capable of causing adverse health effects or disease arising from work activities. COSHH assessments involve gathering information on the products and work practices associated with the use of these hazardous substances. Any risk to

the health of the employees must be identified and provision made to either eradicate the risk or at least control it. Therefore COSHH provides a legal framework to protect people against health risks and sets out the essential precautionary procedures that employers and employees must take.

- Environmental Protection Regulations (Duty of Care), 1991

  The EPA (1990) introduced the duty of care principle, and the Duty of Care Regulations, to which there is also a Duty of Care Code of Practice. The duty of care is a law says that you must take all reasonable steps to keep waste safe. If you give waste to someone else, you must be sure they are authorised to take it and can transport, recycle or dispose of it safely.

- Health and Safety at Work Act, 1974

  The Health and Safety at Work Act makes provision for securing the health, safety and welfare on everyone concerned with work activities, ranging from employers (including self-employed) and employees to manufacturers, designers, suppliers and importers of materials for use at work, people in control of premises and members of the public. The Act further states that all companies, regardless of their size and magnitude must have a written safety policy ensuring effective implementation of all health and safety standards at the workplace.

- Water Resources Act, 1991

  The Water Resources Act is the principal legislation regulating discharges of poisonous, noxious or polluting matters to "controlled waters" in England and Wales. Businesses intending to discharge such substances, or those discharging trade or sewage effluent directly to controlled waters, must obtain consent to do so from the Environmental Agency (EA).

- Control of Pollution Act, 1974

  Control of Pollution Act controls the discharge of poisonous, noxious or polluting substances to controlled waters in Scotland. Businesses intending to discharge such substances, or those discharging trade or sewage effluent directly to controlled waters, must have an authorisation from the Scotland Environment Protection Agency.

- Waste Framework Directive, 75/442/EEC

  This directive (as amended by Directive 91/156/EEC) provides for the establishment of proper waste control regimes. Under the Waste Framework Directive, the prevention or reduction of waste and its harmfulness by encouraging the development of clean technologies, technical product improvements and disposal techniques must be

encouraged. In addition, the recovery of waste (including its use as a source of energy) must also be encouraged and uncontrolled dumping prohibited.

- Control of the Use, Discharge or Emission of Dangerous Substances into the Aquatic Environment Directive, 76/464/EEC

  This directive sets out the maximum concentration limits for certain dangerous substances in controlled waters.

- Hazardous Waste Directive, 91/689/EEC

  This directive aims to introduce greater harmonisation in the management of hazardous waste. In order to formulate a common definition of hazardous waste, it lists wastes that can be classified as hazardous, and includes their constituents and properties.

- Water Industry Act, 1991

  The Water Industry Act deals with the functions and duties of sewerage undertakers, local authority responsibilities for water supply, controls discharges to the sewerage system, and the quality of water supplies. Under this act the discharge of trade effluent to public sewer requires the consent of the relevant water service company (*i.e.* the relevant sewerage undertaker). Consents to discharge will contain conditions relating to the volume and quality of the effluent. For discharges to sewer of substances or from processes prescribed by regulations made under the act, the water company must obtain authorisation from the EA. Under the act, water service companies are empowered to levy trade effluent charges. The act also sets out the powers and duties of local authorities regarding the quality and sufficiency of water supplies provided to premises in their area.

- Control of Pollution (Special Waste) Regulations, 1996

  Special wastes are the most dangerous wastes. The Special Waste Regulations are intended to implement the European Hazardous Waste Directive (91/689/EEC) which sets out requirements for the controlled management of hazardous (special) waste. The Regulations set out procedures to be followed when disposing of, carrying and receiving hazardous waste.

Advancements in technology, materials, machinery, tools and cutting fluids can assist in regulation compliance chiefly through waste minimisation, as described later in section 1.3.2.

1.3.1 Mogden Formula

The Mogden Formula (Equation 1.1) was created before the 1930s and named after the sewage treatment works where it was first used. It apportions a cost to each stage of the treatment process and takes into account the way that a particular firm's effluent, in terms of volume and quality, differs from the normal average composition of sewage in the region. The quality of the discharge is considered in terms of COD as well as the total suspended solids (TSS). Charges are made only for the elements of reception, conveyance, treatment and waste disposal arising from a trade effluent discharged to sewer (Ingold and Stonebridge, 1987). Therefore any business in the UK that discharges a trade effluent to sewer requires consent from a sewerage undertaker who charges the business according to three factors:

i. The nature, composition and volume of the effluent,
ii. Additional expenses incurred to deal with the effluent at the sewerage treatment works, and
iii. Any revenue derived by the sewerage undertaker from the effluent, for example through of the sale of residual sludge as a fertiliser.

These factors are described by the Mogden Formula, which can vary throughout the UK (Envirowise, 2000). A common form is as follows:

$$C_e = R_c + V_c + B_v + \left(\frac{O_t}{O_s}\right)B + \left(\frac{S_t}{S_s}\right)s \qquad 1.1$$

where the parameters and cost values for Anglian Water and Eastern England are defined in Table 1.1.

R_c, V_c, B and s are regional average unit costs. B and s reflect the cost of treating average COD and suspended solids levels per cubic metre (m^3) of effluent, in that region. These factors are multiplied by factors relating the strength (O_t:O_s) and solids content (S_t:S_s) of the trade effluent to that of domestic sewage. If the effluent has fewer suspended solids or a lower COD than average, the ratio (O_t:O_s or S_t:S_s) will be less than one and so charges levied will be lowered accordingly. If the ratio is greater than one, higher charges will be

incurred. Some water companies use a modified version of the formula to take account of specific situations.

Table 1.1 Parameters in Mogden Formula and Typical Values (Croner's 1991)

Parameter	Definition	1997/98 Costs (Anglian Water)
C_e	Total charge for trade effluent, costm^{-3}	
R_c	Unit cost of reception and conveyance of trade effluent in the public foul water sewer, cost m^{-3}	11.42 pence m^{-3}
V_c	Unit cost of volumetric and primary treatment of sewage treated and disposed of in waste water treatment works, cost m^{-3}	17.88 pence m^{-3}
B_v	Additional cost where biological treatment used, cost m^{-3}	3.46 pence m^{-3}
O_t	COD in mg l^{-1} (ppm) of the trade effluent after settlement for a specified period (usually 1 hour)	
O_s	COD in mg l^{-1} (ppm) of average strength settled sewage	465 mg l^{-1}
B	Unit cost of biological oxidation treatment of settled sewage, including the cost of secondary sludge disposal, cost m^{-3}	38.66 pence m^{-3}
S_t	The total weight of suspended solids, in mg l^{-1} (ppm) of the trade effluent at pH 7 of the mixed sewage	
S_s	The total weight of suspended solids, in mg l^{-1} (ppm) of average strength crude sewage	383 mg l^{-1}
s	Unit cost of treatment and disposal for primary sludge, cost m^{-3}	21.88 pence m^{-3}

For example if biological treatment is necessary an additional charge per m^3 (B_v) may be used. The Mogden Formula shows that these charges can be brought down by a reduction in wastewater volume and COD concentration, as well as by recycling part or all of the water. Therefore by introducing new effluent management techniques and/or by investing in effluent treatment technologies for on-site treatment prior to discharge to sewer, many

businesses can reduce the volume of effluent they discharge to sewer, and reduce both its COD and the concentration of suspended solids as well as significantly reducing effluent disposal costs.

The UK EPA (1990) requires continual re-evaluation of waste management practises as technology and techniques improve. As restrictions on the disposal of substances into the environment become tighter the costs of disposal and waste treatment also rise. This motivates industries to minimise the generation of waste, consequently meeting environmental requirements and reducing operating costs (Crittenden and Kolaczkowski, 1995). However, whilst these consent limits and legislations must not be taken lightly, the main concern of this project is waste minimisation.

1.3.2 Waste minimisation

Waste minimisation involves any activity which avoids, eliminates or reduces a waste at its source, allowing recycling of the waste. This results in the requirement of fewer raw materials, as well as reduced present and future costs associated with waste treatment and disposal (Edwards *et al.*, 1996).

The Waste Framework Directive (91/156/EEC) provided a four-step hierarchy for waste management: prevention, minimisation, recycling and finally disposal, where prevention is the most favourable method and disposal the least favourable (Laing, 1992; Thomas *et al.*, 1990). However, prevention is almost impossible for any industrial process, as it implies not creating the waste in the first instance (Anon, 1997).

Crittenden and Kolaczkowski (1995) gave a more practical hierarchy of waste management (shown in Table 1.2) where waste minimisation is concerned with the first three levels of the hierarchy. They state *"companies should strive to elevate waste management practices to these highest options, since conceptually it makes more sense to avoid producing a waste rather than to develop extensive treatment schemes."* This practical approach has two major long-term benefits for a company. Firstly, it can enable them to meet regulatory requirements. Secondly, it can improve profitability, through a combination of factors such as the reduction of liabilities, the promotion of a positive

public image, improvements to the health and safety of employees and an increase in operating efficiency leading to a reduction in production costs.

Table 1.2 Hierarchy of Waste Management Practices

Elimination	Complete elimination of waste
Reduction at source	The avoidance, reduction or elimination of waste, generally within the confines of the production unit, through changes in industrial processes or procedures
Recycling	The use, reuse and recycling of wastes for the original or some other purpose such as input material, materials recovery or energy production
Treatment	The destruction, detoxification, neutralisation *etc.* of wastes into less harmful substances
Disposal	The release of such wastes to air, water or land in properly controlled, safe ways, to render them harmless. Secure land disposal may involve volume reduction, encapsulation, leachate containment and monitoring techniques

1.4 The Waste Oily Water Separation (WOWSEP) process

In order to achieve the aims and objectives (provided in Section 1.1) of the WOWSEP project and its consortium members, a study of an *in-situ* waste treatment system for the removal of soluble components from oily wastewater was conducted. This adsorption study used a novel regenerative carbon and a typical engineering workshop waste stream containing:

a. 80-90% water or a soluble oil emulsion,
b. 5-10% insoluble free and dispersed oils, and
c. Less than 0.5% particulates.

A number of process steps were necessary to treat a waste stream with such diverse impurities. A pre-treatment process for the removal of the particulates, free and emulsified oils was developed by PERA, using a number of existing technologies. The remainder of

the waste, mainly comprising soluble oils and organic chemicals was subject to research using ion exchange, carbon adsorption and steam regeneration at the University of Bath.

Figure 1.0 is a schematic diagram showing the necessary steps for the removal of all these impurities in order to achieve "clean water". Ion exchange is an additional step which may or may not be required depending on the purity requirements of the final product.

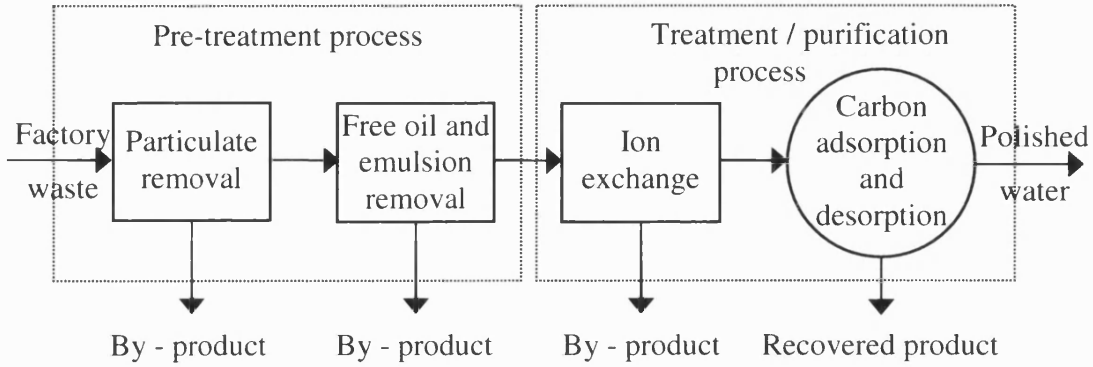

Figure 1.0 Schematic diagram demonstrating stages for wastewater treatment

The requirement of a pre-treatment process for the treatment of factory wastewater is essential because process methods such as adsorption and ion exchange are incapable of removing insoluble compounds efficiently. Therefore the removal of particulates, free and emulsified oils require treatment such as gravity separation, coalescence and filtration (Cheremisinoff, 1995; Sokolovic *et al.,* 1992; Wakeman, 1979; Eller and Gloyna, 1974).

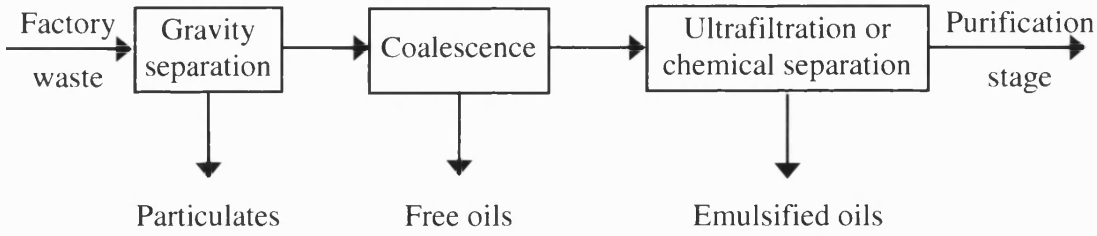

Figure 1.1 Schematic diagram of the WOWSEP pre-treatment process

Figure 1.1 summarises the pre-treatment stages selected for the WOWSEP prototype. The gravity separation unit physically removes particulates whilst the coalescer removes the free oils and the ultrafiltration unit or chemical separation unit breaks down the emulsified oils before the remaining waste is passed to the treatment stage (ion exchange/carbon

adsorption) of the overall process. While chemical separation may be used to break the emulsion this is not the preferred method for this process, as it requires the addition of more chemicals, which defeats the object of purification.

As mentioned, many techniques exist to remove the particulates, free and emulsified oils for the pre-treatment process but few techniques exist to remove the soluble oils. Most of the soluble oils originate from cutting fluids containing a complex composition of chemicals (discussed in greater detail in Chapter 2), which ultimately enter the waste stream. The ability to minimise them is vital to industry.

The initial work in this thesis involved the examination of carbon capacity (equilibrium studies) and the rate of adsorption uptake (kinetic studies), whilst further studies concerned adsorption and regeneration using a wide range of carbon samples and cutting fluid wastes using a combined unit (Figure 1.2). It was anticipated that the carbon adsorption step would remove all the soluble organic contaminants which could then be recovered using steam regeneration. However for a higher level of water purity with close to zero organic content, the additional step of ion exchange was found to be necessary to remove the soluble organic chemicals not adsorbed by the carbon. For scientific purposes, this project examined ion exchange and carbon adsorption, but for the purposes of industry the WOWSEP process concentrated on carbon adsorption alone. It is these purification and regeneration stages that are the central focus of this thesis.

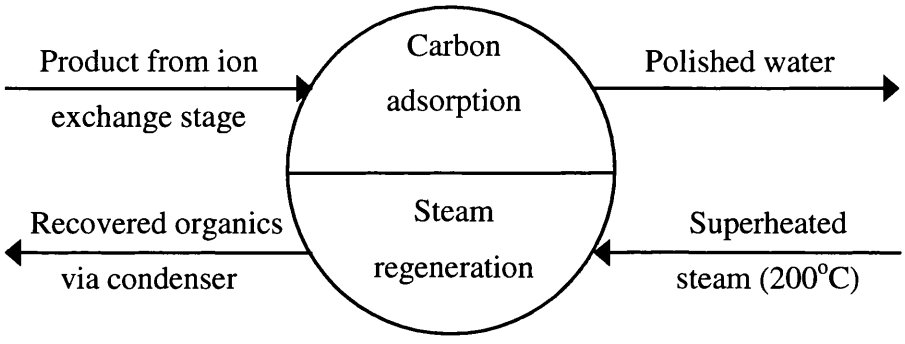

Figure 1.2 Schematic diagram of the carbon adsorption and *in-situ* steam regeneration unit in the WOWSEP process

Carbon adsorption does exist as established technology for wastewater treatment (Ford, 1977, McGuire and Suffet, 1983 and Faust and Aly, 1987), however the novelty and

innovation of this research lies in the use of a novel PRC using an *in-situ* regenerative system with superheated steam. The advantages of the regeneration process are that the carbon and the cutting fluid are relatively costly, therefore single use and disposal of the carbon would be extremely expensive. Consequently regeneration of the carbon and the recovery of the adsorbed phase makes the process even more economically viable. The regeneration being *in-situ* is an additional benefit, reducing costs such as the transportation of the spent carbon for reprocessing or disposal in landfill sites; both of which can be expensive especially for short adsorption cycles requiring frequent carbon replacement and/or disposal.

Data from the initial bench-scale adsorption and regeneration studies identified the optimum requirements to define the specification for the prototype system, such as carbon selection, column dimensions, flowrates and regeneration conditions. This permitted an adsorption column-sizing algorithm to be developed, which was then used to design the prototype rig and support the commercial growth of the WOWSEP process. Other important design considerations for the prototype included: low cost manufacture, application to the majority of small and medium sized enterprises, and flexibility of controlled parameters. The aim of the prototype was to demonstrate that the system was practically, technically and economically feasible. A schematic diagram and photograph of the prototype rig are shown in Figures 1.3 and 1.4 respectively.

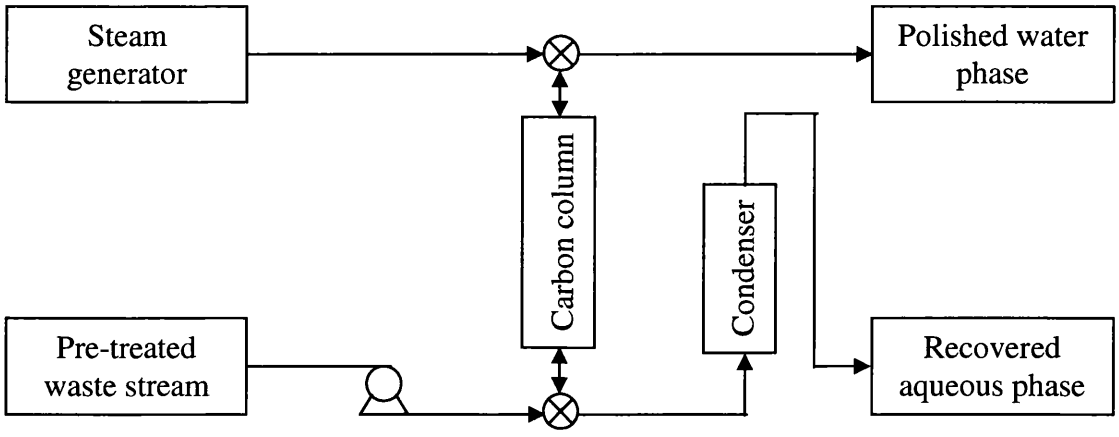

Figure 1.3 Schematic diagram of prototype carbon adsorption/regeneration rig

The prototype was constructed to follow any pre-treatment technology used for the removal of free and emulsified oils. It was based on the stages for wastewater treatment

(Figure 1.0) and the laboratory-scale rig used for bench trials (described in detail in Chapters 7 and 8).

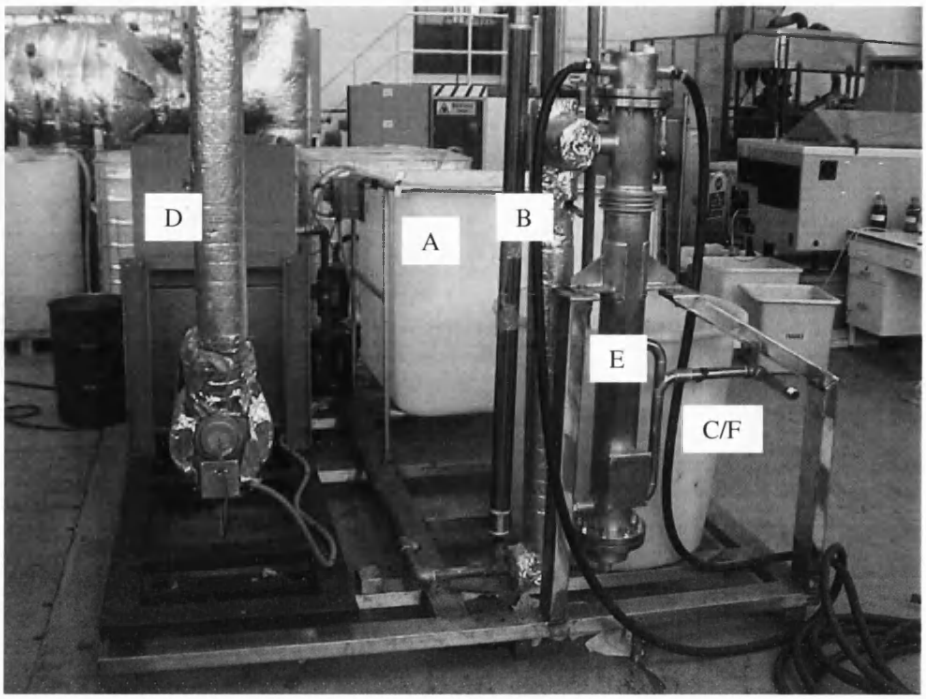

Figure 1.4 Photograph of the prototype carbon adsorption/regeneration rig

The prototype system was commissioned and tested at PERA (Figure 1.4) and validated at an automotive end user site which uses a wide range of water-soluble metalworking fluids (macro, semi-synthetic and synthetic fluid products) during the manufacture of components. The influent for the prototype trials was the product of an existing chemical pre-treatment process. 4000 litres of this feed, with a COD of 680 mg l^{-1}, was pumped from the feed tank (A) upwards through a column containing 16 litres of carbon (B), at a flowrate of 220 l hr^{-1}, for further purification. The polished water was collected and stored in a separate vessel (C) for future reuse on-site or low cost disposal. The ability of the prototype to remove water-soluble organic compounds was monitored by measuring the COD of the effluent (polished) water. Once the carbon was near saturation (60-70% of the breakthrough), it was regenerated using superheated steam at 230°C. The steam was produced by an electrically heated boiler (at 1 bar and 100°C) and its temperature increased to 230°C using an in-line heater (D). The mixture of steam and adsorbate from the regeneration process was cooled in a condenser (E) to produce a small volume concentrate, which was collected in a storage vessel (F). Ion exchange was not included in the

prototype as laboratory-scale trials demonstrated that for the purpose of recycling the polished water in industrial applications, such as floor washing or fluid reformulation, the additional expense for the removal of the organic chemicals was not cost effective.

Figures 1.5 and 1.6 show the breakthrough curve and regeneration profiles obtained from the prototype rig. The relationship of the effluent COD content from the prototype against the volume of waste treated is illustrated Figure 1.5. An immediate breakthrough is shown, with an effluent COD concentration of 79 mg l^{-1}. Thereafter the effluent COD gradually increases. The initial drop in COD concentration from a feed of 680 mg l^{-1} to 79 mg l^{-1} gave a reduction of almost 90%, which is a satisfactory achievement.

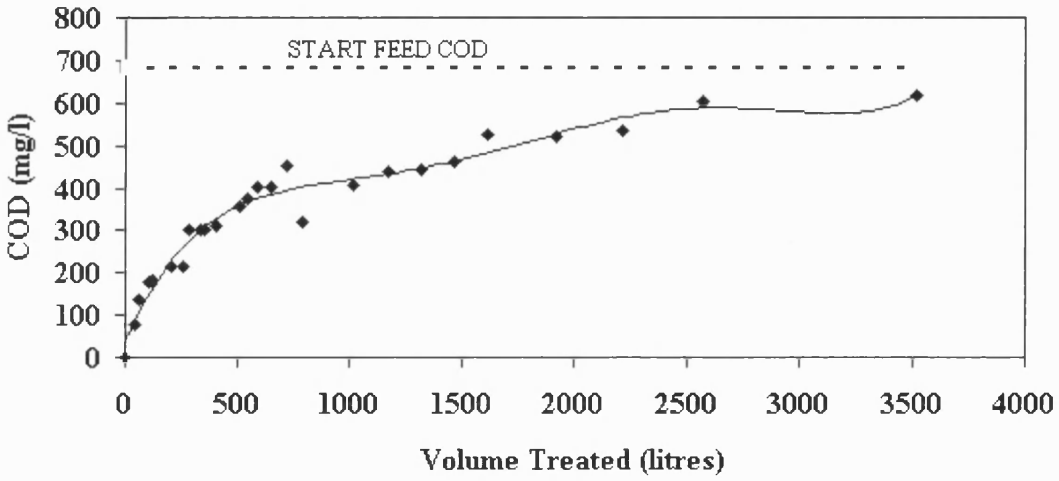

Figure 1.5 Typical breakthrough profile using the prototype rig

Figure 1.6 illustrates the relationship between the COD concentration of the condensate (recovered aqueous phase) against the volume of water required for complete regeneration. The greatest part of the regeneration process occurred in the initial 300 minutes. The two peaks possibly relate to different components desorbing from the carbon at different rates. The total volume of condensate recovered was 600 litres, therefore the ratio for the adsorption feed volume to the recovered condensate volume was calculated to be 20:3 (or 6.67:1).

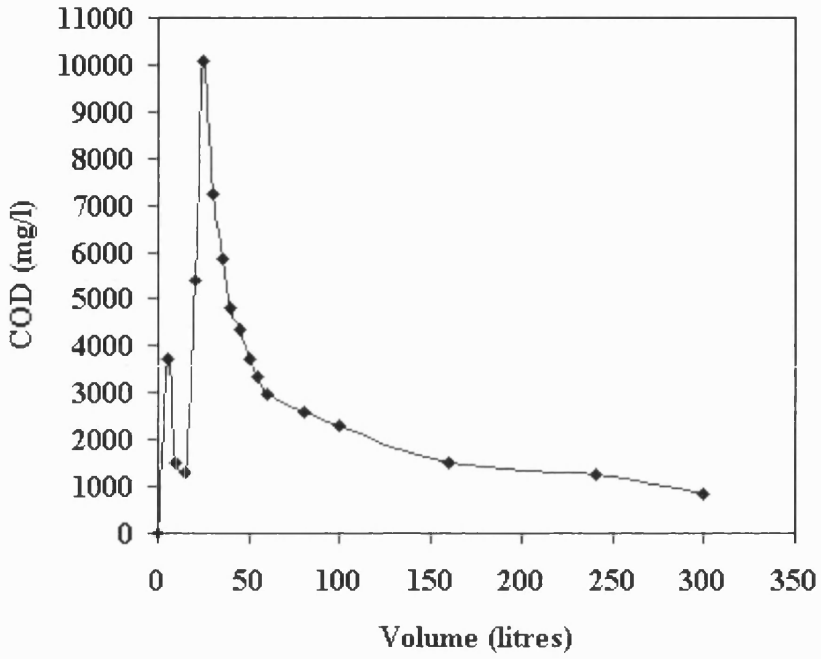

Figure 1.6 Typical regeneration profile using the prototype rig

Repeated adsorption/regeneration trials with this end user waste proved several regeneration cycles could be achieved without significant reduction in carbon performance. All of these results have proved the overall WOWSEP project to be beneficial to any industrial company with a similar oily waste stream.

1.5 WOWSEP benefits

The main benefit of the WOWSEP system is its ability to recycle treated wastewater, which would otherwise be discharged to sewer. This simultaneously provides significant economic savings in terms of reducing mains water consumption and sewerage charges.

The versatility of the WOWSEP process means it could be applied to a broad range of manufacturing industries, from chemical processing through to the disposal of metalworking fluids at end user sites. The technology could also extend to wider applications such as water treatment and power generation industries, as well as to the treatment of run off water from contaminated land. The ability to reuse the treated water for purposes such as mains water (for steam regeneration, cooling systems *etc.*), or process water (general cleaning, reformulation *etc.*) depends entirely on the quality of the water

produced. Likewise the use of the water after treatment defines the extent to which purification must be instigated; otherwise as explained previously for the ion exchange technology, unnecessary costs may be incurred.

Other factors that need to be considered include water hardness and final contaminant concentrations. For example, water hardness can cause problems in fluid re-formulation, and steam generation. The wide-scale use of chemical additives in current waste treatment processes may increase the hardness of the water. Consequently, expensive softening units may be required to counteract the water hardness. However, these problems can be minimised by the use of the WOWSEP process, which does not require any chemical additives.

The calculations from the WOWSEP process show the polished water to have a concentration, approximately 90% less than the feed concentration, which implies it has the potential for reuse in reformulations and/or for general cleaning use.

1.6 Case study

In 2001, Envirowise conducted a case study (Appendix I), based on the economics of the WOWSEP process, for an engineering company producing 1000 m^3 of waste oily water per annum. This case study demonstrated that the yearly cost for off-site disposal without treatment would be £40,000, whereas if the wastewater was treated a net reduction in cost of £27,340 could be achieved. Furthermore, if the wastewater was treated and recycled, the company would make a net saving of £29,455 per annum. Even greater savings could be made if the recovered aqueous phase from the regeneration process could be reused. These significant cost savings are also possible with smaller users.

All the experiments in this project and this case study demonstrate that the fully developed WOWSEP technology can give end-users the benefits of an effective waste oily water treatment system. In brief the benefits include:

- Up to 90% COD reduction in waste water streams
- No off-site transport, disposal or treatment costs
- Reuse of water on-site

- Reduction in on-site water consumption
- Savings on purchase of fresh mains water
- Reduced sewer disposal costs (based on the Mogden formula)
- Reduced carbon disposal/reprocessing costs
- Compliance with current and future legislation
- Potential application to other industry sectors producing wastewater streams (such as textile manufacture, dyers, chemical works and water companies).

This research also led to a cpnference paper (Appendix II) published at the 10th Annual Conference and Exhibition, held in Grand Cayman, Cayman Islands, October 2001 (Critttenden *et al.*, 2001).

1.7 Overview of thesis

This thesis covers extensive research into the removal of soluble oils and organic chemicals from factory wastewater. It investigates the laboratory-scale adsorption and regeneration tests conducted on a variety of carbons and cutting fluid solutions.

Three factors are addressed:

i. the characteristics of the adsorbate,
ii. the characteristics of the adsorbent and
iii. the characteristics of the solution during the laboratory trials.

This Chapter has presented an introduction to oily wastewater as a hazardous waste and the importance of on-site treatment. An overview of the project aims and objectives has been given and the development of the WOWSEP process from funding to design and development as well as trials of the prototype have been described. The following Chapter describes factory waste oily water in detail and its requirement for treatment. It concentrates on cutting fluids, their properties and the treatment methods available to separate the various contaminants. Chapter 3 looks at adsorbent selection, characteristics and properties. Chapter 4 focuses on adsorption principles and theory, whilst Chapter 5 centres on the characteristics of available adsorbent materials, mainly focusing on carbon and its chemical and physical properties, including surface area and pore size distributions.

Chapters 6 and 7 describe experimental work investigating carbon capacity, system kinetics and dynamic column studies respectively. The carbon capacity is studied through batch equilibrium tests using relationships such as Langmuir and Freundlich, whereas kinetic studies look at the diffusivity and rate of adsorption in a stirred cell batch reactor. The dynamic column studies explore a range of factors including the effect of column length, feed flowrate and feed concentration. The effects of flowrate, carbon activation and temperature, with regard to the regeneration of the carbon and recovery of the adsorbed aqueous phase are described in Chapter 8. Finally Chapter 9 discusses the overall conclusions of the work conducted and any future work which should be carried out in order to improve the system further.

2.0 Treatment of Metalworking Fluids

Domestic and industrial oily wastewater streams carry a variety of impurities, such as oils, chemicals and particulates. The oil fraction in domestic waste is a mixture of free (insoluble) and emulsified (partially soluble) oils, which originate from processes such as cooking, cleaning and washing. In addition, industrial waste streams contain soluble oils and other harmful soluble organic and inorganic contaminants. The soluble oils are generally a product of operations such as metal cutting, flushing, washing or as process by-products. These operations use fluids such as machining oils, cooling waters, paint bath flocculants, and mineral spirit cleaners. However the major source of soluble oils is from metalworking fluids, which are generally used to remove heat from cutting surfaces and reduce friction between the tools and work piece (Howard, 1996). With well-established techniques for treating free and emulsified oils, the main concern for water companies and industry is the removal of soluble oils and organic compounds from waste streams. Manufacturing facilities using these solutions discharge them to their local sewer sometimes without prior treatment (Wilson, 1970).

Metalworking fluids have been criticised for being irritating and dermatologically harmful during use (Samitz, 1974) and toxic on disposal. The high toxicity levels present in metalworking fluids makes reformulation with regard to personnel safety (occupational hygiene) essential, particularly as machine operators were openly exposed to these fluids. However, regulations (mentioned in Chapter 1) introduced tighter controls over the disposal of environmentally sensitive substances (Sheng and Oberwalleney, 1997; Miller and Anderson, 1993). Therefore users of metalworking fluids have to consider not only whether a product was acceptable for machining operations, but also its disposal routes and costs. Equally, as well as fluid performance, disposal became a key issue for fluid manufacturers.

Three main disposal routes exist: landfill, atmospheric and the aquatic environment (rivers, sewers *etc.*). Whilst the bulk of spent metalworking fluid is water, the presence of various toxic components make it unsuitable for discharge to sewer or evaporation to the atmosphere. Generally, in the UK, the vast majority of waste fluid including spent metalworking fluids is land filled. The increase in waste and the impact of legislation encouraged industrial companies to employ contractors for the transportation of their waste

off-site for appropriate treatment and/or disposal. Over the years, the contractor's costs escalated and this encouraged industries, even those generating as little as 1 m^3 day^{-1}, to invest in on-site treatment as an alternative to off-site treatment (Burke, 1991).

The rise in oil costs gave cutting fluid manufacturers motivation to research into enhancing metalworking fluid life. It was found that the fluid life could be lengthened by the addition of biocides and fungicides, as well as pH adjusters and sequestrants (such as chelate calcium and magnesium ions). These substances controlled the growth of microorganisms, helped to hinder the growth of bacteria, protected machines against rust and allowed emulsions to re-emulsify and synthetic soaps to re-solubilise (Childers *et al.*, 1990). Hence improvements to the fluid life in effect reduced the amount of cutting fluid disposal. Mosely (1994) stated "*Effective management of metalworking fluids reduces purchase and disposal costs, minimises health risks and creates additional economic benefits*".

Investigations into the treatment of industrial oily wastewater showed that whilst particulates, free and emulsified oils were straightforward to treat using established techniques (such as surface skimming and chemical splitting), the soluble oils and organic compounds were difficult to treat (Childers *et al.*, 1990). The degree of treatment varies depending on the quality of water required, *i.e.* whether it would be used in a wastewater treatment facility, or discharged to sewer under the existing permits or recharged into the aquifer (Napier and Rich, 1984; Stenzel and Merz, 1989).

The complexity in the removal of the soluble contaminants led to the establishment of the WOWSEP consortium and the research on which this thesis is based. This Chapter discusses the importance, content and application of cutting fluids in industry, and explores the requirements for their treatment before being discharged into the environment.

2.1 Metalworking fluids

2.1.1 The role of metalworking fluids in industry

The chief purpose of metalworking fluids is to increase the lifespan of the machine tool. This is achieved through supplying the machine with maximum cooling and lubrication, and by remaining stable when mixed with water, operated at high speed and under high

sheer (Saunders, 1990). The fluids acquire these properties through the unique additives in their formulations. These additives provide several important features (notably, anti corrosion, lubrication and cooling properties), helping them to play a vital role in various types of industries and for numerous applications, as summarised in Table 2.0. Cutting fluids also have the ability to withstand destabilising effects of tramp oils and effectively remove swarf from machines during cutting and grinding processes, promoting a good surface finish (Upton, 1996; Howard, 1996).

Table 2.0 Example of Users, Features and Applications of Cutting Fluids

Users	Features	Applications
Engineering	High quality soluble and straight oils	Cutting
Textile manufactures	Synthetic and semi - synthetic coolants	Grinding
Dyers	Sump cleaners	Drawing
Chemical works	Unique additives	Stamping
Landfill sites	Biostatic fluids	
Water companies	Process and production cleaners	
Steel works	Lubricants	
Power generators		

One type of metalworking fluid is not suitable for all of these users and applications. Indeed, there are three varieties of fluids (macro, semi-synthetic and synthetic), each of which are manufactured to have specific functions, as explained in the following section.

2.1.2 Types of metalworking fluid

The first cutting fluid to be developed was the macro fluid. It was formulated with a high mineral oil content for the purposes of lubrication in machine tools. This high mineral oil content did not provide the macro fluid with any cooling properties and therefore machines could only be used for short periods before becoming too hot to use. This meant that processes were being stalled and production demands were not being met. This loss of time and money, in conjunction with the increased regulation, rising disposal costs, and

environmental concerns, led to companies exerting pressure on the fluid manufacturers to improve the formulation.

The aim of the new formulation was to contain enhanced cooling properties and to provide more environmentally friendly properties. To achieve this, the manufacturers had to lower the mineral oil content, and replace it with a fluid which had a better specific heat capacity than the mineral oil. Research led to the choice of water. It has the best specific heat of the available fluids making it the paramount coolant as well as being environmentally sound (Howard, 1996; Saunders, 1990). As a result the synthetic fluid was developed, which had a much higher water:oil ratio than the macro fluid. However, this new synthetic cutting fluid also had its disadvantages; the low mineral oil content resulted in a loss of lubricating properties and hence caused corrosion and friction between the machines and their components. This made it impossible to use the synthetic fluid for heavy-duty metal cutting or grinding processes.

Studies into the boundary lubrication properties and viscosity (Misra and Skold, 1999; Saunders, 1990; Howard, 1996) of the cutting fluids indicated that when considering the manufacture of consumer goods, quality was just as important as quantity (or rate of production). Therefore the individual cooling or lubricating properties of water and mineral oil respectively, were not sufficient for the cutting fluid applications. Consequently, it was found that a combination of the properties of oil and water was ideal in providing both the lubricating and cooling properties, and therefore essential for a higher production rate. Hence development of the semi-synthetic fluid soon followed.

The semi-synthetic fluid was also water based, providing it with the cooling properties of synthetic fluid, whilst its mineral oil content gave it the lubricating properties of the macro fluid. With the help of additives within the fluid formulation, the semi-synthetic fluids had the ability to perform a commercially acceptable period of time providing they were properly maintained.

2.1.3 Contents of metalworking fluids

As previously mentioned, the macro, semi-synthetic and synthetic cutting fluids all have the same basic objective: to cool and lubricate the machine tool. This implies they all

contain the same basic groups of compounds (Table 2.1). For example, they all contain a lubricant or lubricating agent. Yet, whether this is a mineral oil or a phosphate ester is dependent on the manufacturer, type, grade and purpose of the fluid. This means that each fluid is manufactured with different chemical compounds and compositions, providing them with their own distinct appearances (Table 2.2), properties (Table 2.3), and uses.

Table 2.1 Basic Contents of Metalworking Fluids

Insoluble content	Soluble content
Base fluids (*e.g.* mineral or vegetable oils)	Emulsifiers (*e.g.* alkali fatty acid soap, carboxylic acid salt)
Extreme pressure (performance) additives (*e.g.* sulphur, phosphorous or chlorine contained substances)	Corrosion inhibitors (*e.g.* alcohol amines, borate ester, calcium sulphonate, calcium phosphate, sodium nitrite)
	Anti microbial agents (fungicides, biocides *e.g.* phenols, formaldehyde, boron)
	Lubricating agents (*e.g.* phosphate ester, polyalkylene gycol salt, imidazoline)
	Coupling agents, antifoam agents and dyes

The basic groups, shown in Table 2.1 above, contain many complex soluble and insoluble, organic and inorganic compounds, all of which have their own specific function in the cutting fluid formula. The soluble organic compounds are extremely difficult to destroy (Miller and Anderson, 1993).

The base fluids are necessary to provide lubrication and prevent metallic contact between the workpiece and the machine tool during operation. They were originally made of vegetable oils, which were inexpensive with superior lubrication properties and of which there was a plentiful supply. But the vegetable oils soon became unpopular as they provided a foundation for bacterial growth. Mineral oils, on the other hand, were 'upgraded' from being aliphatic additives in vegetable oils to providing improved lubrication and an enhanced performance level (Dick and Foltz, 1989; Howard, 1996). This presented a better finish quality for many cutting operations without the need for extreme pressure additives, and so replaced the vegetable oils. Corrosion inhibitors found

in the form of animal oils, fatty acids and soda are only required in water based cutting fluids. Their role is to form a soap when combined with water, protecting the machine tool and its components against rust without forming residues and crystalline deposits, while still effectively retaining the cooling properties of water. Emulsifiers are also required in the metalworking fluid formulations enabling the dilution of the concentrated fluids without producing an unstable system. The type of emulsifiers used in the fluid determines the droplet size, appearance (clear, opaque or milky) and the adsorbability of tramp oil by the fluid. Tramp oils aid the fight against anaerobic bacteria (Kim *et al.*, 1994), and when the water element of the emulsion has evaporated, an oily film is left on the machines and its components, protecting them from corrosion.

Cutting fluids were also extremely susceptible to attack from bacteria, yeasts and fungi. Bacterial attack could lead to a decrease in pH, bad odour, reduced performance, breakdown of the emulsion and the possibility of machine corrosion, whilst fungal growth could lead to slimy deposits on machines and blockages in coolant pipes and pumps. This made the incorporation of fungicides and biocides in the fluid formulation for water-based cutting fluids essential. Biostatic agents produce coolants (biostatic fluids) to tolerate low-level infection and inhibit further increases in microbiological contamination. The choice of microbial control agents used is determined by factors such as solubility, pH, operating range, chemical compatibility, cost effectiveness, thermal and physical stability, health and environmental issues (Hill, 1977). Boron products used to be popular as microbial agents, as they kept the fluid in a steady state condition without the requirement of additives. However, increasing environmental concerns relating to the chemical and toxic nature of boron compounds and biocides restricted their use (Wagle, 1983).

Tables 2.2 and 2.3 show that water based (synthetic) cutting fluids have a low mineral oil content, which means they cannot be used in metalworking operations that require high levels of lubrication. Therefore they have generally been used for less severe operations where hydrodynamic lubrication predominates. However, when difficult materials are machined or when used at high speeds/flowrates, hydrodynamic lubrication is not always sufficient. This led to the need for extreme pressure additives, lubricating agents, couplers and antifoam agents to be incorporated in the fluid formulations. The extreme pressure additives react with metal surfaces to form metal chlorides, phosphides and sulphides, easing the metal cutting process, (Misra and Skold, 1999; Dick and Foltz, 1989) whilst the

lubricating agents provide extra lubrication, and the couplers prevent fluid instability (fluid separation).

Table 2.2 Appearance of Macro, Semi-synthetic and Synthetic Cutting Fluids

	Macro	Semi–synthetic	Synthetic
Appearance	Milky white emulsion.	Cloudy green with a micro emulsion.	Clear green solution.
Solubility	75 % insoluble and 25 % soluble.	60 % insoluble and 40 % soluble.	100 % soluble.
Mineral 0il content	50 % - 60 %.	25 % - 35 %.	5 % - 10 %.

Table 2.3 Properties of Macro, Semi-synthetic and Synthetic Cutting Fluids

Macro	Semi-synthetic	Synthetic
Derived from petroleum, animal, marine vegetable or synthetic oils.	A mixture of oil and water.	Simplest fluid consisting of organic and inorganic salts dissolved in water.
Mineral oil content 50 % - 60%.	Mineral oil content 25 % - 35%.	Mineral oil content 5 % - 10%.
Used neat or with performance enhancing additives (no dilution necessary).	Combination of oils and emulsifiers, dilution necessary to form an emulsion.	Dilution necessary but no emulsion formed.
Poor specific heat, hence not used on modern high speed machine tools.	Good specific heat properties, due to water content.	Excellent heat transfer properties.
Excellent lubricant, with large mineral oil content.	Good lubricant and coolant, due to the heat dissipating effect of water.	Require synthetic esters to provide lubrication, as mineral oil content low.
Mineral oils protect machines against corrosion.	Emulsion provides anti corrosion protective film on machines.	Good corrosion control with anti corrosion additives.

The presence of these additives and oils are reflected in the appearances of the cutting fluids. The variations in solubility and mineral oil content are indicated in Table 2.2. For example, the macro fluid has the largest mineral oil content and is the most insoluble, generating a dense, cloudy, opaque emulsion, whilst the synthetic fluid has the least mineral oil content and is the most soluble displaying a clear solution.

Whilst synthetic additives have proved to play an important role in increasing fluid and machine life, inevitably reducing disposal frequency and costs, they are not easy to treat. Ideally cutting fluid manufacturers need to formulate their fluids with additives that produce long life yet are waste treatable. From a formulation perspective, the hard water stability of cutting fluid additives can be studied. The greater the additive stability for magnesium and calcium salts, the longer the fluid life. The additives with the best hard water stability (non-ionic emulsifiers, lubricants and alkanoamine based additives) have been found to be the most difficult to treat. Conversely, the additives with the worst hard water stability (soaps and sulphonates) are easier to treat. Therefore an intermediate additive with moderate hard water stability and moderate waste treatability would probably be the best compromise (Evans, 1977; Childers *et al.*, 1990).

2.1.4 The metalworking fluid market and its significance to the environment

There have been few surveys on the uses of cutting fluids. One conducted in 1980 (cited in Saunders, 1990) revealed that neat oils (macro fluids) were taking up approximately 60% of the cutting fluid market, whilst the soluble oils (semi-synthetic and synthetic) took the remaining 40%. However, there has recently been an overall reduction in the market for cutting fluids due to a number of factors which include technological changes in the design of machining equipment, less frequent fluid changes, health and safety requirements in industry, changes in the development of the cutting fluid and the expensive nature of the cutting fluid. The most significant change to the fluid was the move towards water-mix fluids (Howard, 1996). This change was confirmed by a more recent survey carried out by PERA in 1997 (PERA, Progress Meeting, 1997), which reported that from 337,000 tonnes of metalworking fluid concentrate sold in Europe 53% was semi–synthetic, 40% macro and 7% synthetic. This move away from macro fluids occurred because the water (from synthetic and semi-synthetic cutting fluids) was able to transfer heat two and a half times

faster than oil (in the macro fluids), therefore producing a smaller temperature rise than the equivalent weight of oil for a given heat input (Saunders, 1990).

The survey undertaken by PERA also found that 30% (approximately 100,000 tonnes) of the water-soluble products were used just for metalworking fluid formulations. Water-miscible cutting oils have also been reported to account for 440 million litres of aqueous waste in the UK alone. These figures verify the enormity of the pollution problem this may cause throughout the world, with metalworking fluids only forming part of the soluble pollutants entering the wastewater streams. A large percentage of this pollution is not recyclable or treatable by conventional methods and, as a result, the ability to minimise this waste is of great importance to industry. Therefore an alternative technology must be sought, or a combination of existing methods used to purify this waste. It is the search for this treatment that is the heart of this research.

2.2 Treatment of wastewater containing metalworking fluids

The removal or separation of free and emulsified oils (coalescers, ultrafiltration) is well documented, but little is known about the removal of soluble oils (Hu *et al.*, 2002). An *Athens* (Compendex Plus) search (formerly known as *BIDS*) of the treatment of wastewater from 1973 to 2003 provided 23,701 "hits", whereas a search over the same period for the treatment of metalworking fluids only gave 24 "hits". These searches demonstrate a lack of information and understanding on cutting fluid waste streams.

The previous section presented the composition of cutting fluids to be a complex mixture of many chemicals (summarised in Table 2.1). Major research efforts by suppliers, such as Agip Petroli, and changes in manufacture have created a significant improvement in the performance of water-based cutting fluids, as well as being more environmentally friendly than the macro fluids (Mosely and Brandolese, 1993). Irrespective of this, water-based fluids contain hazardous compounds which find their way into waste streams. For example, they have the greatest measure of soluble oils and organic chemicals, which result from the substitution of mineral oils with synthetic organic additives (emulsifiers, corrosion inhibitors *etc.*). These soluble compounds are the most difficult and expensive to treat and potentially the greatest threat to the environment (Childers *et al.*, 1990).

In general, wastewater containing cutting fluids comprises a mixture of particulates, free, emulsified and soluble oils, all of which originate from diverse sources. The particulate matter may emanate from several sources, such as fine metallic swarf from metal cutting operations, debris from grinding processes and general dirt and dust from factory workshops. The principal sources of free oils are leakages from hydraulic circuits and total loss lubrication systems (Mosely *et al.*, 1994). Gravity separation and turbulence may enable some particulates and free oils to be retained in holding tanks, whilst suspended solids and the remainder of the free oils are carried out with the waste stream. Emulsions and soluble contaminants are not separated out in the holding tanks but remain in the bulk fluid to be directly carried away into wastewater streams with the suspended solids and free oils. The microbial contaminants are kept to a minimum however, through the presence of the biocides and biostatic agents in cutting fluid formulations (Skold, 1991).

The harmful, soluble chemicals in the cutting fluid waste streams include amines, such as diethanolamine and monoethanolamine (DEA, MEA), nitrites, nitrosating agents (including many biocides), nitrosamines, secondary amines and boron esters (Howard, 1996). These originate from the corrosion inhibitors in the water-based fluids. Nitrosamines have been proved to be carcinogenic and can cause a variety of tumours if they enter a living body, attacking organs such as the liver, kidney or lungs (Mosely *et al.*, 1994; Howard, 1996). The nitrosamines are formed by a reaction which occurs when sodium nitrite comes in contact with an amine, both of which used to be present in cutting fluid formulations. It was vital to remove this health risk and so cutting fluid manufacturers were forced to remove the nitrite fraction from their formulations (Archibald and Bowes, 1990).

Nonetheless both compounds (sodium nitrate and amines) may still find their way into waste streams through several other routes. Amines are still used as corrosion inhibitors in the formulation of cutting fluids and nitrites can be formed through the biodeteriation of nitrates, workpiece hardening using nitrite salts, nitrite containing anti corrosion products and absorption of nitrous fumes. Consequently, the chance of nitrosamine formation still exists and fluids containing amines are now under scrutiny in certain markets. For these reasons, the monitoring of amines and nitrites is now mandatory and research into their removal from waste streams is essential.

Many cutting fluid manufacturers claim their fluids to be biodegradable, but semi-synthetic and synthetic oils are not easily biodegradable due to the large presence of aromatic molecules. Generally aromatic molecules are not as easily degradable as linear aliphatic molecules (Saunders, 1990; Childers *et al.*, 1990). This suggests that it is the water-based fluids which need to be predominantly targeted for treatment.

2.2.1 Treatment methods

There are many methods available for the treatment/separation of various contaminants, examples of which are shown in Table 2.4.

Table 2.4 Separation Methods for Pre-treatment and Treatment of Various Contaminants Found in Waste Streams containing Cutting Fluids

Contaminants	**Methods of removal**					
Particulates	Natural sedimentation	Centrifugation and hydro-cyclonation	Filtration (porous, vacuum)	Surface skimming	Backwash filtration	Magnetic separation
Free oils	Micro-filtration	Centrifugation and hydro-cyclonation	Oleophillic belt, tube, wheel and mop	Aeration devices	Coalescence	Surface skimming
Emulsified oils	Ultrafiltration	Flocculation poly-electrolyte	Chemical splitting	Centri-fugation	Biological aeration filters	Dissolved air flotation
Soluble contaminants	Distillation	Evaporation	Chemical splitting	Ion exchange	Adsorption	
Microbiological growth	Ultraviolet radiation	Pasteurisation	Biocides	Biostatic agents		

These methods either alter the chemistry of hazardous substances to make them safe for disposal, or remove the harmful contaminants so that they can be dealt with separately. The method used is dependent on its simplicity, cost effectiveness and the contents of the waste stream. These factors usually make physical treatment methods (adsorption, evaporation and filtration) the first consideration for the separation of wastes containing liquids and solids (Cheremisinoff, 1990). While each process effectively separates solids

from a liquid phase, it is ultimately the quality, quantity and character of the solids in relation to the carrier liquid that will determine the method used for the treatment. Methods such as sedimentation, clarification and flotation are often preceded by chemical splitting to improve the efficiency of the separation or to convert insoluble pollutants to suspended solids for physical removal (Cheremisinoff, 1990). Chemical splitting involves the reaction of two solutions, creating a third, which is normally easier to dispose of or separate using physical means. This is the most common method of treating wastewater due to its ease of adaptability to different volumes of wastewater. Examination of Table 2.4 highlights two points:

i. one treatment method can be used to separate more than one contaminant, and
ii. a variety of methods can be used for the separation of one contaminant.

In theory, both of these statements are plausible and possible, but neither is practical. For a multicomponent waste stream it is very unusual to see one method treat the whole stream, unless the required treatment is not very specific. Besides, depending on the properties and characteristics of the waste, each method has a greater affinity for one type of contaminant over another (Coulson and Richardson, 1991).

The affinity of one contaminant over another in distillation is dependent on the volatility of one component above another, whilst in absorption it is the solubility, in extraction it is the distribution coefficient, and in adsorption it is the attraction (bond strength). This makes the first statement inept and compromises the efficiency of the treatment. For example, activated carbon is commonly used for the adsorption of organic compounds; however, activated carbon beds may also be used as particulate filters. Hence, whilst using one step to remove two types of contaminant sounds advantageous, it also has its disadvantages. In the above example, when using carbon beds for adsorption as well as a filter, the voids in the carbon bed may frequently become blocked, creating pressure build-ups. This then obstructs the adsorption process from taking place efficiently. Equally, the second statement is also impractical. The use of more than one method for the removal of one contaminant would suggest the methods being used are incompetent, thereby making the overall treatment uneconomical. Consequently, for the treatment of a multicomponent waste stream, it is more common to see a variety of methods used in series, each removing a particular contaminant.

Table 2.5 Basic Functions and Properties of Separation Methods for Pre-treatment and Treatment

Separation method	Contaminant	Functions and properties
Natural sedimentation or gravity settling	Particulates	Gravitational separation of particulates using settling tanks and weirs is dependent on the difference between the relative density of water and the solids being removed. This method is cheap, simple and suitable for low turnover systems, although it is not suitable for fine particles.
Magnetic separation	Particulates	This technique can only be applied to waste containing ferrous swarf particulates. The fluid waste is pumped into a tank or trough which has a partially immersed rotating magnetic disc or belt. After extraction of the ferrous debris, a scraper removes the extracted material from the disc or belt.
Filtration (*e.g.* porous and vacuum)	Particulates	The removal of particulates by means of an inert porous filter medium, *e.g.* paper or cloth. There are several types of filters available which may use gravity, pressure or vacuum conditions to increase the speed of filtration.
Surface skimming	Particulates, free oils	Basic manual removal of any solids or free oils suspended on the surface of a liquid waste.
Oleophillic belts, tubes, wheels and mops.	Free oils	This technique utilises the attraction of an oil film to a continuous rotating endless belt, rope, wheel or mop which is in contact with the contaminated surface of the fluid. Free oils are then removed from the belt, mop *etc.* by means of a scraper or squeeze roller system.
Coalescence	Free oils	This device makes small oil droplets, into larger droplets through the process of coalescence and produces a bulk oil phase which separates by gravity. There are several types of coalescer available *e.g.* filters, mixed media or parallel plates. The latter two are most commonly used for the removal of free oils.
Aeration devices (*e.g.* dissolved air flotation)	Particulates, free and emulsified oils	Aeration devices are agitators that cause fluids to foam. Particulates and tramp oils attach themselves to the bubbles which are then skimmed off. This method is not suitable for coarse particles, although it has the ability to break emulsions by dissolving air into the liquid waste. This is then released into a main tank where the air comes out of solution as fine bubbles. A flocculent is added to complete the process.

Table 2.5 Basic Functions and Properties of Separation Methods for Pre-treatment and Treatment (Continued)

Separation method	Contaminant	Functions and properties
Hydro-cyclonation	Particulates, free and emulsified oils	Contaminated fluid is pumped tangentially into a conical vessel shaped to impart a vortex. The solids are thrown against the walls of the vessel and discharged by gravity from the bottom. The vortex creates a vacuum at the axis of the vessel resulting in clean fluid passing to the top from where it is removed and is re-circulated up through a central pipe. The efficiency of the hydrocyclone is governed by a number of factors including viscosity of the input stream, input and output pressures and size distribution of the particulates. The presence of excessively large particles can give rise to clogging at the solids discharge outlet.
Centrifugation	Particulates, free and emulsified oils	Both hydrocyclones and centrifuges operate on the same principles, but centrifuges have moving parts. They have a high-speed spinning bowl which causes rapid separation of particles and immiscible liquids with different specific gravities. Several factors for the speed of separation of a solid particle in a fluid are involved including fluid viscosity, particle and fluid densities and the applied gravitational force. Centrifugal cleaning of aqueous waste is particularly efficient for the removal of fine particulates and where a high degree of clarification is required. Due to their high capital cost, centrifugal systems find limited application in low volume waste streams, but are more widely used on high volume systems. The presence of particulates has a significant effect on the overall efficiency of the process.
Reverse osmosis	Emulsified oils	Reverse osmosis membranes have very small pores (10^{-4}-10^{-3}microns), which only allow water molecules through, holding back organic molecules and inorganic salts, requiring a minimum operating pressure of 500psi (*c.*35 bar).
Ultrafiltration	Emulsified oils	Ultrafiltration membranes have pore sizes of 10^{-3}-10^{-1} microns, which only allow low molecular weight organics, water and inorganic salts to pass through, with the higher molecular weight organics are retained. Operating pressures up to 50psi (*c.*3.5bar) are required.
Microfiltration	Free oils	Microfiltration has the same principles as ultrafiltration and reverse osmosis, but it has a larger membrane pore size of 10^{-1}-8.0 microns, thus only retaining very large molecules *e.g.* oil.

Table 2.5 briefly explains the basic function and properties of the various separation methods available (Cheremisinoff, 1990; Coulson and Richardson, 1991; Burke, 1991; Perry and Green, 1984).

As previously mentioned, this project was mainly set out to treat the soluble oils arising from the use of metalworking fluids. However, commercial confidentiality restricted the precise measures or ingredients of the cutting fluids to be disclosed. Analysis of the variety of components in the cutting fluid could in itself lead to another PhD research project. This uncertainty made the remnants of cutting fluids present in wastewater streams difficult to identify and consequently treat.

2.3 Pre-treatment stages

The selection of the pre-treatment stages for the WOWSEP process was as crucial as the selection of the purification methods. When selecting a treatment method, not only must the ease and cost of separation or the required final purity of the wastewater be considered, but more importantly the purity of the effluent at the end of each step. This is because the effluent of one stage becomes the influent of the next and this factor can either enhance or reduce the efficiency of each stage.

The pre-treatment stages in the WOWSEP process were designed to successively remove the particulates, free and emulsified oils, whilst the remainder of the wastewater, mainly consisting of soluble organic contaminants, was to be treated in the purification stage. Generally, particulates and suspended solids are the easiest to separate. If they are not removed early on in the process they could be a hindrance to subsequent stages by causing blockages *etc.* This provided the reasoning to eliminate them first.

Tables 2.4 and 2.5 showed various options for this treatment stage. Many of them are unsuitable for the WOWSEP process however. For example, while natural sedimentation (gravity separation) is simple and does not require complicated expensive equipment, it does not remove the suspended solids. Surface skimming does not remove dense particulates and magnetic separation only removes metallic particulates. This leaves filtration and centrifugation or hydrocyclonation. Centrifuges and hydrocyclones require large amounts of energy and complicated mechanical equipment. The presence of

excessively large particles in hydrocyclones and centrifuges can give rise to clogging at the solids discharge outlet, which may add further complications to the process *e.g.* cleaning. In contrast, filtration is relatively inexpensive and safer to operate as large amounts of energy are not required and the mechanical equipment required is far less complex than that for centrifuges and hydrocyclones. Filtration is a simple, popular process, which has been previously recommended by many authors (Stenzel, 1993; Coulson and Richardson, 1991; Lyman, 1978), as an independent separation method for the removal of suspended solids (<50parts per million (ppm)) and metals, especially if carbon adsorption is used for the removal of soluble organics in the purification stage, minimising the backwash requirements.

Insoluble oils are generally easier to treat than soluble oils (Childers *et al.*, 1990). Therefore following the removal of the particulate matter, the next contaminants to be removed from the waste stream were the insoluble free oils. Many of the methods shown in Tables 2.4 and 2.5 (*e.g.* aeration devices, coalescence) do not remove the free oils but either break them down or increase the droplet size for ease of removal by surface skimming which is usually carried out using oleophillic mops. Centrifuges and hydrocyclones can also be used to separate the free oils, but as previously mentioned they are extremely energy intensive and therefore expensive to operate. Microfiltration is a possibility but a more common method for the treatment of free oils by a small machine user is the oleophillic belt skimmer. Lyman (1978) suggested that the concentration of free oil and grease should be less than 10 ppm before entering a carbon adsorption column for it to operate effectively.

Emulsified oils are not so easy to treat as free oils or particulates. The most common methods for the removal of an emulsion are ultrafiltration and chemical splitting. Conventional treatment for emulsions, at present, is by chemical splitting (McCoy, 1994), which can be undertaken by two methods acid-alum split or charge neutralisation with polyelectrolytes (Hu *et al.*, 2002). Of these two methods, charge neutralisation is particularly favourable as it produces less sludge and is more cost effective (Burke, 1991). The following sections examine these methods in more detail.

2.3.1 Chemical splitting

The prime objective in chemical splitting is to break an emulsion down by the addition of chemicals, allowing the oil phase to separate from the aqueous phase, such that the free oil may then be removed. For example, the inorganic salt separation (acid-alum split) method uses sulphuric acid (H_2SO_4), aluminium sulphate (Al_2SO_4) and sodium hydroxide (NaOH) (as stated by Burke, 1991):

- 300-500 mg l^{-1} of H_2SO_4 is added to a fixed volume of metalworking fluid with mild agitation, until the pH is lowered to 2.0-3.0.
- Approximately 50-60% (in weight) liquid concentrate of Al_2SO_4 is then added to the solution (typically 500-5000 mg l^{-1}). This amount is directly proportional to the hard water stability of the solution being treated.
- After approximately 5 minutes of agitation, a 50% solution of NaOH is added to increase the fluid pH to a value between 4.5 and 9.0. The actual amount of NaOH to be added is dependent on the optimised flocculant formation between the Al_2SO_4, NaOH and the characteristics of the metalworking fluid being treated.
- After a further five minutes of agitation, the mixture is allowed to settle until the flocculant rises to the surface. It must be noted that the flocculant may settle if there is insufficient oil in the starting solution, or if an excessive amount of Al_2SO_4 is added.

If the exact chemistry of the fluid being treated or the interaction of mixtures of the waste metalworking fluids were unknown or unavailable, the procedure and amounts of each solution for the acid-alum split method would have to be decided by trial and error.

2.3.2 Polymer method (charge neutralisation)

The polymer method is similar to the inorganic salt separation, such that the addition of highly charged cations destabilise the anionic charges or vice versa. Occasionally the use of acids, inorganic salts and sodium hydroxide is required. The difference is that polymers are based on highly charged organic compounds and the chemistry of these compounds is more focused (Kemmer, 1979). In practice, small amounts of oil will always remain in the water phase and therefore total separation is not achieved. The degree of separation can be

improved however by the use of flocculating or collecting agents *e.g.* aluminium or iron hydroxide.

2.3.3 Membrane technology

Membrane technology utilises porous polymeric membranes as a means of separating materials of different molecular weights and sizes. The selection of the separation route is dependent on factors such as the membrane pore size, molecular weight cut-off and permeation flux. The permeation rate through the membrane is pore size and pressure dependent, as pressure must be applied across the membrane to force the aqueous phase and/or low molecular organics through the membrane. The Ultrafiltration Handbook (1989) suggests there are three different membrane processes for different size molecules: microfiltration, ultrafiltration and reverse osmosis (Table 2.5). Microfiltration membranes have fairly large pores (up to 8 microns), thereby allowing almost all organic molecules to penetrate through the membrane. This gives an insufficient separation of semi-synthetic and synthetic fluid emulsions. Reverse osmosis membranes, on the other hand, only allow very small molecules, (*e.g.* water) to pass through the membrane pores and therefore become easily fouled by large organic molecules, especially oils (Skold, 1996; Burke, 1991). This is not economical as regular cleaning or membrane replacement would be required. Therefore a basic, inexpensive, easy to clean and operate ultrafiltration unit (which only consists of a tank, pump, filter, membrane and interconnecting pipes) is the most likely workable membrane process for the separation of emulsified organic compounds. Ultrafiltration is also safer than the chemical method and it provides a respectable performance and a membrane life greater than 4 years (Hu *et al.*, 2002). However, the ultrafiltration process also has its limitations:

- The system temperature must be below 40°C for any continuous period of time. This avoids membrane damage.
- The solid content and the quantity of free oils must be extremely low. This avoids plugging of the micropores in the membrane, especially as fouling may be irreversible.
- Solvents may destroy the membrane.
- The membranes must be kept wet and clean at all times, as they are prone to bacterial fouling if not washed regularly, and are difficult to clean when dry.
- Low molecular weight organics and dissolved metals may pass through the membrane.

For the purposes of the WOWSEP process, a combination of filters and a gravity separation unit was used for the removal of particulates and coalescers for the free oils. Both chemical splitting and ultrafiltration were independently used for the treatment of the emulsion and their effects on the final purification stage were studied.

2.4 Purification stage

The pre-treatment processes should theoretically have removed the particulates, free and emulsified oils. However, the inorganic salt or ultrafiltration methods do not provide an effective removal of the soluble organic contaminants, such as the amines, non-ionic additives and alkoamines (Miller and Anderson, 1993; Burke, 1991). These substances remain in the effluent from the pre-treatment stages which subsequently becomes the influent to the purification stage.

When selecting the purification method(s) with the said pre-treatment stages a few points need to be considered:

1. The effect of chemical splitting on the purification stage.
2. The effect of ultrafiltration on the purification stage.
3. The possibility of recovering the soluble organics from the purification stage.

The first two points are important as they affect the contents and concentration of the influent to the purification stage and hence its performance.

Line 4 of Table 2.4 shows five simple and possible methods for the use of this purification step: distillation, evaporation, chemical splitting, adsorption and ion exchange. Distillation and evaporation are easy to understand and troubleshoot. They give consistent results over a wide range of fluids and provide an almost universal application (Coulson and Richardson, 1991). However, they are both very energy intensive processes and require knowledge regarding the properties of each compound present in the influent (*e.g.* boiling points and volatilities), which in this instance are unknown. Distillation separates contaminants with respect to their relative volatilities, and therefore in a multicomponent system compounds would be separated at different intervals with respect to the temperature of the system at that particular time. The components being distilled can then be condensed and collected for reuse or disposal at, for example, to a Publicly Owned

Treatment Works (POTW). Evaporation, on the other hand, separates compounds with respect to their boiling points. The evaporated fluids are not condensed, as in distillation, or sent to a POTW, but are generally released directly into the atmosphere. However evaporation is only suitable for small volumes unless a large floor space is available to aerate the effluent water in a lined pond, reducing disposal volumes (Burke, 1991). It must be noted, however, that evaporation can only be used if it complies with the current air pollution permits, and care must be taken at all times as fumes can be corrosive, have a foul odour and if the correct fluid and operational safeguards are not taken, fires or explosions may be caused. Vacuum assisted evaporators are also available which use less energy than standard evaporators and absorb all the fumes. The disadvantage, however, is that they increase the complexity and add extra maintenance to the operation. Chemical splitting was studied as one of the pre-treatment stages. It is also an option for the purification stage (Table 2.4). On the whole, it seems inappropriate to use it as a purification stage, especially as it involves the addition of extra chemicals contradicting the purpose of purification. Miller and Anderson (1993) thoroughly examined techniques such as chemical oxidation, ultraviolet light with catalysts, membrane technologies, and biodegradation to follow the ultrafiltration process, whilst Sheng and Oberwalleney (1997) examined the effects of recycling on different techniques such as sedimentation, magnetic separation, skimming, barrier filtration and centrifugation.

In contrast to all the other methods, adsorption and ion exchange are straightforward processes that do not require the addition of chemicals, and are not energy intensive. Regeneration of the adsorbent (or resin) and recovery of the adsorbate must also be uncomplicated. Both processes have very similar principles for the separation of compounds. The main difference is that in adsorption there is no exchange of ions between the adsorbent and the adsorbate molecules, whereas in ion exchange, ions are displaced in the insoluble exchange material (resin) by ions in the solution.

Adsorption on activated carbon is a well-established technology; its equipment is simple and readily available (Coulson and Richardson, 1991). It is one of the best commercially proven methods for removing organic chemicals (up to 93%) and can be used to eliminate hazardous substances from wastewaters, as well as for the recovery of valuable substances (Hashimoto *et al.*, 1985; Chow and David, 1978; Belkin *et al.*, 1994). Applying activated

carbon efficiently to a specific fluid requires careful examination in order to evaluate the objective of the treatment system and problems that may be brought upon the system.

Recovery of the soluble contaminants and regeneration of the adsorbent or resin is also an important issue and whilst adsorption and ion exchange processes are similar, their regeneration processes are different. The ion exchange resin requires the addition of counter ions to elute the adsorbed ions from the resin. The addition of further chemicals is not ideal, as this then produces another waste to dispose of. Regeneration of an adsorbent (*e.g.* carbon), on the other hand, could be achieved using a carrier medium such as steam, which strips the adsorbed molecules from the adsorbent. The steam can then be condensed and the adsorbed molecules recovered for reuse.

Taking all of these factors into account and the fact that adsorption is a clean, simple and cost effective technology that is widely used for the treatment of wastewater; it was decided that it would be the most suitable method for the purification step of the WOWSEP process. The selection of a suitable adsorbent is discussed in greater detail in the next Chapter.

3.0 Adsorbent Selection

There is a wide selection of adsorbents available on the market, ranging from activated carbon (organic), to ion exchange resins and zeolites (inorganic), cellulose, wool and polysaccharides, each specialising in a particular application. The most common of these are the organic and inorganic adsorbents, otherwise known as general-purpose adsorbents.

When selecting an adsorbent three main criteria need to be considered (Fox and Kennedy, 1985):

1. Type of adsorbate molecules present and their attraction to the adsorbent.
2. The type and form of adsorbent materials *e.g.* powdered activated carbon, granular polymeric adsorbents, *etc.*
3. The design criteria *e.g.* equilibrium capacity, adsorbent lifetime, dynamic adsorption rate, ease of regeneration, mass balances and cyclic studies and the process economics (Rousseau, 1987). However adsorbents are often selected by experimental trial and error.

The following sections in this Chapter look at the variety of adsorbents available on the market and their characteristics and properties, such as structure, surface areas and applications. Chapter 4 provides a detailed account of adsorption theories, while Chapters 5, 6, 7 and 8 discuss the experimental data associated with the final adsorbent selection for the WOWSEP process.

3.1 Organic adsorbent materials

Carbon is the oldest, least expensive and most widely used non-polar organic adsorbent (Cheremisinoff, 1990; Fox, 1985). It appears in numerous forms, for instance charcoal and activated carbon, and its usage dates back to over 3500 years ago, centuries before Christ (BC) (Lyman, 1978; Cheremisinoff and Moressi, 1978). The use of activated carbon in the form of carbonised wood (charcoal) has been described as early as 1500 BC in an ancient Egyptian papyrus (cited in Rodriguez-Reinoso, 1997). Before the 13th century, ancient Hindus successfully used charcoal to filter their water; thereafter the development of carbon materials and their applications began to increase rapidly (cited in Cheremisinoff

and Moressi, 1978). Hippocrates and his disciples recommended dusting wounds with powdered charcoal to remove their unpleasant odour. However, carbon was not used industrially until the end of the 18th century. In 1773 the Swedish chemist, Karl Wilhelm Scheel, discovered the adsorption of gases on to charcoal, and in 1785 Russian academic, Lowitz, noted charcoal's ability to remove colours from liquids (cited in Jankowska *et al.*, 1991a; Cheremisinoff and Moressi, 1978). This led to the use of charcoal as a decolourising agent for sugar syrup, in England in 1794, and initiated research on adsorption from the liquid phase. The manufacture of better quality gas adsorbent carbons was encouraged during World War 1 for use in gas masks, for protection against poisonous gases (Bansal *et al.*, 1988; Rodriguez-Reinoso, 1997). In the mid 19th century, England started to use carbon for the removal of odours and tastes from drinking water (Cheremisinoff and Cheremisinoff, 1993; Fox, 1985; Huang, 1978). Ostrejko (1900) discovered that when vegetable charcoal was treated with mineral chloride it showed a decolouring power of ten times that of the untreated charcoal. By the 20th century carbon and its derivatives had been thoroughly researched such that they were being used universally in numerous techniques and applications, for example water and wastewater treatment in wineries (Lopez, 1999), paper and pulp industries (Roth, 1982; Khalili *et al.*, 2002), pharmaceutical industries (Jankowska *et al.*, 1991a; Rodriguez-Reinoso, 1997; Lyman, 1978), food industries (Lopez, 1999; Fox, 1985; Huang, 1978) and petrochemical and petroleum industries (Kisarov *et al.*, 1980; Sokolov and Kuz'min, 1979; Huang, 1978). The following sections describe various forms of carbon and other organic adsorbents.

3.1.1 Engineering porous carbons

Engineering porous carbons (and graphite) were chiefly used from the mid 20th century for a variety of applications. They are manufactured using organic raw materials (such as wood and walnut hulls) and heated in red heat with an ample air supply. This drives off any hydrocarbons and sustains combustion, resulting in a basic macroporous char with pore widths in excess of 50nm and surface areas of 5-100m^2g^{-1} (similar to that of the initial stages of activated carbon manufacture). However, due to these low surface areas engineering porous carbons were mainly used as particulate filters, gas diffusers and lightweight carbon components, where the spent carbon could be recovered and reused after chemical or thermal regeneration.

3.1.2 Carbon molecular sieves

In the 1960s research established that carbonisation of certain polymers gave rise to a high surface area material, called molecular sieves. This material was able to selectively exclude molecules, depending on its pore size. The effective pore sizes could be reduced, for the exclusion of small molecules, by performing a further simple carbonisation process (Walker, 1966). In the early 1970s Bergbau Forschung used coal based molecular sieves (carbon molecular sieves) for the first time industrially (cited in Jüngten *et al.*, 1981). The coal pore structure was modified by carbon deposition in the pore mouths through the cracking of an inorganic precursor (Moore and Trimm, 1977). During the 1970s and 1980s the trend had drifted towards the use of activated carbon. However by the 1990s, interest in the use of carbon molecular sieves with a high pore volume combined with the use of chemical deposition returned (Cabrera *et al.*, 1993). The organic carbon molecular sieves were shown to have a similar function to inorganic zeolite molecular sieves (described in Section 3.2.3). However the slit like pores of the carbon molecular sieves enhanced selectivity in certain process situations, in comparison with the rounded apertures of zeolites. The most common commercial use of carbon molecular sieves is the separation of nitrogen from air (Knaebel, 1995).

3.1.3 Activated carbon

Activated carbon is the collective name for a group of microcrystalline, non-graphitic materials processed to develop a high degree of internal porosity and surface area. This permits the adsorption of gases or vapours and dissolved or dispersed substances from liquids. Generally, adsorption applications require carbon to have surface areas greater than $600 m^2 g^{-1}$, rendering engineering porous carbons, with their lower surface areas, inadequate. Activation of the char removes carbon from the interior of the particle producing an internal porous structure (Figure 3.0), thereby creating an unstructured, disorganised microporous material, with variable pore size distributions (Guillot *et al.*, 2002), large internal surface areas and pore volumes (Metcalf and Eddy, 1991).

The raw materials used for the manufacture of activated carbon may originate from almost any carbonaceous material (*e.g.* blood, bones, wood, nutshells *etc.*). These raw materials may then take either of two activation routes: gas or chemical (although occasionally both

may be used). Gas activation is achieved by preliminary carbonisation of the raw material followed by oxidation either through heating at low temperatures in air or at higher temperatures with steam or carbon dioxide. Chemical activation, on the other hand, is dependent upon the action of inorganic chemicals on the raw materials to dehydrate the organic molecules during the carbonisation (or calcination) process.

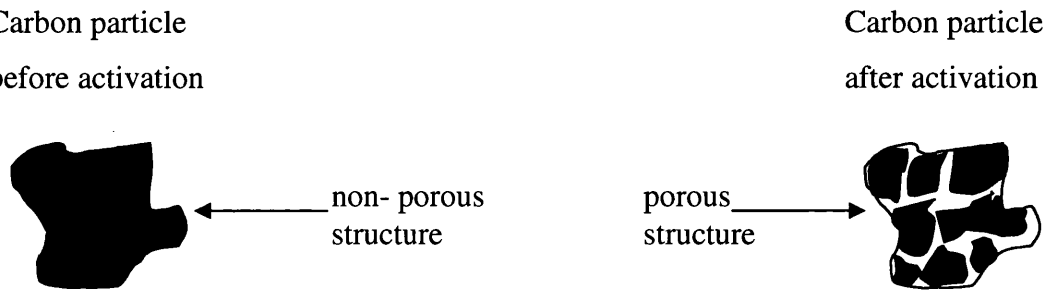

Figure 3.0 Carbon particle before and after activation

These activation processes produce two types of carbons: liquid phase or gas phase, depending on the raw material and activation process used. Liquid phase carbons (such as decolorising adsorbents made from coal, peat, lignite or sawdust) are mixed with oxidising agents (*e.g.* alkali metal hydroxides, carbonates, sulphates, phosphates) and heated with a temperature between 500°C and 900°C, cooled, washed, filtered and dried. This produces powders with surface areas in the range of 300 m^2 g^{-1} and pore sizes greater than 3 nm. The larger pore sizes allow rapid diffusion of molecules to occur. Gas phase activated carbons, on the other hand, may be manufactured by either chemical or gas activation. Chemical activation uses raw materials such as sawdust and peat with phosphoric acid or zinc chloride. Further activation is then employed using steam to produce vapour phase quality. Gas activated carbons are initially calcined at 400-500°C and then selectively oxidised further (with steam or carbon dioxide) at 800-1000°C to develop the required internal porosity and surface activity. These gases are preferred for the oxidation as they are less exothermic and easier to control than low temperature oxidation with air. Gas phase carbons so produced are hard granules or pellets with surface areas in the range of 800-1200 m^2 g^{-1} and smaller pore sizes of less than 3 nm (Rousseau, 1987).

Generally, activated carbon has a variable pore structure, with pores in the sub 2 nm range and surface areas of 300-3000 m^2 g^{-1} (Rousseau, 1987), where the variation in the pore size and surface area results from modifications of base material, temperature and impurities.

The activated carbon that possesses the highest surface area (3000 m^2 g^{-1}) is produced from petroleum coke.

Impurities in conventional activated carbon usually consist of 0.5% inorganic residues after acid washing. As manufactured, the inorganic content in carbons represents 5-10% wt/wt in the form of metal ions, sulphates, phosphates and chlorides. The type and distribution of impurities affects the way the activation process works, leading to heterogeneous products. For example, the presence of metal impurities act as catalysts for the oxidation process in the manufacture of activated carbon. Variations of the metal content lead to large deviations in pore structure and hence surface area.

As described earlier, the use and applicability of carbon has increased over the centuries. In the early 1970s, activated carbon became the most popular adsorbent in the treatment of industrial and municipal wastewaters. It was used to eradicate pollutants such as hazardous organic compounds, bad odour and taste. It was used also for the clean up of gases containing volatile organic compounds, as well as for the constant increasing demands for the purity of natural and synthetic products (Chow and David, 1978; Fox, 1985; Bernardin and Bilello, 1979; Rodriguez-Reinoso, 1997).

Carbon's extensive range of raw materials, activation methods and temperatures, has made it a general purpose adsorbent with functions for a broad selection of applications and an affinity for an assortment of adsorbates. This diversity gives carbon its versatility, making it susceptible to competitive adsorption, eventually leading to the requirement and hence development of application-specific carbonaceous and synthetic polymeric resins. This approach also enables activated carbon to become tailored for specific applications (Hassler, 1967; Sweatman and Quirke 2001). For example, in the 1980s, Japan introduced a coconut shell precursor based on the modification of the pore structure by carbon deposition. The variation in raw material increased the activated carbon's surface area, making it more suitable for adsorption applications (Ohsaki and Abe, 1984). The removal of compounds such as mercury, ammonia, hydrogen sulphide, hydrogen cyanide, phosgene, arsine and nerve gases required activated carbons to be impregnated with compounds such as sulphuric acid, iron oxide, zinc oxide and heavy metal salts respectively (Gayazov *et al.*, 1985; Huang, 1978). However tailoring a carbon for a multicomponent system, and to be application-specific makes it necessary to have several

process steps prior to, or following, the carbon adsorption column so that all non-adsorbable species can be removed.

Common uses for carbon are the recovery of nitrogen from air; recovery of ethene from methane and hydrogen; odours from gases; water purification including the removal of phenol, halogenated compounds, pesticides and chlorine; recovery of solvent vapours and the purification of helium (Coulson and Richardson, 1991).

3.1.4 Phenolic resin carbons (PRC)

MAST Carbons Ltd., driven by the need for a new catalyst support with improved characteristics, have extended carbon research even further and developed a polymer-based PRC (MAST, 1998).

The important feature of the PRC as a novel catalyst support is the development of a high surface area, controlled porosity and a complex net-shape-forming capability (MAST, 1998). The materials do not have mesopores in their standard form and while this may seem like a disadvantage for some processes, other features, most notably their ability to produce a tightly defined micropore and controlled macropore structure compensates for this (Tennison *et al.*, 1993). These properties provide for a wide array of applications ranging from biomedical applications to large-scale gas and liquid separation processes.

Table 3.0 Comparison of Phenolic Resin Carbon with Other Industrial Carbons According to MAST Carbons Ltd.

Phenolic resin carbons (PRC)	**Other industrial activated carbons**
Capability of near net shape forming	Poor physical properties
Wide range of physical forms	Strictly limited physical forms
High purity	Low purity
Micro and macro structure only	Micro, meso and macro pore structure
Good reproducible porous structure	Poor reproducible porous structure
Controllable porous structure	Variable pore structure
Physically strong and resistant to attrition	Fairly brittle

The initial stages of the manufacturing process for PRCs are similar to those for activated carbons, where a polymer precursor material is turned into a non-porous char. This char is then carbonised through heating in a non-oxidising atmosphere to over 550°C. As the temperature increases the resin releases volatiles until only a carbon skeleton of the original shape remains. The carbonised material is then activated by oxidation to remove any blocked pores and generate a high internal surface area. This process offers a route to manufacture porous carbons in a wide variety of shapes and structures, including adsorbents, structural materials, catalyst supports and asymmetric microporous carbon membranes. The PRCs range from large monolithic adsorbents to granular particles. Table 3.0 shows the differences between the PRC and other industrial carbons.

3.1.5 Polymeric adsorbents

Polymeric adsorbents, more commonly known as ion exchange resins, are of spherical shape with a high pore volume. They have a diverse variety of forms, such as inert copolymers of polystyrene and divinylbenzene. The polymer beads typically have a diameter of 0.3-1 mm, which shrink and swell upon cyclic use. They are very expensive, approximately ten times the cost of other commercial materials such as carbon. Internally the polymer beads contain gel-like microbeads joined together at a few points creating a macropore structure, with surface areas between 5-800 $m^2 g^{-1}$, and pore diameters of 2-200 nm (20-2000 Å), or if activated 0.3-200 nm.

Polymeric resins are not limited to surface bonding but also involve stronger chemical bonding such as ion pairing and hydrogen bonding. Ion exchange works on a related principle to that of physical and chemical adsorption. During physical adsorption, molecules adhere onto the substrate by molecular cohesion and dipole-dipole (van der Waals) interaction, enabling the separation of non-polar substances from polar solvents (Purolite International Ltd., 1998a). The general principle is that hydrophobic (non-polar) materials are attracted to hydrophobic surfaces from relatively hydrophilic (polar) solutions or vice versa.

An ion exchange resin can be either cationic (negatively charged) or anionic (positively charged), and its use is dependent on the nature of the solution and whether it is the anions (negatively charged ions) or cations (positively charged ions) that are required to be

removed. Ion exchange resins are more application-specific than activated carbons and so the problem of competitive adsorption is not as great.

Polymeric adsorbents are used in applications such as recovery and purification of antibiotics and vitamins, decolourisation, decaffeination, blood purification, separation of halogenated light organics from water and treatment of industrial wastes *e.g.* phenolics and volatile organic carbons (Rodriguez-Reinoso, 1997; Lyman, 1978). Although ion exchange resins are most effective in selectively removing or polishing metals and cyanide (CN) bearing waste streams (Cheremisinoff, 1990). They have also commonly been used for the adsorption of organic chemicals from contaminated wastewater (Hutton, 1978). However their oldest and most enduring application is for water treatment, to soften or demineralise water before industrial use and to recover components from an aqueous effluent before it is discharged or recirculated (Coulson and Richardson, 1991).

The main difference between polymeric adsorbents and polymeric resins is the type of adsorbate-adsorbent bonding. Polymeric adsorbents use non ionic bonding, which is physical in nature, whereas with polymeric resins (*e.g.* ion exchange resins) use ionic bonding, which is chemical in nature (Fox and Kennedy, 1985).

3.1.6 Macroreticular resins

The technology of synthetic polymeric adsorbents is an offshoot of the synthetic ion exchange resin technology. In the 1950s there was a major development in polymer chemistry extending from the improvement of ion exchange resins and greatly influencing ion exchange technology, producing macroreticular ion exchange resins. The main difference between the two resins is the fixed pore structure of the macroreticular polymer beads, permitting molecules to move in and out of the resin, thereby increasing diffusion rates of the ionic species. This is in contrast to the conventional ion exchange resins which do not contain a true physical porosity and the exchangeable ions diffuse through the swollen bead structure to the exchange sites. In addition, increased cross-linking of the polymer matrix in the macroreticular resin makes it less susceptible to oxidation and more durable.

3.1.7 Macronets

In 1969, Davankov and Tsyurupa (Davankov *et al.*, 1969) discovered and patented macronets by further developing the macroreticular ion exchange resin. The principle of macronets was that the porosity was not introduced during polymerisation but during a post polymerisation process in which the polymer was hyper-crosslinked in a swollen state. The final product had a polymeric network with a controlled pore structure, high surface area and regenerable properties. This controllable pore structure created macronets with a high proportion of micropores which in turn produced surface areas in excess of 900 $m^2 g^{-1}$ (*e.g.* MN500), whereas standard synthetic ion exchange resins (*e.g.* Purasorb AP250 and AP400) have larger micropores and therefore do not have surface areas larger than 600 $m^2 g^{-1}$ (Purolite International Ltd., 1998b).

As well as a large number of micropores providing high surface areas, the macronets have macropores providing rapid access to their internal surfaces, as with adsorbents. The macronets also have an ion exchange functionality with the capability of the addition of functional groups providing further selectivity and the possibility of making the polymers hydrophilic, thereby enabling chemical regeneration. Another advantage of macronets is their ability to swell as a result of liquids and gases that do not normally solvate the polymeric matrix, which limits the expansion between its ionic forms.

Macronets have been shown to have many beneficial properties over activated adsorbents (such as carbon); for example they are physically robust with breaking weights of 750 g/bead making them easier to handle without any dust problems. They can also be regenerated by conventional ion exchange techniques such as hydrochloric acid or caustic soda and they can be regenerated *in-situ* using steam stripping. These properties show macronets to have a dual role: as an adsorbent and as an ion exchange resin, properties which have led them to replace activated carbon and other adsorbents in applications such as:

- The decolourisation and removal of tastes and odours of sweetener syrups (*e.g.* corn syrups, cane syrups).
- The removal of pesticides and herbicides from potable water sources.
- The removal of phenol and chlorinated phenols, detergents and dyes from wastewaters.

- The removal of mineral oil from water.
- The debittering of citrus fruit juice and caffeine isolation.
- The removal of organics from gases.

Generally, polymers and resins have a vast array of applications, such as water purification including the removal of phenol, chlorophenols, ketones alcohols, aromatics, pesticides, antibiotics, detergents, emulsifiers and dyestuffs; the recovery and purification of steroids, amino acids, and polypeptides; the removal of colours from syrups, recovery of proteins and enzymes and the separation of aromatics from aliphatics.

3.2 Inorganic adsorbent materials

There are many common inorganic adsorbents such as activated alumina and silica. However other inorganic materials such as calcium chloride, calcium oxides, magnesium, zinc and sodium bicarbonate can also act like absorbents.

3.2.1 Activated alumina

Activated aluminas are amorphous inorganic adsorbents with the general formula $Al_2O_3 \cdot nH_2O$. They are manufactured by the controlled heating of hydrated alumina in air at 400°C. At this temperature, water molecules evaporate in the form of steam and the crystal lattice ruptures along the planes of weakness. This produces activated alumina with a well-defined pore structure, with mean pore diameters in the range of 2-5 nm, pore volumes in the range of 0.2-0.3 $cm^3\ g^{-1}$ and surface areas in the range of 200 to 500 $m^2\ g^{-1}$ (Rousseau, 1987), and as the formula suggests a high affinity for water and hydroxyl groups.

Activated aluminas are available in the form of granules, beads, extrudates and powders, where the beads and extrudates have dimensions of 1-8 mm and 2-4 mm, respectively. Their main benefits are a high capability of retaining its adsorptive capacity at elevated temperatures and a resistance to attrition in moving bed applications. Although in terms of capacity or selectivity activated aluminas cannot compete with molecular sieves (Coulson and Richardson, 1991).

Activated alumina has applications ranging from drying processes for liquids and gases, the removal of oxygenates and mercaptans from hydrogen feed streams, fluoride ions from water, hydrogen chloride from hydrogen in petroleum refineries, but this adsorbent is mostly used as a catalyst or catalyst support and as a desiccant (Knaebel, 1995).

3.2.2 Silica

Silica has the formula SiO_2 and exists in many varieties, such as silica gel, porous borosilicate glass and aerogels. Silica gel is a rigid, three dimensional, non-crystalline network of spherical microparticles made of amorphous colloidal silica. It is produced from a silicate solution, such as sodium silicate, which is acidified to a pH less than 10, forming a gel of polymeric colloidal silicilic acid as an agglomerate of microparticles. This gel has a polar surface exhibiting an adsorptive preference for unsaturated organic compounds (Cheremisinoff and Moressi, 1978; Rousseau, 1987).

When the gel is heated, the water evaporates leaving a hard, open-celled, porous, glassy structure with pore diameters of 3nm and internal surface areas ranging between 100-900 $m^2\ g^{-1}$ (Knaebel, 1995). The surface area is highly dependent on the raw materials used, the manufacturing process and consequently on the density of the particles and the pore size: the smaller the pores the higher the density and surface area. For example "regular density" silica is prepared by gelling, in an acid medium, creating pore diameters of 2-4 nm, pore volumes ranging from 0.37-0.4 $cm^3\ g^{-1}$ and surface areas of 750-800 $m^2\ g^{-1}$. "Intermediate density" silicas are in powder form with pore sizes of 12-16 nm, pore volumes of 0.9-1.1 $cm^3\ g^{-1}$ and surface areas of around 300 $m^2\ g^{-1}$. "Low density" silicas or areogels are extremely fine powders, with surface areas as low as 100-200 $m^2\ g^{-1}$ and are very rarely used as adsorbents (Rousseau, 1987). The form of silica varies from beads with diameters of 1-3 mm to granules with diameters of 2-4 mm as well as gels and powders. They are used for processes such as the separation of hydrocarbons, dew point reduction for natural gases, drying of liquid hydrocarbons, but due to its hydrophilic surface they have a high affinity for water and are most commonly used to remove moisture from the air.

In 1903, the selective adsorption of various liquid substances on silica gel was observed, where each substance appeared as a different colour in the gel. This adsorptive process was referred to as the chromatographic method (Jankowska *et al.*, 1991a).

3.2.3 Zeolites

There are approximately forty naturally occurring zeolites and one hundred and fifty synthesised minerals collectively known as molecular sieves (Coulson and Richardson, 1991). These molecular sieves are inorganic crystals, generally comprising of alumino-silicates with generic formula $M_{2/n}\cdot Al_2O_3\cdot xSiO_2\cdot yH_2O$, where M is a single cation with valence n, x is the silica to alumina ratio (≥ 1) and y is the molar water hydration (Rousseau, 1987). They have a complex, crystalline lattice structure, comprising a tetrahedral of silica (SiO_4) and alumina (AlO_4) crystals which are linked by sharing oxygen atoms. Mobile cations and water molecules occupy the channels and voids, and may be replaced through ion exchange. Heating the zeolitic molecular sieve removes the water, leaving the crystalline structure permeated by micropores. This process is reversible and the zeolites can be rehydrated.

Zeolites are manufactured through the crystallisation of gels in a closed hydrothermal system with temperatures varying from approximately 20°C (room temperature) to 200°C. The time required for the process varies from 2-3 hours to 6-7 days. The crystalline cake which is produced, filtered and washed (and may be ion exchanged to a different cationic form), before being mixed with suitable clay binders. This forms a cage-like structure with rounded uniform micropores, where adsorption occurs inside of the crystal lattice through selective pore filling. These micropores only allow molecules of a certain size, shape and polarity to enter the zeolite structure and it is this mechanism which give zeolites the name of molecular sieves, and so the usual surface area concepts are not applicable. The crystals are dried and fired to the final product giving a high resistance to mechanical attrition.

Different source materials and different manufacturing conditions produce various molecular sieves with pore dimensions ranging from 0.3–1 nm. Commercial zeolites are produced in the form of beads with diameters of 0.5–3 mm, extrudates with diameters of 1–6 mm, granules with mesh sizes of 20x40 to 6x12, and powders. Hydrophilic molecular

sieves have a larger alumina content whilst hydrophobic molecular sieves have a large silica content.

Zeolites also have many applications, such as the removal of water from azeotropes, drying of gases, purification of hydrogen, separation of normal paraffins from naphtha, separation of p-xylene from other xylene isomers, recovery of carbon monoxide from methane and hydrogen, as well as the separation of oxygen from air and for pollution control including the removal of mercury, SO_x and NO_x from gases.

3.3 Adsorbent characteristics

Adsorption works on the basis of molecules physically binding onto active adsorptive sites present on the surface of an adsorbent. The correct choice of adsorbent is crucial for a successful adsorption system. Generally, adsorbents are available in the form of irregular granules, extrudates, pellets and formed spheres with sizes up to 6 mm. The size of the adsorbent reflects the need to introduce as much surface area as possible into a given volume of bed whilst at the same time minimising the pressure drop for flow through the bed. For an adsorbent to be commercially attractive, and to utilise its adsorption capacity to a maximum, it should have the following characteristics (Coulson and Richardson, 1991):

- Pore size distribution: to maximise the surface area, which is proportional to the pore volume and inversely proportional to the pore radius.
- Large enough pore diameter to allow the adsorbate molecules to migrate through the pores to the adsorbing surface but small enough to exclude undesirable molecules from entering the internal structure. This makes the pore size distribution important in determining the effectiveness of the adsorbate.
- Capability of being regenerated easily, efficiently and economically, in comparison to the cost of buying fresh adsorbent for each cycle and having to pay for disposal of the spent adsorbent.
- Mechanically strong to withstand the bulk handling and vibration from any industrial unit, and
- Long life *i.e.* not age rapidly or lose its adsorptive capacity through continual recycling.

These characteristics need to be taken into account when selecting an adsorbent for a given application. The following section describes the properties of adsorbents which need to be made available in the selection process.

3.4 Adsorbent properties

When choosing a suitable adsorbent, users generally look at the porosity and surface area of the adsorbent to define the quality of the solid. However the surface chemistry of the adsorbent is now also recognised as playing an important role in determining the adsorptive properties (Bansal *et al.*, 1988; Rodriguez-Reinoso *et al.*, 1992). The adsorbent properties have a direct effect on the cost and performance of the product as well as on the mode of application. When examining the suitability of an adsorbent, both the chemical and the physical properties need to be considered for each particular system. The following sections briefly describe the significance of these properties in an adsorption process.

3.4.1 Chemical properties

The adsorptive properties of activated carbon (as an example) are determined not only by its porous structure but also by its chemical composition. The chemical properties include the pH, degree of ionisation, the type of functional groups present on the adsorbent, and the extent to which these properties may be changed when in contact with the solution. Each of these properties allows the adsorbent to become application specific. However, for the use of general-purpose adsorbents, the chemical nature of its surface is of much less significance than its physical nature, such as surface area (Cheremisinoff and Moressi, 1978).

3.4.1.1 Functional groups

Many adsorbents, such as macronets, are manufactured for specific functions by the addition of functional groups on the adsorbent surfaces, for example carboxyl, phenolic hydroxyl, quinoline-type carbonyl and lactones, as shown in Figure 3.1.

This provides the means for the formation of chemical interactions between the adsorbate molecules and the surface of the adsorbent, such as ion exchange and hydrogen bonding (chemisorption). The acidic or basic nature of the functional groups gives the adsorbent a surface charge which allows the attraction or repulsion of a charged adsorbate. These interactions are usually irreversible, not allowing the adsorbent to be regenerated. This can either be an advantage or a hindrance to a process, depending on the particular application, the economics of the process, the cost of the adsorbent, and the requirement for regeneration. These surface functional groups can be characterised by several methods, including direct titration, neutralisation, methylation, infrared internal spectrometry and polargraphic methods (Cookson, 1978).

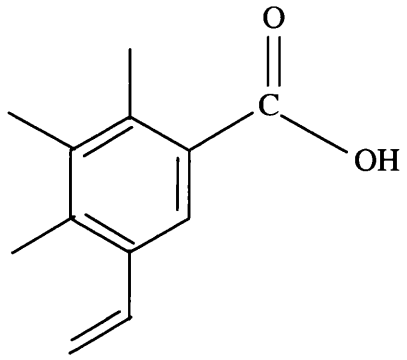

Carboxylic group

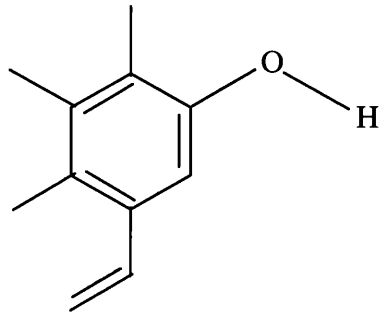

Phenolic hydroxyl group

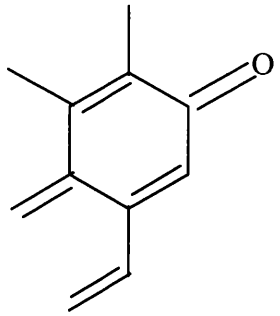

Quinoline-type carbonyl group

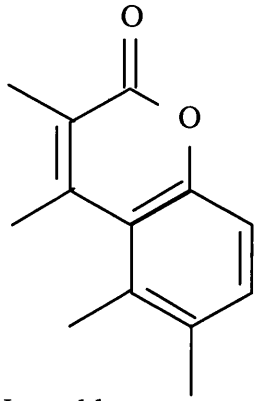

Normal lactone group

Figure 3.1 Oxygen surface functional groups

3.4.1.2 pH

The pH of an adsorbent is determined from the precise nature of the raw materials from which it is manufactured. It is measured from the pH of a water extract obtained under

prescribed conditions and governs the presence of metals and other common compounds in the adsorbent as well as the addition of any functional groups. Generally, acid-washed carbon has a slightly acidic pH ranging from 5 to 7, whilst carbon washed with water has a slightly alkaline pH of 7 to 9. Unwashed carbons may have a higher pH between 9 and 11, depending on the raw material and the activation method used.

The optimal pH of an adsorbent is entirely reliant upon the nature of the solution to be purified and its application after treatment. It may occasionally be necessary to alter the pH of the solution or the adsorbent in order to enhance the adsorption process. To change the pH of an adsorbent pre-treatment (such as acid washing) may be required to remove the residual inorganic salts. However, it is generally easier to alter the pH of the solution rather than the adsorbent, although this introduces an additional impurity which may also require removal from the system or make regeneration of the adsorbent more complicated. Therefore the pre-treatment of the solution or the ability of the adsorbent to change the chemical characteristics of the solution to be treated, can have either beneficial or adverse effects on the adsorption process. This is an important factor if the solution is to be reused, particularly if it is water for human consumption.

3.4.1.3 Polarity

The chemical nature (polarity) of an adsorbent surface varies with adsorbent type and influences the attractive forces between molecules. For example, alkaline surfaces are characteristic of vegetable base carbons and this surface polarity affects adsorption of dyes, colours and unsaturated organic compounds. Non-polar activated carbons make the adsorption of inorganic electrolytes difficult and the adsorption of organic compounds more favourable (Cheremisinoff and Cheremisinoff, 1993).

3.4.1.4 Degree of ionisation

The degree of ionisation of an adsorbent is dependent upon the functional groups present on its surface which in turn accounts for the attraction of certain molecules to the active sites of the adsorbent.

3.4.2 Physical properties

Physical properties of an adsorbent are dependent upon its form, density, internal surface area, pore size and pore distribution. The latter three properties directly affect the adsorption performance by determining the adsorbent capacity available and the molecular sizes of adsorbates to be adsorbed.

As mentioned previously in Section 3.2, for an adsorbent to be commercially attractive it should have a large internal surface area, a pore size distribution, good regeneration capability, long lifetime and it should be mechanically strong. All of these properties are physical, showing their importance alongside chemical properties.

3.4.2.1 Particle geometry

The effective size and shape, the mean particle diameter and the uniformity coefficient define particle geometry. There are two general types of adsorbents: powder (with a particle size of less than 0.18 mm) and granular (including pellets and extrudates). However other special forms do exist, such as monoliths, fibres (from isotropic coal and petroleum pitch), cloths (from viscose rayon) and felts, which are attracting more attention and becoming increasingly useful in many gas phase applications (Rodriguez-Reinoso, 1997). The particle geometry determines the initial head loss or pressure drop and mass transfer characteristics of an adsorption system, (Rousseau, 1987) and is therefore important in the design of a fixed bed adsorber unit. Generally, the pressure drop and the mass transfer rate per unit length of a packed bed is inversely proportional to the particle size to a power ≥ 1. This suggests that if the particle size was to be increased, the pressure drop would decrease, but on the other hand reducing the particle size increases the mass transfer rate. As the pressure drop and mass transfer criteria are not compatible, trade offs must be made in the design criteria.

As well as contributing to mass transfer rates and pressure drops across a bed, the particle size also contributes to the hydraulics, filterability and handling characteristics of a system (Cheremisinoff and Morresi, 1978). Filterability acts on the same basis as sieves or screens, and is determined by the particle size distribution, which defines the fraction of material permitted to pass through to the adsorbent pores or to be retained at the adsorbent

surface. This is a crucial design factor if there are suspended solids or particulates present in the feed solution, but whether it is advantageous or disadvantageous depends on the function of the adsorbent and the purity of the product required.

The mean particle diameter is a calculation of the average particle size based on results of sieve analysis, the effective size is the diameter (mm) of the largest particle and the uniformity coefficient is defined as the ratio of the mean particle to the effective size (Bernardin, 1985).

3.4.2.2 Density

The density of an adsorbent is another significant factor in the design of an adsorption system. Its measurement comes in numerous forms: structure, particle or packing (tamped) density, which may be evaluated as a dry or wet density. However, adsorbent density values are usually reported as a bulk density (ρ_b) or as the weight of dry material per unit bulk volume packed in a column.

McBain distinguishes 4 kinds of densities for porous materials: bulk, apparent, effective and true (cited in Černý, 1970a).

1. Bulk density (ρ_b) is measured as the dry mass (g) per unit volume (ml) of sample. The unit of volume includes the volume of the mass of the adsorbent in air, including pore system and voids between the particles. For the usual kinds of active carbon the bulk density ranges from 380-500gl^{-1} (Černý, 1970a; Jankowska *et al.*, 1991a).

2. Apparent density (otherwise known as the dry particle density or mercury density) (ρ_p), is described as the mass of 1 ml of adsorbent granules, excluding the volume of interstitial space between them. It is measured using mercury as it completely fills the interstitial space under atmospheric pressure (1 atm). However mercury also fills the largest pores of the adsorbent, the width of the pores that will be filled depending on the total pressure of mercury. Therefore to define this density exactly, the pressure under which it is measured should be quoted. With pressures under 1atm, the apparent densities of activated carbon usually range from 0.6 to 0.8 g ml^{-1}.

3. Effective density (otherwise known as the specific gravity, real density or specific density) is determined with a liquid which penetrates into the adsorbent pores. Their varying adsorbability leads to different degrees of compression in the pores and various liquids produce several values for a single adsorbent.

4. True density (otherwise known as the absolute or helium density), is described as the mass of 1 ml of the adsorbent, excluding the volume of the pores. This quantity is measured using helium, which penetrates relatively well even into narrow pores of the adsorbent and for which the absorbability at room temperature is assumed to be very low or negligible. However this assumption is not always justified, and research (Černý, 1970a) has shown that the density of carbonaceous adsorbents determined at room temperature to be higher by 10-15% if a correction is not made for the adsorption of helium and other factors. The true density can also be determined from x-ray diffraction.

Relationships have been formed between the various types of density. For example, ρ_p is related to ρ_b and to the fraction of external voids (ϵ) in a packed bed as follows:

$$\rho_p(1-\epsilon) = \rho_b \qquad 3.1$$

The crystalline density of a solid (ρ_c) is usually quoted in property tables for pure chemical compounds. It is related to ρ_p and to the internal porosity (χ) of particles as:

$$\rho_c(1-\chi) = \rho_p \qquad 3.2$$

Similarly the wet density of an individual particle (ρ_w) is related to these factors and to the liquid density (ρ_f) by:

$$\rho_w = \rho_p + \rho_f\chi \qquad 3.3$$

A less exact relation can be drawn between the pore surface area per unit weight of dry solid (σ) and the mean pore radius (r), such that:

$$\sigma = \frac{A\chi}{\rho_p r} \qquad 3.4$$

where A is a constant which may vary with different types of porous adsorbents, but is often in the order of 3 (Perry and Green, 1984).

Generally, uses of granular activated carbon (GAC) and synthetic adsorbents use the wet (backwashed and drained) density to calculate the quantity needed to fill a certain bed volume, while the dry (apparent) density is used as a specification value and a quick measure of its reactivation performance. Powdered activated carbons (PACs), on the other hand, are often described by the tamped (packed) density.

3.4.2.3 Porosity

Černý (1970a) proposed that an important characteristic of active carbon is the total volume of its pores–the micropores, transitional (meso) pores and macropores. This quantity can best be determined by measuring the true and apparent density of the adsorbent (when its determination from the adsorption isotherm is possible).

The pore structure is a major factor in the adsorption process and activated carbons owe a large portion of their adsorption properties to it. Activated carbon is a processed carbon material with a highly developed porous structure and a large internal surface area. It consists of 87-97% carbon, as well as hydrogen, oxygen, sulphur, nitrogen and various other compounds either originating from raw material used in its production or generated during manufacture (Jankowska *et al.*, 1991a). The porous nature includes the pore shape, pore volume and distribution, as well as the surface area, all of which affect the extent to which molecules can be adsorbed.

Pores in carbonaceous materials are developed during high temperature activation in the presence of oxidising gases, where the spaces between crystallites are cleared from various carbonaceous compounds and unorganised carbon. During this activation process, Dubinin *et al.* (1964) observed two stages: firstly, the formation of macropores from the burn off of the edge groups of the microcrystallite; secondly, the formation of micropores from the burn off of microcrystallite planes.

The most suitable activation process is one that forms the largest number of pores, thereby creating a large total surface area (*i.e.* large internal surface area) and hence a large

adsorptive capacity. The outer (geometric) surface area of the particle is negligible in comparison to its internal surface area. Pores have many shapes and forms, for example ink bottled shape (a contracted entrance), capillaries (open at both ends or one end closed), slits between two planes, v-shaped and tapered (De Boer, 1958; Barrer *et al.*, 1956).

Activated carbon usually has pores belonging to a number of groups, each with a different range of effective radius. Previously there used to be two groups of pore sizes, macro and micropores (Dubinin *et al.*, 1964; Černý, 1970a). However, the International Union of Pure and Applied Chemistry (IUPAC) (1985) and Dubinin (1975) now define three regions of pore sizes, namely, macropores, mesopores and micropores.

1. Macropores are large voids which open directly to the external surface of the adsorbent particle, with a primary function of providing a pathway for the transport of molecules to the internal structure of the particle, although they are not filled by capillary condensation. In the case of carbon, they are formed during activation with oxidising agents. Macropores are typically greater than 50 nm (500 Å), with an effective radius of 500-2000 nm, a volume of 0.2-0.8 ml g^{-1} and a specific surface area of 0.5-2.0 m^2 g^{-1} (Dubinin, 1966; Smišek and Černý, 1970). The specific surface area of macropores is negligible in comparison to the total surface area, which indicates that the macropores do not play any appreciable role in the adsorption process. The exception is the adsorption of large molecules (*e.g.* viruses). Macropores provide a passageway for molecules to access the interior mesopores and micropores (Cheremisinoff and Morresi, 1978).

2. Mesopores (transitional pores) branch off from macropores. They have two main functions: (i) capillary condensation under high-pressure vapours, and (ii) as transportation arteries providing a passage for the adsorbate to get from the macropores to the micropores. They lie between the bulk material defined by the interparticle voids and the microstructure. According to Dubinin's classification, transitional pores are those in which capillary condensation may take place with the formation of the meniscus of the liquid (gas adsorbents do not require mesopores as capillary condensation does not take place in gas adsorption). This phenomenon commonly produces the hysteresis loop on the adsorption isotherm. Monomolecular and polymolecular adsorption occurs on the surface of these various pores. The typical

pore size ranges from 2-50 nm, with an effective radius from 1.5-200 nm and a volume between 0.02-0.50 ml g^{-1}, corresponding to a specific surface area of 20 and 100 m^2 g^{-1}, which does not exceed 5% of the total surface area (Smišek and Černý, 1970; Jankowska *et al.*, 1991a).

3. Micropores are the smallest of the three pore sizes where, according to Dubinin's classification, capillary condensation does not take place. This is because the pores are completely filled at the relative pressure corresponding to the beginning of the hysteresis loop. The micropores are of greatest significance because of their extremely large specific surface area, specific volume and hence adsorptive capacity. In the case of carbon, they are the small, slit shaped spaces between the graphite crystallites generated during the carbonisation process, and only very few lead to the external surface of the particle (Rodriguez-Reinoso, 1997; Smišek and Černý, 1970; Wang and Do, 1999; Guillot *et al.*, 2002; Stoeckli *et al.*, 2001). The micropores are typically developed during carbon activation and result in the large surface areas for adsorption to occur (Cheremisinoff and Morresi, 1978). They have pore sizes comparable with adsorbed molecules with effective radii of <2 nm, pore volumes of 0.15-0.60 ml g^{-1} and a specific area of at least 95% of the total specific area which may have values of more than 1000 m^2 g^{-1} (Wolf, 1958; Smišek and Černý, 1970; Jankowska *et al.*, 1991a). The energy of adsorption in micropores is substantially greater than that for adsorption in mesopores (or at a non-porous surface) causing particularly large increases of adsorption capacity for small equilibrium pressures of adsorbates.

3.4.2.4 Pore size distribution (psd)

Figure 3.2 shows schematically the three pore sizes, where the macropores open out directly to the external surface of the particle, transitional pores (mesopores) branch off from the macropores and likewise the micropores branch off from the mesopores. The micropores are of greatest significance for adsorption due to their very large specific surface area and their large specific volume. The formation of all three pore sizes in an adsorbent is known as a pore size distribution (psd).

The psd is dependant upon the nature of the adsorbent and it determines the size of the molecules that enter the adsorbent particle for adsorption. It is a related property that

indicates the fraction of space within the particle occupied by the macropores, mesopores and micropores. The greater the pore size variation in the adsorbent, the greater its ability to adsorb compounds of various molecular sizes. The pore dimensions correlate with capacity and kinetics, although their relationships are extremely complex.

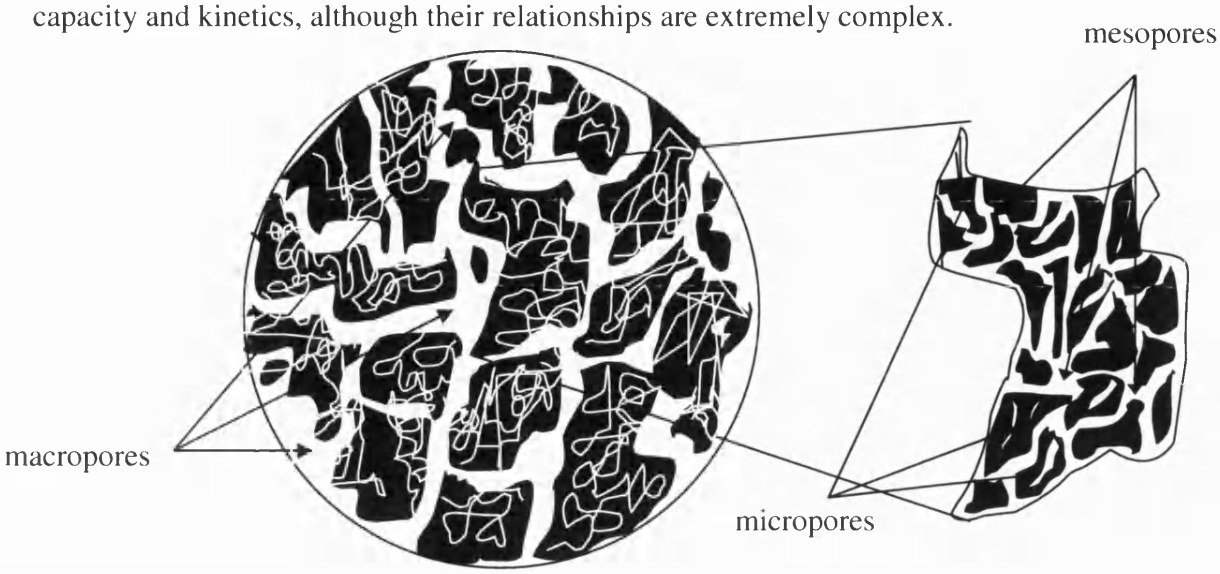

Figure 3.2 Pore arrangement in an adsorbent particle

3.4.2.5 Adsorption capacity

For an economic separation process, an adsorbent with high selectivity, capacity and life is required (Ruthven, 1984; Schork *et al.*, 1993). The adsorbent capacity mainly depends on fluid-phase concentration, temperature and initial conditions of the adsorbent. This adsorptive capacity, otherwise known as the loading, is defined as the quantity of adsorbate adsorbed per unit weight of adsorbent. It is usually the most important of the attributes because it is the key economic factor in the adsorption process as it dictates the amount of adsorbent required and accordingly, the volume of adsorber vessels. It is best determined experimentally (as discussed in Chapter 6) with the given wastewater (Cheremisinoff and Cheremisinoff, 1993) via plots known as isotherms (detailed in Chapter 4), presented at given fixed temperatures (Knaebel, 1995). Adsorption capacity is also expressed by surface area, psd, molasses and iodine numbers.

3.4.2.6 Molasses number

The molasses number was developed for the decolourisation of cane sugar and relates to the adsorption of large molecules. The molasses decolourisation test is specifically

directed towards the use of activated carbon in the sugar and glucose industries and predominantly covers the medium sized pores. This test requires a weighed amount of carbon to be shaken with a molasses solution in a water bath for thirty minutes, and filtered under strictly controlled conditions. The optical transmission is measured and compared with filtrates of a standard carbon treated in the same way. Both transmissions are compared and have to be matched within certain limits by changing the amount of carbon under investigation. The results are expressed as a number of mg giving the same decolourising effect as the standard weight of standard carbon.

3.4.2.7 Iodine number

The adsorption properties of activated carbon are generally estimated by determining the isotherms of adsorption from the liquid phase. For example, iodine adsorption, determines the iodine number. The iodine number (expressed as a measure of the mass (g) of iodine adsorbed per gram of carbon) is a quick, simple test which estimates the specific surface area of activated carbon (*i.e.* the carbon's capacity to adsorb small molecules). It also correlates well with the Brunauer Emmett and Teller (BET) surface area, which is described in detail in Chapter 4 (Rodriguez-Reinoso, 1997). This method requires activated carbon to be boiled in 5% hydrochloric acid (HCl) and then cooled. After cooling, a 0.1 N iodine solution is added to the solution and shaken for 30 seconds. It is then filtered, and the filtrate titrated with 0.1 N sodium thiosulphate solution with starch as an indicator.

Other adsorption tests include methylene blue, phenol and butane adsorption. Another physical property that needs to be considered is the particle's resistance to abrasion, which is a measure of the product's ability to handle attrition.

3.4.2.8 Selectivity

The selectivity is a ratio of an adsorbent's attraction for one component over another, at a given fluid concentration. The ratio generally approaches a constant value as the concentration drops towards zero. In temperature or pressure swing applications the selectivity may be more important than the capacity, due to the fact that the higher the capacity the more difficult the regeneration.

3.4.2.9 Regeneration capability

The reuse of an adsorbent has become an economic necessity in many applications. At present, off-site regeneration is common for activated carbon applications, whilst most other modern adsorption systems regenerate on-site (Knaebel, 1995). Regeneration is essential, especially as it permits adsorbents to operate sequential cycles with uniform performance. The heat of adsorption provides a measure of the energy required for regeneration, the lower the heat of adsorption the easier the regeneration.

There are three methods of regeneration: temperature swing, pressure swing and chemical displacement (or elution). The latter is most common in ion exchange systems, whilst the former two methods are more common with adsorbents. The choice of regeneration method is dependent on the process and its conditions. Chemical and solvent regeneration is commonly used to determine the "working capacity" of an adsorbent. It involves the adsorbent to be washed through with a chemical. This chemical either reacts with or replaces the adsorbate, desorbing it from the active sites of the adsorbent. However thermal regeneration is more favourable than chemical regeneration, even though it is more difficult to perform. This is due to an additional waste product produced by chemical regeneration, which would require disposal or further treatment. Thermal regeneration on the other hand produces a by-product which may be recycled.

Few regeneration methods can be economically operated to 100% efficiency as some capacity is lost on each successive regeneration. The loss of capacity is usually greatest in the first regeneration cycle and then decreases with every consecutive regeneration cycle. Laboratory studies, conducted previously by MAST Carbons Ltd. (1997), using the PRC and a refined effluent have demonstrated both an extremely high capacity for the higher molecular weight organics and more importantly, the ability to regenerate the carbon completely using steam at a maximum of 200°C without any significant loss in capacity.

3.4.2.10 Surface area

The surface area is a fundamental property which is usually related to adsorption capacity. The larger the surface area of the adsorbent, the better it is suited to the removal of organic species from aqueous solutions. However, whilst surface area is the most significant

property of an adsorption process, any interpretation based solely on surface area is incomplete (Cookson, 1978).

Porosity yields the surface area that provides the carbon with the ability to adsorb gases or liquids (Rousseau, 1987). The surface area is contained within the internal pore structure of the adsorbent particles, regardless of particle size, and the total surface area can amount to thousands of square metres per gram of adsorbent. But, it must be noted that there may be a vast difference between the surface area available to a particular adsorbate and the total surface area of the adsorbent. However, from the three porous structures (macro, meso and micro pores) it is the smallest (micro) pores that provide almost all of the surface area, whilst the largest (macro) pores are almost insignificant with regard to the surface area.

Overall, the carbon used in the WOWSEP process was the MAST PRC carbon. This was primarily because MAST Ltd. was a member of the WOWSEP consortium, and one of the objectives of this project was to test their carbons and to examine its advantages over an industrially produced carbon.

4.0 Adsorption Theory

4.1 Adsorption principles

Adsorption is a simple, convenient, low cost treatment process (Chow and David, 1978). It is a surface phenomenon (Knaebel, 1995), which occurs when two phases (liquid/solid or gas/solid) come into contact. This creates an interface between the bulk fluid (gas or liquid) and solid (adsorbent) phases, forming a concentration gradient. This concentration gradient causes a transfer of molecules (adsorbates) from the bulk solution to the interior pores of the solid, where adsorption takes place. The adsorption process involves the 'hopping' of adsorbate molecules along the surface of the adsorbent until they arrive at adsorptive sites to which they bind (adsorb) by forces (*e.g.* van der Waals or dipole-dipole interactions). The adsorption that occurs in the macro and mesopores of the adsorbent surface is generally negligible due to its relatively small surface area. In comparison, the high surface area of the interior micro and sub-micropores of the adsorbent surface makes adsorption in these regions significant.

There are two types of adsorption process: physical and chemical. They differ by the strength of the bonds that attach the adsorbate to the adsorbent. Physical adsorption usually occurs at temperatures under 200°C (*c.*400°F). It operates on the basis of adsorbate molecules being attached to an adsorbent by weak, physical forces such as van der Waals forces. This allows the process to be easily reversed and thus the adsorbent to be regenerated. Chemisorption (chemical adsorption) on the other hand, utilises stronger chemical forces such as hydrogen bonding to bind the adsorbed molecules to the solid surface. In some instances, this may involve the exchange or sharing of electrons or even molecules breaking up into atoms or radicals. Generally, chemisorption is restricted to a single layer of molecules on the surface of the adsorbent, but it may be followed by additional layers of physically adsorbed molecules (Coulson and Richardson, 1991). The stronger chemical bonds are more difficult to break than the weaker physical bonds, making regeneration almost impossible (Cheremisinoff and Cheremisinoff, 1993). However increasing the temperature to above 200°C may provide the activation energy to make or break chemical bonds. Table 4.0 summarises the differences between physical adsorption and chemisorption.

Table 4.0 Differences between Physical Adsorption and Chemisorption

Physical adsorption	Chemisorption
Low heat of adsorption	High heat of adsorption
Less than 2 or 3 times the heat of evaporation	Greater than 2 or 3 times the heat of evaporation
Non specific	Highly specific
Monolayer or multilayer coverage	Monolayer coverage only
No dissociation of adsorbed species	Dissociation of adsorbed species
Significant at relatively low temperatures (<200°C)	Possible over a wide range of temperatures
Fast process	Slow process
Non activated	Activated
Reversible	Generally irreversible
No electron transfer, but polarisation may occur.	Electron transfer leads to bond formation between adsorbate and surface

4.2 Adsorption mechanisms

The transfer of molecules from the bulk solution to the surface of the adsorbent and into its pores is known as the mass transfer of molecules. This mass transfer process consists of three basic steps (Tchobanoglous and Franklin, 1991; Rosene, 1981):

1. External mass transfer (or macrotransport) involves the movement of adsorbate molecules through the bulk phase to the liquid-solid interface by advection and diffusion.
2. Intraparticle (internal) mass transport (or microtransport) involves the diffusion of adsorbate molecules through the macro and mesoporous system, and to the adsorptive sites in the micropore and sub-micropore regions of the adsorbent.
3. Adsorption occurs on the adsorbent surface, mainly in the micropore and submicropore region.

These mechanisms are illustrated in Figure 4.0, where the steps for an adsorbing solute are:

1 = bulk diffusion or fluid mixing

2 = external mass transfer

3 = phase boundary

4 = pore diffusion

5 = solid diffusion

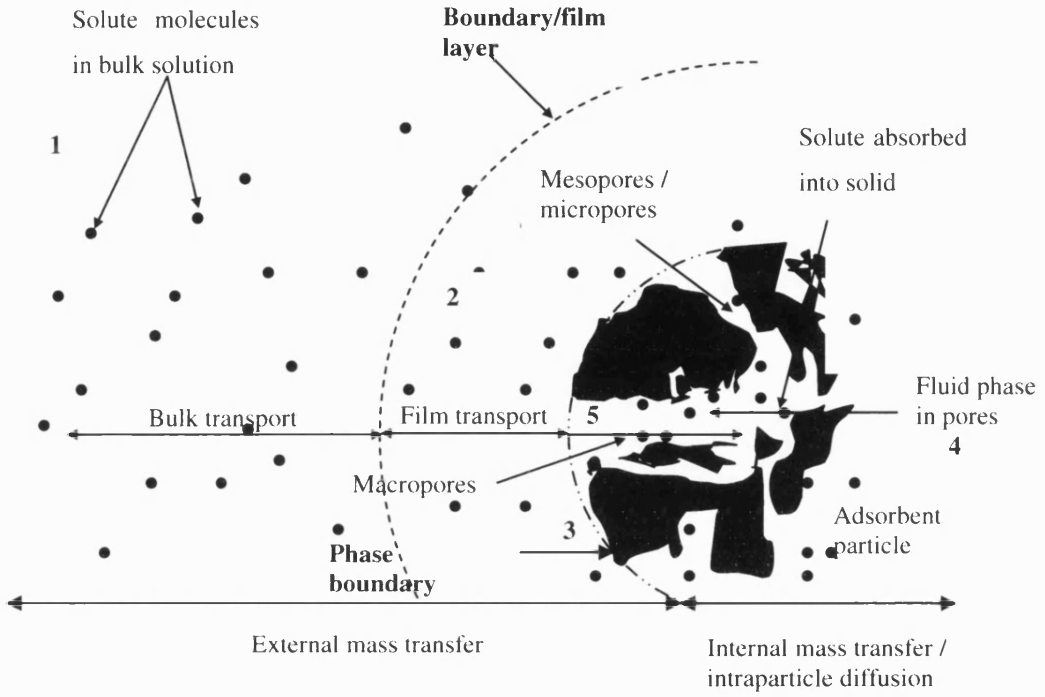

Figure 4.0 Diagram demonstrating the mass transfer mechanisms of solute particles from the bulk solution to the interior of an adsorbent particle

Steps 1 and 2 involve the external transfer of mass while steps 3-5 involve the internal mass transfer (or intraparticle mass transfer). These steps entail the diffusion of molecules from one phase to another. Each step has a different driving force (*e.g.* diffusion, convection) and so gives rise to different mathematical models.

The mechanisms of diffusive transport are based on the assumptions: (i) transport only occurs through the pores, (ii) flux through the solid can be neglected (iii) pores are randomly orientated (giving a longer diffusional path and reducing the concentration gradient in the direction of flow) and (iv) a psd exists (*i.e.* there is a variation in pore diameter) (Ruthven, 1984). Generally, the rate controlling (slowest) step is used in the design of a process, and adjusted for any other contributory resistances.

4.2.1. Bulk diffusion

Bulk diffusion includes the rapid transport of the adsorbate in the bulk fluid, either by mixing, molecular diffusion, or convective flow. Mixing (or lack of mixing) between contacting phases in a packed bed may occur through the existence of a velocity distribution, dead zones or through inefficient mixing. For example, in column operations with low flowrates, breakthrough curves may be broadened by axial dispersion (or molecular diffusion).

4.2.2. External mass transfer (dispersion mechanism)

Figure 4.0 shows external mass transfer to occur between the external surface of an adsorbent particle and the surrounding fluid phase. External mass transfer takes place when the mean free path (*i.e.* average distance travelled between molecular collisions) is small relative to the pore diameter. The resistance to the flow of fluid arises from collisions between diffusing molecules, where the diffusion in liquid filled pores is predominantly the same as in gaseous systems. It involves two mechanisms: (i) bulk (molecular) diffusion, which concerns the transport of the adsorbate in the bulk solution by mixing, and (ii) film diffusion involving the transport of the adsorbate across the boundary layer at the external surface of the particle.

These mechanisms may be affected by the hydrodynamic conditions (fluid mixing) outside the particles. If an adsorbate molecule and adsorbent particle are under static conditions (*i.e.* there is no forced circulation of the fluid phase and the pressure is the same throughout the system), then the external mass transfer takes place by molecular diffusion. This is driven by a concentration difference between the external surface of an adsorbent particle and the surrounding fluid phase. It may also extend across the boundary layer which surrounds each particle. In contrast, under turbulent flow conditions the mass transfer is controlled by convection, which controls the effective thickness of the boundary layer. Convective flow must also be considered in addition to external diffusion when there is a concentration differnce in the system as a result of the forces applied to the fluid phase. Thus, the driving force for bulk diffusion is the concentration gradient across the boundary layer (dc/dt), whilst the degree of mixing determines the extent of the film diffusion.

The rate of mass transfer or diffusional flux, N (g s^{-1}), for the adsorbate is given by the relationship between the concentration in the bulk fluid and at the adsorbent surface:

$$N = k_f A_p (c - c_e) \qquad 4.1$$

where k_f is the external mass transfer coefficient (m s^{-1}), A_p is the external surface area (m^2), c is the fluid phase concentration at time, t (g m^{-3}) and c_e is the fluid phase concentration in equilibrium with the external adsorbent surface (g m^{-3}).

For a batch of fluid, the adsorption rate of mass transfer may be written as:

$$N = -V\left(\frac{dc}{dt}\right) \qquad 4.2$$

where V is the volume (m^3) of the fluid phase. When $t = 0$, $c = c_o$ and $c_e = 0$ (*i.e.* initial conditions), the mass transfer resistance is controlled by the boundary layer of the particle. Therefore by equating Equations 4.1 and 4.2, the value of k_f can be determined:

$$k_f = \frac{-V}{A_p c_0}\left(\frac{dc}{dt}\right)_{t \to 0} \qquad 4.3$$

However k_f may also be estimated from correlations such as the Reynolds Analogy (Equation 4.4) in terms of the Sherwood number (*Sh*), Schmidt number (*Sc*), Reynolds number (*Re*) and the friction factor (*f*). This relationship is only valid for well-agitated vessels, where the concentration of the adsorbate and adsorbent particles in the solution are uniform throughout the vessel, physical properties are constant, there is a very small net bulk flow at the fluid/solid interface, no chemical reactions occur in the fluid, there is no radiant energy interchange and there is no pressure, thermal or forced diffusion.

$$\frac{f}{2} = \frac{Sh}{Sc\,Re} \qquad 4.4$$

Sh, *Sc* and *Re* (dimensionless numbers) are described in terms of D_i (molecular diffusivity of solute i in m^2 s^{-1}), d_p (particle diameter in m), ρ (fluid density in kg m^{-3}), u (fluid

velocity in m s^{-1}), μ (fluid viscosity in kg m^{-1} s^{-1}) and ν (or μ/ρ) (momentum diffusivity of the solute in m^2 s^{-1}), are described by:

$$Sh = \frac{k_f d_p}{D_i} = \frac{2}{3} Re^{\frac{1}{2}} Sc^{\frac{1}{3}} \qquad 4.5$$

$$Sc = \frac{\nu}{D_i} \qquad 4.6$$

$$Re = \frac{\rho u d_p}{\mu} \qquad 4.7$$

4.2.3. Reaction kinetics at phase boundaries (chemisorption only)

The reactions at phase boundaries of porous adsorbents are usually very fast; therefore the rate of adsorption and desorption are often controlled by mass transfer within the pore network (Ruthven, 1984). There are exceptions to this rule, such as in chemisorption and affinity adsorption systems which are used for biological separations, where the kinetics of bond formation can be extremely slow.

4.2.4. Pore diffusion

Intraparticle mass transfer (pore diffusion) concerns the rate at which the adsorbate is transferred from the surface to the interior of the particle. If the pores are sufficiently wide, diffusing molecules escape the attractive force of the adsorbent surface. The adsorbate is then transported by convective flow, bringing the concentration in the pore and the surrounding liquid phase into equilibrium. The driving force for such a diffusion process can be approximated by the difference in mole fraction or concentration of the diffusing species within the pores. However, in narrow pores the frequency of collisions of the molecules with the wall of the pores exceeds the frequency of collisions between molecules, in which case surface diffusion dominates over pore diffusion.

4.2.5. Surface diffusion in the adsorbed phase

Having diffused through the external boundary layer, the molecules then diffuse to the particle interior and subsequently to the adsorptive sites. Here, the molecules either bind to the pore surfaces by weak, physical, non-polar forces (such as van der Waals, London Dispersion and charge-transfer forces), or stronger chemical, polar forces (such as dipole-dipole interactions and hydrogen bonding) and other Lewis acid-base interactions (Fox and Kennedy, 1985). As most adsorbents have a psd, the transportation of the adsorbate molecules inside the particle (intraparticle transport) may be limited by solid diffusion, pore diffusion, or a combination of these mechanisms (Perry and Green, 1984). The micropore diffusional rate involves the adsorption step and is generally considered to be rapid.

Knudsen diffusion occurs in small pores and at low pressures, where the mean free path is greater than the pore diameter. This causes the molecules to collide with the pore walls more frequently than between other diffusing molecules. Therefore the molecules attach and migrate over the adsorbent's surface. This is known as surface diffusion and occurs when there is a direct contribution to the flux from the transport of fluid through the physically adsorbed layer on the surface of the macropore. However, as previously mentioned, the rate of adsorption and desorption in porous adsorbents occurs by molecular diffusion processes, which are generally controlled by mass transfer within the pore network rather than kinetics of sorption at the surface. This suggests that molecular diffusion is normally controlled by particle diffusion rather than film diffusion, and changes in the external environment of the particle do not generally affect the rate controlling mechanisms.

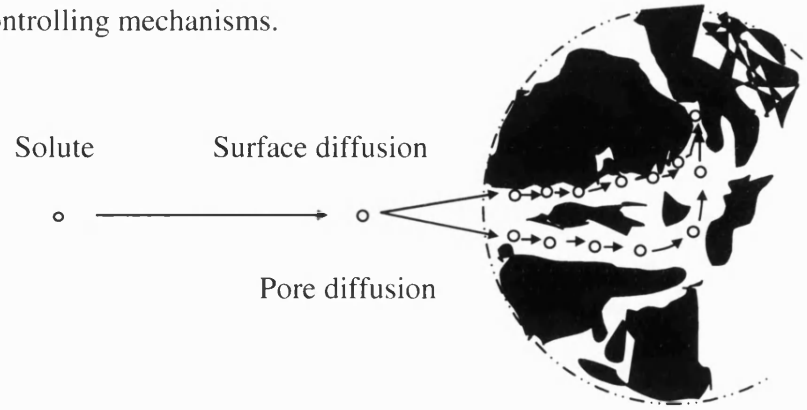

Figure 4.1 Diagram demonstrating the difference between pore diffusion and surface diffusion

Figure 4.1 illustrates the difference between surface and pore diffusion. Surface diffusion occurs if the pores are narrow, and the diffusing molecules are unable to escape the attractive force of the adsorbent surface. Assuming the adsorbent has a homogeneous surface within a uniform structure (which implies that the adsorption sites are energetically identical), the transport of molecules then occurs by an activated process involving 'hopping' between adsorption sites.

Since there is little, if any, bulk flow through the pores, intraparticle transport can be considered as a diffusive process and kinetic data may be correlated in terms of diffusivity as defined by Fick's Law (Ruthven, 1984):

$$J = -D(c)\frac{\partial c}{\partial x} \qquad 4.8$$

where J is the flux (kmol m^{-2} s^{-1}), D is the diffusivity in a cylindrical pore (kmol m^{-1} s^{-1}), which is dependent on concentration but independent of concentration gradient ($\partial c/\partial x$) (m^{-1}).

Making the assumption that transport only occurs through the pores and the flux through the solid can be neglected, the pore diffusivity (D_p) and porosity of adsorbent particles (ε_p) can be included in Ficks Law:

$$J = -\varepsilon_p D_p \frac{\partial c}{\partial x} \qquad 4.9$$

Fick's Law can be used to describe both pore and solid diffusion as long as the driving force is expressed in terms of the appropriate concentrations.

4.3 Isotherms

Adsorption isotherms are relationships between the adsorbent capacity and residual concentration. The capacity of an adsorbent for a particular adsorbate is influenced by the interaction of three properties: (i) the concentration of the adsorbate in the fluid phase (c), (ii) the concentration of the adsorbate in the solid phase (c_s) and (iii) the temperature (T), or

pressure (p) of the system. The isotherms are represented by curves which portray the concentration of the solute on the adsorbent as a function of the feed concentration, at constant temperature and at equilibrium. Equilibrium is achieved when the rate of adsorption equals the rate of desorption. Experimental data have shown the equilibrium distributions to be dependent on the above three properties, and for gas phase systems the concentration (c) is often replaced by the pressure (p). Therefore for liquid systems A (the quantity of the adsorbed substance per unit surface area or mass of the adsorbent) is a function of c and T (*i.e.* A=f(c, T)) and for gaseous systems A=f(p, T) (Černý, 1970b; Jankowska *et al.*, 1991b).

The adsorption equilibrium may be represented in one of three ways. One property is kept constant whilst the other two are plotted in graphical form (Coulson and Richardson, 1991; Černý, 1970b). For liquid phase systems:

1. The commonest practice is to keep T constant and to plot c versus c_s to give an adsorption isotherm ($c=f(c_s)_T$).
2. When c_s is kept constant, the plot of c versus T is known as an adsorption isostere ($c=f(T)_{Cs}$).
3. Keeping c constant, and plotting c_s versus T gives adsorption isobars ($c_s=f(T)_C$). However this is most common for gas phase systems.

Generally, adsorption experiments produce isotherms either based on capacity or on the adsorption rate. This depends on whether the experiments are run to equilibrium or as a function of time. Both sets of data provide information on adsorbent selection and can also be used to predict the amount of adsorbent required or the usage rate for a fixed bed system.

Single component isotherms provide the ability to establish whether the compounds of interest are suitable for adsorption and which compounds are likely to control the cost effectiveness of adsorbent treatment. Multicomponent isotherms establish the least adsorbable contaminant of interest, such that column studies may be used to monitor the breakthrough of only that contaminant (Stenzel, 1993). Therefore, suitable interpretation of equilibrium isotherms can give preliminary information on the viability of treatment, the evaluation of economic feasibility and the requirement of any additional tests.

Factors that can affect adsorption and the shape of the isotherm are:

- Adsorbent preparation – manufacturers often provide instructions on the pre-treatment of adsorbents such as drying, washing or sieving. For example, the rate at which carbon reaches equilibrium is dependent upon particle size (smaller particles reach equilibrium faster). To increase the rate of adsorption and thereby decrease the time necessary to complete the isotherm it is recommended that adsorbents (*e.g.* granular activated carbon) should be pulverised such that 95 wt% will pass through 325 mesh screen (US standard sieve). This is because, in theory, all adsorbents manufactured in the same way to identical shape and size should have a similar porous structure and hence reach the same equilibrium capacity (Schuliger, 1978).
- pH – adsorption from a solution is highly dependent on its pH.
- Temperature – as the temperature increases, the rate of diffusion increases, but the equilibrium capacity of the adsorbent reduces for a given bulk fluid concentration.
- Contact time –the contact time between the adsorbate and the adsorbent should be long enough to allow the system to reach equilibrium.
- Sample filtration – on completion of the adsorption process, the adsorbent must be separated from the remaining adsorbate solution, before analysis.

The characterisation of non-porous materials is relatively straightforward, whereas interpretation of porous solid isotherms is more complicated. Microporosity in adsorption processes is most difficult to describe accurately, whilst mesoporosity is more easily understood and macroporosity behaves as an open surface to adsorption. However, as macropores (within microporous carbons) only account for a maximum of 1% of the adsorption processes they are not as important during the characterisation and calculation of the surface area as micropores (Arnold, 1995).

There are six types of isotherm shown in Figure 4.2 classified by Gregg and Sing (1982). These isotherms were originally designed for gas phase systems, although many of the same principles can also be related to liquid phase systems. The first five isotherms were originally classified by Brunauer *et al.* (1940):

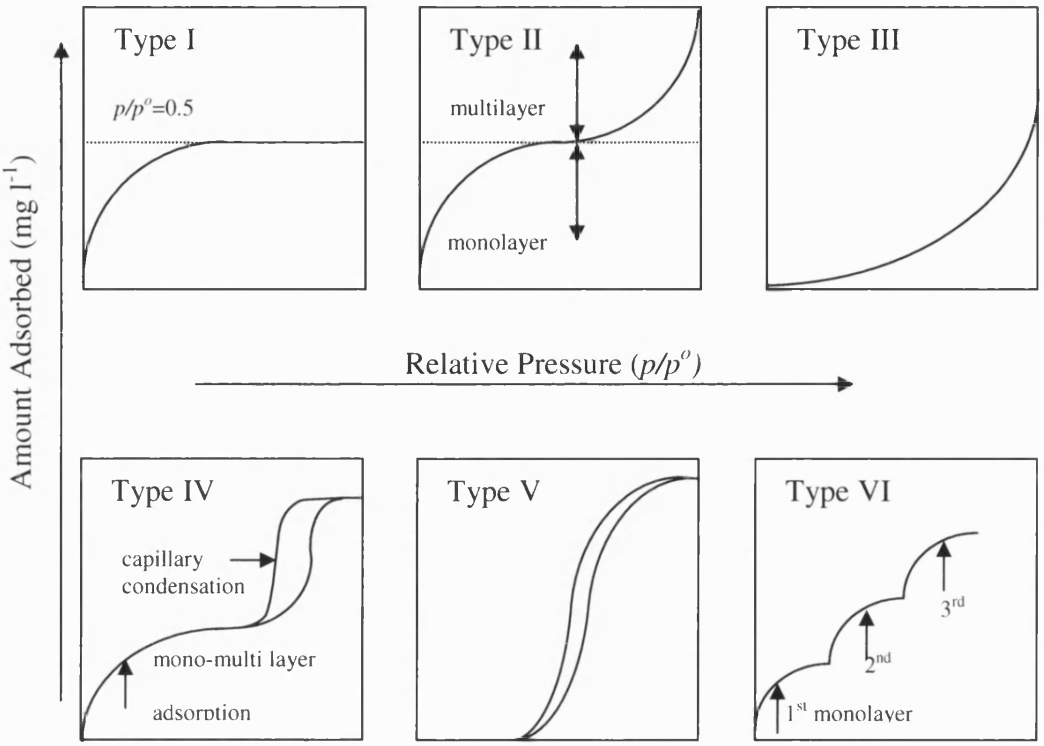

Figure 4.2 Classification of isotherms according to Gregg and Sing (1982)
where the relative pressure is the ratio of the actual pressure (p) and the saturated vapour pressure (p^o) at a given temperature

I. Type I isotherms increase rapidly to a relative pressure of approximately 50% (p/p^o=0.5) and then levels off. The isotherms are reversible and favourable to the uptake of solutes, although the uptake is limited to monolayer coverage only. This is due to adsorption being governed by accessible micropore volume filling at low relative pressures (p/p^o<0.1) rather than the internal surface area. The initial 'knee' at low relative pressures then procedes to a large almost flat plateau. The 'knee' corresponds to a wide micropore size distribution whilst the plateau represents the small contribution from larger porosity (Rodriguez-Reinoso, 1997). The isotherm curve is shown to be concave downwards to the relative pressure axis and adsorption is completed at a relative pressure of approximately 0.5. The loading (amount adsorbed) comes to a limiting value, as the relative pressure approaches 1.0. It is typical of adsorbents such as activated carbon and molecular sieves which have an insignificant small external surface area. Type I isotherms follow the Langmuir Model (Section 4.4.2). Examples are the adsorption of nitrogen at 77K (-196°C), and ammonia at 273K (0°C) onto microporous carbon.

II. Type II isotherms increase to a point at which it begins to level off concave to the relative pressure axis and then begins to increase again at an inflection point convex to the relative pressure axis. Type II isotherms are common, reversible isotherms, typical of non-porous and mixed micro and mesoporous solids. They describe the physical adsorption of gases where the monolayer coverage is succeeded by unrestricted multilayer adsorption at higher p/p^o values. The isotherms may be favourable or unfavourable, as verified by the alternating concave and convex curves. The inflection point indicates the end of the monolayer and the beginning of the multilayer. These isotherms follow the Brunauer Emmett and Teller (BET) model (Section 4.4.3). An example is the adsorption of benzene onto carbon black.

III. Type III isotherms are rare, reversible isotherms, originating from non-porous and microporous solids, which are convex towards the relative pressure axis. They are unfavourable to the uptake of solutes, with characteristics of weak gas-solid (adsorbate-adsorbent) interactions. This causes the uptake at low relative pressures to be small. The heat of adsorption is equal to or smaller than the heat of condensation of the pure adsorbate. These isotherms are most commonly found with the adsorption of water vapour onto pure non-porous carbons.

IV. Type IV isotherms may be favourable or unfavourable. They have a slight knee, which corresponds to micropore filling at low relative pressures (<0.1), although adsorption is significant on the non-microporous surface. Similar to the Type II isotherm the Type IV isotherm then increases slowly with alternating concave and convex curves, relating to monolayer-multilayer adsorption. However, unlike Type II isotherms, Type IV isotherms describe restricted multilayer formation with a hysteresis loop. The hysteresis loop is associated with the mesopores where capillary condensation takes place with limited uptake over a range of high relative pressures and occurs when desorption takes place along a different path from adsorption.

V. Type V isotherms may also be favourable or unfavourable. They originate from certain microporous or mesoporous adsorbents. They are uncommon. They are convex towards the relative pressure axis and have weak adsorbate-adsorbent interactions. An example of a process which follows the Type V isotherm is the adsorption of water onto activated carbon. The sigmoidal shape of the isotherm is characteristic of capillary condensation. However, the functional form of the Langmuir isotherm cannot be used to describe this adsorption equilibrium. It is evident that a fundamentally

different mechanism is at work, in which capillary condensation and adsorption play an interdependent role (Huggahalli and Fair, 1996).

VI. Type VI isotherms are stepwise isotherms, which represent complete formation of successive monomolecular layers. Halsey (1948) proposed stepwise isotherms to arise from extremely homogeneous (*i.e.* all active sites have the same potential energy), non-porous surfaces. Each step height corresponds to the respective monolayer capacity. Examples include the adsorption of argon and krypton on graphitised carbon black at liquid nitrogen temperatures (77K).

4.4 Single component equilibrium models

To effectively characterise the dynamic adsorptive behaviour of any compound from the fluid to the solid adsorbent phase, it is important to have a reasonable description of the equilibrium state in both phases and to understand the mechanism of adsorption better. Unfortunately, a single model is unable to describe all the mechanisms and isotherm shapes. Therefore many theoretical and empirical mathematical models have been developed for porous and non-porous adsorbents to explain the shapes of isotherms. However, these models usually ignore structural features of the adsorbent, except in the most general of ways *e.g.* pore width. Isotherms, on the other hand, incorporate information concerning effective surface areas, psds, micropore volumes *etc.* However, obtaining this information may be difficult, as direct experimental evidence is limited. Consequently, all models are based on assumptions and matched against experimental isotherms. The following sections discuss various models which are commonly used to form isotherms and to calculate surface areas.

Whilst many models have been developed to describe gaseous phase adsorption, not so many describe liquid phase adsorption as it is less understood. In some cases, however, gas phase adsorption models may also be used for the liquid phase. Therefore only the relevant gas phase and liquid phase models have been discussed in the following sections.

4.4.1 Henry's Law

Henry's Law is the simplest form of an adsorption isotherm. It expresses the proportionality between the amount adsorbed relative to the amount of adsorbent, q, with

units $g_{adsorbate}\ g_{adsorbent}^{-1}$ or $g\ g^{-1}$, and the equilibrium concentration, c ($g\ m^{-3}$), (or pressure, p ($N\ m^{-2}$)), of the adsorbate in the liquid or gaseous phase respectively. For example, when an adsorbate, A, is brought into contact with an adsorbent, B, a complex, $A \bullet B$, is produced. At equilibrium this reaction is reversible (Equation 4.10):

$$A+B \leftrightarrow A \bullet B \qquad 4.10$$

During physical adsorption there is no change in molecular state on adsorption (*i.e.* no association or dissociation). Assuming a homogeneous adsorbent surface with low uniform adsorbate concentration, Henry derived an expression to describe the equilibrium:

$$\frac{qf_s}{cf} = K \qquad 4.11$$

where f_s and f are the dimensionless activity coefficients on the adsorbent surface and the concentration of the fluid phase at equilibrium, respectively. K ($m^3\ g^{-1}$) is the equilibrium constant, known as Henry's coefficient, which is a function of temperature, c is the adsorbate concentration in the fluid phase ($g\ m^{-3}$) and q is the loading of the adsorbate onto the adsorbent ($g\ g^{-1}$).

At low c, all molecules are isolated from their neighbouring molecules, and for small values of q ($f=f_s \approx 1$), the concentration of the adsorbed substance in the surface layer in linear form becomes:

$$q = Kc \qquad 4.12$$

This relationship is known as Henry's Law.

Three other common expressions describing the equilibrium phenomenon are the BET, Langmuir and Freundlich equations. These models were developed by empirical observation and describe adsorption capacities in terms of the equilibrium concentration and constants specific to the adsorbate. The BET and Langmuir models were originally developed for gas phase systems. In general, the BET model is used to characterise adsorbents, used in gaseous and aqueous phase systems, through the calculation of their surface areas. The Langmuir model is also often used for liquid phase systems, but

moreover as a comparison to the liquid phase Freundlich model, such that an assessment of the models which best suit a particular system can be made. The theory of these models is explained in the following sections, whilst experimental results of the BET model is discussed in Chapter 5 and the Langmuir and Freundlich models in Chapter 6.

4.4.2 Langmuir model

The Langmuir isotherm is the simplest theoretical model for monolayer adsorption. It was originally developed to represent chemisorption for site-specific adsorption of gaseous systems on non-porous surfaces and was later found to comply with porous surfaces as well. It is a single component isotherm based on dynamic equilibrium. The assumptions which form the basis of this model are that the adsorbed gas behaves ideally in the vapour phase, the adsorbed phase does not extend beyond the first layer (monolayer loading only), the adsorbent surface is homogeneous, there are no interactions between adjacent molecules on the surface and all adsorption is localised (*i.e.* molecules do not migrate over the adsorbent surface).

The model balances the relative rates of uptake (adsorption) and desorption:

$$Rate\ of\ Adsorption = k_a p(1-\theta) \tag{4.13}$$

$$Rate\ of\ Desorption = k_d \theta \tag{4.14}$$

where θ is the fractional coverage of adsorbent by adsorbate, k_a and k_d are equilibrium constants for adsorption and desorption respectively (as functions of temperature), and p is the equilibrium pressure.

At equilibrium, the rate of adsorption equals the rate of desorption. Therefore equating Equations 4.13 and 4.14:

$$k_a p(1-\theta) = k_d \theta \tag{4.15}$$

which in terms of θ and the dimensionless ratio of the adsorption and desorption equilibrium rate constants (b), gives:

$$\theta = \frac{bp}{1+bp} \tag{4.16}$$

$$\text{where } b = \frac{k_a}{k_d} \tag{4.17}$$

b is known as the Langmuir equilibrium constant. It is related to the adsorption energy and the temperature, and it follows the vant Hoff equation:

$$b = b_o \exp^{\left(-\Delta H/RT\right)} \tag{4.18}$$

where b_o is the nature of frequency factor (dimensionless), ΔH is the heat of adsorption (kJ kmol^{-1}), R is the universal gas constant (kJ kmol^{-1} K^{-1}) and T is the temperature (K). The expression in Equation 4.18 shows the value of b to decrease as the temperature increases, verifying adsorption to be an exothermic reaction (*i.e.* $\Delta H<0$).

Replacing the equilibrium pressure, p (N m^{-2}), with concentration at equilibrium, c (g m^{-3}), for liquid phase systems, Equation 4.16 becomes:

$$\theta = \frac{bc}{1+bc} \tag{4.19}$$

The fractional coverage may also be expressed as the ratio of the loading, q, of adsorbate per unit mass of adsorbent at equilibrium (g g^{-1}) against the maximum monolayer loading, q_s (g g^{-1}). Therefore Equation 4.19 becomes:

$$\frac{q}{q_s} = \frac{bc}{1+bc} \tag{4.20}$$

This is a common form of the Langmuir equation, which conveys asymptotic behaviour of the monolayer. At saturation, the concentration (c) approaches infinity and the equilibrium loading (q) approaches the maximum monolayer loading (q_s) and therefore the fractional coverage (θ) approaches unity.

The Langmuir plot is the relationship between the qualities of the adsorbate per unit of adsorbent (loading) against the concentration at equilibrium of the adsorbate in solution. This isotherm is usually Type I classified and provides information on the adsorptive capacity of a particular adsorbent with a particular adsorbate. It also shows the maximum loading of the adsorbent and provides an understanding on the quality of adsorption, the steeper and sharper the isotherm the better the adsorption.

In linear form, Equation 4.20 becomes:

$$\frac{1}{q} = \frac{1}{q_s bc} + \frac{1}{q_s} \qquad 4.21$$

At very low concentrations $bc<1$ Equation 4.20 reduces to:

$$q = q_s bc \qquad 4.22$$

If $q_s b$ is thought of as K (Henry's coefficient) then Equation 4.22 is the equivalent of Henry's Law (Equation 4.12).

4.4.3 Freundlich model

Freundlich isotherms are used as a screening method to determine the feasibility of using an adsorbent in fixed bed adsorbers. The degree of adsorption of organics depends primarily on their molecular weight, molecular structure, density, solution concentration and solubility. Freundlich isotherms provide an estimate of adsorption capacity of GAC for a compound, define the local equilibrium at the surface of GAC and predict the relative breakthrough order of compounds by comparing the adsorption capacity values (Kuennen *et al.*, 1989).

Freundlich proposed an equation for liquid phase adsorption at equilibrium. The model is useful for dilute solutions over small concentration ranges. It is based on the following assumptions:

- that there is no association or dissociation of molecules after they are adsorbed on the surface,
- there is no chemisorption (*i.e.* the process is purely physical with no change in the configuration of the molecules in the adsorbed state),
- the adsorbent surface is heterogeneous (each active site has a different potential energy), and
- each site obeys the Langmuir model.

The Freundlich plot, similar to the Langmuir plot, is a relationship between the loading of the adsorbate per unit mass of adsorbent, q (g g^{-1}), and the concentration of the adsorbate at equilibrium, c (g m^{-3}):

$$q = Kc^{1/n} \qquad 4.23$$

where K (m^3 g^{-1}) and n (n>1; dimensionless) are empirical constants, dependent on the nature of the solid, adsorbate and temperature.

This isotherm represents the exponential distribution of heats of adsorption (Perry and Green, 1984). For low concentrations, the amount adsorbed is proportional to the first power of the concentration (converting Equation 4.23 to Henry's Law (4.12)). At high concentrations the Freundlich isotherm becomes concentration independent. At medium concentrations the proportionality is expressed by the fractional exponent *1/n*. This fractional exponent approaches unity as the concentration decreases and tends to zero as the concentration increases (Jankowska *et al.*, 1991b), whilst the amount adsorbed increases to infinity with increasing concentration. Therefore the Freundlich model is unsatisfactory for high surface coverage (q approaching infinity), and does not reduce to the linear form (Equation 4.24) at low concentrations. At low surface coverage (q approaching zero), the Freundlich model does not approach Henry's Law. Therefore intermediate conditions between the Langmuir and Freundlich assumptions are more realistic.

Linearising Equation 4.23 gives:

$$\ln q = \ln K_f + \frac{1}{n}\ln c \qquad 4.24$$

The Freundlich parameters, *1/n* and K_f are obtained from the logarithmic Freundlich graph. They are the gradient of the line and the point at which it crosses the y axis respectively. The Freundlich constant, *1/n*, is significant of the energy (or intensity) of adsorption which reflects the ease or difficulty of removing that compound, while the Freundlich constant, K_f, is a relative indicator of the adsorbability of the compound or the adsorption capacity (Walter and Weber, 1992; Stenzel, 1993). Hence a high *1/n* value implies a weak interaction of bonds while a high K_f value implies a high adsorbent capacity. The Freundlich relationship is usually used to express the experimental results, analytically, and compare the determined constants to aid selection of an adsorbent.

4.4.4 Brunauer Emmett and Teller (BET) model

The Langmuir model has been shown to give an appropriate representation of a system's behaviour at low concentrations. However, the Langmuir model has been shown to be unsatisfactory near saturation regions where monolayer loading no longer exists and where molecular interactions and the heterogeneity of adsorptive sites become more pronounced. This was discovered by BET (1938), who found that not all adsorption systems obeyed Langmuir's monolayer coverage theory, but many formed multimolecular layers of molecules on the adsorbent's surface. BET developed a model to extract the monolayer capacity and hence the specific surface area (Ruthven, 1984), as well as the increase in uptake at higher relative concentrations (>c/c_s = 0.5). The model extended the Langmuir model to account for multilayer adsorption (Černý, 1970b; Arnold, 1995; Gregg and Sing, 1982).

Therefore the model derived was based on the assumptions that the Langmuir model could be applied to every layer of adsorbed molecules. The molecules in the first layer provide the adsorption sites for the molecules in the second layer and the molecules in the second layer provide sites for the third layer *etc.*, such that only the first layer of adsorbed molecules is in direct contact with the adsorbent and bound by adsorption forces. The second and subsequent layers are not influenced by these forces, but have the same properties as that of the liquid state. The heat of adsorption for the second and further layers is constant and equal to the heat of condensation of the substance adsorbed (*i.e.* the forces acting in the condensation of vapours). The concept of localisation, from

Langmuir's model, is still maintained in all layers and the forces of interaction between the adsorbed molecules are neglected. This produces the expression:

$$\frac{q}{q_s} = \frac{b\left(c/c_s\right)}{\left(1-c/c_s\right)\left(1-c/c_s+b\,c/c_s\right)} \qquad 4.25$$

However, BET recommended that if the number of molecular layers, even at saturation concentrations, is restricted (*e.g.* by pore walls) to a finite number, N, then:

$$\frac{q}{q_s} = \frac{b\left(c/c_s\right)\left[1-(N+1)\left(c/c_s\right)^{N}+N\left(c/c_s\right)^{N+1}\right]}{1-\left(c/c_s\right)\left[1+(b-1)\left(c/c_s\right)-b\left(c/c_s\right)^{N+1}\right]} \qquad 4.26$$

where c is the concentration at equilibrium (g m^{-3}), c_s is the saturation concentration (g m^{-3}), and N is the number of molecular layers; with N=1 for monolayer coverage (Equation 4.26 reduces to 4.20). This equation is typical of a Type II isotherm, which is used to describe unrestricted multilayer formation. However, BET observed that whilst the model was good for physical adsorption, it fails at the most active parts of the surface at relative concentrations (c/c_s) below 0.05 and above 0.35. This suggests the BET model is only valid for $0.05 < c/c_s < 0.35$.

The surface area is a relative term, usually measured by evaluating the monolayer coverage within the surface of an adsorbent by an adsorbate with known density and molecular dimensions. The BET model is principally used to measure the total surface area through the adsorption and desorption of nitrogen under varying pressures at 77K (Chapter 5), rather than for process design (Cheremisinoff and Moressi, 1978). However, the BET model is always criticised, as the measured surface areas are rarely accurate. This is due to the interpretation of data being difficult when applied to complex and disordered adsorbent pore structures, and also because adsorption does not occur in molecular layers but by macropore filling (Gregg and Sing, 1982). Although, if the term "effective surface area" is used, then the values obtained are helpful in indicating adsorption capacity. However, the

BET equation does not describe the process of adsorption in porous adsorbents, but it does provide a means of comparison between materials (Arnold, 1995).

There are many other adsorption models (*e.g.* the Kelvin equation, Polanyi's Potential, Dubinin's, Dubinin-Polyani, Dubinin-Astakov theories, t and α_s plots), which describe adsorption but they mainly refer to the adsorption of the gaseous phase, not the aqueous phase.

4.5 Multicomponent equilibrium models

When two or more adsorbates exist with the possibility of occupying the same adsorption sites (competitive adsorption), isotherm relationships become more complex. The experimental measurements of multicomponent isotherms are extremely time consuming due to the number of variables. Therefore theoretical predictions of multicomponent and binary mixtures from single component adsorption data have become popular. The simple isotherms have been fairly successful in these predictions. However, there is still no method established with universal proven applicability (Ruthven, 1984).

4.5.1 Ideal Adsorbed Solution Theory (IAST)

The IAST model was successfully developed by Myers and Prausnitz in 1965 to predict the adsorption of multicomponent gas mixtures onto activated carbon (Kuennen *et al.*, 1989; Crittenden *et al.*, 1985). Similar to Raoult's Law which describes vapour-liquid equilibrium, the IAST was proposed to describe vapour-solid equilibrium, although more recently, the IAST has been also been used to predict liquid-solid systems using their respective single solute isotherm parameters (Wang and Tien, 1982).

The model considers that the spreading pressure, an intensive property which is the change of surface tension as the result of adsorption, is unchanged as a single solute is mixed with other components in adsorption (*i.e.* the spreading pressure is the same for all species) (Wang and Tien, 1982). The model indicated that by assuming constant temperature, a thermodynamically inert solid phase with the same surface area available to all adsorbates (*i.e.* no steric effects), the Gibbs surface model for adsorption can be applied, the adsorbent's monolayer capacity is different for various molecules and the monolayer

behaves as an ideal solution, then the basic equations in the IAST model can predict the behaviour of the mixture from single component data. This data may be given either in numerical or algebraic form, using Gibbs Theory and Raoult's Law (Noll *et al.*, 1992; Ruthven, 1984).

For example, for a multicomponent (liquid-solid) system, the single solute mass balance for component i is:

$$q_i = \frac{V(c_{oi} - c_i)}{W_s} \qquad 4.28$$

where q_i is the surface loading from component i (g g^{-1}), V is the volume of solution (m^3), W_s is the mass of adsorbent (g) and c_{oi} and c_i are the initial liquid phase concentration and equilibrium liquid phase concentration (g m^{-3}), respectively.

Using Dalton's law (which proposes the sum of all partial pressures to be equal to the total pressure) in a similar manner, the sum of individual loadings, q_i, is defined to be the total surface loading, q_T

$$q_T = \sum_{i=1}^{N} q_i \qquad 4.29$$

and z_i, the mole fraction of component i on the surface of the carbon (dimensionless), is defined by the ratio of the individual loading to the total loading.

$$z_i = \frac{q_i}{q_T} \qquad 4.30$$

Analogous to Raoult's Law (for an ideal gas, the partial pressure is equal to the mole fraction of the constituent, and for an ideal mixture, the partial pressure is related to the concentration in the liquid phase), the single solute liquid concentration (c_i^o, g m^{-3}) is in equilibrium with the single solute surface loading (q_i^o, g g^{-1}), which causes the same spreading pressure or reduction in surface tension in the mixture.

$$c_i = z_i c_i^o \qquad 4.31$$

Rearranging Equation 4.29 and applying Dalton's Law, suggests for a multicomponent system, the total loading is equal to the summation of all the ratios of the individual loadings to the mole fraction for each component. This gives an expression for no area change per mole upon mixing from the single solute isotherms at the spreading pressure of the mixture (π_m).

$$\frac{1}{q_T} = \sum_{i=1}^{N} \frac{z_i}{q_i^o} \qquad 4.32$$

Equating the spreading pressures, π_i^o (N m^{-2}), of the pure component systems to that of the mixture, where at constant temperature and spreading pressure, $\pi_i^o = \pi_j^o = \pi_m$ (subscripts i and j relate to components i and j, respectively).

The integral is evaluated using the single solute isotherm expression, according to the Gibbs equation:

$$\frac{\pi A}{RT} = \int_o^{p_i^o} q^o(p) \frac{dp}{p} \qquad 4.33$$

$$\frac{\pi_m A}{RT} = \int_o^{q_1^o} \frac{d \ln c_1^o}{d \ln q_1^o} dq_1^o = \frac{\pi_1^o A}{RT} = ... = \int_o^{q_N^o} \frac{d \ln c_N^o}{d \ln q_N^o} dq_N^o = \frac{\pi_N^o A}{RT} \qquad 4.34$$

where A is the surface area of the adsorbent (m^2) and the spreading pressure, π, is defined as the difference between the interfacial tension of the pure solvent-solid interface and that of the solution-solid interface at the same temperature (N m^{-2}), T is the system temperature (K) and R is the universal gas constant (kJ kmol^{-1} K^{-1}).

The IAST was originally developed for dilute systems, although the model was later found to give valid predictions even at high concentrations and low temperatures. However for high temperature and high relative concentrations systems, the IAST could not always be applied, and where the results were reasonable, they were generally not quite as good as the non-uniform Polanyi based model (Manes and Greenbank, 1981).

4.5.2 Extended Langmuir model

The Langmuir model (Equation 4.20) has been extended to account for multicomponent systems.

$$\frac{q_1}{q_{s_1}} = \frac{b_1 c_1}{1 + b_1 c_1 + b_2 c_2 + b_3 c_3 + ... + b_j c_j} \quad 4.35$$

$$\frac{q_2}{q_{s_2}} = \frac{b_2 c_2}{1 + b_1 c_1 + b_2 c_2 + b_3 c_3 + ... + b_j c_j} \quad 4.36$$

$$\frac{q_j}{q_{s_j}} = \frac{b_j c_j}{1 + b_1 c_1 + b_2 c_2 + b_3 c_3 + ... + b_j c_j} \quad 4.37$$

where c is the concentration (g m^{-3}), q is the equilibrium loading (g g^{-1}), q_s is the maximum monolayer loading, b is the dimensionless Langmuir equilibrium constant, and each subscript relates to a particular component.

For these relationships to be thermodynamically consistent, it must be assumed that q_{s1} equals q_{s2} *etc.* However, for physical adsorption of a wide variety of molecular sizes such an assumption is unrealistic. Different values of q_s may be utilised if these relationships are regarded as analytical rather than physical, although this causes concentration limitations and any extrapolation must be done with care (Suzuki, 1990).

4.5.3 Langmuir-Freundlich model

Due to the limited success of the Langmuir model (Equation 4.20) in predicting mixture equilibria, several authors have modified the equations by introducing the power law expression of the Freundlich form (Equation 4.23):

$$\frac{q_1}{q_{s_1}} = \frac{b_1 c_1^{n_1}}{1 + b_1 c_1^{n_1} + b_2 c_2^{n_2} + b_3 c_3^{n_3} + ... + b_j c_j^{n_j}} \quad 4.38$$

$$\frac{q_2}{q_{s_2}} = \frac{b_2 c_2^{n_2}}{1 + b_1 c_1^{n_1} + b_2 c_2^{n_2} + b_3 c_3^{n_3} + ... + b_j c_j^{n_j}} \quad 4.39$$

$$\frac{q_j}{q_{s_j}} = \frac{b_j c_j^{n_j}}{1 + b_1 c_1^{n_1} + b_2 c_2^{n_2} + b_3 c_3^{n_3} + \ldots\ldots + b_j c_j^{n_j}} \qquad 4.40$$

These expressions, like the extended Langmuir model, are not thermodynamically consistent on their own, unless $q_1 = q_2$ *etc.* They have been shown to provide a reasonably good empirical correlation of binary equilibrium data for a number of simple gases on molecular sieve adsorbents and are therefore widely used for design purposes. But similar to the extended Langmuir model, the lack of proper theoretical foundation suggests this theory should also be used with caution.

4.5.4 IAST-Freundlich model

Another simple relationship was derived to predict multicomponent adsorption by incorporating the Freundlich model (Equation 4.23) which represents single solute behaviour with the IAST model (Equation 4.34):

$$n_i = \frac{d \ln c_i^o}{d \ln q_i^o} \qquad 4.41$$

Integration of the above Equation (4.41) between i=1 to i=N, and rearrangement gives:

$$n_1 q_1^o = \ldots\ldots = n_N q_N^o \qquad 4.42$$

and substituting Equation 4.42 into Equations 4.30, 4.31 and 4.32, and incorporating the power law of the Freundlich model gives:

$$c_i = \frac{q_i}{\sum_{j=1}^{N} q_j} \left[\frac{\sum_{j=1}^{N} n_j q_j}{n k_i} \right]^{n_i} \qquad 4.43$$

This improved model (Equation 4.43) is known as the Freundlich-IAST model. It has proved to be more efficient with a greater scope of applicability as it incorporates the use of IAST for the estimation of the multicomponent adsorption equilibria data (Wang and

Tien, 1982). It is generally used in mass transfer models, where Freundlich parameters are extended to account for multicomponent mixtures and to take into account competitive interactions at the GAC surface (Kuennen *et al.*, 1989; Crittenden *et al.,* 1985).

4.6 Kinetic models

4.6.1 Homogeneous Surface (Solid) Diffusion Model (HSDM)

The homogeneous surface diffusion model (HSDM) was developed and analysed by several researchers (Weber and Chakravorty, 1974; Mathews and Weber, 1975; Crittenden and Weber, 1978a; Traegner and Suidan, 1989) to describe adsorption onto granular activated carbon (Roy *et al.*, 1992). The model has been coupled with the Freundlich model and the ideal adsorbed solution theory (IAST), for single and multicomponent systems respectively, to include diffusion resistances for liquid and intraparticle (micropore) phases (Crittenden and Hand, 1984). However, in order for this model to be useful, it must be capable of predicting the effluent concentrations of adsorbates in complex mixtures and the impact of process variables on process performance such that the least cost operation can be identified.

The model assumes the adsorbent to be spherical in shape and in a fixed position in the adsorber, *i.e.* the surface concentration depends only on the radial position and plug flow occurs in the adsorbent bed if the mass transfer zone is >30 adsorbent particle diameters. Equilibrium between the liquid and solid phase adsorbate concentrations is assumed to exist only at the outer surface of the adsorbent particle, where subsequent diffusion occurs along the pore surfaces rather than within the pores (Suzuki, 1990). Liquid-phase diffusion resistance also occurs at the external surface and it can be described by a linear concentration gradient, and solid or surface diffusion is the principal intraparticle mass transport mechanism which is independent of concentration. The impact of pore structure and concentration can be simulated with a single effective diffusivity (Lee *et al.*, 1983; Crittenden and Hand, 1983). For desorption, the model assumes complete reversibility with identical mass transfer parameters and in multicomponent systems the adsorbates diffuse independently of one another, such that the interaction of the solutes is fully accounted for by multisolute equilibrium expressions (Crittenden and Hand 1984).

HSDM equations are presented in many publications (Roy *et al.*, 1992 and 1993; Crittenden and Weber, 1978b; Ari *et al.*, 1981). The HSDM was confirmed to be successful in predicting effluent concentration of known solutes in complex mixtures of unknown composition when significant competitive interactions did not occur during the adsorption processes. It was also successful in predicting desorption and displacement of single and bi-solute fixed bed data. The model was not so successful in predicting effluent concentrations of non-specific measures of organic concentrations *e.g.* TOC. However, in the future, suggested improvements in the model may allow the prediction of TOC or known adsorbates in competing mixtures of unknown compositions (Crittenden and Hand, 1984). Therefore the ability for HSDM to predict the impact of process variables on adsorber performance made it useful for the preliminary design of fixed bed adsorbers. For example Lee *et al.* (1983) found the HSDM to be capable of successfully simulating effluent concentration history profiles for commercial humic acid, and Lo and Alok (1996) developed a computer simulation model for GAC adsorption to predict the effluent concentration of synthetic organic chemicals in a multicomponent system, incorporating the IAST and HSDM.

4.6.2 Pore Surface Diffusion Model (PSDM)

The PSDM includes the same mechanisms as HSDM, except pore diffusion is also accounted for, where the adsorbate is assumed to diffuse into a liquid phase within the carbon particle and equilibrate locally along the pore wall (Weber and Chakravorty, 1974). It incorporates intraparticle transport (described by pore and surface diffusion), external mass transfer (described by the linear driving force approximation), local adsorption equilibrium at GAC surface throughout the carbon pore (defined by Freundlich isotherm parameters), multicomponent equilibrium at GAC surface (described by the IAST model) and advection considered to dominate axial transport (Kuennen *et al.*, 1989).

4.7 Ion Exchange Theory

The principles of ion exchange are similar to those of adsorption (especially chemisorption) and chromatography, although it has it own specific applications (Coulson and Richardson, 1991; Slater, 1991; Pharmacia Biotech, 1996). Theoretically all three processes are comparable, but their mechanisms are quite different. As previously

explained adsorption operates on the basis of the strength of attractive forces between the adsorbent and components in the adsorbate. Chromatography, on the other hand, uses high selectivity to separate components of closely similar physical and chemical properties, separation results from differing velocities which occurs due to the variety of distribution coefficients of the components in the mixture between the stationary and mobile phases. Ion exchange, on the other hand, involves the selective transfer of one or more solutes from a fluid phase to a batch of rigid particles, through the replacement of ions in the fluid phase with those in the solid phase. Hence ion exchange is so called as there is an 'exchange' of equivalent numbers of similarly charged ions between a stationary (immobile) phase (which maybe a crystal lattice or gel) and a fluid (mobile) phase surrounding the resin.

It is stated in literature (Aristotle, 330BC) that ion exchange was first discovered when seawater lost salts when percolated through sand, although this process was referred to as adsorption (Moses). In 1850, two English chemists Thompson (Thompson, 1850) and Way (Way, 1850 and Way, 1852) studied the exchange of ammonia ions in fertilisers and calcium ions in soil, using naturally occurring alumino-silicates (Lemberg, 1870). Hence alumino-silicates (now often referred to as zeolites or molecular sieves) were the first ion exchangers to be discovered. However, it was soon found that alumino-silicates become unstable in the presence of mineral acids, so an exchange involving hydrogen ions (H^+) was impossible. Therefore a group of acid resisting exchangers were developed. The first manufactured exchanger was sulphonated coal, after which a synthetic phenol formaldehyde exchanger was developed and then more versatile synthetic cross linked polymers (otherwise known as resins) were developed.

Ion exchange resins can be considered as a homogeneous gel throughout which a network of hydrocarbon chains is distributed. Attached to these chains bound immobile ionic groups, which can be either positively or negatively charged (anionic or cationic, respectively). There are many types of exchange materials with various physical forms *e.g.* beads, membranes, fibres and liquids. These ion exchangers can be used to separate ionic species in various liquids (Arden, 1968 and Helffrich, 1962).

Table 4.1 Mechanism of the Ion Exchange Process in Water Softening Units.

1. Starting conditions (equilibration) 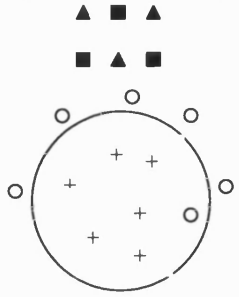	The ion exchange material is brought to equilibrium with a starting buffer, containing counter ions (*e.g.* Cl^- (anions) or Na^+ (cations)), such that the required pH and ionic strength required to bind the desired solute molecules is attained.
2. Adsorption of molecules 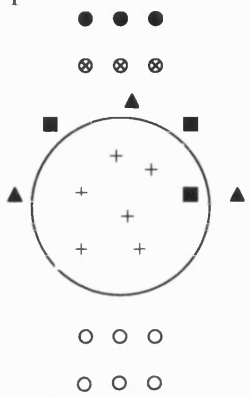	The solution to be purified is introduced to the system. Solute molecules carrying the appropriate charge displace the counter ions and bind on to the resin.
3. Start and end of desorption 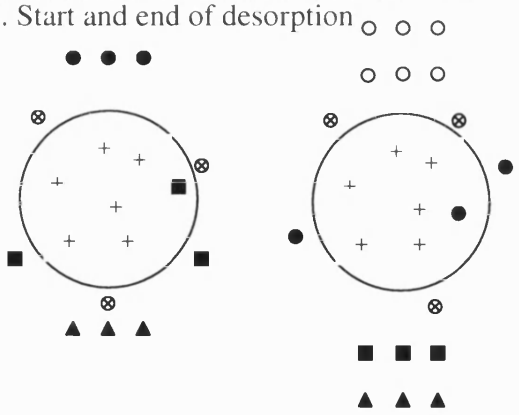	The bound molecules are removed (eluted) from the system, by the addition gradient ions in an eluting buffer. The eluting buffer has a greater ionic strength than (and/or a change in pH) to the solution to be purified. The more weakly bound substances are eluted from the resin first.
4. Regeneration 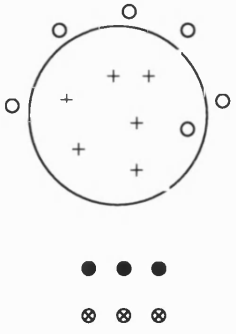	The regeneration of the resin is brought about by the re-introduction of the starting buffer, consequently removing the gradient ions. The system is now re-equilibrated and the starting conditions achieved, ready for the next separation.

Key: o = starting buffer counter ions ■ = substance to be separated

▲ = substance to be separated ⊗ = gradient ion

● = gradient ion

Ion exchange involves the replacement of ions on the resin with ions of the equivalent charge from the solution. Ions with the same polarity (charge) as the framework are known as co-ions, whilst ions of opposite polarity are termed counter ions, and it is only the latter which have the potential to exchange. Negatively and positively charged ions in the mobile fluid phase are called anions and cations, respectively. For example, a cationic exchange resin has incorporated into it immobile anionic (positively) groups bonded to each other through cross linkage. The charges of these fixed anionic groups are balanced by diffusible cationic (negatively charged) groups, which are exchangeable cations (positively charged) from the fluid phase. Overall, positively charged (anionic) exchangers replace negatively charged counter ions (anions) and vice versa.

The bonds that hold the molecules onto the ion exchange resin may be electrostatic bonds, chemical bonds or van der Waals forces. Electrostatic interaction is only significant if the resin has an ionic structure. As with adsorption, the van der Waals forces in ion exchange are weak and can be broken by physical means such as steam stripping, thus enabling adsorbed substances to be removed and the exchanger to be regenerated. Chemical bonding or chemisorption (*e.g.* ion pairing) is much stronger than the electrostatic or van der Waals bonds and is not restricted to surface bonding. The adsorbed substances are then removed by chemical treatment, *i.e.* there is a replacement of ions attached to the resin.

In general, the cationic exchanger is usually regenerated with sulphuric acid (H_2SO_4), whilst the anionic exchanger is usually regenerated with sodium hydroxide (NaOH), (Foust *et al.*, 1960). Table 4.1 briefly explains each step involved in the ion exchange process.

The oldest and most enduring application for ion exchange is for water treatment, the most popular process being water-softening or demineralising (Coulson and Richardson, 1991; Foust *et al.*, 1960; Perry and Green, 1984). This process removes the positive calcium ions from the water and replaces them with sodium ions from a cationic resin. The process is reversible and the resin regenerable through the addition of sodium chloride solution (NaCl), eluting calcium ions from the resin and restoring the resin to its original cationic condition (Equation 4.44). This is known as elution.

$$Ca^{2+} + 2Cl^- + 2Na^+R_c^- \Leftrightarrow 2Na^+ + 2Cl^- + Ca^{2+}(R_c^-)_2 \qquad 4.44$$

where Ca^{2+} = calcium ions Cl^- = chloride ions
Na^+ = sodium ions R_c^- = cationic resin

The ion exchangers used for this treatment process are synthetic resins, consisting of hydrophobic polymer matrices highly substituted with ionic groups and a high capacity for small ions and excellent flow properties. However, the hydrophobicity of the matrix tends to denature labile biological materials (Pharmacia Biotech, 1996). Therefore, the low permeability of these matrices provide a low capacity for large macromolecules (*e.g.* proteins). The first exchangers developed to accommodate biological materials were developed by Peterson and Sober (1956) using cellulose as a base, and as it is a hydrophilic in nature it does not have the tendency to denature biological substances (*e.g.* proteins). However, the disadvantages of these resins are that they have low capacities (at higher capacities the cellulose becomes soluble in water) and due to their irregular shape they also have poor flow properties (Pharmacia Biotech, 1996).

The rate at which ions diffuse between exchanger and liquid is determined by concentration differences between the two phases as well as the necessity of maintaining electroneutrality in both phases. Similar to adsorption, the actual mechanisms for the diffusion of the molecules into the resin particles are similar to that of adsorption:

i. Diffusion of ions from the bulk liquid phase to the surface of the resin.
ii. Diffusion of the ions from the surface of the resin into the resin to the active sites of exchange.
iii. Exchange of the ions at the active site.
iv. Diffusion of the replaced ions from within the resin to its surface.
v. Diffusion of the replaced ions from the resin surface to the bulk liquid.

Any of these steps maybe rate limiting. The actual transfer of the ions (step iii) is best described by a kinetic reaction rate, whereas the other steps are described by the diffusion process. Therefore the equation that maybe used to describe the diffusion steps is the rate equation for counter diffusion (Equation 4.1).

The maximum resin capacity (total ionic capacity) is equal to the total number of exchangeable ions per unit mass of resin (Coulson and Richardson, 1991). However, it is not always easy to determine this as sometimes there may not always be an ion on every molecule *e.g.* for styrene based anion exchangers, there is not always an anionic group on every benzene ring. Therefore if the resin is not completely ionised, the effective capacity (which is less than the maximum capacity) is usually calculated. If equilibrium between the liquid and resin is achieved the capacity is calculated using the contact time and is called the dynamic (available) capacity. As with adsorption the capacity at breakpoint is often quoted as it is until this time that a resin/adsorption bed can be used efficiently, before being regenerated or disposed of. In general, the capacity of the ion exchanger does not relate to its loading, but the actual capacity of each individual component which binds onto the resin. For a porous resin matrix, molecules which are small enough to enter the pores will have a greater dynamic capacity than those molecules which are restricted to the charged substituents on the surface of the resin. Therefore non-porous matrices have considerably lower capacities than porous matrices, but they have a higher efficiency as the diffusion distances are shorter.

In general, the phase equilibrium relationships in ion exchange are similar to those of adsorption isotherms. Equilibrium in ion exchange is dependent upon (Foust *et al*, 1960):

- Temperature
- Degree of ionisation of solvent
- Degree of ionisation of solute
- Degree of ionisation of resin

The experimental conditions which affect the observed capacity are pH, the ionic strength of the buffer, the nature of the counter ion, the flowrate (which is related to the dynamic capacity, such that when the flowrate is increased, the dynamic capacity is decreased) and temperature.

This Chapter has shown that adsorption is most affected by the intraparticle mass transfer of an adsorbate molecule. From all of the single component models and the multicomponent models discussed, the single component BET model will be used in Chapter 5 to characterise the adsorbents and the single component Freundlich and Langmuir models will be compared to examine the equilibrium isotherms (Chapter 6). In this instance, the multicomponent isotherms will not be utilised as the precise components

of the cutting fluid are unknown, making it difficult to identify them. This Chapter has also summarised the basic principles of ion exchange, which was shown to be similar to the adsorption process.

The following Chapter investigates the internal structure of adsorbent materials and discusses the surface area and pore size distributions, particularly of activated carbon, as this was used as the main adsorbent for the WOWSEP process. Ion exchange resins were also studied as they were utilised as an additional purification step to the WOWSEP process.

5.0 Adsorbent Characterisation

In order to investigate adsorption, it is necessary first to characterise the adsorbents. The mass transfer of molecules through pores limits the rate at which an adsorbent can adsorb any species. Therefore the adsorption of molecules from a solution is strongly dependent on the porous nature of the adsorbent, and it owes a large portion of its adsorptive properties to this. Characterisation of an adsorbent involves the examination of its internal and external surfaces and is of great importance to both the producer and user. The complete characterisation of an adsorbent includes a study of its adsorptive, chemical, physical and mechanical properties (Rodriguez-Reinoso, 1997). The two most important characteristics responsible for the adsorptive nature of the material are: the psd (which is a function of the surface area) and the chemical reactivity of the surface (Mattson and Mark, 1971). Hence the first stage in the characterisation of an adsorbent is usually the examination of its internal and external structure (porosity analysis) followed by the determination of its surface area.

5.1 Introduction

5.1.1 Carbon structure

Activated carbon is a microcrystalline, non-graphitic form of carbon where an activation process develops the internal porosity (Rousseau, 1987; Cheremisinoff and Cheremisinoff, 1993). The internal and external surfaces have an extremely complex system. Therefore examination of its surface chemistry requires an understanding of the molecular and crystalline structure. The basic structure of activated carbon is closely approximated to the structure of pure graphite (Figure 5.0). It is composed of fused regular hexagons held approximately 0.335 nm (3.35 Å) apart by weak van der Waal forces. They have an inter-atomic carbon-carbon bond distance of 0.142 nm within each parallel layer (Cookson, 1978; Mattson and Mark, 1971; Bernal, 1924; Černý, 1970a). Each carbon atom has four electrons, three of which form regular covalent bonds with adjacent atoms while the fourth electron vibrates between several covalent bond structures.

Riley (1947) proposed two types of structures for activated carbons. The first consisted of elementary crystallites, which, in two dimensions, is similar to graphite. However it

differed from graphite in the respect that the parallel planes were not perfectly oriented with respect to the perpendicular axis. The planes consisted of irregular microcrystallites, which were a few layers in thickness and less than 10nm in width, with high levels of imperfections. The angular displacement of one layer with respect to the other was found to be random and the layers overlapped one another irregularly. Biscoe and Warren (1942) named this arrangement as a "turbostatic structure" (Figure 5.1). The second type of structure is a disordered, cross-linked space lattice of the carbon hexagons, which resulted from their deflection from the planes of graphitic layers.

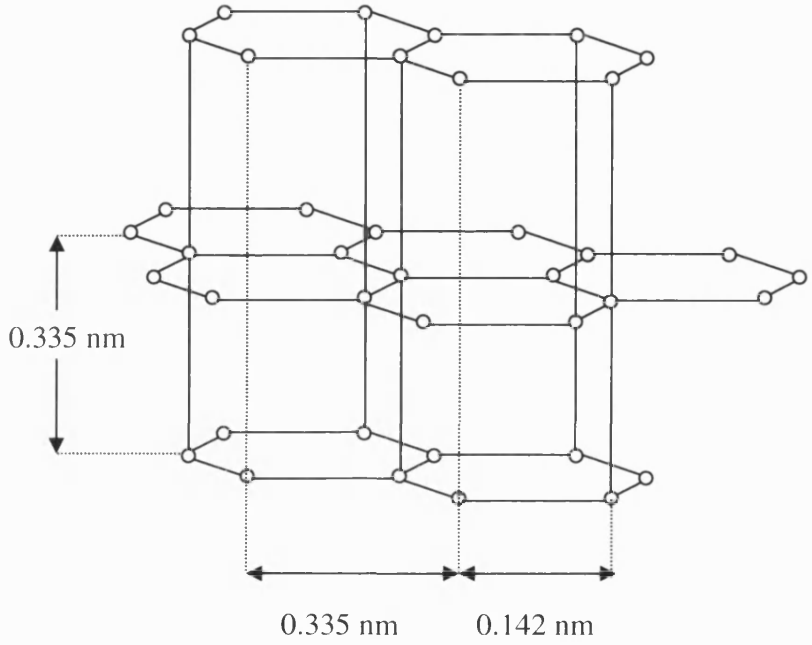

Figure 5.0 Carbon atom arrangement in a graphite crystal

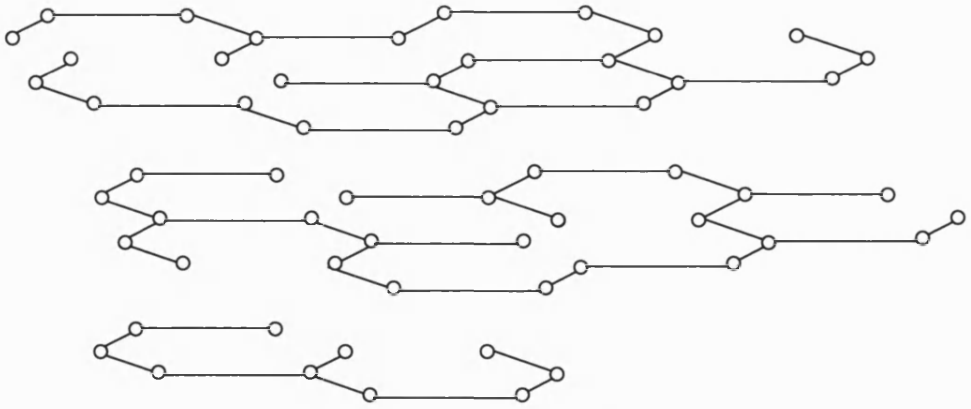

Figure 5.1 Turbostatic structure of carbon

Many x-ray detailed analyses (Riley, 1947; Franklin, 1950 and 1951; and Cookson, 1978) confirmed these structures of carbon. Franklin studied the manufacture of charcoal using

pyrolysis of polyvinylidene chloride (PVDC) at 1000°C. The pyrolysis was shown to contribute significantly to the porous nature of the carbon. It also provided a better understanding of the crystalline structure, with 65% of the carbon in charcoal being arranged in graphitic layers, the remaining 35% being highly disordered.

5.1.2 Porosity

The characterisation of porosity in activated carbon is not a straight forward task since there is not a single technique to provide information on the whole range of pore sizes. The determination of both mesoporosity and macroporosity is well documented, but that of microporosity is subject to many uncertainties.

The macropores and most of the mesopores can be assessed by mercury porosimetry, a simple technique based on the penetration of mercury into the pores under the effect of pressure. However, the use of mercury is not ideal due to its hazardous nature and therefore is no longer popular. As previously mentioned (Section 4.4.5), the mesoporosity of activated carbon can be evaluated by the analysis of the hysteresis loop observed on desorption, following the adsorption of vapours to unit relative pressures.

The adsorption of gases and vapours is a classic and convenient approach to the general characterisation of the microporosity in activated carbons. However, the complex and disorganised structure of the microporosity in activated carbon makes interpretation of porosity data difficult. Other techniques such as immersion calorimetry, electron microscopy *etc.* are complementary to the characterisation of activated carbons and have been gaining momentum during the last few years (Stoeckli, 1990).

5.1.3 Surface area

A critical factor in an adsorption process is the surface area of the adsorbent. The concept of surface area, in the case of activated carbons, should be used with care because the application of any values obtained from the common methods (BET, Langmuir *etc.*) relates to the volume of liquid contained within the micropores as well as the pore walls. Therefore the term apparent or effective surface area should be used (Rodriguez-Reinoso, 1997). However, "surface area" alone does not describe an adsorbent clearly. Adsorbents,

including carbons, with similar effective surface areas can be structurally different and values may vary depending on temperature and adsorbates. Therefore, when quoting surface areas it is important to qualify them by including the technique, adsorbate, and temperature.

The surface area is normally measured by equilibrium adsorption of a gas or vapour under isothermal conditions. Once the adsorption isotherm is obtained it is analysed by an appropriate method (BET or Langmuir) to evaluate the monolayer capacity from which the surface area may be calculated. The BET equation is most commonly used to calculate the surface area, although it is open to criticism on a number of grounds (detailed in Section 4.4.4).

5.2 Adsorbent characterisation methods

This section gives a brief overview of the different methods available for the characterisation of adsorbents. While all of these characterisation methods were not used in this project, a summary of their properties they have been provided in Table 5.0 and their applications discussed for general background.

Many methods (such as direct titration, neutralisation, infrared internal spectrometry and polargraphic methods) have been developed to characterise adsorbents, some chemically (for the presence of functional groups) and others physically (to measure the surface area and pore size). Maximisation of the surface area and control of the surface oxides are of importance in producing an "active" product, although the optimum activation conditions for a given application cannot be predicted without some experimental trial and error (Mattson and Mark, 1971).

The most popular physical characterisation is the calculation of the surface area using nitrogen adsorption at 77K and 1 bar, and the BET model (Bradley *et al.*, 1991; Amarasekera *et al.*, 1995; Lu and Lau, 1995; Guo and Lau, 1999). Bradley *et al.* looked into the physical and chemical characterisation of copper, chromium and silver impregnated activated carbons. They made a comparison of surface area (using the BET method), micropore volume and characteristic energy (using the Dubinin-Radushkevich (D-R) equation), micropore width (using the Stoeckli equation), surface composition and

surface chemistry (using x-ray electrophoton spectroscopy) between the impregnated and non-impregnated carbon.

Table 5.0 Properties and Applications of Various Characterisation Methods

Methods	Properties and applications
Scanning Electron Microscopy (SEM)	• Measures macro and meso pores (pores >5 nm). • Investigates external and internal surfaces. • Carbon gives better resolution than other adsorbents. • Silicalite contains a lot of gas in structure, therefore SEM may be unsuccessful if not degassed prior to characterisation.
Mercury intrusion porosimetry	• Measures macro and mesopores, >3 nm. • Applied in the range of 7.5 nm at 200 MPa to 15 μm at 1.01325×10^5 Pa (atmospheric pressure).
Low field Nuclear Magnetic Resonance (NMR)	• Measures pores >5 nm. • Used to correlate chemical shift to pore sizes in adsorption of xenon onto zeolite NaY using ^{129}Xe probe.
Transmission Electron Microscopy (TEM), High Resolution Transmission Electron Microscopy or Spectroscopy (HRTEM or HRTES)	• Gives higher resolution than SEM. • Shows presence of single shell fullereness and mono-dispersed nano size carbon spheres. • Demonstrates the uniformity and pore structure of hyper cross-linked polymeric foams.
Small Angle X-ray Scattering (SAXS)	• Unsuccessful in distinguishing between pore and micrographites, due to limited technology.
X-ray Diffraction (XRD)	• Data indicates fused hexagonal layered structure dominates for graphite (Cookson, 1978).
Chromatographic methods	• Used to characterise porosity of adsorbent polymers *e.g.* macronet isoporous styrene polymers shown to have a narrow pore size of 0.7 nm.
Thermoporosimetry	• Used for wet porous adsorbents (*e.g.* wet silica gels). • Solidification temperature of liquid produced in pores is dependent on pore width and measured using a scanning differential calorimeter.
Adsorption of nitrogen, carbon dioxide and methane	• Well-established techniques. • Relationship between gases adsorbed and pressure at constant temperature – known as adsorption isotherms. • Adsorption of nitrogen at its boiling point of 77K is most common method for evaluating surface area. However results extremely dependent on model used to derive the distribution.

Characterisation of sewage sludge derived adsorbents, using BET surface area, micropore area and pore size/volume distribution, was investigated for the removal of hydrogen sulphide by Lu and Lau (1995). Whilst Amarasekera *et al.* (1995) studied the adsorption of carbon dioxide adsorption at 273K onto four brown coals, concentrating on the micropore surface areas, psd and pore volumes. As a comparison, BET surface areas were determined for two of the brown coals by nitrogen adsorption at 77K. The surface areas were found to be consistent with published values, indicating it to be a valuable and effective method in characterising the surface areas of carbons.

A study involving the impregnation of potassium hydroxide and sulphuric acid on activated carbon was carried out by Guo and Lua (1999). The study consisted of the effects of impregnation concentrations and soaking times, which were measured by adsorption isotherms, porosity, surface area and psd. A reasonably high BET surface area was found to predominantly originate from microporosity. Chemical characterisation showed that impregnation significantly affected the surface chemistry of the carbon (*i.e.* inorganic component and surface organic functional groups on the carbon surface).

Other methods for the characterisation of adsorbents, besides the adsorption of nitrogen include adsorption of carbon dioxide and methane, using methods such as adsorption potential distributions, Fourier Transform Infra Red (FTIR) spectroscopy, Density Functional Theory (DFT) and Accelerated Surface Area and Porosimetry (ASAP) *etc.*

Aukett *et al.* (1992) also conducted a study of microporous, potassium hydroxide activated carbon. However, they studied the adsorption of methane rather than nitrogen. They produced a molecular simulation of the process which showed the adsorption of methane was due to an enhanced heat of adsorption, brought about by the overlap of the wall forces from opposing pore walls in the microstructure.

Adsorption potential distributions were used to estimate the specific surface area and pore size of microporous carbons by Kruk *et al.* (1999). They revealed two peaks, the first relating to monolayer formation on the micropore surface and the other relating to the micropore filling. The trough between the two peaks was identified as the point of completion of the monolayer. It was this trough that allowed the evaluation of the specific surface area, which was found to be in good agreement with the DFT. The DFT was also

used alongside the Dubinin-Stoeckli (D-S) method, the Subtracting Pore Effect (SPE) and alpha plots by El Merraoui *et al.* (2000) to study the micropore size distribution of pitch based activated carbon fibres. Isotherms were obtained using these methods to determine the psd. The psd obtained from the DFT showed a definite peak at small pore widths (approx. 0.6nm) and a broad peak at larger size micropores. The mean narrow pore widths from the DFT and D-S models were found to be similar, but there was a large difference for the wider pores. The SPE method, on the other hand, found the mean pore widths to be smaller than those obtained by DFT and D-S. A comparison of these methods shows the difference in characterisation of the carbon and hence exaggerates the importance of choosing the correct analysis method.

In 1996, Krupa and Cannon studied the pore structure of granular activated carbon (GAC) using dye adsorption. They looked at the comparison of virgin and reactivated GACs, using nitrogen adsorption and the DFT model and compared these models to the Barrett, Joyner and Halenda (BJH) model. The pore sizes that provided the greatest adsorption capacity correlated well with the dimensions of the adsorbates: small compound adsorption correlated most strongly with micropore volume, whilst the larger dye adsorption correlated most strongly with mesopore and large micropore volumes.

Sweatman and Quirke (2001) compared the characterisation of porous materials using carbon dioxide, nitrogen and methane adsorption at ambient temperatures 25°C (298K) and high pressures. The results revealed more micropore structure for the adsorption of carbon dioxide at 20 bar, than the adsorption of nitrogen and methane at 20 bar (20×10^5 N m^{-2}) and carbon dioxide at 1bar (1×10^5 N m^{-2}). The carbon dioxide psds were so accurate that the adsorption of methane and nitrogen could be predicted with reasonable precision.

A second study by Lu *et al.* (1996) and another by Fenelonov *et al.* (1997) examined the evolution of the surface and pore structure in chemical activation, using accelerated surface area and porosimetry (ASAP). Lu *et al.*'s research studied the surface area development of sewage sludge during pyrolysis, looking at the effects of hold time and temperature, whilst Fenelonov *et al.* (1997) studied the adsorption of nitrogen at 77K. The former study established the surface area to increase with rising temperature and hold time. However, between 550°C and 650°C the surface area was reduced. This was due to the formation of pore enlargements through the loss of volatiles in the intermediate thermoplastic phase.

There was also a reduction in mesopore volume due to sintering at high temperatures and prolonged times. The optimum temperature and hold time were found to be 850°C and 2 hours respectively.

Gomez-Serrano *et al.* (1997) obtained similar results by investigating the characterisation of activated carbon treated with a range of sulphuric acid concentrations. The chemical composition, thermal behaviour and texture was studied using chemical analysis, Fourier Transform Infrared (FTIR) spectroscopy, thermogravimetric analysis, gas adsorption, mercury porosimetry, and density measurements. The mass of the carbon samples increased greatly after contact with the sulphuric acid. The presence of HSO_4^- and SO_4^{2-} ions was detected by FTIR spectroscopy, which provides useful information about structures *e.g.* surface functional groups, and basic spectra of the activated carbon for comparison with spectra of the same carbon containing species (Mattson and Mark, 1971). The mass increase was dependent on the preparation method of the activated carbon samples. During activation (30-800°C), the carbon had a large mass loss at temperatures below 400°C, but as the temperature was increased above 400°C, the mass loss was reduced. The introduction of the sulphuric acid in the activated carbon pores produced a drastic reduction in the surface areas and in the microporosity of the material, which in turn affected the psd in the micro and mesopore ranges.

A comparison on the effect of steam and carbon dioxide activation in the micropore size distribution of activated carbon was investigated by Molina-Sabio *et al.* (1996). The development of the char was examined using immersion microcalorimetery of liquids with different molecular sizes (benzene, 2, 2, dimethylbutane, iso-octane and alpha pinene). The study was carried out with three carbons, two prepared by steam and one by carbon dioxide activation. Burn off ranged from 8-70%. The carbon dioxide activation created microporosity, while the early stages of steam activation widened the micropores. The resulting activated carbons exhibited a lower micropore volume. The different porous structures produced by steam and carbon dioxide activation are related to the oxygen surface groups in the carbon, measured by temperature programmed desorption. The results indicated that carbon dioxide activation created a large number of groups evolving as carbon monoxide, which were thermally more stable than those produced by steam activation.

Strelko *et al.* (2002) also investigated the characterisation of carbon adsorbents with oxidised surfaces. However, they used elemental analysis, electrophoretic mobility measurements and potentiometric titrations to assess the surface reactivity and functional group content of a series of oxidised active carbons. The oxidation of carbon in hot air resulted in a greater proportion of relatively weak acidic surface functional groups, *e.g.* phenolic, in comparison to nitric acid modifications, which produced a greater amount of carboxylic groups. Within the range of the pH values studied, the electrophoretic mobility measurements suggested that the carbon surface was negatively charged. The pH titrations indicated that the surface acidity of the active carbons was stronger than that of a commercial polymeric carboxylic acid ion exchange resin.

Characterisation of carbonaceous materials is not only limited to differences in their crystalline (porous) structure such as microporosity, oxygen content and particle size (Austin and Hedden, 1958 and Steward and Davidson, 1958), but also by other properties, such as helium and mercury densities, magnetic susceptibility and optical properties (Kipling, 1964 and Blayden and Wescott, 1963).

Nuclear Magnetic Resonance (NMR) using ^{129}Xe probe was used by Ito and Fraissard (1987) and Conner *et al.* (1989) to correlate chemical shift with pores size, for the adsorption of Xe onto zeolite NaY and silica, respectively. The chemical shift was shown to increase as the pore size decreased for the zeolite, while the opposite was shown for the silica. Glaves *et al.* (1988) suggested the application of low field NMR spin lattice relaxation for pores greater than 5 nm (macropores). However, some microporosity was observed during an investigation of the formation and development of the structure in the polymerisation of ethylene using NMR by Ferreo *et al.* (1992). On the whole, it is extremely difficult to extract information from the resulting infrared Electron Spin Resonance (ESR) and NMR spectra, due to the heterogeneous surface of carbon, the metal like optical constants and other difficult to handle physical properties of these materials.

Chromatography is a method used to characterise adsorbent polymers. There are many chromatographic methods available, for example inverse steric exclusion chromatography, and gel permeation chromatography. Jerebek and Setinek (1989) used inverse steric exclusion to characterise swollen polymers, while Tysurupa and Davankov (1980) used gel permeation chromatography to characterisation macronet isoporous styrene polymers.

Quinson *et al.* (1986) used thermoporosimetry to evaluate the psd of wet porous adsorbents (*e.g.* silica gel).

A study by Jankowska (1991a) used Small Angle X-ray Scattering (SAXS) method for the characterisation of activated carbon. This was first attempted in the 1940s and had a qualitative character. The scattering of x-rays at small angles (10^{-4}–10^{-1} rad), occurs in media with electron density differences, which varies between 1-100 nm. In the case of adsorbents, such as activated carbons, pores inside the solid phase may constitute such scattering centres. Analysis of the curves describing the dependence of the scattering intensity (I) on the angle (φ) provides information on the magnitude and in many cases also on the shape of the inhomogeneities of the solid. In the 1950s, the following equation was developed for describing the intensity distribution of x-ray scattering

$$I_\varphi = I_e N n^2 \exp - \frac{4\pi R \varphi^2}{3\lambda^2} \qquad 5.1$$

where I_φ is the intensity of scattering at angle φ, I_e is the intensity of scattering for one electron, λ is the wavelength of the x-ray radiation, N and n are the number of inhomogenities in the solid scattering the x-rays and the number of electrons in each of them, respectively, and R is the inertia radius, characterising the mean numerical dimensions of the inhomogeneity.

SAXS was also applied to carbon by Fugiwara *et al.* (1991), and to Styrosorb polymers by Davankov and Tsyurupa (1980) but both with little success. Fugiwara *et al.* found it difficult to distinguish the pore and micrographites with the present technology, while Davankov and Tsyurupa found inconclusive information on the microporous nature of the adsorbents.

Another study by Jankowska (1991b) used electron microscopy to characterise the porous structure of activated carbon. This is a straightforward method. Its main advantage over other methods such as adsorption is its ability to determine the shape and size of the pores (especially mesopores) directly, as well as being able to observe the external surface of the adsorbent. The information obtained may also conform differential curves of pore volume distributions according to radii, this is often in good agreement with results obtained from

adsorption tests or mercury porosimetry. However, electron microscopy also has its drawbacks: its measurements are limited to pores greater than 5 nm, *i.e.* mesopores and macropores, a wide psd produces unreliable results, and the preparation methods are lengthy and complicated. It is therefore important not to use electron microscopy on its own, but as a complementary method alongside methods such as adsorption and porosimetric tests.

There are many forms of electron microscopy: Scanning Electron Microscopy (SEM), Transmission Electron Microscopy (TEM), High Resolution Electron Microscopy (HRTEM) and Controlled Atmosphere Transmission Electron Microscopy (CATEM). Carrot *et al.* (2001) examined Activated Carbon Fibres (ACF) using SEM alongside XRD and low temperature nitrogen adsorption. TEM gives a higher resolution than SEM. Steckle *et al.* (1996) used TEM to show the uniformity and pore structure of hypercrosslinked polymeric foams, while Wang and Kang (1997) showed the presence of single shell fullereness in monodispersed nano size carbon spheres. HRTEM is even better than TEM as it gives a higher resolution (Oshida *et al.* 1995; Endo *et al.*, 1995; Innes *et al.*, 1989). Buglass *et al.* (1990) used a combination of HRTEM and CATEM to characterise reduced and passivated states of a series of carbon supported ruthenium catalysts. CATEM allowed the microstructural and chemical developments to be followed unambiguously, therefore proving to be a valuable technique for the study of catalyst reduction.

Steriotis *et al.* (1997) studied the structure of an asymmetric tubular carbon membrane, where the analysis of samples was carried out using SEM and nitrogen adsorption small angle neutron scattering.

Characterisation and calculations of psd for activated carbon were conducted by Kruk *et al.* (1999); Guillot *et al.* (2002); Stoeckli *et al.* (2001); Davies *et al.* (1999), who all assumed the geometry of micropores to be slit shaped. Kruk *et al.* used the specific surface areas to calculate the average micropore sizes. They discovered the average micropore size increased the normalised adsorption as the low relative pressures ($<10^{-3}$) gradually decreased. For larger micropore samples, the surface area became increasingly similar to the normalised adsorption on a macroporous non-graphitised carbon. Gradual development of the secondary micropore filling was also seen. Model isotherms were created by Guillot *et al.* from computer simulations to assess the psd on the basis of

experimental isotherms, while Stoeckli *et al.* investigated the characterisation of micropores in activated carbons using the D-R equation. They used different techniques to derive psd and average pore widths *e.g.* molecular probes adsorbed from the vapour and liquid phases and analysis of adsorption data from computer simulations. The presence of constrictions was confirmed by determining the enthalpy of immersion into liquids with critical diameters of 0.6-0.9 nm. Davies *et al.* (1999), on the other hand calculated the psd of activated carbons from given experimental adsorption isotherms. They discovered the psd to be relevant to the development of the pore network models in the internal structure of activated carbons and other amorphous adsorbents. The difficulty of determining suitable methods for the calculation of reliable, stable and representative psd arose when they attempted to fit the psd to previously produced data.

Overall this section has provided a background to adsorbent characterisation. Many methods (physical and chemical) have been discussed along with their properties and applications, a summary of which was shown in Table 5.0. However, chemical characterisation was not as important in this study as many of the adsorbents used were specifically developed for the adsorption of organics. Therefore the remainder of this Chapter concentrates on the physical characterisation of adsorbents, mainly looking at their porosity and surface area; using SEM, ASAP and the BET evaluation.

5.3 Scanning Electron Microscopy (SEM)

5.3.1 Experimental procedure

A sample of adsorbent was adhered onto an aluminium plate using double sided sticky tape and spluttered with gold for approximately 4 minutes. The adsorbent was then examined under a JSM T330 SEM at an accelerating voltage of 15 kV and a high transmission (HT) current. Appropriate photographic images of the adsorbents were taken at various magnifications. The adsorbents studied were:

- MAST carbons
  - E15-35-C (Figures 5.2-5.6)
  - E15-40-C (Figures 5.7-5.10)
  - E15-50-C (Figures 5.11-5.14)

- E-1-0-C (Figures 5.26-5.28)

➢ Sutcliffe Speakman (SS) carbon
  - 208EA (Figures 5.15-5.20)
  - 607C (Figures 5.21-5.25)

➢ Purolite C150H (Figures 5.29-5.31)

➢ Amberlite XAD-4 (Figures 5.32-5.34)

➢ Silicalite (Figures 5.35-5.37)

Even though the WOWSEP process is a liquid phase system, some of the adsorbents studied were manufactured for use in gas phase systems. Whilst it seems unusual to use gas phase adsorbents for a liquid phase system, as previously discussed, the exact nature of the components present in the cutting fluid were unknown. However, it was known that the cutting fluid was a complex mixture of components. Liquid phase adsorbents are generally thought of to have smaller pores than gas phase adsorbents and with the cutting fluid mixture more than likely to have large complex molecules, it was deemed necessary to characterise, try and test the adsorption capability of the gas and liquid phase carbons in this project.

The MAST carbon samples vary in their activation levels. E-15-35-C, E-15-40-C and E-15-50-C are gas phase carbons with activation levels of 35%, 40% and 50% respectively. MAST E-1-0-C, on the other hand, is a carbon manufactured for liquid phase adsorption. 208EA and 607C are carbons manufactured on a large scale by Sutcliffe Speakman (SS) for liquid and gas phase adsorption, respectively. Purolite C150H and Amberlite XAD-4 are ion exchange resins. Purolite C150H is a macroporous, strong acidic polystyrene resin with excellent resistance to attrition and osmotic shock. It is usually used for treatment of condensates, continuous processes and special applications *e.g.* galvanic plating, sugar. Rohm and Haas manufactures Amberlite XAD-4 as a commercial, porous, polystyrene, polymeric resin, which is mainly used for the clean up of wastewater streams *e.g.* phenolic streams, and Silicalite is a form of zeolite (described in Chapter 3). All of these samples were analysed on the SEM by Ms. A O'Reilly, a senior technician in the Department of Chemical Engineering at the University of Bath.

5.3.2 Results and discussions

The following scanning electron micrographs (Figures 5.2 – Figure 5.37) either show an overview, external or internal surface image of the adsorbent samples, at various magnifications, as summarised in Table 5.1.

The overview micrographs for MAST carbons E-15-35-C (Figures 5.2 and 5.3), E-15-40-C (Figure 5.7) and E-15-50-C (Figure 5.11) show all three activated carbons to be cylindrical in shape. Figures 5.4, 5.8, 5.12 and 5.13 present the external surfaces, whilst Figures 5.5 and 5.6, 5.9 and 5.10, and 5.14 show the internal surfaces at various magnifications, of the same respective MAST carbons. Figures 5.5, 5.9 and 5.12 show internal and external surfaces of the carbon granules at a magnification of x200. As can be seen, there is uniformity between both the internal and external surfaces where both the surfaces are showing a sponge-like structure throughout the carbon particles with a very similar disarray of pores. The even higher magnification micrographs (Figures 5.4 and 5.6, 5.8 and 5.10, 5.13 and 5.14) show the pores in the carbon particles to be irregularly shaped. All the pores shown are greater than 50nm in diameter, hence they are all macroporous in size.

The overview micrographs (Figures 5.15 and 5.21) show the SS carbons 208EA and 607C, respectively, to be asymmetrical granular particles. The external surface of 208EA (Figures 5.16, 5.17 and 5.18) reveals the carbon to have uniform layers of graphitic sheets with voids between each sheet as described by the work of Riley 1947; Franklin, 1950 and 1951; and Cookson, 1978 (detailed in Section 5.1.1). Likewise the micrographs presenting the cross sectional area (Figure 5.21) and external surfaces of SS 607C carbon (Figures 5.22 and 5.23) also suggest it is comprised of layered graphitic material. However, Figure 5.22 presents a more 'fingerprint' disorganised layered structure, in contrast to the organised layers of SS 208EA (Figure 5.16). These layered sheets suggest more organised 'slit-like' micropores are present in their structure (as mentioned in Section 5.2), although this cannot be confirmed as SEM does not give a high enough resolution to characterise micropores.

Table 5.1 Summary of Scanning Electron Micrographs

Figure	Adsorbent	Description	Magnification (x)
5.2	MAST E-15-35-C	Overview	35
5.3	MAST E-15-35-C	Overview	35
5.4	MAST E-15-35-C	External surface	2000
5.5	MAST E-15-35-C	Internal surface	200
5.6	MAST E-15-35-C	Internal surface	1000
5.7	MAST E-15-40-C	Overview	35
5.8	MAST E-15-40-C	External surface	2000
5.9	MAST E-15-40-C	Internal surface	200
5.10	MAST E-15-40-C	Internal surface	15,000
5.11	MAST E-15-50-C	Overview	35
5.12	MAST E-15-50-C	External surface	200
5.13	MAST E-15-50-C	External surface	1500
5.14	MAST E-15-50-C	Internal surface	1000
5.15	Sutcliffe Speakman 208EA	Overview	35
5.16	Sutcliffe Speakman 208EA	External surface	200
5.17	Sutcliffe Speakman 208EA	External surface	3500
5.18	Sutcliffe Speakman 208EA	External surface	2000
5.19	Sutcliffe Speakman 208EA	Internal surface	75
5.20	Sutcliffe Speakman 208EA	Internal surface	500
5.21	Sutcliffe Speakman 607C	Overview	75
5.22	Sutcliffe Speakman 607C	External surface	200
5.23	Sutcliffe Speakman 607C	External surface	3500
5.24	Sutcliffe Speakman 607C	Internal surface	500
5.25	Sutcliffe Speakman 607C	Internal surface	2000
5.26	MAST E-1-0-C	Overview	35
5.27	MAST E-1-0-C	External surface	3500
5.28	MAST E-1-0-C	Internal surface	5000
5.29	Purolite C150H	Overview	35
5.30	Purolite C150H	External surface	3000
5.31	Purolite C150H	Internal surface	5000
5.32	Amberlite XAD-4	Overview	35
5.33	Amberlite XAD-4	External surface	3500
5.34	Amberlite XAD-4	Internal surface	5000
5.35	Silicalite	Overview	35
5.36	Silicalite	External surface	1000
5.37	Silicalite	Internal surface	5000

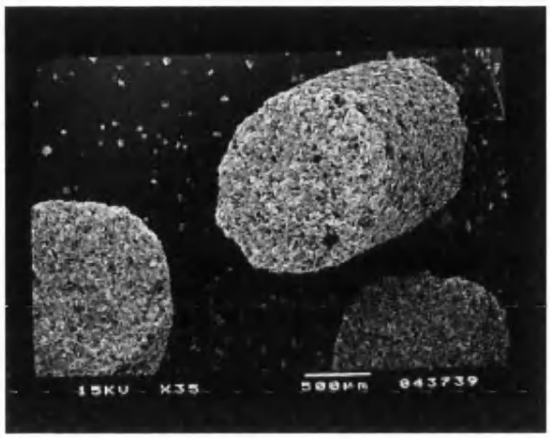

Figure 5.2 E-15-35-C Overview

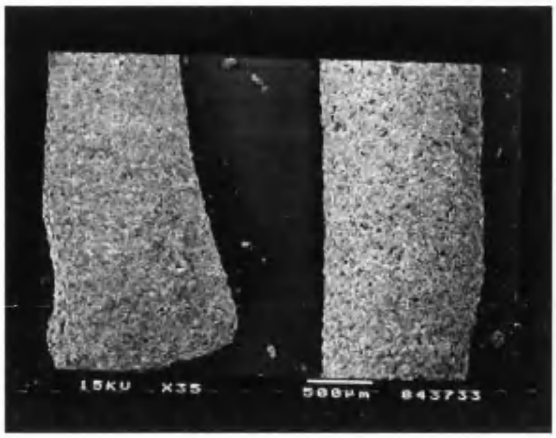

Figure 5.3 E-15-35-C Overview

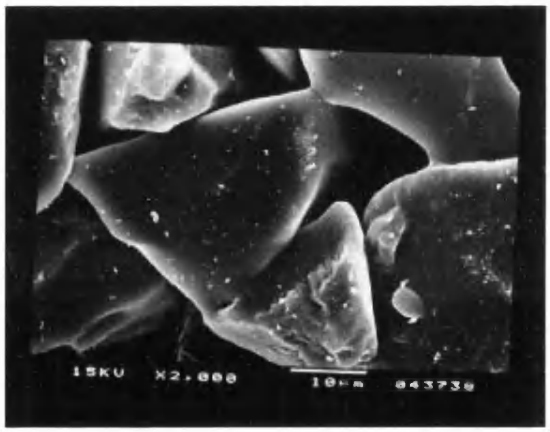

Figure 5.4 E-15-35-C External surface

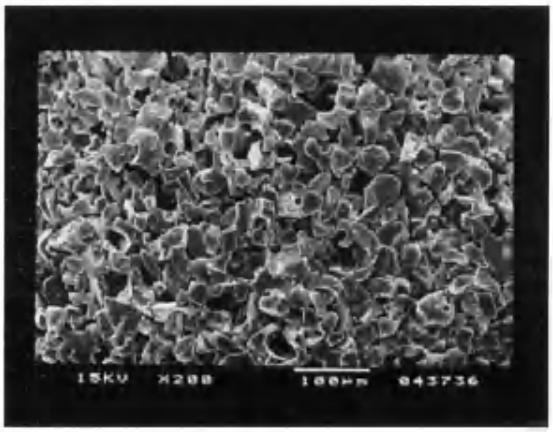

Figure 5.5 E-15-35-C Internal surface

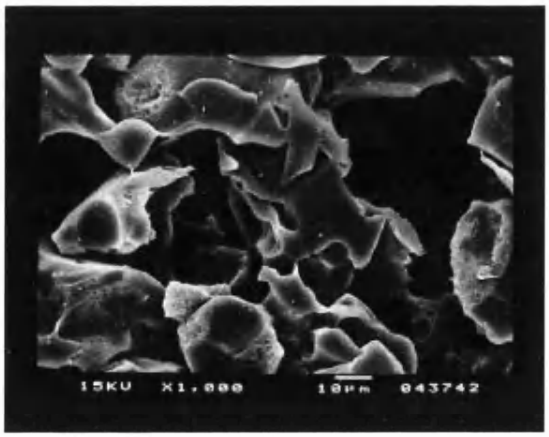

Figure 5.6 E-15-35-C Internal surface

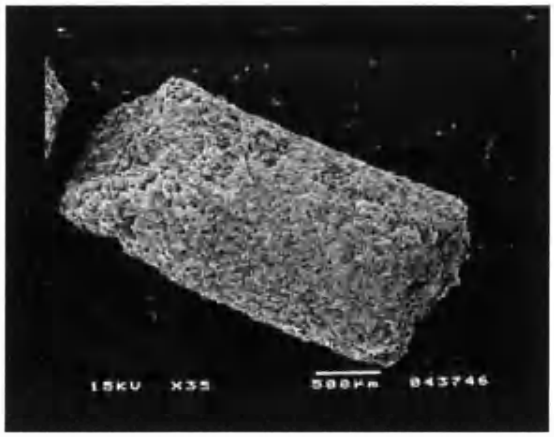

Figure 5.7 E-15-40-C Overview

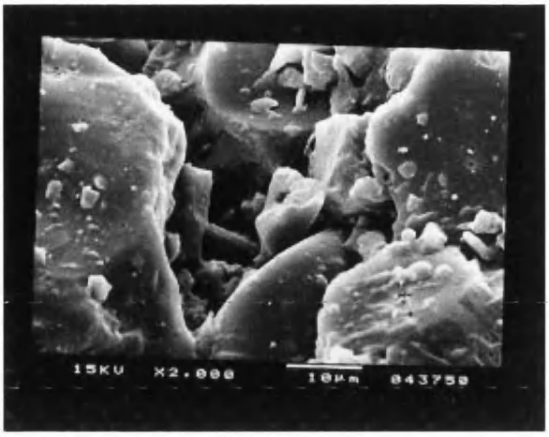

Figure 5.8 E-15-40-C External surface

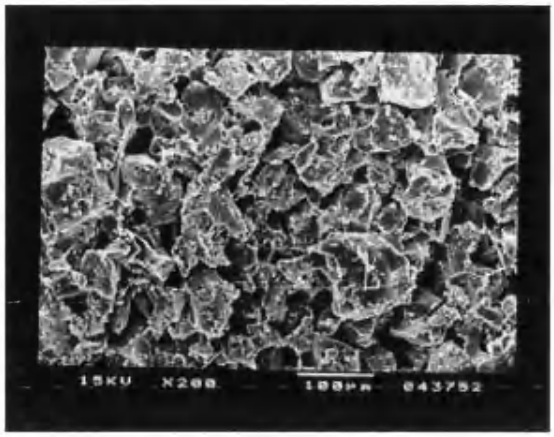

Figure 5.9 E-15-40-C Internal surface

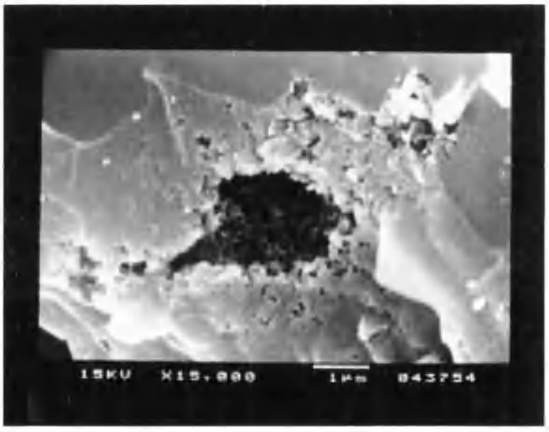

Figure 5.10 E-15-40-C Internal surface

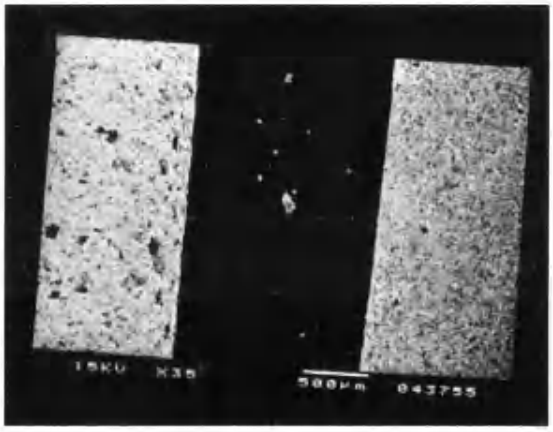

Figure 5.11 E-15-50-C Overview

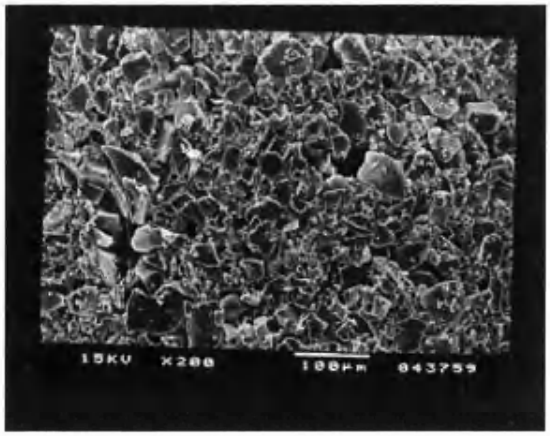

Figure 5.12 E-15-50-C External surface

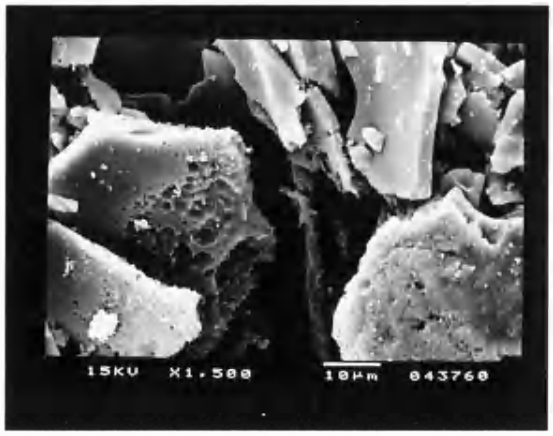

Figure 5.13 E-15-50-C External surface

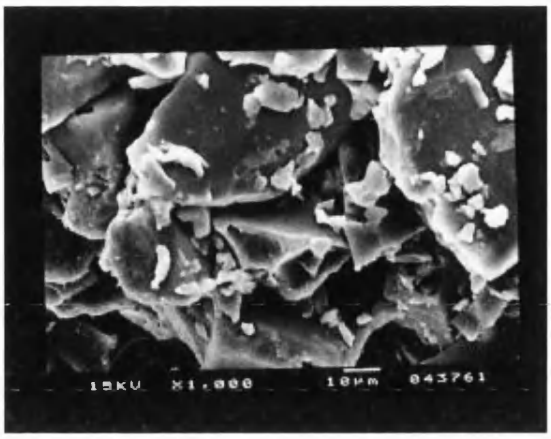

Figure 5.14 E-15-50-C Internal surface

Figure 5.15 SS 208EA Overview

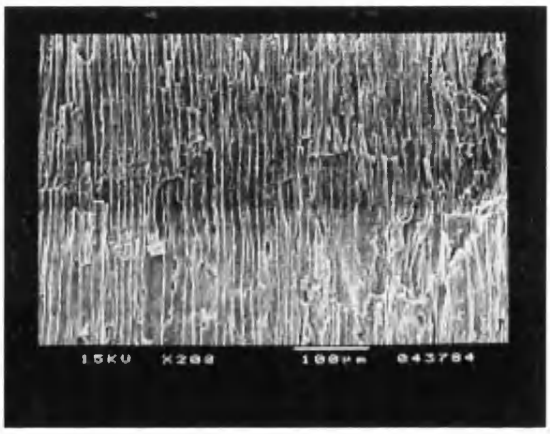

Figure 5.16 SS 208EA External surface

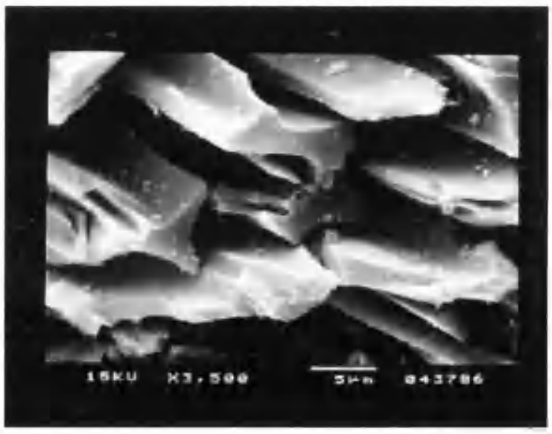

Figure 5.17 SS 208EA External surface

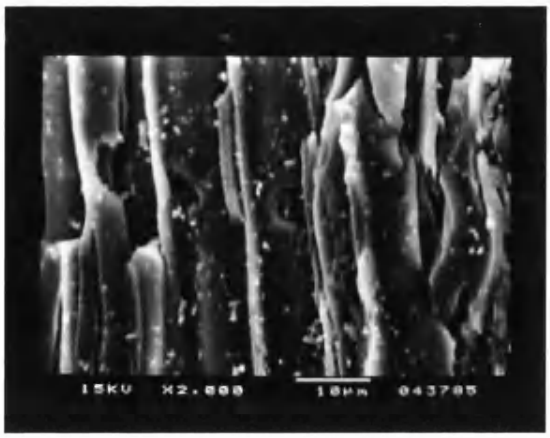

Figure 5.18 SS 208EA External surface

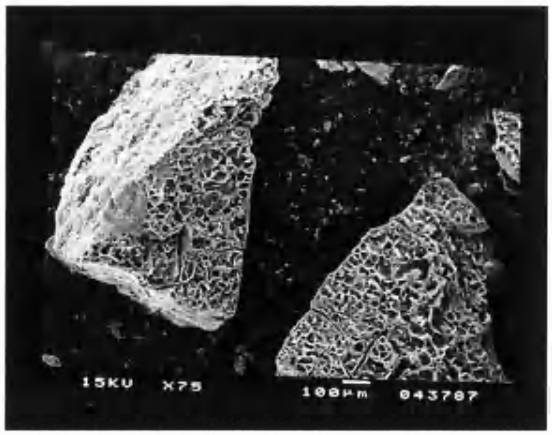

Figure 5.19 SS 208EA Internal surface

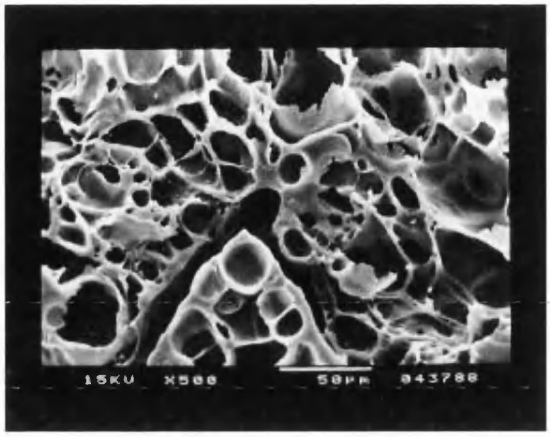

Figure 5.20 SS 208EA Internal surface

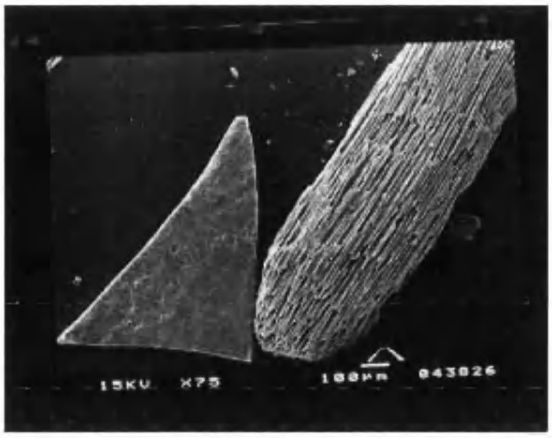

Figure 5.21 SS 607C Overview

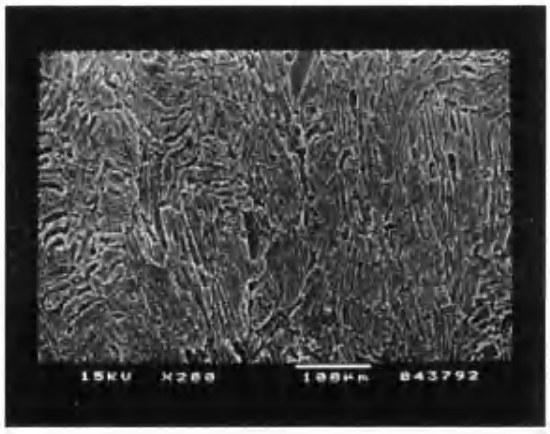

Figure 5.22 SS 607C External surface

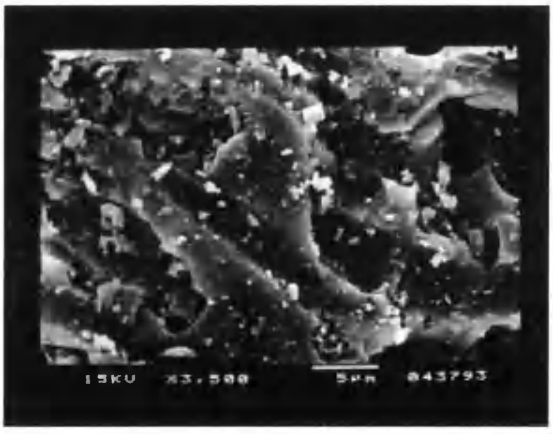

Figure 5.23 SS 607C External surface

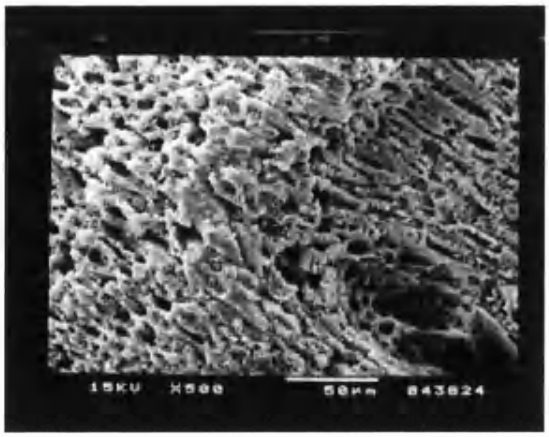

Figure 5.24 SS 607C Internal surface

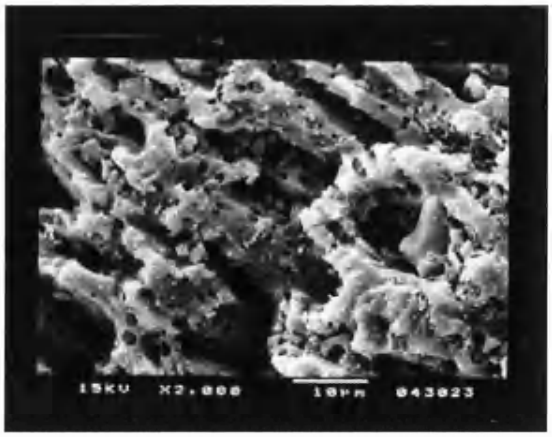

Figure 5.25 SS 607C Internal surface

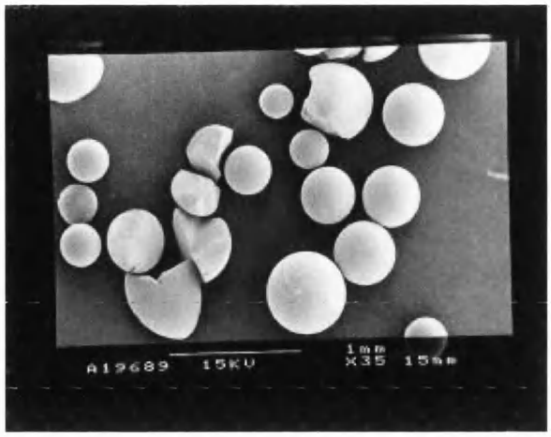

Figure 5.26 E-1-0-C Overview

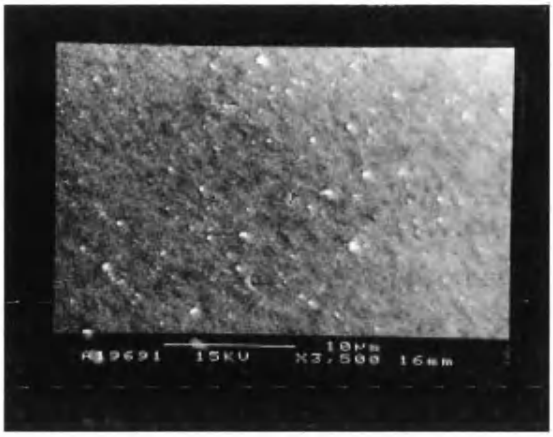

Figure 5.27 E-1-0-C External surface

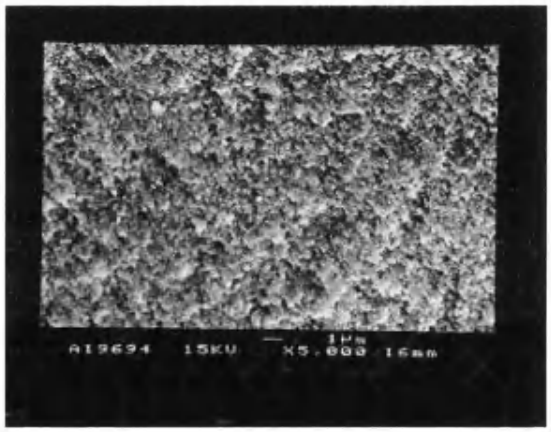

Figure 5.28 E-1-0-C Internal surface

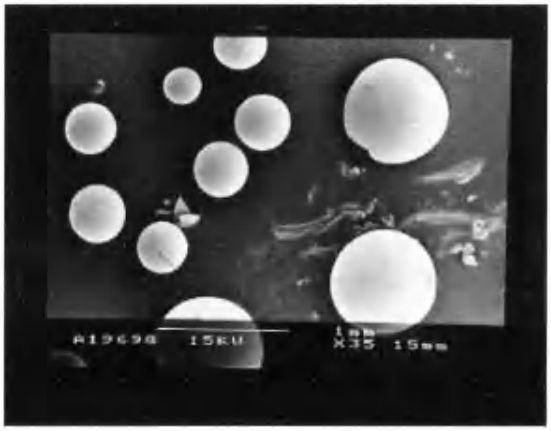

Figure 5.29 C150H Overview

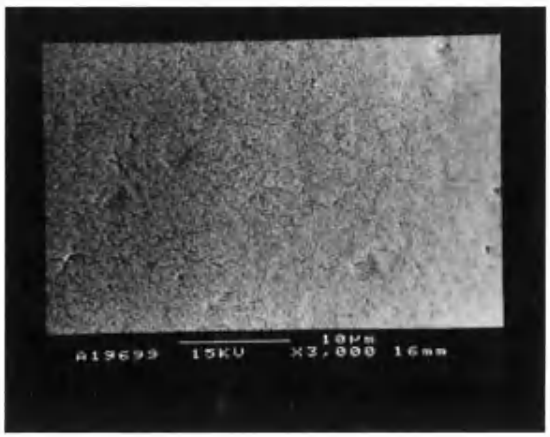

Figure 5.30 C150H External surface

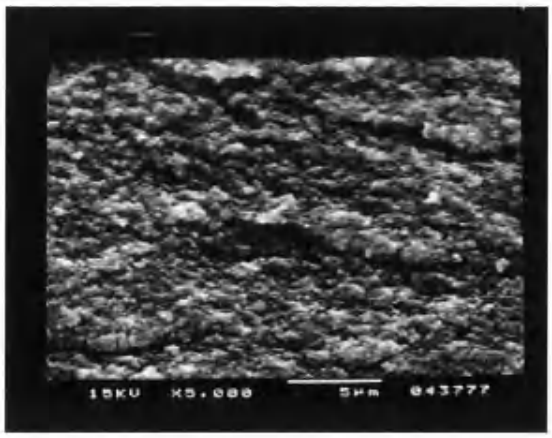

Figure 5.31 C150H Internal surface

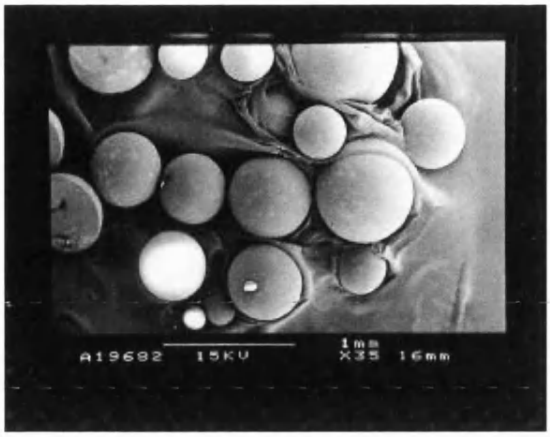

Figure 5.32 XAD-4 Overview

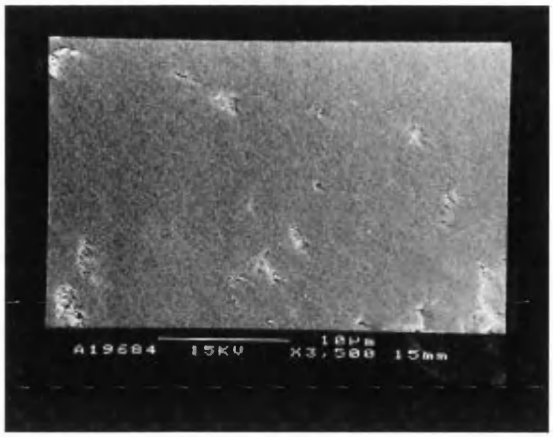

Figure 5.33 XAD-4 External surface

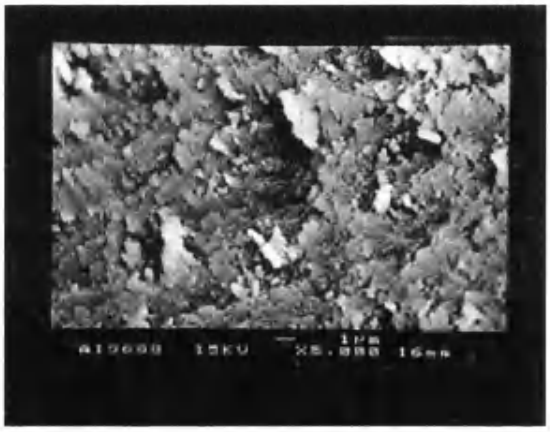

Figure 5.34 XAD-4 Internal surface

Figure 5.35 Silicalite Overview

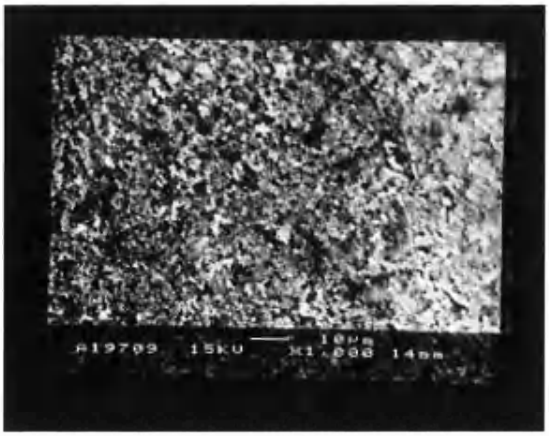

Figure 5.36 Silicalite External surface

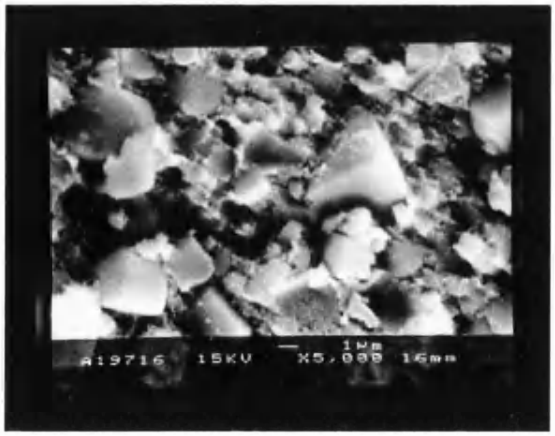

Figure 5.37 Silicalite Internal surface

Contrary to the external surfaces, the internal surfaces of SS 208EA (Figures 5.19 and 5.20) illustrate the carbon to have irregular shaped and spaced voids, whilst the internal surfaces of SS 607C (Figure 5.24 and 5.25) generally show layered parallel planes of graphitic material, with occasional anomalies. SS 607C is also shown to be a much denser material (Figure 5.24) in comparison to the internal micrograph of SS 208EA (Figure 5.20), which is shown to be "honeycomb" like, at the same magnification (x500).

MAST E-1-0-C, Purolite C150H and Amberlite XAD-4 are all shown to be perfect spherical beads in the overview micrographs (Figures 5.26, 5.29 and 5.32). The external surfaces for these adsorbents are illustrated (Figures 5.27, 5.30 and 5.33) as smooth non-porous surfaces with few imperfections, shown more so at magnifications greater than x3000. The internal surfaces (Figures 5.28, 5.31 and 5.34) also show the adsorbents to be dense with very little porous structure detectable by SEM even at high magnifications of x5000.

Silicalite is portrayed (Figure 5.35) as a smooth, imperfect spherical particle. The external surface (Figure 5.36) shows an adsorbent with a dense non-porous structure at a magnification of x1000, whilst the internal structure (Figure 5.37) shows a disorganised porous structure at a magnification x5000. A comparison of the pore voids of Silicalite (Figure 5.37), E-1-0-C (Figure 5.28) and the ion exchange resins (Figures 5.31 and 5.34), at the same magnification, shows the Silicalite pores to be much larger than that of the ion exchange resins and E-1-0-C.

It must be noted that both Purolite C150H and Amberlite XAD-4 demonstrated significant charging when viewing the internal structures at magnifications below x1000, revealing that pores less than 100nm could not be seen, whilst higher magnifications were showing no resolution.

5.3.3 Conclusions

The SEM micrographs largely show the macroporous structures (>50nm) of the adsorbents.

The MAST and Sutcliffe Speakman (SS) carbons (E-15-35-C, E-15-40-C, E-15-50-C, 208EA and 607C) were shown to be extremely macroporous materials, whilst the ion exchange resins (C150H and XAD4), Silicalite and MAST E-1-0-C were shown to have a smooth, non-porous surface.

The SS carbons (208EA and 607C) are industrially manufactured commercial activated carbons. Figures 5.15 and 5.21 show the carbons to be irregularly shaped granular particles, with layers of graphitic material (Figures 5.16 and 5.22). SS 208EA has is shown to have organised, parallel layers (Figures 5.16, 5.17 and 5.18) of graphitic material, whilst 607C has disorganised layers of material (Figures 5.22, 5.23 and 5.24). A comparison of the internal (Figure 5.20) and external (Figure 5.18) surfaces for 208EA shows the internal structure is more disorganised proving the activated carbon to be a heterogeneous product. Likewise, a comparison of the internal (Figure 5.24) and external (Figure 5.22) surfaces of 607C also show a heterogenous product. This heterogeneity generally comes from the presence of inorganic impurities (*e.g.* metal ions, sulphonates, phosphates, and chlorides) which affect the activation process, producing random macroporosity and hence a weak physical structure.

E-15-35-C, E-15-40-C and E-15-50-C MAST carbons are shown to be regular cylindrical particles (Figures 5.2, 5.7 and 5.11, respectively), with a similar appearance to "cigarette ash". The internal and external surfaces for all three carbons are shown to be very similar in structure (for example Figures 5.5 and 5.12), suggesting a unique homogeneous surface, unlike that of commercial carbons as shown by the SS carbon SEM micrographs. This homogenous surface aids in the physical strength of the carbon particles, whilst the random voids of a heterogeneous material weakens the overall structure. The macropores of the MAST carbons are also shown to be three dimensional in structure (*e.g.* Figure 5.4), increasing the strength of the product and as no binders are used in the manufacturing process a combination of these two properties provides outstanding permeability for the carbon particle. The level of activation does not seem to have had a marked effect on the macropore structure of these MAST carbons, as shown by Figures 5.5, 5.9 and 5.12, for carbon activation levels 35%, 40% and 50%, respectively.

Therefore the novel manufacturing process of the MAST PRC carbons, where binders are not used, produce a much physically stronger, homogeneous carbon material with a controlled, reproducible macropore structure.

In contrast, the ion exchange resins (C150H and XAD-4), Silicalite, MAST carbon (E-1-0-C), are shown to be smooth spherical materials, with a dense internal structure and much smaller pores. The dense internal structure of the ion exchange resins and the liquid phase MAST carbon may show a non-porous structure because the pores are too small to be seen by the JSM T330.

In general, SEM was shown to be a valuable technique to study the internal and external structure of various adsorbents. The MAST carbons were shown to have a homogenous, macroporous internal and external surface, whilst the commercially manufactured SS carbons were shown to have a heterogeneous macroporous internal and external surface.

5.4 Accelerated Surface Area and Porosimetry (ASAP)

The literature review (Section 5.2) describes a range of techniques available for estimating porosity and surface area, the most common being the adsorption of nitrogen at its boiling point (77K or -196°C), from which adsorption isotherms are obtained. These isotherms are studied using methods such as BET and Langmuir to obtain the following information (Arnold, 1995):

- Estimates of surface area and pore size
- Assessments of the surface chemistry of the adsorbent *e.g.* functional groups
- The nature of the adsorbed phase
- Assessments of the efficiency of industrial carbons employed in separation and purification techniques

In this study the isotherms obtained from the ASAP method are used to estimate the surface areas of the adsorbents.

5.4.1 Experimental procedure

This work was also carried out by Ms. A O'Reilly, a senior technician in the Department of Chemical Engineering, University of Bath. The surface area and pore size distributions of the nine adsorbents, detailed in Section 5.3.1, were examined using the Micrometrics ASAP 2010. The adsorbent samples were first dried in an oven for a minimum of 8 hours at approximately 70°C, and then degassed for a minimum of 24 hours at 100°C, and sealed to ensure the adsorbent could not be contaminated by exposure to the atmosphere. The adsorbent was then exposed to liquid nitrogen (> 99.99% purity) at its boiling point 77K (-196°C), to create adsorption isotherms. The sample mass was calculated by subtracting the mass of the empty nitrogen degassed sample tube from the nitrogen degassed adsorbent filled sample tube. Table 5.2 gives a summary of the conditions for each adsorbent sample.

Table 5.2 Summary of ASAP Micrometric Condition Settings for each Adsorbent Sample

Adsorbent	Sample mass (g)	Warm freespace (cm^3)	Equilibrium intervals (s)	Adsorbate	Analysis bath temperature (K)	Cold freespace (cm^3)	Low pressure dose ($cm^3\ g^{-1}$ STP)
E-15-35-C	0.4601	16.06	10	Nitrogen	77.30	54.24	25
E-15-40-C	0.4462	16.91	10	Nitrogen	77.30	56.44	25
E-15-50-C	0.4258	16.16	10	Nitrogen	77.30	54.89	25
SS 208EA	0.3319	17.38	10	Nitrogen	77.30	54.71	15
SS 607C	0.2911	16.41	10	Nitrogen	77.30	53.12	15
E-1-0-C	0.5753	18.86	10	Nitrogen	77.30	63.16	10
C150H	0.4456	16.18	20	Nitrogen	77.30	51.29	2
XAD-4	0.4276	16.36	10	Nitrogen	77.30	52.02	10
Silicalite	0.1989	16.75	20	Nitrogen	77.30	54.41	10

5.4.2 Results and discussions

Figures 5.38 to 5.46 show the nitrogen adsorption and desorption isotherms acquired from ASAP studies and used to calculate the surface area of adsorbents.

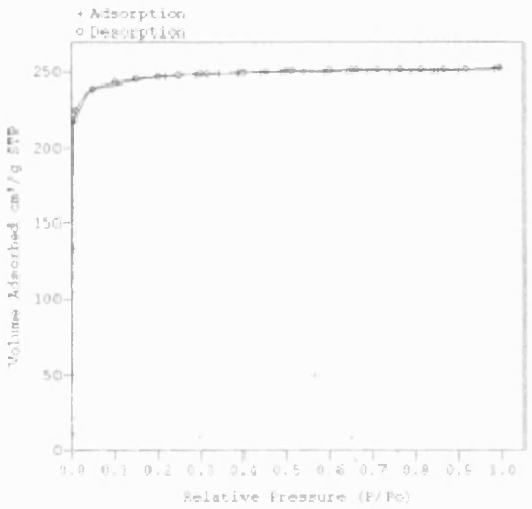

Figure 5.38 Adsorption /desorption isotherms for E-15-35-C

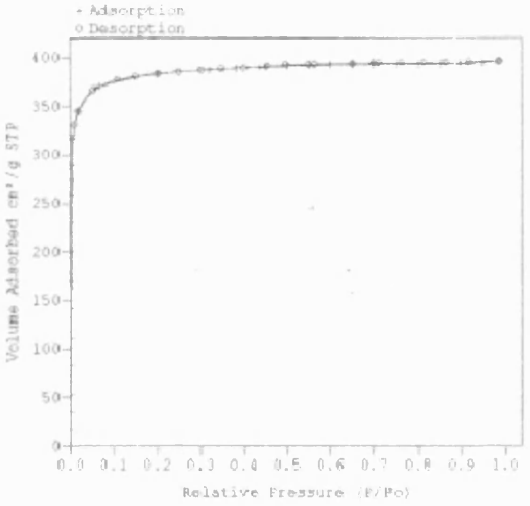

Figure 5.39 Adsorption / desorption isotherms for E-15-40-C

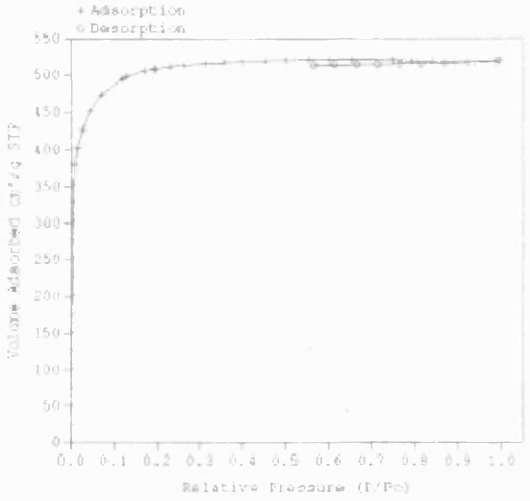

Figure 5.40 Adsorption / desorption isotherms for E-15-50-C

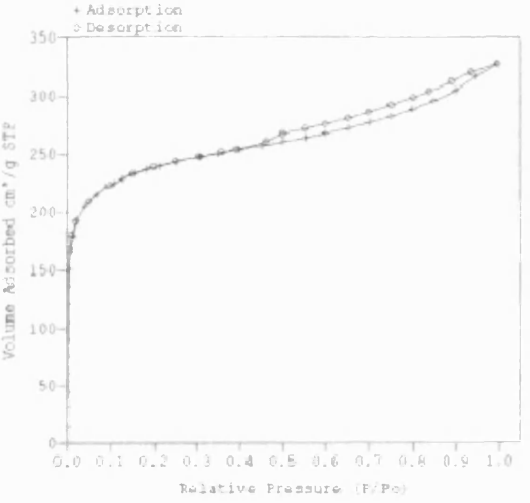

Figure 5.41 Adsorption / desorption isotherms for SS 208EA

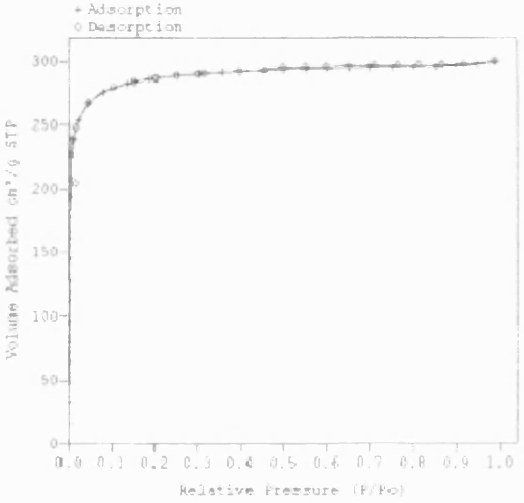

Figure 5.42 Adsorption / desorption isotherms for SS 607C

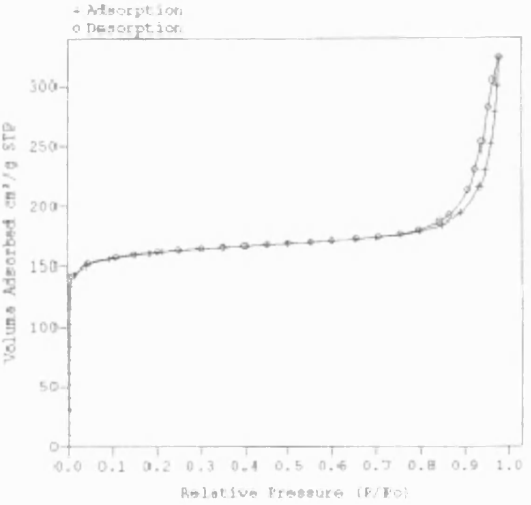

Figure 5.43 Adsorption / desorption isotherms for E-1-0-C

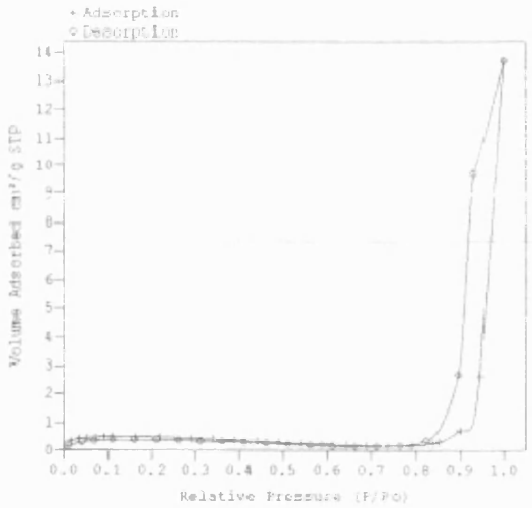

Figure 5.44 Adsorption / desorption isotherms for C150H

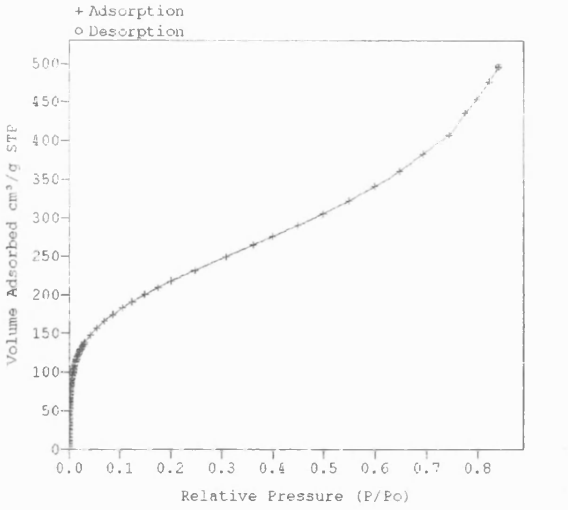

Figure 5.45 Adsorption / desorption isotherms for XAD-4

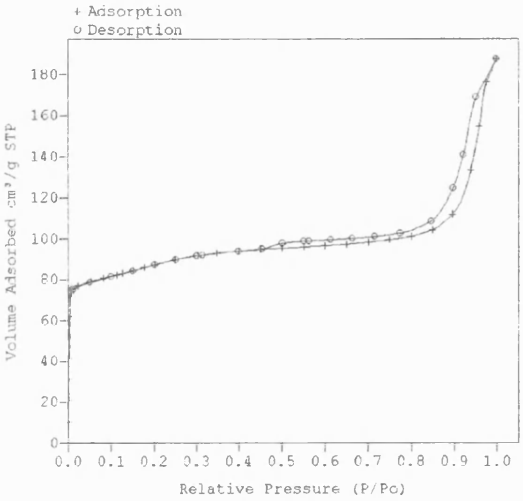

Figure 5.46 Adsorption / desorption isotherms for Silicalite

The y axis is the volume of nitrogen adsorbed (cm^3g^{-1}) at standard temperature and pressure (STP) and the x axis is the relative pressure (P/P_o). According to BET's isotherm classification described in Section 4.3 (Figure 4.2), the gas phase carbons MAST E-15-35-C (Figure 5.38), E-15-40-C (Figure 5.39), E15-50-C (Figure 5.40) and SS 607C (Figure 5.42) appear to possess a Type I isotherm typical of microporous solids. Conversely, the liquid phase carbons MAST E-1-0-C (Figure 5.43) and SS 208EA (Figure 5.41), Amberlite XAD-4 (Figure 5.45) and Silicalite (Figure 5.46), appear to possess Type II isotherms, and Purolite C150H (Figure 5.44) possesses a Type III isotherm.

The liquid phase carbons (Figures 5.41 and 5.43) and Silicalite (Figure 5.46) show a hysteresis loop, which is complementary to Type IV isotherms, whilst Purolite C150H (Figure 5.44) also shows hysteresis, but this shape isotherm with hysteresis is not explained by the BET classifications. In fact, Figure 5.44 demonstrates that Purolite has an extremely low affinity for nitrogen and hence the isotherm is not very accurate.

Table 5.3 summaries the surface areas determined by BET (Equation 4.25) and Langmuir (Equation 4.16) models as described in Chapter 4. It also gives the single point surface area calculated at an approximate relative pressure of 0.21. The BET and single point surface areas to be fairly similar in their values, but the Langmuir surface areas were calculated to be much greater. However, all three models generally show the same trend for the adsorption of nitrogen, where MAST E-15-50-C possess the highest surface area, followed by MAST E-15-40-C, SS 607C, MAST E-15-35-C, SS 208EA, Amberlite XAD-4, MAST E-1-0-C, Silicalite and Purolite C150H to posses the lowest surface area. Although, Purolite showed such a low affinity for nitrogen that the surface area could not be analysed accurately.

Table 5.3 Summaries of BET, Langmuir and Single Point Surface Areas From ASAP Nitrogen Adsorption Results

Adsorbent	BET surface area ($m^2 g^{-1}$)	Langmuir surface area ($m^2 g^{-1}$)	Single point surface area ($m^2 g^{-1}$)	Relative pressure (p/p_o)
E-15-35-C	845.82	1074.14	841.34	0.22
E-15-40-C	1340.19	1668.97	1332.85	0.20
E-15-50-C	1789.42	2212.59	1716.05	0.23
SS 208EA	843.75	1028.93	822.31	0.21
SS 607C	1021.05	1244.91	991.35	0.21
E-1-0-C	568.87	698.36	553.63	0.21
C150H	1.70	2.20	1.66	0.21
XAD-4	743.64	886.36	758.51	0.20
Silicalite	309.31	373.63	304.04	0.21

The BET surface areas show that there is a relationship between activation and surface area, such that the carbon with the highest activation (E-15-50-C) has the higher surface

area. The liquid phase carbons are also shown to have a lower surface area compared to gas phase carbons.

Chapters 3 and 4 explained that the surface area of an adsorbent largely comes from its microporosity. In addition, as Table 5.3 shows, that the higher the carbon activation the higher the surface area, which in turn suggests the greater the microporosity. Therefore it can be said that whilst SEM does not provide information on microporosity , the ASAP studies do. It is shown that MAST E-15-50-C not only has the highest surface area, but also contains the greatest quantity of micropores.

5.4.3 Conclusions

Generally, the gas phase carbons have larger surface areas than the liquid phase carbons. The highest surface area is shown to belong to the greatest activated carbon (MAST E-15-50-C). This confirms assumptions that suggest activation produces a larger number of micropores. Various nitrogen adsorption isotherms were studied for BET classification. The gas phase carbons demonstrated the Type I isotherm, whilst the liquid phase carbons and Silicalite showed hysteresis, typical of the Type IV isotherm, Amberlite illustrated an isotherm characteristic to the Type II isotherm, and Purolite was unsuccessful in adsorbing nitrogen at 77K.

Overall, the SEM micrographs were useful in showing the macroporosity of the adsorbents whilst the ASAP nitrogen adsorption studies illustrates which adsorbent has the highest surface area and hence microporosity. On the whole the SEM micrographs (Figures 5.2-5.37) showed the MAST carbons (E-15-35-C, E-15-40-C and E-15-50-C) to have the greatest macroporosity and the ASAP studies (Figures 5.38-5.46) showed MAST E-15-50-C to have the greatest microporosity. Therefore, these studies suggest MAST E-15-50-C would be the best material for the WOWSEP process.

This Chapter has characterised and studied the structure of the adsorbents, hence the next stage would be to study the loading capabilities of the adsorbent with the adsorbate of interest. The next Chapter addresses the kinetic and equilibrium properties of the various adsorbents and cutting fluid.

6.0 Batch Kinetic and Equilibrium Studies

6.1 Kinetic studies

Activated carbon has been gaining ever-increasing usage as a general purpose adsorbent for organics from the aqueous phase. It is generally modelled as having a homogeneous surface with one pore size throughout the particle, even though it is accepted that activated carbon has heterogeneous surface properties and a wide range of pore sizes (Peel *et al.*, 1981). This complex internal pore structure has made it difficult to fully understand the actual mechanisms of transport within the particles.

In multicomponent systems, the adsorbent has a different affinity for each of the adsorbates. Poorly adsorbed compounds have little effect on adsorbent usage rates, while strongly adsorbed compounds adsorb more competitively, largely affecting the usage rates. Therefore the study of the capacity of a particular adsorbent with a particular adsorbate is essential. Generally, higher molecular weight substances are more strongly attracted to carbon, so long as they are small enough to enter through the carbon pores. More specifically, variations in conditions such as: (i) the characteristics of the bulk solution (pH, temperature, concentration), (ii) the physical and chemical characteristics of the adsorbate (solubility, polarity, hydrophobicity, shape, size and weight) and (iii) the physical and chemical characteristics of the adsorbent (surface area, pore size, chemical composition), influence the equilibrium process and the adsorbent loading. A change in conditions may even lead to regeneration of the spent carbon, although this is dependent on the directional change and magnitude of adsorption (Cheremisinoff and Moressi, 1978; Kittredge, 1980).

As described in Chapter 2, metalworking fluids contain many complex chemicals. The precise names and compositions of these chemicals could not be released for this research due to commercial confidentiality. Nonetheless, D. A. Stuart Oil provided several so-called 'individual components' (only trade names were provided) from R5/026/3 semi-synthetic fluid, none of which were pure components but were made up of from a number of chemicals. Attempts were made to analyse each of these 'individual components' using methods such as Fourier Transform Infra Red (FTIR), X-ray spectroscopy, TOC and High Performance Liquid Chromatography (HPLC). Whilst it may have been theoretically

possible to analyse these components, it was not found to be a straightforward process. The high density and low water solubility properties of most of these compounds led to analytical complications, such as contamination of the analysers and inconsistent reproducibility, which made the analysis unsuccessful. A breakdown of the contents of a cutting fluid plus their analyses would possibly require the time and effort of a complete PhD. Therefore the R5/026/3 semi-synthetic cutting fluid used in the following experiments was initially treated as a pseudo-single homogeneous organic solution and analysed as total organic carbon (TOC). This assumption was later found to be invalid (as discussed in greater detail in Chapter 7).

During kinetic experiments each carbon particle has to purify a certain volume of liquid. This is achieved through the five steps (bulk diffusion, external mass transfer, phase boundary, pore and surface diffusion) discussed in Chapter 4. The latter three steps describe the adsorption process itself, which is the final stage of getting a molecule from the bulk phase on to the surface of an adsorbent. When every particle has achieved this, the system reaches equilibrium. An equilibrium state is likely to exist between the adsorbate molecules immediately above the surface and those on the surface. The relative importance of the boundary–film and intra-pellet (pore) diffusion in mass transfer is measured by the Biot number (*Bi*). This is another method of measuring the adsorption rate of a system, where a large *Bi* indicates that the rate is being controlled by pore diffusion. The *Bi* is determined on the assumption that there is no accumulation of adsorbate at the external surface of the adsorbent:

$$Bi = \frac{k_f r}{D_{eff}} \qquad 6.1$$

where D_{eff} is the effective particle diffusivity ($m^2\ s^{-1}$), r is the radius of the particle (m) and k_f is the external mass transfer coefficient ($m\ s^{-1}$), previously described in Chapter 4, and is determined by Equation 4.3:

$$k_f = \frac{-V}{A_p c_0}\left(\frac{dc}{dt}\right)_{t\to 0} \qquad 4.3$$

where V is the volume (m^3) of the fluid phase, A_p is the external surface area (m^2), c is the fluid phase concentration at time, t (g m^{-3}) and c_e is the fluid phase concentration in equilibrium with the external adsorbent surface (g m^{-3}). When $t = 0$, $c = c_o$ and $c_e = 0$ (*i.e.* initial conditions). The overall mass transfer coefficient (K, m s^{-1}) at 20°C was used calculate the value of D_{eff} (Equation 6.2) and hence the Bi (Equation 6.1):

$$K = \frac{D_{eff}\pi^2}{r^2} \qquad 6.2$$

Overall the kinetic experiments provide information on the contact time required between an adsorbate and adsorbent in order to reach equilibrium, as well as the rate of adsorption and the system's practical applications (Bernardin, 1985). The rate of adsorption of an adsorbate onto carbon depends on both the external and internal mass transfer kinetics of a system. The internal mass transfer may include the solid phase surface diffusion and/or pore diffusion processes (McKay, 1984), and is important because the mass transfer process controls the cycle time of fixed bed adsorption processes (Knaebel, 1995).

6.1.1 Experimental procedure

20 g (± 0.05 g) of adsorbent were placed into a glass vessel containing a motor controlled impeller. The vessel was placed in a temperature-controlled water bath, where the temperature was set to 20°C (± 0.1°C). 100 ml of adsorbate solution was then added to the adsorbent and the motorised impeller was started at a speed of 170 rpm, such that the adsorbate and adsorbent were well agitated (Figure 6.0). The agitation ensured complete mixing of the adsorbate/adsorbent combination and the high impeller speed made certain that no significant boundary film layers existed around the adsorbent particles. Simultaneously a stopwatch was started and samples of the adsorbate solution were withdrawn and analysed using the TOC analyser at intervals.

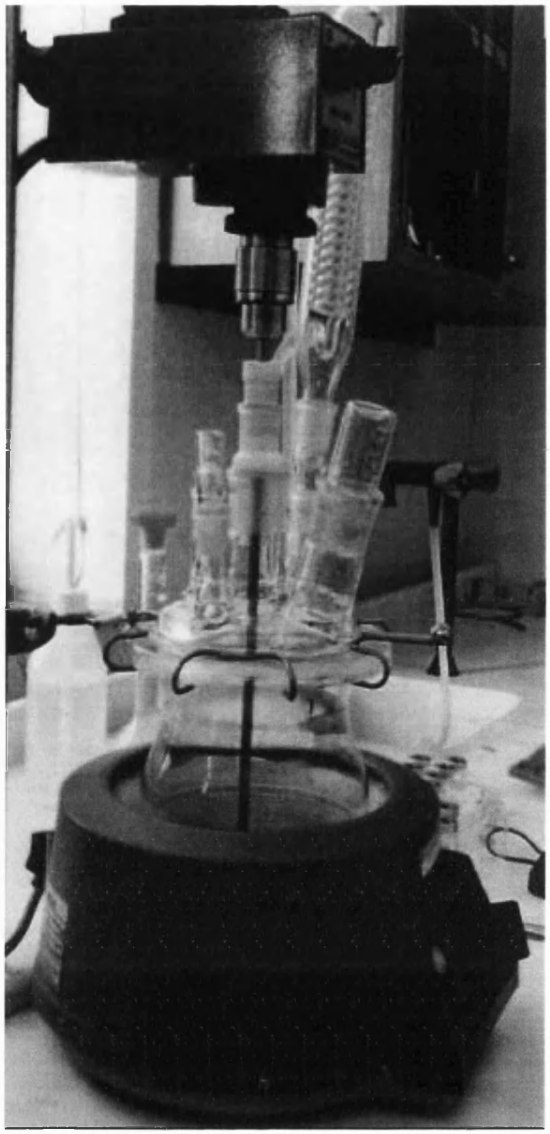

Figure 6.0 Apparatus for kinetic studies

6.1.2 Analysis method

There are three main methods of analysis for organic compounds, namely chemical oxygen demand (COD), biological oxygen demand (BOD) and total organic carbon (TOC). The standard BOD test requires a five-day incubation period (and is often called the BOD_5 test) with a sample of bacteria. This is followed by a measurement of oxygen consumed for the biochemical degradation (oxidation) of organic (carbonaceous demand) and inorganic (nitrogen and hydrogen) material during the period (Greenberg *et al.*, 1989a). COD measures the oxygen equivalent of the organic content of a sample that is susceptible to oxidation by a strong chemical oxidant, although the presence of oxidisable inorganics

may interfere with the analysis (Greenberg *et al.*, 1989b). TOC measurement, on the other hand, has recently come to the forefront of technology as a fast, simple, convenient, reliable, and direct means of assessing water quality (Crane, 1996; Burke, 1991). It is independent of the oxidation state of the organic matter and does not measure other organically bound elements, such as nitrogen and hydrogen, and inorganics that can contribute to the oxygen demand measurement by BOD and COD (Greenberg *et al.*, 1989c). The more common of these methods for the analysis of wastewater are COD and BOD. However, these methods are laborious, time consuming and less reliable than TOC. Therefore the analysis method used in this research project was TOC, using the Dohrmann DC180 analyser (Figure 6.1).

6.1.2.1 Dohrmann DC180 TOC analyser

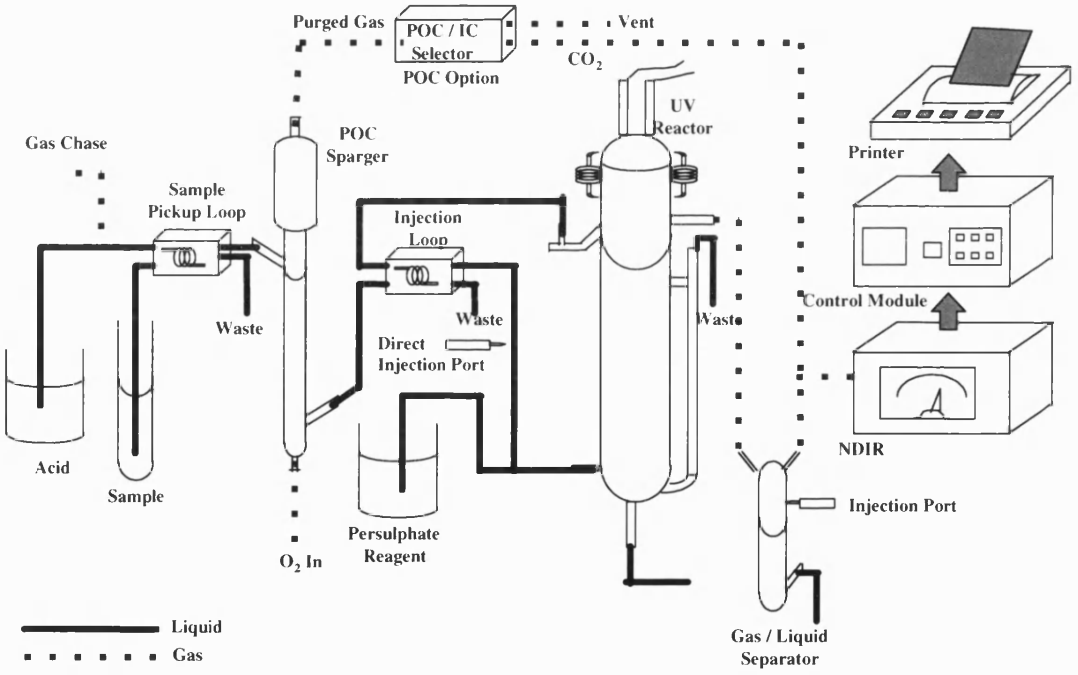

Figure 6.1 Schematic diagram of the Dohrmann DC180 TOC analyser

The DC180 TOC analyser was designed to operate with different modes for the measurement of various types of carbon: inorganic carbon (IC) (*e.g.* carbon dioxide or carbonic acid), organic carbon (OC), purgeable organic carbon (POC), non-purgeable organic carbon (NPOC) and total carbon (TC). The TOC measurement could either be based on a sum of the POC and NPOC or as a difference of the TC and IC. If the TOC

measurement is based on POC and NPOC, and the POC fraction is small compared to the NPOC, a higher throughput can be achieved by analysing for NPOC only. Figure 6.1 is a schematic diagram showing the operations of the DC180. As there was no POC or IC present in the cutting fluid samples, the mode of analysis for this project was NPOC only using the direct injection port. The direct injection port bypasses the sparger and introduces the sample straight into the ultraviolet (UV) reactor. Therefore the purged gas produced by the sparger is not analysed by the non-dispersive infrared (NDIR) detector, but vented. The UV light and oxygen rich persulphate in the reactor ensures complete oxidation of all the organics, producing carbon dioxide (CO_2). The CO_2 product is then transferred to the NDIR detector for measurement, which sends a signal to the control module and recalculates the CO_2 measurement to TOC. The TOC results are then printed.

6.1.3 Results and discussions

As mentioned earlier the main aim of the kinetic studies was to provide information on the uptake rate of the carbon. A graph of concentration versus time shows uptake behaviour of the carbon against time. Generally, a steeper graph represents faster adsorption.

In order to separate the soluble oils from the neat cutting fluid, the WOWSEP team at PERA pre-treated the neat fluid using two methods: ultrafiltration and chemical splitting. Kinetic studies were then conducted using MAST E-15-50-C and SS 607C carbons and the resulting two pre-treated fluids.

Figure 6.2 shows a comparison of kinetic experiments conducted using MAST E-15-50-C and SS 607C with the ultrafiltered cutting fluid. The y axis is a ratio (C/C_o) of the concentration of the solution at a given time (C, mg l^{-1}) over its initial concentration (C_o, mg l^{-1}), and the x axis represents the Time in minutes. Initially, both graphs are almost identical, showing a steep initial drop in concentration. This suggests that the initial rate of adsorption is high. After the first 30 minutes or so, the E-15-50-C graph starts to level off and equilibrium is achieved after approximately 100 minutes. The SS 607C graph, on the other hand, shows that after the first 30 minutes the uptake rate decreases, however equilibrium is not reached until approximately 230 minutes. Overall the MAST E-15-50-C graph is steeper and sharper than the SS 607C indicating it has better kinetic properties than SS 607C.

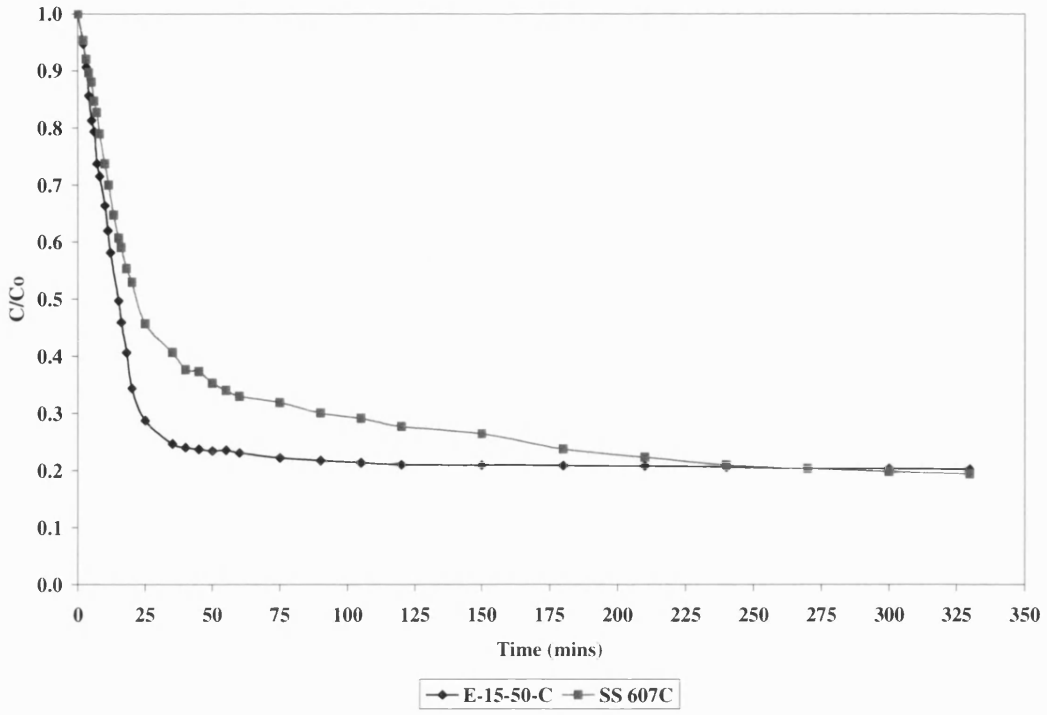

Figure 6.2 A comparison of batch kinetic studies for MAST E-15-50-C and SS 607C carbons with ultrafiltered cutting fluid

Table 6.0 shows *Bi* and the rate of adsorption $\left(\left.\frac{dc}{dt}\right|_{t\to 0}\right)$ of the systems shown in Figure 6.2.

Table 6.0 Biot Numbers and Rates of Adsorption for MAST E-15-50-C and SS 607C Carbon with Ultrafiltered Cutting Fluid

Figure	**Adsorbent**	**Adsorbate**	$\left.\frac{dc}{dt}\right\|_{t\to 0}$ **(mg cm^{-3} s^{-1})**	**Biot number**
6.2	MAST E-15-50-C	Ultrafiltered cutting fluid	-105.92	1.141
6.2	SS 607C	Ultrafiltered cutting fluid	-69.812	5.625

The rate of adsorption is represented by the initial gradient, for the first 30 minutes. The numerical values of $\left(\left.\frac{dc}{dt}\right|_{t\to 0}\right)$ shows that MAST E-15-50-C has a larger value and hence a greater rate of adsorption. The negative sign shows that the concentration is decreasing as

the time is increasing. In addition, MAST E-15-50-C is shown to have a lower *Bi* number than SS 607C, but both values are low enough to indicate that adsorption is film diffusion controlled, even with a higher agitation rate. According to Equation 6.1, the lower the *Bi* the higher the D_{eff} must be.

Figure 6.3 shows a comparison of ultrafiltered and chemically split cutting fluids using MAST E-15-50-C. As in Figure 6.2, both graphs have a large initial drop in concentration, but the chemically split cutting fluid is shown to have a slightly shallower curve than the ultrafiltered cutting fluid. This indicates that the chemically split cutting fluid has a lower adsorption rate. After the initial drop in concentration, the C/C_o ratio levels off into a plateau. This is when the system has reached equilibrium. Figure 6.3 also shows that the time taken for equilibrium to be achieved for the chemically split fluid is longer than the ultrafiltered fluid. Nevertheless, both adsorbates achieved equilibrium within an hour.

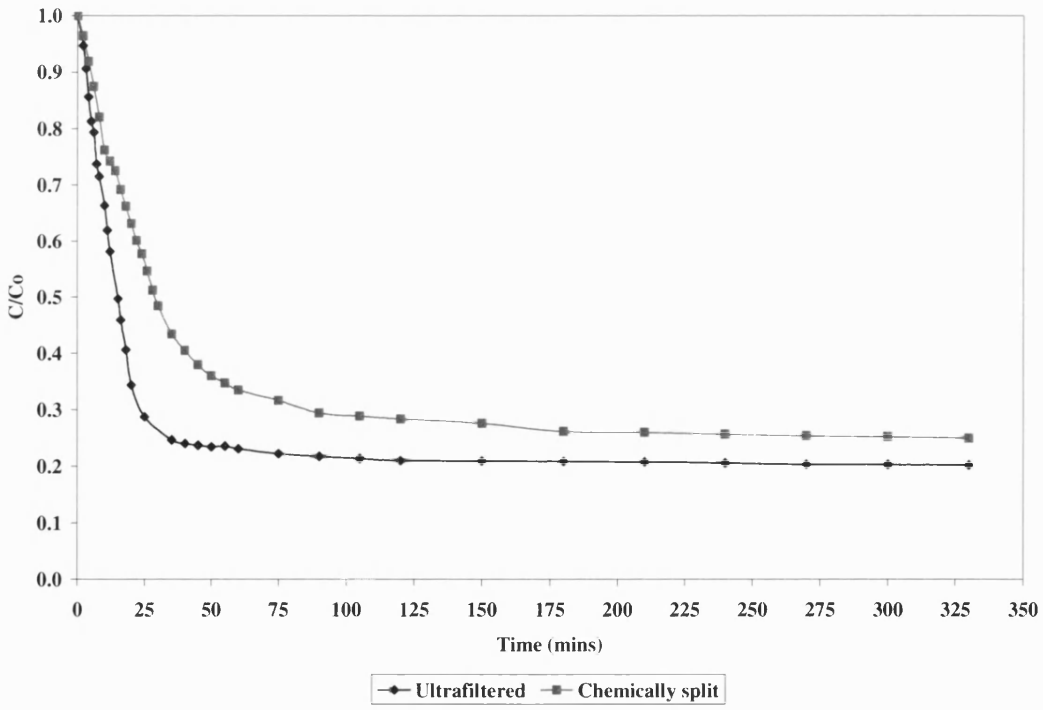

Figure 6.3 A comparison of batch kinetic studies for ultrafiltered and chemically split cutting fluids with MAST E-15-50-C carbon

Table 6.1 shows the *Bi* and $\left(\left.\frac{dc}{dt}\right|_{t\to 0}\right)$, calculated for the systems shown in Figure 6.3. The chemically split solution is shown to have a much lower *Bi* and gradient than the

ultrafiltered solution. This suggests that even though the *Bi* numbers are different for each solution. However, the values are still low, indicating adsorption to be film diffusion controlled. The higher *(dc/dt)* number for the ultrafiltered solution suggests the adsorption system has better kinetic properties when using MAST E-15-50-C with ultrafiltered cutting fluid.

Table 6.1 Biot Numbers and Rates of Adsorption for Ultrafiltered and Chemically Split Cutting Fluids with MAST E-15-50-C

Figure	Adsorbent	Adsorbate	$\left(\frac{dc}{dt}\Big\|_{t\to 0}\right)$	Biot number
6.3	MAST E-15-50-C	Ultrafiltered cutting fluid	-105.92	1.141
6.3	MAST E-15-50-C	Chemically split cutting fluid	-39.854	0.562

6.1.4 Conclusions

The kinetic experiments show that a combination of MAST E-15-50-C and ultrafiltered solution has a higher rate of adsorption and better kinetic properties than SS 607C and the chemically split solution. In addition, calculation of the low Biot Numbers showed that adsorption in this system was controlled by film diffusion.

Whilst it would have been interesting to see how the impeller speed affects the rate of adsorption and the *Bi* number, the main purpose of conducting the kinetic studies was moreover to obtain information on the time taken for the system to reach equilibrium. Bernardin (1985) stated *"Generally four hours with vigorous agitation is sufficient for approaching equilibrium, but this can vary with the sample. To better estimate the optimum contact time for a particular system a single carbon dosage should be contacted with a sample of solution and the concentration change measured over time"*. However, the results from these kinetic experiments showed the greatest part of adsorption and equilibrium is achieved relative quickly, within the first 30 minutes. Therefore the following section studies the loading capacity, through equilibrium experiments of the carbon using various adsorbates and adsorbents.

6.2 Equilibrium studies

Having characterised the adsorbents (Chapter 5) and calculated the time required for the process to reach equilibrium (kinetic studies) the next stage was to conduct a series of batch equilibrium studies. Initially, equilibrium studies are used to establish whether adsorption would occur to any appreciable extent between the adsorbate and the adsorbent. If adsorption is found to be feasible a series of batch tests are conducted to determine the thermodynamic relationship between the adsorbent and the adsorbate. This relationship is often expressed as an isotherm (detailed in Chapter 4). It provides information on the loading capacity of the carbon and the quantity of adsorbent necessary to achieve the target concentration. The isotherm may also reveal the presence of background organic compounds and indicate what portion of these compounds can be regarded non-adsorbable (Stenzel and Merz, 1989; Bernardin, 1985). If these non-adsorbable compounds are established at the equilibrium stage, then their presence can be accounted for at the purification stage or they can be removed before the purifying carbon column. As in the kinetic studies, due to the uncertainty of the chemical content of the cutting fluid, the fluid was considered a homogeneous single component solution. However, as mentioned previously this assumption was later found to be unrealistic.

6.2.1 Experimental procedure

1 g (± 0.05 g) of adsorbent and 5 ml of adsorbate (at a known concentration, *e.g.* 1000 mg l^{-1}) were measured and placed in a glass sample vial. The vial was covered with Viton Rubber (oil and chemical resistant) and crimp sealed with an aluminium washer and cap (Figure 6.4).

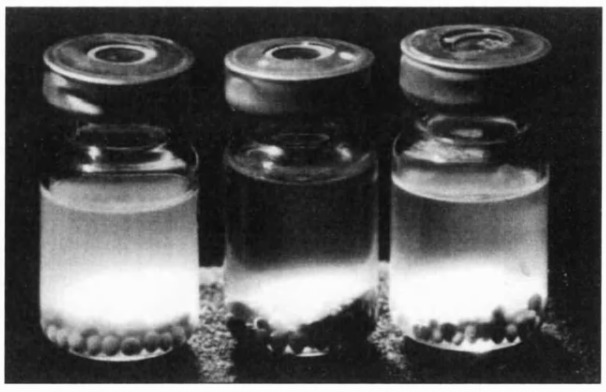

Figure 6.4 Sample vials containing an adsorbent and adsorbate solution

The vial was clipped onto a tray, which was placed in an agitated, temperature controlled water bath (Figure 6.5) with the same conditions as in the kinetic studies (agitated at 170 rpm with a constant temperature of 20°C). Simultaneously, 5 ml of the same adsorbate solution, without the adsorbent, was placed as a control in an empty vial, sealed and placed under the same conditions in the water bath. To obtain an isotherm, this procedure was repeated with the same adsorbent, but with different starting adsorbate concentrations.

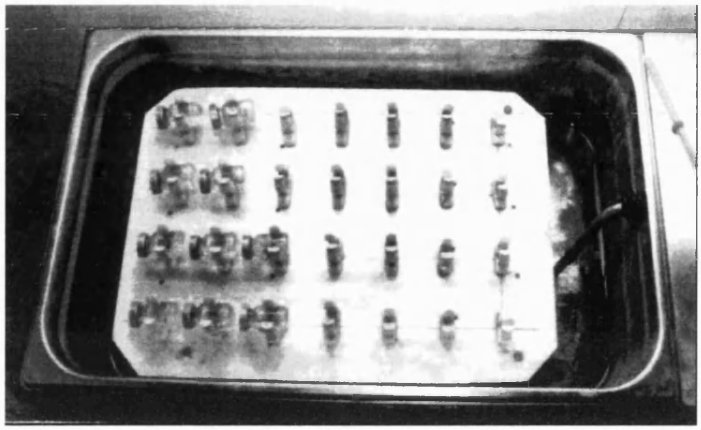

Figure 6.5 Agitated water bath containing sample vials

The samples were left in the water bath for a minimum of 24 hours. The kinetic studies, described earlier in this Chapter (Figures 6.2 and 6.3), showed that the greater part of adsorption had taken place within the first 30 minutes, and Bernardin (1985), had stated that four hours is sufficient for approaching equilibrium. In order to confirm this incubation period, a sample was taken every hour from a couple of vials and the TOC was tested. It was found that the major part of adsorption had occurred within the first hour and complete adsorption had occurred within approximately 6 hours. This would suggest that 24 hours would be adequate time for equilibrium to be achieved. After 24 hours, the resulting solutions were then filtered (using filter paper) to remove the adsorbent particles and analysed. This procedure was repeated for different adsorbents and adsorbates (with various initial concentrations) to obtain various isotherms.

6.2.2 Results and discussions

The principal adsorbent and adsorbate being investigated in this research was MAST PRC and pre-treated (ultrafiltered or chemically split) semi-synthetic cutting fluid (R5/026/3,

provided by D. A. Stuart Oil), although other adsorbents and adsorbates were used as comparisons.

When carbon is placed in a solution containing dissolved organic substances, adsorption is expected to take place until a balance is struck between the carbon and the organic substances, *i.e.* the rate of adsorption equals the rate of desorption. This is the point at which the carbon can accept no more organic substances and equilibrium is achieved. The thermodynamic equilibrium relationship between the organic compounds in the water (measured as TOC concentration (c, mg l^{-1})), and the organic compounds adsorbed on the carbon was expressed as the loading (q, mg mg^{-1}).

Chapter 4 discussed the theory of equilibrium experiments and suggested many models for equilibrium relationships. Commonly used models are the Langmuir, Freundlich and BET models. The Freundlich model is used extensively in water treatment applications (Faust and Aly, 1987). The BET model was used in the ASAP studies to calculate the surface area of adsorbents (Chapter 5). In this Chapter, experimental data from a simple mass balance developed for a batch system (Figure 6.6) are compared to the Langmuir and Freundlich models (Figures 6.7 and 6.8, respectively). The carbons being compared were MAST E-15-35-C, SS 607C and SS 208EA, and the adsorbate solution under study, initially, was propionic acid. Propionic acid was used as a 'standard' against which all other adsorbate solutions could be compared as it is known to adsorb onto activated carbon.

A simple mass balance over the batch system (Equation 6.3) assumes that there is no change in adsorbate volume (V, l) or adsorbent mass (M, mg). In this equation c_i and c are the initial and equilibrium concentrations (mg l^{-1}), and q_i and q are the initial and equilibrium loadings (mg mg^{-1}), respectively.

$$M(q - q_i) = V(c_i - c) \qquad 6.3$$

Assuming the adsorbent is initially free of any adsorbate (q_i=0), the equilibrium loading may be expressed as

$$q = \frac{V(c_i - c)}{M} \qquad 6.4$$

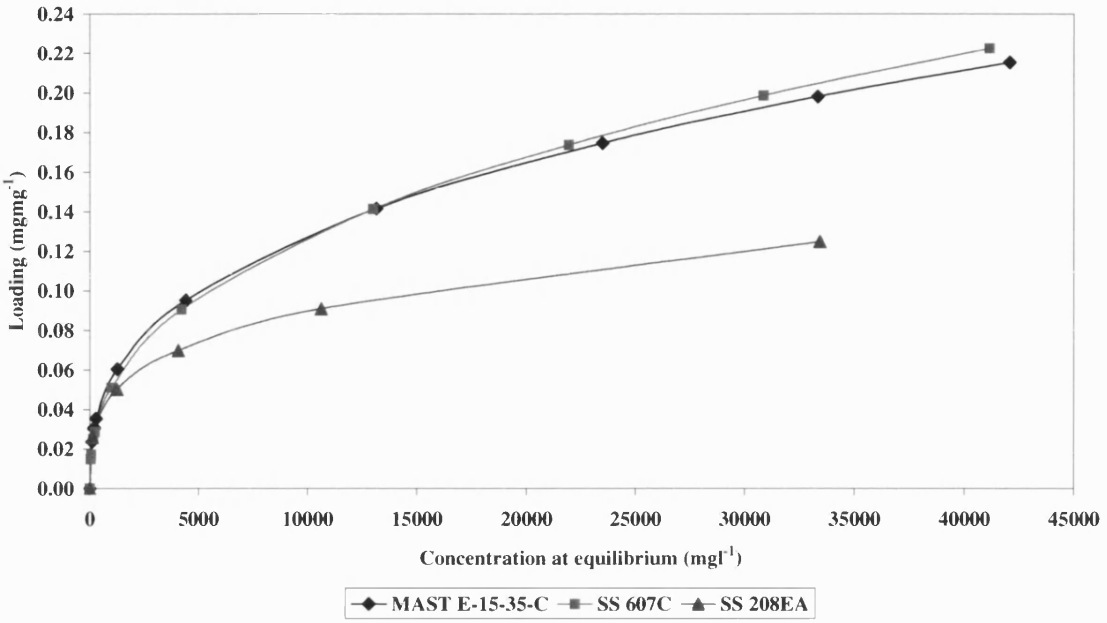

Figure 6.6 A comparison of experimental data obtained from a simple propionic acid mass balance over a batch equilibrium system using MAST E-15-35-C, SS 607C and SS 208EA carbons

The experimental isotherms in Figure 6.6 are similar to the BET Type I isotherm, which is typical of microporous solids (detailed in Chapter 4). The isotherms start with a sharp increase in loading, which proceeds into a "knee" and then levels off towards a plateau. This plateau tends towards the maximum loading of the carbon, which is associated with the completion of the monolayer coverage. However, the plateau in Figure 6.6 is not flat but still increasing slightly. This suggests that the maximum loading has not been achieved, although the shallow gradient indicates that it is not far off.

Figure 6.7 shows the corresponding linearised Langmuir plots (Equation 4.21) obtained by plotting the reciprocal loading and concentration of the experimental data for propionic acid with MAST E-15-35-C, SS 607C and SS 208EA (from Figure 6.6). If this system were to follow the Langmuir model then the reciprocal plots would produce straight line graphs. However, as can be seen, none of the three carbons produce straight line (linear)

graphs. This indicates that the adsorption of propionic acid onto carbon does not follow the Langmuir model.

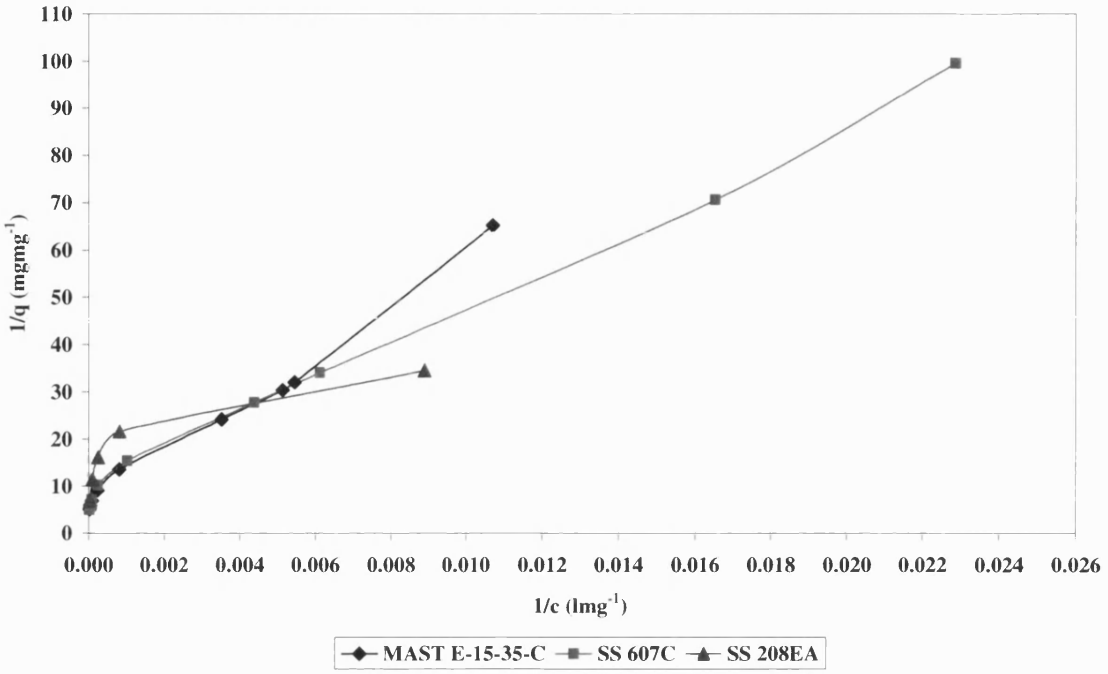

Figure 6.7 A comparison of Langmuir plots for propionic acid and MAST E-15-35-C, SS 607C and SS 208EA carbons

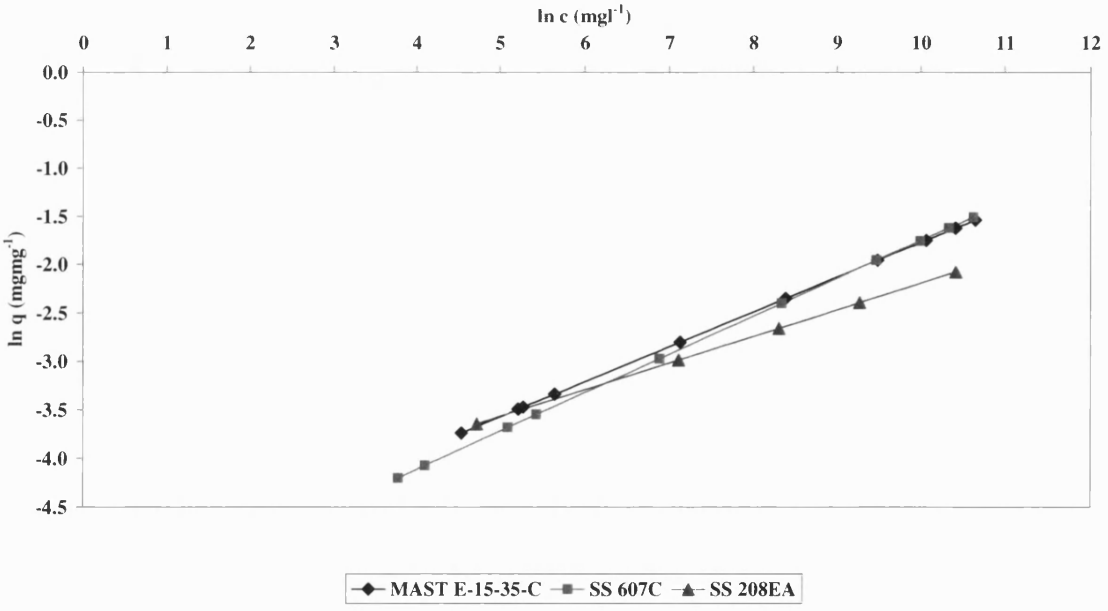

Figure 6.8 A comparison of logarithmic Freundlich plots for propionic acid and MAST E-15-35-C, SS 607C and SS 208EA carbons

Figure 6.8 shows the logarithmic Freundlich plots (Equation 4.24) obtained from the same experimental data for propionic acid with MAST E-15-35-C, SS 607C and SS 208EA carbons as in Figure 6.6. If the system followed the Freundlich model, then the logarithmic plots would produce straight lines. It can be seen that these are, as expected, linear, which confirms that the adsorption of propionic acid on carbon follows the Freundlich model. Once more this is what would be expected as the Langmuir model was developed for gaseous phase systems while the Freundlich model was developed for aqueous phase systems. As with the experimental isotherms (Figure 6.6) the Freundlich lines for MAST E-15-35-C and SS 607C are very similar, while the SS 208EA line has a shallower gradient.

As explained in Chapter 4, the Freundlich parameters, $1/n$ and k_f are the gradient of the line and the point at which it crosses the y axis, respectively, and are obtained from the logarithmic Freundlich graph. Larger values of $1/n$ indicate a weaker interaction between the adsorbate and the adsorbent, hence making regeneration more favourable, whilst greater values of k_f indicate a larger adsorbent capacity.

Table 6.2 presents the Freundlich constants for the experiments shown in Figure 6.8. The values show SS 607C to have the largest $1/n$ value which suggests a weaker interaction between the propionic acid and SS 607C carbon, whilst SS 208EA has the lowest $1/n$ value implying the strongest interaction between the propionic acid and SS 208EA carbon. As SS 208EA has the largest k_f value this suggests it also has the largest adsorption capacity, whereas SS 607C has the lowest adsorption capacity.

These results show the relationship between propionic acid and MAST E-15-35-C, SS 607C and SS 208EA carbons. However, this thesis is concerned with the treatment of metalworking fluid waste. Chapter 2 discussed the requirement for pre-treatment of the spent cutting fluid before the carbon adsorption unit. Whilst the WOWSEP process incorporates a gravity separation unit for the removal of particulates and a coalescence unit for the separation of free oils, a process method was required for the removal of emulsified oils. The available options (ultrafiltration, flocculation, polyelectrolyte, chemical splitting, centrifugation, biological aeration filtration, dissolved air flotation) were presented in Table 2.4.

Table 6.2 Freundlich Parameters Obtained for Equilibrium Batch Studies of Propionic Acid with MAST E-15-35-C, SS 607C and SS 208EA Carbons

Figure	Carbon	Adsorbate	Freundlich equation	*1/n*	k_f
6.8	E-15-35-C	Propionic acid	(lnq)=0.361(lnc)-5.375	0.361	0.0046
6.8	SS 607C	Propionic acid	(lnq)=0.394(lnc)-5.689	0.394	0.0034
6.8	SS 208EA	Propionic acid	(lnq)=0.275(lnc)-4.943	0.275	0.0071

As previously mentioned the simplest, easiest and most convenient methods available were ultrafiltration and chemical splitting. Therefore, to decipher which of the two methods would better compliment the carbon adsorption unit, equilibrium studies were conducted for each method using MAST E-15-50-C and SS 607C (Figure 6.9).

Generally, Figure 6.9 shows that both MAST E-15-50-C and SS 607C have a higher loading for the ultrafiltered solution than the chemically split solution. At concentrations less than approximately 600 mg l^{-1} the MAST E-15-50-C appears to have a higher loading than SS 607C for the ultrafiltered cutting fluid. At concentrations above this SS 607C outperforms MAST E-15-50-C. However, for the chemically split fluid MAST E-15-50-C outperforms SS 607C throughout the concentration range.

Figure 6.10 shows the corresponding Freundlich lines obtained from the same experiments presented in Figure 6.9. The MAST E-15-50-C lines for the ultrafiltered and chemically split solutions are almost parallel which suggests they behave in a similar manner. However, the MAST E-15-50-C/ ultrafiltered line is slightly above that of MAST E-15-50-C/chemically split line which indicates the MAST carbon has a slightly larger capacity for the ultrafiltered solution than the chemically split solution. Likewise, the Freundlich lines for SS 607C with the ultrafiltered and chemically split solutions show the ultrafiltered line to run higher than the chemically split line, again suggesting that SS 607C also has a larger adsorption capacity for the ultrafiltered cutting fluid.

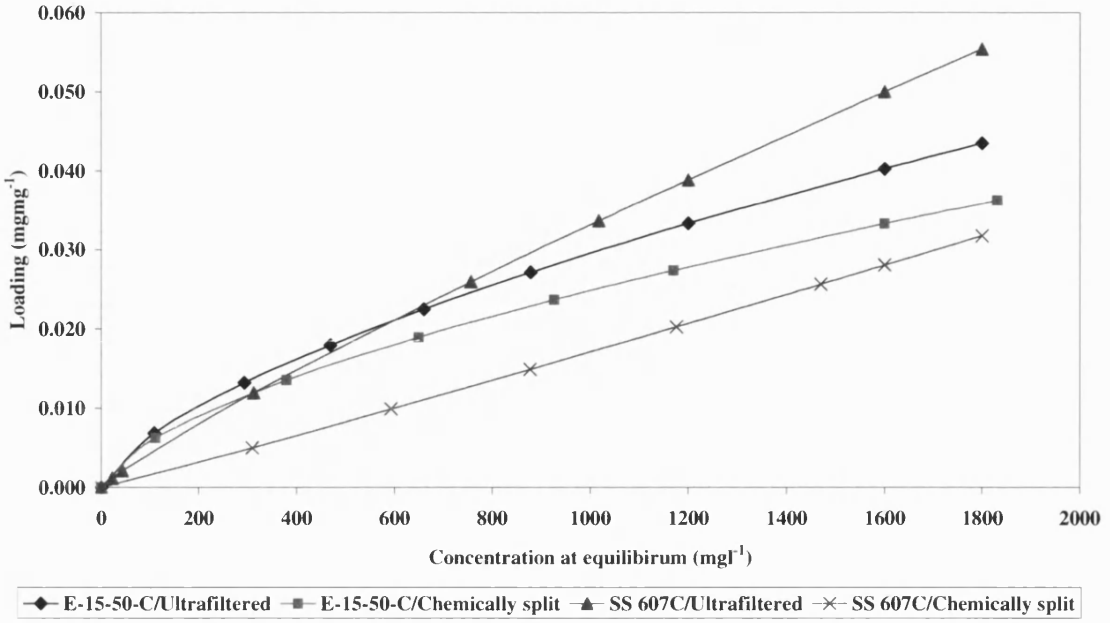

Figure 6.9 A comparison of experimental data obtained from equilibrium batch studies for MAST E-15-50-C and SS 607C carbons with ultrafiltered and chemically split cutting fluids

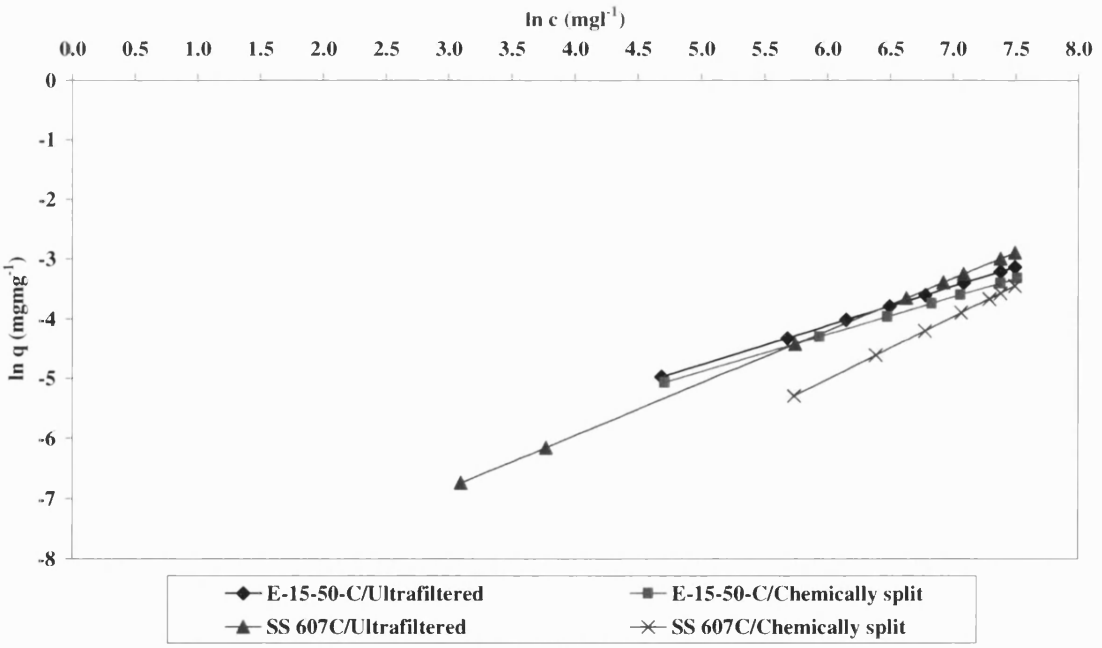

Figure 6.10 A comparison of logarithmic Freundlich plots for MAST E-15-50-C and SS607 carbons with ultrafiltered and chemically split cutting fluids

A comparison of MAST E-15-50-C and SS 607C for the ultrafiltered cutting fluid, on the other hand, shows the Freundlich lines to intersect. In addition, the graph shows that SS 607C has a higher loading at residual concentrations nearer to the initial concentrations, but the slightly steeper gradient of the SS 607C line indicates a higher sensitivity to concentration (*i.e.* a weaker adsorbate-adsorbent interaction). This is further confirmed by the Freundlich parameters shown in Table 6.3, where SS 607C has a higher *1/n* value than MAST E-15-50-C for the ultrafiltered cutting fluid. This implies that the ultrafiltered solution has a weaker interaction with SS 607C and than E-15-50-C. In addition, E-15-50-C has a much larger value of k_f for both adsorbate solutions than SS 607C suggesting it also has a larger adsorption capacity.

Table 6.3 Freundlich Parameters Obtained for Equilibrium Batch Studies of MAST E-15-50-C and SS 607C Carbons with Ultrafiltered and Chemically Split Cutting Fluids

Figure	Carbon	Adsorbate	Freundlich equation	*1/n*	k_f
6.10	E-15-50-C	Ultrafiltered	(lnq)=0.657(lnc)-8.059	0.657	0.00032
6.10	E-15-50-C	Chemically split	(lnq)=0.626(lnc)-8.018	0.626	0.00033
6.10	SS 607C	Ultrafiltered	(lnq)=0.876(lnc)-9.457	0.876	0.00008
6.10	SS 607C	Chemically split	(lnq)=1.049(lnc)-11.311	1.049	0.00001

Figure 6.11 shows a comparison of equilibrium isotherms for propionic acid, ultrafiltered and chemically split cutting fluid data using MAST E-15-50-C carbon. The graph shows the propionic acid to have a much steeper and sharper curve with a considerably higher loading (approximately 0.065 mg mg^{-1}) than the ultrafiltered (approximately 0.039 mg mg^{-1}) and chemically split (approximately 0.033 mg mg^{-1}) cutting fluids at an equilibrium concentration of 1800 mg l^{-1}. However, the graphs also show the ultrafiltered and chemically split isotherms are still increasing and have not yet reached their maximum values. Figure 6.12 shows the corresponding Freundlich lines for the experimental data shown in Figure 6.11. As expected the propionic acid line is above those for the ultrafiltered and chemically split cutting fluids, suggesting that E-15-50-C has a larger adsorption capacity for propionic acid. This is also verified by the Freundlich constants shown in Table 6.4, where propionic acid has the highest k_f value and the lowest *1/n* value.

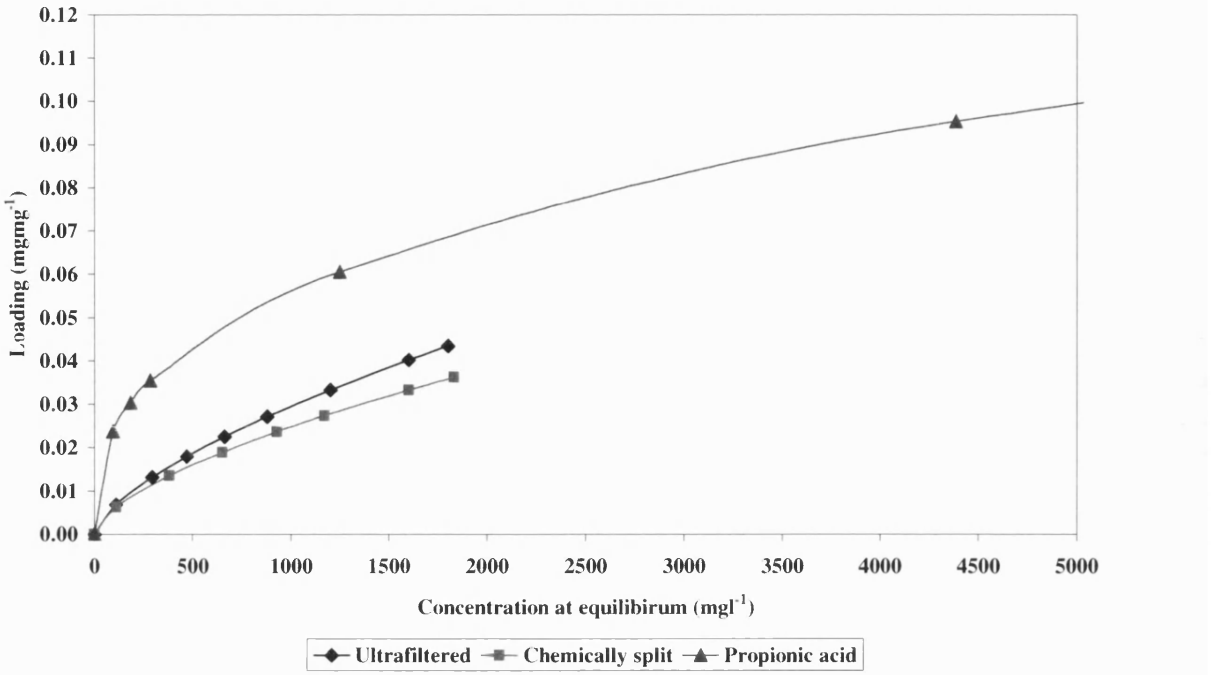

Figure 6.11 A comparison of experimental data obtained from equilibrium batch studies for propionic acid, ultrafiltered and chemically split cutting fluid with MAST E-15-50-C

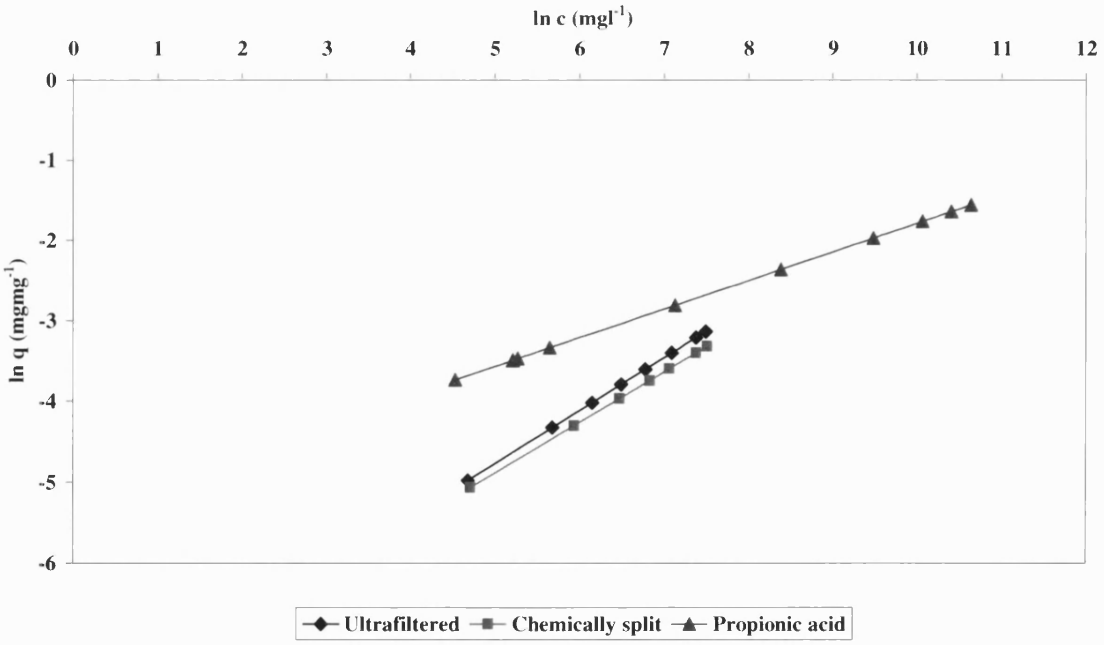

Figure 6.12 A comparison of logarithmic Freundlich plots for MAST carbon with ultrafiltered cutting fluid, chemically split cutting fluid and propionic acid

Figure 6.6 showed the highest loading for propionic acid with MAST E-15-50-C carbon to be approximately 0.2 mg mg^{-1}. The results for cutting fluids shown in Figure 6.11 therefore reveal ultrafiltered and chemically split solutions may be using no more than 20% of the available carbon capacity on a mass basis, which would suggest the carbon still has an available adsorption capacity and the possibility of the presence of soluble non-adsorbable compound(s). However, so far it has been assumed that the cutting fluid is a homogeneous, single component solution. Chapter 2 described the typical contents of a cutting fluid solution showing that it is not a single component solution but a multi-component solution. Therefore, as a first approximation, the solution is now regarded to be a binary mixture, consisting of an adsorbable organic fraction (referred to as "organics") and a non-adsorbable amine fraction (referred to as "amines").

Table 6.4 Freundlich Parameters Obtained for Equilibrium Batch Studies of MAST E-15-50-C Carbon with Ultrafiltered Cutting Fluid, Chemically Split Cutting Fluid and Propionic Acid

Figure	Carbon	Adsorbate	Freundlich equation	*1/n*	k_f
6.12	E-15-50-C	Ultrafiltered	(lnq)=0.657(lnc)-8.059	0.657	0.00032
6.12	E-15-50-C	Chemically split	(lnq)=0.626(lnc)-8.018	0.626	0.00033
6.12	E-15-50-C	Propionic acid	(lnq)=0.361(lnc)-5.375	0.361	0.0046

The removal of the "amines" is required for a more efficient purification process (again, this is confirmed later in Chapter 7). As described in Chapter 4, ion exchange is simple, easy to use and inexpensive, which classifies it as is a potential method for the removal of the "amine" fraction. In addition, as its function is similar to that of carbon adsorption, the same (or part of the same) equipment as the adsorption unit could be used for the laboratory-scale studies, further reducing process costs. Batch equilibrium experiments were conducted with six ion exchange resins (namely Duolite, Dowex 50, Dowex Macroporous (M), Amberlite XAD-4, Purolite C150H and Purolite MN500) and compared with the two carbons adsorbents (MAST and Sutcliffe Speakman) using the ultrafiltered and chemically split solutions. All of the ion exchange resins are based on polystyrene. Dowex M and Dowex 50 are weak anion and strong cation exchangers, respectively. Purolite C150H, Amberlite XAD-4 and Duolite are copolymers of styrene and divinylbenzene, whilst Purolite MN500 is a crosslinked polystyrene resin. Both Purolite

C150H and MN500 are strong acidic, cationic resins, with a macroporous structure. However, MN500 is a macronet, which is described in Chapter 3 as a solid with a microporous structure, presenting it with a high surface area (>900 m^2 g^{-1}). This allows MN500 to act as an adsorbent as well as an ion exchange resin. In addition, macronets may also be steam regenerated *in-situ*, (as with adsorbents) or chemically (as with ion exchange resins).

The equilibrium study results produced by the ultrafiltered solution and the various adsorbents are shown in Figure 6.13.

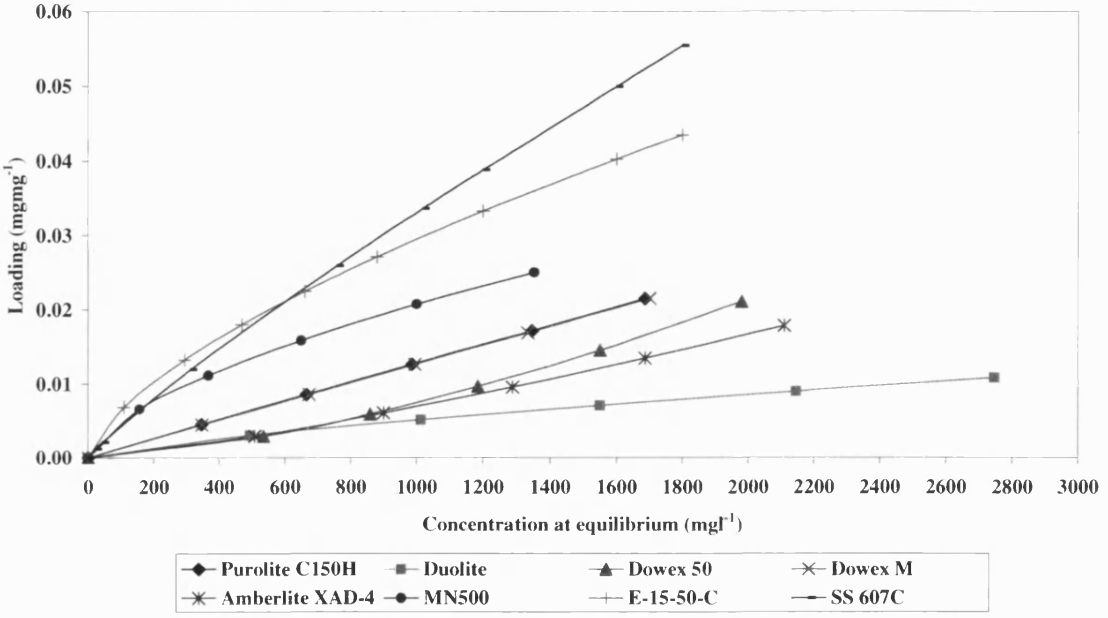

Figure 6.13 A comparison of experimental data obtained from equilibrium batch studies for ultrafiltered cutting fluid with various ion exchange resins, MAST E-15-50-C and SS 607C

Of the ion exchange resins, MN500 gave the steeper, sharper graph, similar to the carbon adsorbents, while Duolite gave the shallowest isotherm. Duolite was also shown to have the lowest Freundlich line in Figure 6.14, which suggests it is the least desirable ion exchange resin. MN500, on the other hand, has a Freundlich line reasonably close to those of the carbons, suggesting it has a good adsorption capability. This was as expected because the MN500 has a macro and microporous structure comparable to that of an adsorbent.

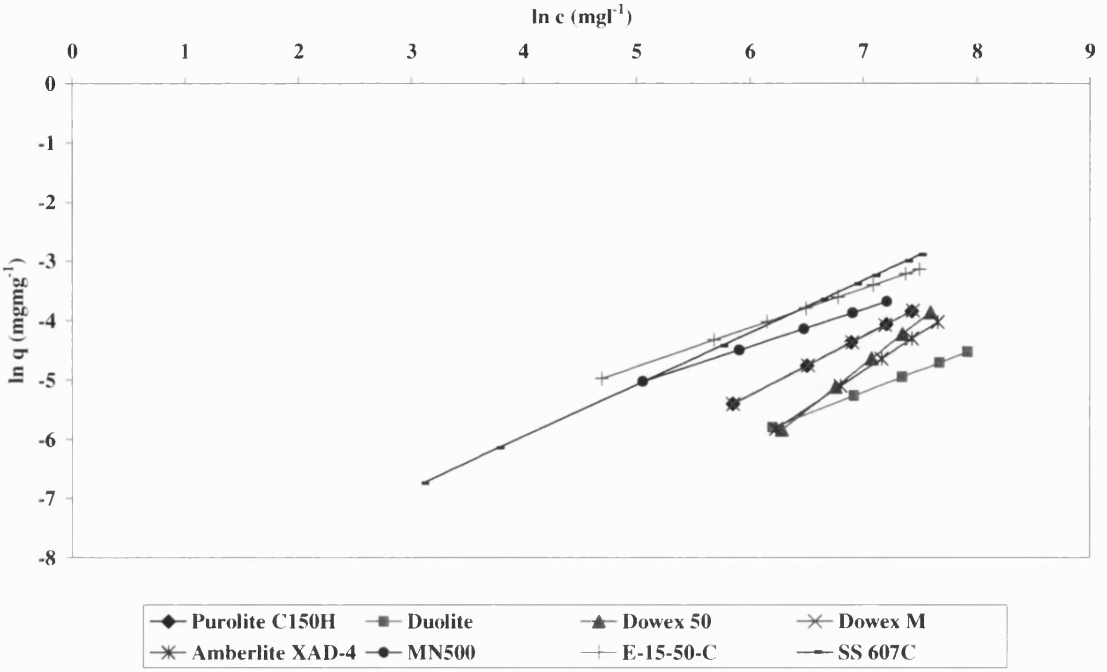

Figure 6.14 A comparison of logarithmic Freundlich plots for ultrafiltered cutting fluid with various ion exchange resins, MAST E-15-50-C and SS 607C

The Freundlich parameters (Table 6.5) show Dowex 50 to have the lowest adsorption capacity (lowest k_f value) and the weakest interaction between the resin and adsorbate (highest $1/n$ value), while MN500 and MAST E-15-50-C have the largest adsorption capacities (highest k_f values) and strongest interactions (lowest $1/n$ values).

Equilibrium batch experiments with the ion exchange resins were also carried out using chemically split cutting fluid (Figure 6.15). Similar to Figure 6.13, Figure 6.15 shows the carbons and MN500 to have the highest isotherms while Duolite has the lowest isotherm. Purolite C150H and Dowex M are shown to have almost identical isotherms as in Figure 6.13. MN500 was shown to behave more like a carbon with the ultrafiltered cutting fluid (Figure 6.13), however with the chemically split cutting fluid (Figure 6.15) it appears to behave more like a mixture of the carbon and the ion exchange resins (the MN500 graph starts off like the carbons, but the line finishes with the ion exchange resin).

Table 6.5 Freundlich Parameters Obtained for Equilibrium Batch Studies of Ultrafiltered Cutting Fluid with Various Ion Exchange Resins, MAST E-15-50-C and SS 607C

Figure	Carbon	Adsorbate	Freundlich equation	*1/n*	k_f
6.14	C150H	Ultrafiltered	(lnq)=0.987(lnc)-11.177	0.987	0.0000140
6.14	Duolite	Ultrafiltered	(lnq)=0.744(lnc)-10.411	0.744	0.0000301
6.14	Dowex 50	Ultrafiltered	(lnq)=1.517(lnc)-15.371	1.517	0.0000002
6.14	Dowex M	Ultrafiltered	(lnq)=0.989(lnc)-11.193	0.989	0.0000138
6.14	XAD-4	Ultrafiltered	(lnq)=1.268(lnc)-13.727	1.268	0.0000011
6.14	MN500	Ultrafiltered	(lnq)=0.621(lnc)-8.165	0.621	0.0002845
6.14	E-15-50-C	Ultrafiltered	(lnq)=0.657(lnc)-8.059	0.657	0.0003162
6.14	SS 607C	Ultrafiltered	(lnq)=0.876(lnc)-9.457	0.876	0.0000781

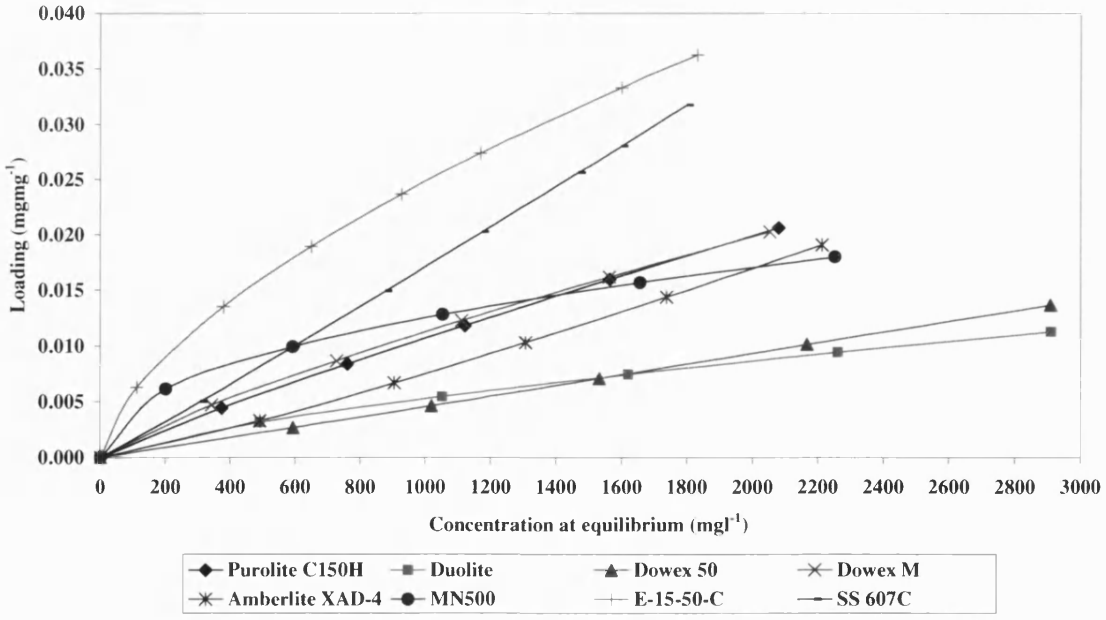

Figure 6.15 A comparison of experimental data obtained from equilibrium batch studies for chemically split cutting fluid with various ion exchange resins, MAST E-15-50-C and SS 607C

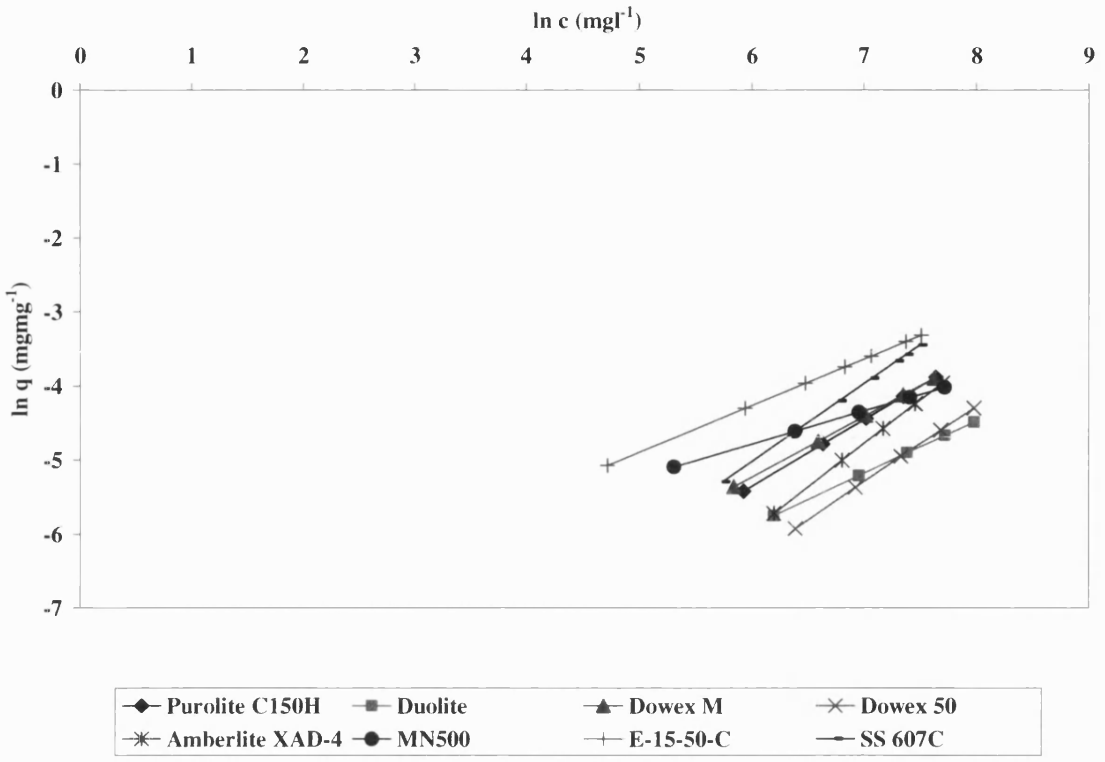

Figure 6.16 A comparison of logarithmic Freundlich plots for chemically split cutting fluid with various ion exchange resins, MAST E-15-50-C and SS 607C

Table 6.6 Freundlich Parameters Obtained for Equilibrium Batch Studies of Chemically Split Cutting Fluid with Various Ion Exchange Resins, MAST E-15-50-C and SS 607C

Figure	Carbon	Adsorbate	Freundlich equation	*1/n*	k_f
6.16	C150H	Chemically split	(lnq)=0.895(lnc)-10.717	0.895	0.0000222
6.16	Duolite	Chemically split	(lnq)=0.711(lnc)-10.154	0.711	0.0000389
6.16	Dowex 50	Chemically split	(lnq)=1.026(lnc)-12.964	1.026	0.0000038
6.16	Dowex M	Chemically split	(lnq)=0.817(lnc)-10.127	0.817	0.0000400
6.16	XAD-4	Chemically split	(lnq)=1.169(lnc)-12.964	1.169	0.0000023
6.16	MN500	Chemically split	(lnq)=0.444(lnc)-7.445	0.444	0.0005846
6.16	E-15-50-C	Chemically split	(lnq)=0.626(lnc)-8.018	0.626	0.0003295
6.16	SS 607C	Chemically split	(lnq)=1.049(lnc)-11.311	1.049	0.0000122

A comparison of the corresponding Freundlich plots (Figure 6.16) and Freundlich constants (Table 6.6) shows that XAD-4 has the highest *1/n* value and the lowest k_f value, suggesting it has the weakest adsorbate/adsorbent interaction and the lowest adsorbent capacity, whilst MN500 has the lowest *1/n* value and the highest k_f value suggesting it has the strongest adsorbate/adsorbent interaction and the highest adsorbent capacity.

Despite the minor differences, both the ultrafiltered cutting fluid and the chemically split cutting fluid generally have similar trends.

The SEM micrographs and ASAP studies (Chapter 5) also showed a difference between the carbons and ion exchange resins. The SEM micrographs barely showed any porosity for Purolite C150H (Figure 5.31) and Amberlite XAD-4 (Figure 5.34), even at magnifications of x5000, while the ASAP studies showed MAST E-15-50-C to have the highest capacity of all the adsorbents tested.

Even though MN500 gave better adsorption properties than the other ion exchange resins, practical reasons such as its availability and expense prevented its use in the WOWSEP process. Therefore, Purolite C150H was the ion exchange resin used for the remaining experiments.

Figure 6.17 shows a comparison of experimental data for the ultrafiltered cutting fluid with E-15-50-C carbon, C150H ion exchange resin and a 50/50 mixture of E-15-50-C and C150H. The graph shows their respective loadings, at an equilibrium concentration of 1600 mg l^{-1}, to be approximately 0.041 mg mg^{-1}, 0.020 mg mg^{-1} and 0.071 mg mg^{-1}. These values show the highest loading is shown to be achieved by E-15-50-C mixed with C150H.

If it were to be assumed that the cutting fluid was a homogeneous single component solution, then it would be expected that the loading of this on to carbon and the ion exchange resin would be the same regardless of whether the batch studies were conducted with a single adsorbent /ion exchange resin or a mixture of the two. However, as can be seen, this is not the case and the loading of the mixture is greater than that of the summation of the two individual loadings. This would suggest it would be beneficial to the WOWSEP process to have ion exchange as an additional step to carbon adsorption.

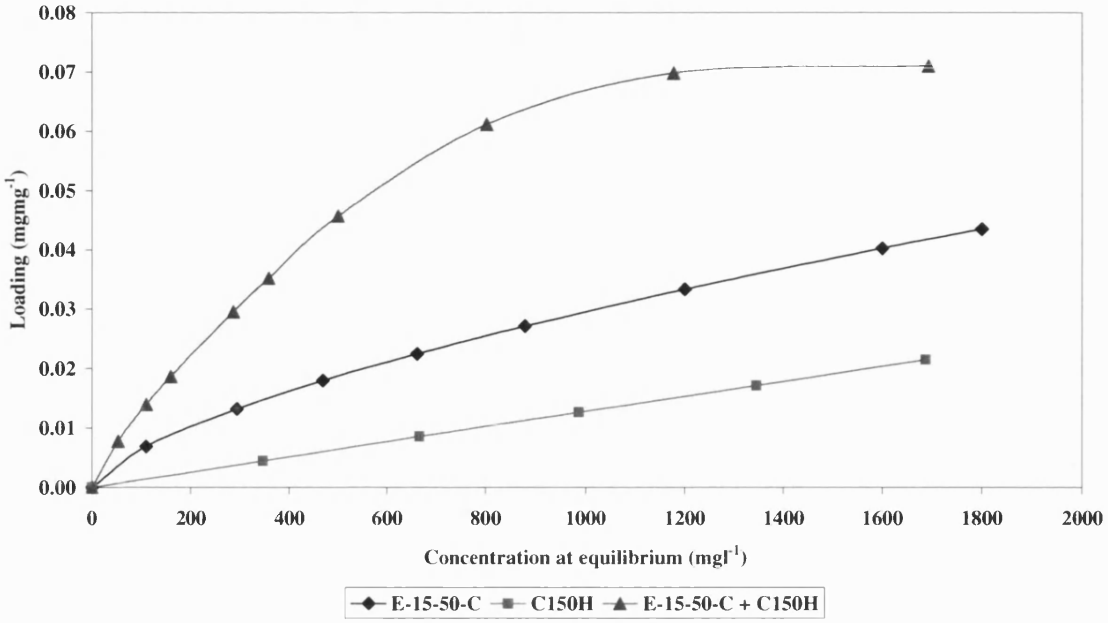

Figure 6.17 A comparison of experimental data obtained from equilibrium studies for ultrafiltered cutting with fluid MAST E-15-50-C, Purolite C150H and a 50/50 mixture MAST E-15-50-C and Purolite C150H

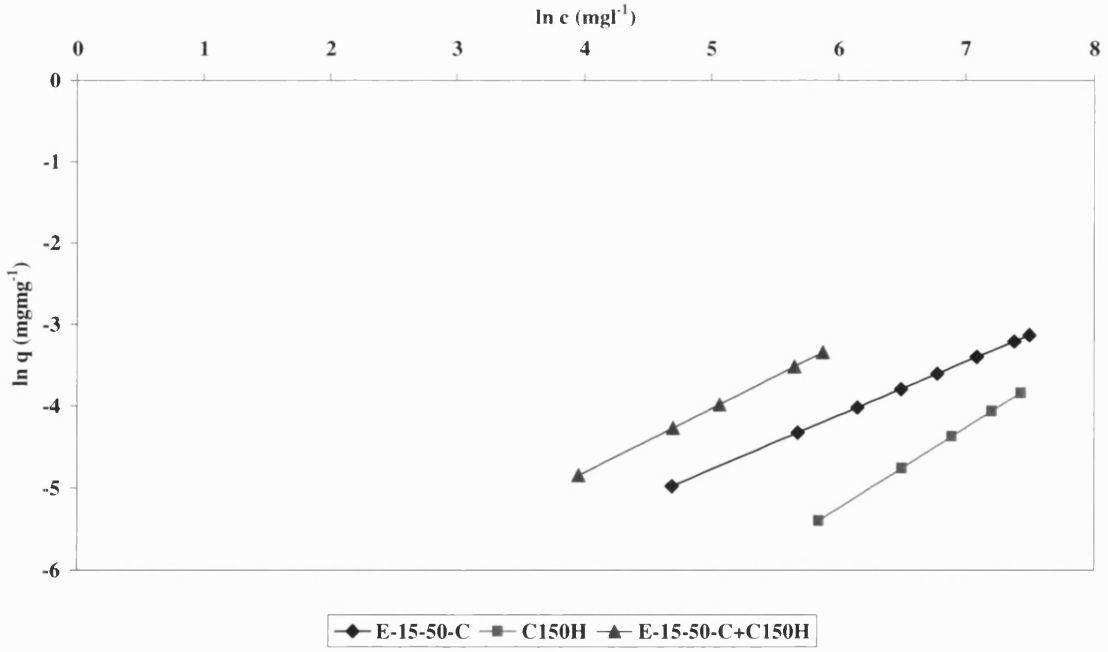

Figure 6.18 A comparison of logarithmic Freundlich plots for ultrafiltered cutting fluid with MAST E-15-50-C, Purolite C150H and 50/50 Mixture of MAST E-15-50-C and Purolite C150H

Figure 6.18 shows the corresponding Freundlich lines obtained from the experimental data presented in Figure 6.17, the Freundlich constants, of which, are shown in Table 6.7. Figure 6.18 shows that the carbon/resin mixture has the highest loading for the ultrafiltered cutting fluid followed by the carbon alone and then the ion exchange resin. Likewise, the carbon/resin mixture is shown to have the highest k_f value (in Table 6.7) indicating it has the highest adsorption capacity.

Table 6.7 Freundlich Parameters Obtained for Equilibrium Batch Studies of Ultrafiltered Cutting Fluid with MAST E-15-50-C, Purolite C150H and 50/50 Mixture of MAST E-15-50-C and Purolite C150H

Figure	Carbon/resin	Adsorbate	Freundlich equation	*1/n*	k_f
6.18	E-15-50-C	Ultrafiltered	(lnq)=0.657(lnc)-8.059	0.657	0.00032
6.18	C150H	Ultrafiltered	(lnq)=0.987(lnc)-11.177	0.987	0.00001
6.18	E-15-50-C/C150H	Ultrafiltered	(lnq)=0.781(lnc)-7.938	0.781	0.00036

It must be noted, however, that the maximum loading for the C150H/E-15-50-C mixture with the ultrafiltered cutting fluid has still not quite reached that of the propionic acid (with either carbon) at the same equilibrium concentration (shown in Figure 6.11). This indicates that there may be further compounds which are non-adsorbable. However, as previously explained, due to the complexity of the mixture, and given the fact that confidentiality restricted vital information and as time constraints were tight, it was not possible to investigate this matter further. Therefore for the purposes of the WOWSEP process, carbon adsorption alone was regarded to be sufficient, and ion exchange was deemed to be an additional process if extra purification were to be required.

6.2.3 Conclusions

Generally, the equilibrium studies have shown that an additional step to carbon adsorption would be appropriate for further purification of cutting fluid waste. Ion exchange removed at least one of the soluble components present in the ultrafiltered and chemically split cutting fluids, which was not removed by carbon. Therefore ion exchange was found to be beneficial to the WOWSEP process.

Table 6.8 Summary of the Maximum Loadings and Freundlich Parameters obtained for Equilibrium Batch Experiments shown in Figures 6.6 to 6.18

Figure	Carbon/resin	Adsorbate	Max loading on graph (mg mg^{-1})	*1/n*	k_f
6.6/6.8	E-15-35-C	Propionic acid	0.1952	0.361	0.0046295
6.6/6.8	SS 607C	Propionic acid	0.1998	0.398	0.0033180
6.6/6.8	SS 208EA	Propionic acid	0.1369	0.275	0.0071346
6.9/6.10	E-15-50-C	Ultrafiltered	0.0435	0.657	0.0003163
6.9/6.10	E-15-50-C	Chemically split	0.0362	0.626	0.0003290
6.9/6.10	SS 607C	Ultrafiltered	0.0554	0.876	0.0000782
6.9/6.10	SS 607C	Chemically split	0.0317	1.049	0.0000122
6.11/6.12	E-15-50-C	Ultrafiltered	0.0435	0.657	0.0003163
6.11/6.12	E-15-50-C	Chemically split	0.0362	0.626	0.0003290
6.11/6.12	E-15-50-C	Propionic acid	0.1120	0.361	0.0046295
6.13/6.14	C150H	Ultrafiltered	0.0215	0.987	0.0000140
6.13/6.14	Duolite	Ultrafiltered	0.0108	0.744	0.0000301
6.13/6.14	Dowex 50	Ultrafiltered	0.0211	1.517	0.0000002
6.13/6.14	Dowex M	Ultrafiltered	0.0216	0.989	0.0000138
6.13/6.14	XAD-4	Ultrafiltered	0.0179	1.268	0.0000011
6.13/6.14	MN500	Ultrafiltered	0.0251	0.621	0.0002845
6.13/6.14	E-15-50-C	Ultrafiltered	0.0435	0.657	0.0003163
6.13/6.14	SS 607C	Ultrafiltered	0.0554	0.876	0.0000782
6.15/6.16	C150H	Chemically split	0.0206	0.895	0.0000222
6.15/6.16	Duolite	Chemically split	0.0113	0.711	0.0000389
6.15/6.16	Dowex 50	Chemically split	0.0137	1.026	0.0000038
6.15/6.16	Dowex M	Chemically split	0.0203	0.817	0.0000400
6.15/6.16	XAD-4	Chemically split	0.0191	1.169	0.0000023
6.15/6.16	MN500	Chemically split	0.0180	0.444	0.0005846
6.15/6.16	E-15-50-C	Chemically split	0.0362	0.626	0.0003295
6.15/6.16	SS 607C	Chemically split	0.0317	1.049	0.0000122
6.17/6.18	E-15-50-C	Ultrafiltered	0.0435	0.657	0.0003163
6.17/6.18	C150H	Ultrafiltered	0.0215	0.987	0.0000140
6.17/6.18	E-15-50-C+C150H	Ultrafiltered	0.0710	0.781	0.0003569

The purpose of Purolite MN500 to act as both an ion exchange resin and an adsorbent has been demonstrated in these studies: (i) like the ion exchange resins, it has been shown to remove some of the soluble compound(s), which could not be removed by the carbon, and (ii) like the carbons it has produced a BET Type I adsorption isotherm.

The information obtained from the equilibrium experiments provided the means to select the 'best' adsorbent for use in the laboratory-scale tests. The equilibrium studies alongside SEM and ASAP studies have shown MAST E-15-50-C carbon to have the greatest adsorbent capacity, with the exception of the MAST/Purolite mixture.

Table 6.8 gives a summary of the maximum equilibrium loadings and Freundlich constants obtained for all the experiments mentioned in the batch studies. It clearly shows that the equilibrium loadings of the cutting fluid, whether ultrafiltered or chemically split, is much lower than that achieved with propionic acid (which was used as a benchmark organic chemical).

When comparing the equilibrium loadings from the dynamic column experiments detailed in the next Chapter (Chapter 7) and those from the batch equilibrium experiments reported in this Chapter, it will be seen that the batch equilibrium loadings are much lower for the cutting fluid. The reasons for the differences in equilibrium results from the batch (static) and the column (dynamic) methods are associated with the complex structure of the cutting fluid. An explanation for these findings will be discussed in greater detail in Chapter 7.

7.0 Dynamic Column Studies

Chapter 6 discussed kinetic and equilibrium studies, which showed the maximum adsorbent capacity using propionic acid, the extent to which cutting fluids are able to adsorb onto carbon, as well as the advantage of using ion exchange. Overall, the kinetic and equilibrium studies proved that further studies concerning the dynamic adsorption of cutting fluids onto carbon would be worthwhile.

One of the aims of this research project was to design, build and apply an integrated system for the downstream purification of factory wastewater containing soluble oils and organic chemicals in the form of metalworking fluids. This was achieved through the development of a process consisting of carbon adsorption and ion exchange units, with the potential of the carbon bed being regenerated *in-situ.*

This Chapter begins with a general introduction to dynamic column studies, with a brief overview of the design considerations required to build an integrated adsorption/regeneration system, followed by a more specific experimental procedure which was adopted for the WOWSEP process. An investigation of factors and initial design conditions (such as influent flowrate, concentration, column length *etc.*), which may affect the overall quality of the process, was conducted. A model was also created to explain various ambiguities in the results and the conclusions provide an overview of the results.

7.1 Introduction

Adsorption processes are, in many cases, associated with dynamic column studies. These studies are more complex than simple stirred tank batch processes that reach equilibrium as mass transfer resistances and unsteady state needs to be considered (Gean-Koplis, 1993), although unsteady state may also occur in more complex batch processes. The results of dynamic column studies provide information on the way the system is operated (for example the time taken for breakthrough to occur) and the overall dynamics of the system (which determines the efficiency of the process) rather than just equilibrium considerations (which determine whether a specific adsorbate can be adsorbed by a specific adsorbent and to what extent).

Column studies involve a feed solution being pumped through a carbon column (either in an upward or downward direction depending on the system design). Adsorption takes place from the inlet of the column and proceeds to the exit. Initially, the bed inlet is assumed to contain no solute (*i.e.* C_o=0, where C_o is the inlet feed concentration). When the fluid first comes into contact with the carbon the greater part of mass transfer from the bulk fluid to the carbon takes place (*i.e.* adsorption). During the course of adsorption, the concentration near the inlet of the column increases, forming a saturated zone, called the mass transfer zone (mtz). The fluid concentration or adsorbent loading profile of the adsorbable component over the mass transfer zone is known as the mass transfer front (mtf). After the feed passes through a region of the bed whose depth is equal to the mass transfer zone, the concentration of the contaminant in the feed is reduced from its feed value to its minimum value. No further adsorption occurs within the bed below the mass transfer zone. As the top layers of activated carbon granules become saturated with the organic contaminant material, the mass transfer zone moves through the bed until breakthrough occurs, at time T_b (Metcalf and Eddy, 1991). Breakthrough is described as the point at which the effluent concentration is at the maximum allowed for disposal. It often has a C/C_o ratio in the range of $0.01<C/C_o<0.05$ (where C is the effluent concentration). At the leading edge of the transfer front, the impurity concentration in the carrier fluid is equal to the breakthrough concentration. At the trailing edge of the transfer front, the impurity concentration in the carrier fluid is largely equal to that in the feed (C_o). Therefore if the effluent concentration is measured continuously, breakthrough of the adsorbable components is observed when the mass transfer zone approaches the exit. This occurs from time T_b to T_e (where T_e is the time at the end of breakthrough) and is usually when C/C_o=1.0 (Suzuki, 1990).

Generally, the adsorbent bed is viewed as a sum of two sections: the equilibrium section (the loading for which can be obtained from equilibrium batch studies) and the Length of Unused Bed (LUB). The LUB is defined as the additional quantity of adsorbent added to the column to compensate for the presence of a mass transfer zone during dynamic adsorption and it corresponds to the bed length from which breakthrough is observed in the effluent concentration (at time T_b), through to time T_e.

The most common way to represent breakthrough data is in graphical form, of effluent concentration (C) versus time (T) (Figure 7.0). This is known as a breakthrough (or

loading) graph. The effluent concentration is often represented as a ratio of C/C_o (dimensionless) to facilitate the interpretation of the results on a comparable basis.

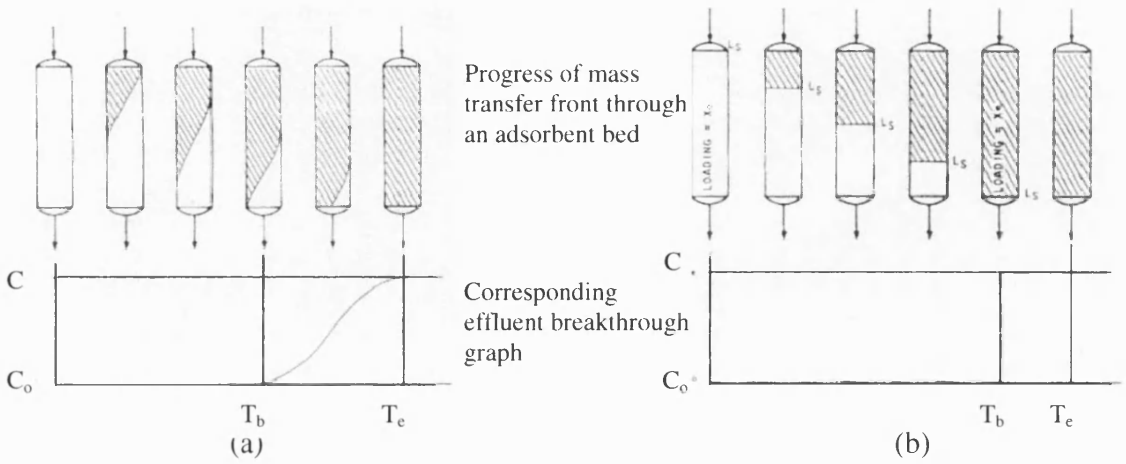

Figure 7.0 (a) Stable mass transfer front, (b) Stoichiometric mass transfer front (cited in Collins, 1965)

Breakthrough profiles show the composition of the effluent from the carbon column as a function of throughput, and provide information on many dependent design variables such as adsorbent capacity. This makes them the best experimental determination of column performance. Additionally, breakthrough data are often used to select an adsorbent by comparing two or more adsorbents under identical conditions and to evaluate other parameters such as the change in adsorbent capacity with multiple cycles, counter-current operation and multiple column adsorption (Fox and Kennedy, 1985).

When studying adsorption breakthrough profiles, the general features to consider are:

- The shape of the breakthrough curve - This is significant as it indicates the feasibility of bed utilisation. Ideally, a steep, narrow s-shaped curve (shown in Figure 7.0(a)) is desirable as it represents a stable mass transfer zone and a viable system. The major part of adsorption takes place in a relatively narrow mass transfer zone, at any time. As the solution continues to flow, the s-shaped mass transfer zone moves down the column. The effluent concentration remains near zero until the mass transfer zone reaches the column outlet. At this point (breakpoint) the outlet concentration starts to rise rapidly until the end of the breakthrough curve.

- The width of the mass transfer zone - This signifies the efficiency of the system. A narrow mass transfer zone gives a steep breakthrough curve and suggests most of the bed capacity is used at the breakpoint. This makes efficient use of the adsorbent bed and lowers the energy costs for regeneration. On the other hand, a broad, shallow breakthrough curve is produced by a low flowrate, which subsequently spreads the mass transfer zone. Therefore the shape of the adsorption isotherm ultimately depends on the width and shape of the mass transfer zone, which is governed by factors such as flowrate, mass transfer rate to the particles and diffusion in the pores.

- The breakthrough time - This is arbitrarily chosen to satisfy the specific needs of a process. Ideally, for an effective system, at the time of breakthrough, the process should be stopped and the bed replaced.

- The Empty Bed Contact Time (EBCT) - This is the time taken for the feed solution to pass through the column. It is dependent on column length and flowrate; a slower flowrate produces a larger EBCT, resulting in a greater lifetime for the columns. In practice, an EBCT of 15 minutes is common (Horner, 1999). The EBCT is one of the major design variables for liquid phase carbon adsorption, along with system configuration (a combination of the number of beds required and whether they should be placed in series or parallel) and carbon usage rate (although the former two factors have an influence on the latter). For a single adsorber, the EBCT is normally chosen to be large enough to minimize carbon usage rate (FRTR, 2005). The EBCT is discussed in more detail in Section 7.4.

- The mass balances and loadings – The mass balances consider the mass of adsorbent, the column length, the adsorbate flowrate, the feed concentration of adsorbate, the total throughput of the adsorbate and the total mass of adsorbate adsorbed. From these values the loading is calculated by dividing the mass adsorbed by the mass of adsorbent. The loading therefore takes into account factors such as mass of adsorbent (therefore indirectly the column length) and the initial influent concentration. Generally the loading is more useful in design considerations than the total mass adsorbed.

- The presence of non-adsorbable compounds – These can produce immediate breakthrough. However an early breakthrough may be caused by other factors in the system design (such as short column length, high flowrate, high influent concentration, adsorbate pH *etc.*) or early breakthrough may be attributed to the mesoporous nature of adsorbent, *e.g.* the non-adsorbable compounds may block the mesopores, preventing the diffusion of adsorbable molecules into the micropore structure of the adsorbent.

7.2 Design of an adsorption column

The main parameters that need to be considered when designing an adsorption column are the contact time, carbon usage rate and pre-treatment requirements. Initial assumptions are normally made of isothermal adsorption, uniform flow, single adsorbates and constant intraparticle diffusivity. This information is not revealed by equilibrium isotherm studies. Hence dynamic column studies are essential.

Primarily, column studies are conducted on a laboratory-scale as this provides more information than a full-scale process. This is especially true if fresh adsorbent is used and regeneration is contemplated. In order to efficiently carry out laboratory-scale column tests, information on the adsorbent characteristics, column diameter, feed flowrate, adsorbent bed depth, adsorbent mass, contact time, influent concentration, and the desired effluent concentration is required. Much of this information is obtained through repeated trial and error experiments. Initial data (such as adsorption isotherms, loading curves and regeneration curves) obtained from laboratory-scale experiments, define the outline for a theoretical design, and suggests additional experimental work to better define and improve the full-scale process design. The conceptual design identifies process configuration, adsorbent selection, integration of adsorption with other processes, major items of capital equipment and their sizes, general operating conditions, general mass and energy balances and cost estimating (Fox and Kennedy, 1985). Therefore laboratory-scale tests and the conceptual design of a full-scale system must be carried out in parallel, as an iterative process. However, since the conceptual design is based upon experimental data, the amount of uncertainty in the design is a direct function of the quality and the amount of data supporting it. So, whilst the design is a fairly costly step it is extremely important and it ultimately leads to the commercialisation of an adsorption process.

7.3 Experimental procedure

Bench-scale dynamic adsorption experiments were performed using a laboratory-scale rig (Figures 7.1 and 7.2). The labels 'A, B, C, D, E and F' in Figure 7.1, refer to the pieces of equipment shown in the schematic diagram (Figure 7.2).

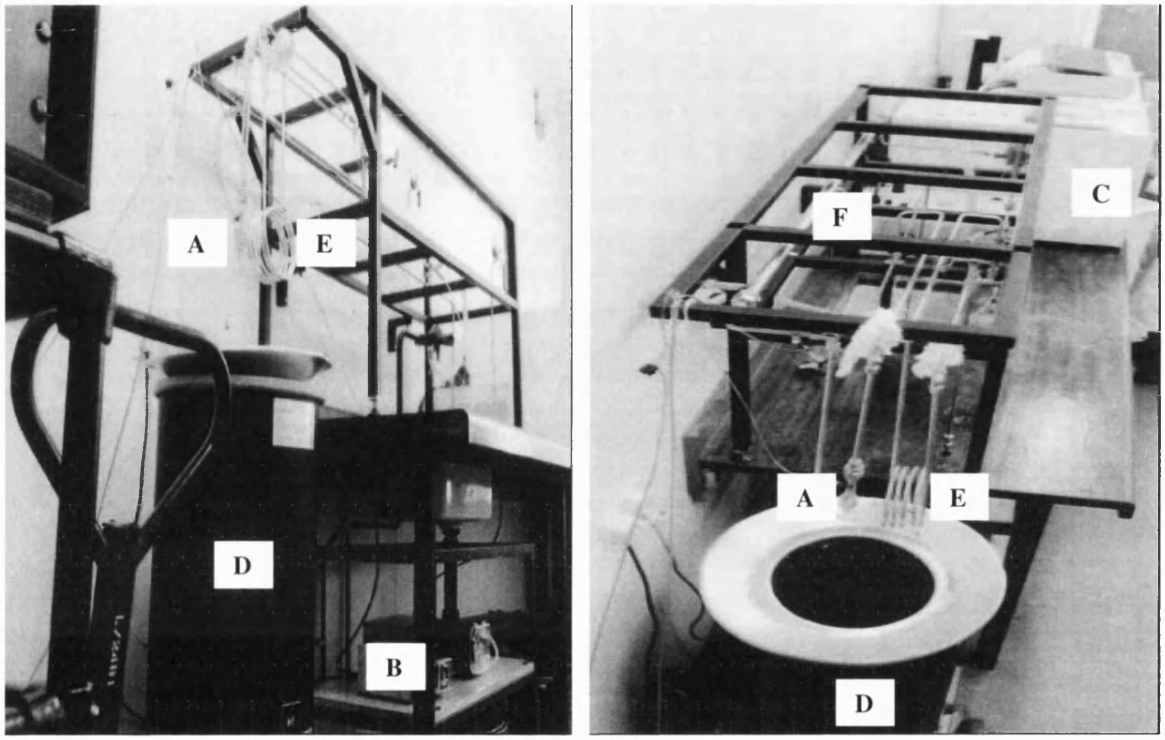

Figure 7.1 Photographs of laboratory-scale rig

The laboratory-scale rig consisted of a 1.27 cm (½") stainless steel column (A), packed with granular activated carbon. Stainless steel meshes were placed at either end of the column to restrain the carbon and provide an even flow distribution, and prevent channelling of the feed solution. This system was designed such that preliminary adsorption and regeneration studies (Chapter 8), of soluble oils and organic chemicals from factory wastewater, could take place *in–situ*, thus saving on cost, and complexity of construction.

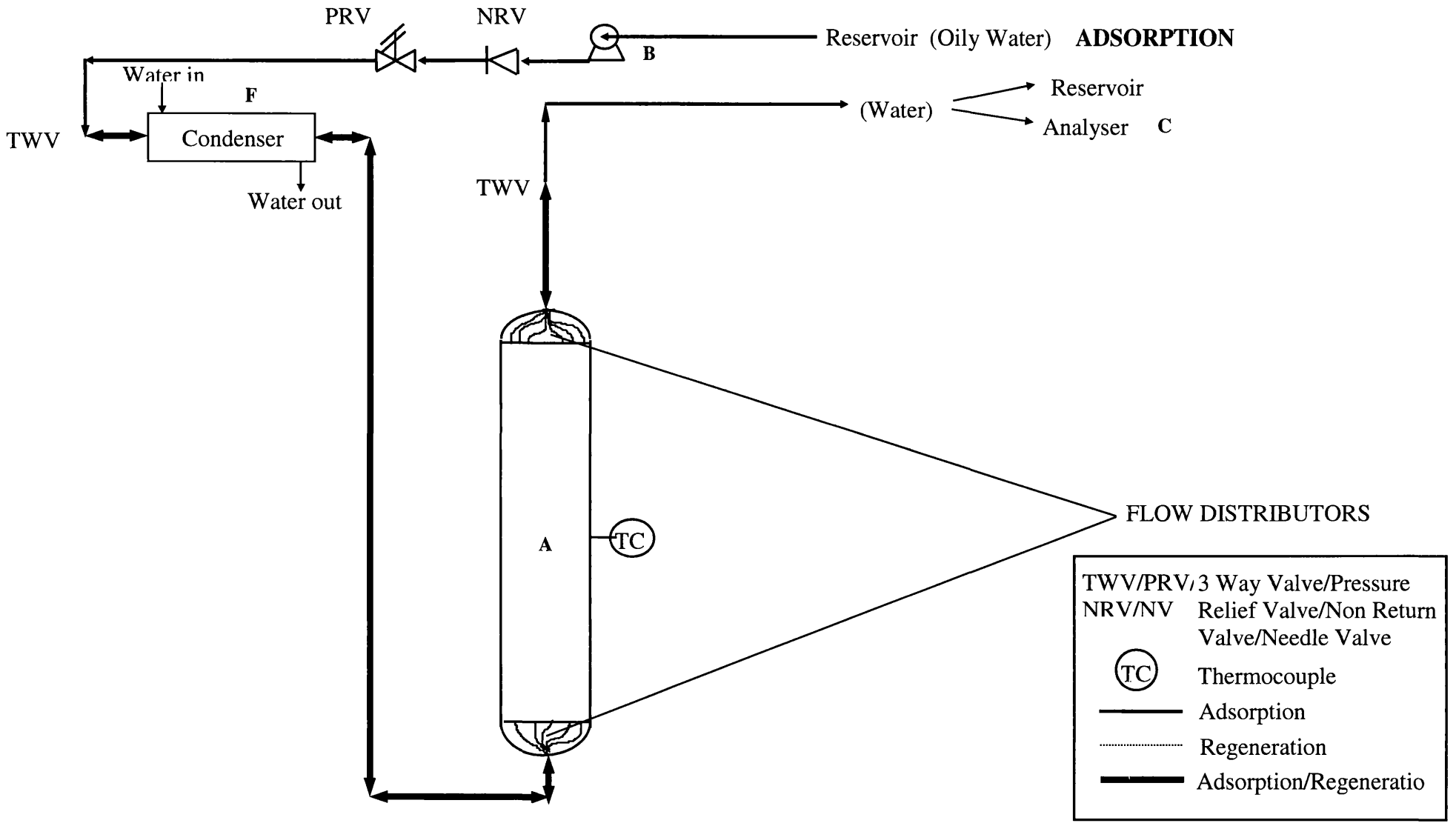

Figure 7.2 Schematic diagram of the adsorption side laboratory-scale rig

Before initial use, the system was primed with ultra-pure water, in order to rinse out any surplus carbonaceous materials. This ensured any subsequent measurements of carbon adsorption to be truly representative. The feed, at a known concentration, was then pumped upwards, using a Watson Marlow peristaltic pump (B), through the column at the desired flowrate. The effluent was collected and analysed using a Dohrmann DC180 TOC analyser (C). The other major pieces of equipment, such as the fluidised sand bath (D), the regeneration coil (E) and the condenser (F) were used for the regeneration studies.

Effluent samples were taken periodically, analysed using the TOC analyser and plotted to produce breakthrough curves, making the initial assumption (later proved to be invalid from a scientific point of view, although not from an industrial point of view) that the total organic fraction of the feed was a pseudo-single component. All the adsorption experiments were carried out at ambient room temperature (approx 20°C) in order to represent typical industrial conditions. The main variables in these experiments were: adsorbent bed length ranging from 10-100 cm, feed flowrate ranging from 150-600 cm^3 hr^{-1} and feed concentrations ranging from 120-11,000 mg l^{-1} TOC. A comparison of naturally derived coconut shell carbons supplied by Sutcliffe Speakman (SS) and a variety of novel "phenolic resin carbons" (PRC) supplied by MAST Carbon Ltd. were used for the dynamic column studies. The feed used was R5/026/03, a semi-synthetic cutting fluid supplied by D. A. Stuart Oil Ltd., but pre-treated (by chemical splitting or ultrafiltration) by PERA. Other simpler fluids (such as butyl glycol and propionic acid) were also used for comparative purposes.

7.4 Results and discussions

As previously mentioned, in order to design an efficient and effective prototype for the WOWSEP process, a series of laboratory experiments had to be conducted. These experiments study the effect of various factors such as feed flowrate, feed concentration, bed length, loading until breakthrough and complete (equilibrium) loading *etc.* Table 7.0 gives a summary of all the conditions and values of the loadings for the experiments discussed in this Chapter.

Table 7.0 Summary of Conditions for Adsorption Breakthrough Experiments

Figure	Adsorbent	Feed solution	Column (cm)	Mass dry adsorbent (g)	C_o (mg l^{-1})	Flowrate (cm^3 hr^{-1})	EBCT (mins)	Residence time (mins)	Breakthrough time (mins)	% mass adsorbed	Loading until breakthrough (mg mg^{-1})	Complete loading (mg mg^{-1})
7.3	SS 607C	Neat R5/026/03	10	3.41	402.10	301.24	2.23	13.83	12	15.81	0.0020	0.017
7.3	SS 607C	Ultrafiltered	10	3.25	127.65	294.36	2.28	14.51	13	31.01	0.0029	0.025
7.3	SS 607C	Chemically split	10	2.41	169.60	295.87	2.27	14.08	13	14.82	0.0014	0.046
7.4	E-15-50-C	Chemically split	20	4.70	1050.00	150.00	8.95	32.24	20	36.84	0.0045	0.198
7.4	E-15-40-C	Chemically split	20	5.10	1049.50	150.00	8.95	32.24	21	37.87	0.0068	0.187
7.4	SS 607C	Chemically split	20	6.50	1073.50	150.00	8.95	32.24	25	31.57	0.0034	0.125
7.5/7.6	E-15-35-C	Ultrafiltered	20	5.24	168.60	291.05	4.61	16.62	15	16.78	0.0005	0.024
7.5/7.6	E-15-35-C	Butyl glycol	20	5.24	1151.67	282.66	4.75	17.11	18	22.61	0.0063	0.102
7.5/7.6	E-15-35-C	Propionic acid	20	5.24	991.60	289.94	4.63	16.68	20	19.90	0.0058	0.071
7.7	E-15-35-C	Propionic acid	20	5.24	991.60	289.94	4.63	16.68	20	19.90	0.0058	0.071
7.7	E-15-35-C	Propionic acid	20	5.24	985.75	154.60	8.69	31.28	39	33.42	0.0037	0.072
7.8	E-15-35-C	Propionic acid	20	5.24	985.75	154.60	8.69	31.28	39	33.42	0.0037	0.072
7.8	SS 607C	Propionic acid	100	29.29	749.10	150.00	44.76	68.07	631	79.21	0.0375	0.045
7.9	E-15-35-C	Butyl glycol	10	2.25	1117.00	286.95	2.34	14.51	13	17.34	0.0075	0.074
7.9	E-15-35-C	Butyl glycol	20	5.24	1151.67	282.66	4.75	17.11	15	22.61	0.0063	0.102
7.9	SS 607C	Butyl glycol	100	33.67	868.00	150.00	44.76	68.06	1600	92.27	0.1067	0.112
7.10	SS 607C	Chemically split	100	28.80	1380.05	150.00	44.76	68.06	40	39.32	0.0022	0.141
7.10	SS 607C	Butyl glycol	100	33.67	868.00	150.00	44.76	68.06	1600	92.28	0.1067	0.112
7.10	SS 607C	Propionic acid	100	29.29	749.10	150.00	44.76	68.06	631	79.21	0.0375	0.045
7.10	SS 607C	MEA	100	29.48	658.90	150.00	44.76	68.06	40	47.69	0.0013	0.010

Table 7.0 Summary of Conditions for Adsorption Breakthrough Experiments (continued)

Figure	Adsorbent	Feed solution	Column (cm)	Mass dry adsorbent (g)	C_o (mg l^{-1})	Flowrate (cm^3 hr^{-1})	EBCT (mins)	Residence time (mins)	Breakthrough time (mins)	% mass adsorbed	Loading until breakthrough (mg mg^{-1})	Complete loading (mg mg^{-1})
7.11	C150H	Chemically split	20	5.45	1102.70	150.00	8.95	32.24	20	35.97	0.0016	0.060
7.12	C150H+MAST	Chemically split	20	8.68	1124.00	150.00	8.95	32.24	20	50.53	0.0011	0.059
7.13	C150H	Ultrafiltered	20	6.70	1113.00	150.46	8.93	32.14	20	47.83	0.0014	0.072
7.14	C150H+MAST	Ultrafiltered	20	8.35	1074.00	150.00	8.95	32.24	20	68.13	0.0011	0.079
7.15	E-15-50-C	Chemically split	20	4.70	1050.00	150.00	8.95	32.24	20	36.84	0.0045	0.198
7.15	E-15-50-C	Organics	20	6.65	453.55	150.46	8.93	32.14	240	79.94	0.0278	0.110
7.15	E-15-50-C	Amine	20	4.82	931.15	150.00	8.95	32.24	21	12.29	0.0052	0.025
7.15	C150H	Chemically split	20	5.45	1102.70	150.00	8.95	32.24	20	35.97	0.0016	0.060
7.15	C150H	Organics	20	6.30	474.40	150.00	8.95	32.24	20	17.13	0.0006	0.003
7.15	C150H	Amine	20	6.45	673.55	150.00	8.95	32.24	240	74.29	0.0575	0.081
7.16	C150H+MAST	Chemically split	20	8.68	1124.00	150.00	8.95	32.24	20	50.53	0.0011	0.059
7.16	C150H (Before)	Chemically split	20	8.55	1066.00	150.00	8.95	32.24	20	41.63	0.0010	0.054
7.16	C150H (After)	Chemically split	20	8.25	1096.50	150.46	8.93	32.14	20	51.53	0.0011	0.057
7.23	E-15-40-C	Chemically split	20	4.80	1054.75	150.00	8.95	32.24	21	36.89	0.0045	0.196
7.23	E-15-40-C	Chemically split	20	5.00	1056.25	150.00	8.95	32.24	20	36.03	0.0067	0.183
7.23	E-15-40-C	Chemically split	20	5.20	1042.68	150.00	8.95	32.24	20	34.31	0.0067	0.196
7.23	E-15-40-C	Chemically split	20	5.00	1037.50	150.00	8.95	32.24	26	36.20	0.0068	0.180
7.23	E-15-40-C	Chemically split	20	5.10	1049.50	150.00	8.95	32.24	21	37.87	0.0068	0.187

As described earlier, the EBCT is the time taken for the feed solution to pass through the column. The residence time is the time taken for the feed to flow through all the pipe work and reach the adsorbent bed. The breakthrough time is the time taken for the adsorbate to be detected in the effluent stream. The percentage mass adsorbed is calculated by integrating the area under the breakthrough curve and dividing it by the throughput of adsorbate and multiplying it by 100. The loading is calculated using Equation 4.28 (Chapter 4). The loading until breakthrough is the loading calculated up to when the mass transfer zone starts, or when adsorbate is found in the effluent and complete (equilibrium) loading is the loading calculated after the adsorbent cannot accept anymore adsorbate, the system reaches equilibrium *i.e.* when $C/C_o = 1$.

As Table 7.0 shows, many experiments were conducted to find the optimum conditions, for the WOWSEP prototype. These experiments are discussed in the following sections.

7.4.1 The effect of pre-treatment to the cutting fluid on the adsorption system

The previous Chapter mentioned that ultrafiltration and chemical splitting of the neat cutting fluid was carried out by the team at PERA. Three initial dynamic column studies were carried out to observe the difference in adsorption behaviour between these three fluids with SS 607C carbon, using a 10 cm column, an influent flowrate of approximately 300 $cm^3\ hr^{-1}$, and feed concentrations of 402.10 mg l^{-1}, 127.65 mg l^{-1} and 169.90 mg l^{-1} for the neat, ultrafiltered and chemically split cutting fluids, respectively. The EBCT and residence time of the system were approximately 2.25 and 14.15 minutes, respectively. The obtained data of C/C_o versus time are shown in Figure 7.3. Pre-treatment by ultrafiltration and chemical splitting, not only reduced the TOC concentration of the neat cutting fluid, but as can be seen in Figure 7.3 changed the shape of the breakthrough curve. All three solutions resulted in an immediate breakthrough (*i.e.* at a time equal to that of the residence time).

The neat and chemically split cutting fluids gave a breakthrough concentration of approximately 80% and 70% of the feed concentration, while the ultrafiltered cutting fluid gave a breakthrough concentration around 50% of the feed. The immediate breakthrough suggests that there may be component(s) which are not adsorbing onto the carbon. This is

confirmed by a study of the corresponding mass balances (total mass adsorbed onto the carbon) and the complete equilibrium loadings (mg mg^{-1}) given in Table 7.1.

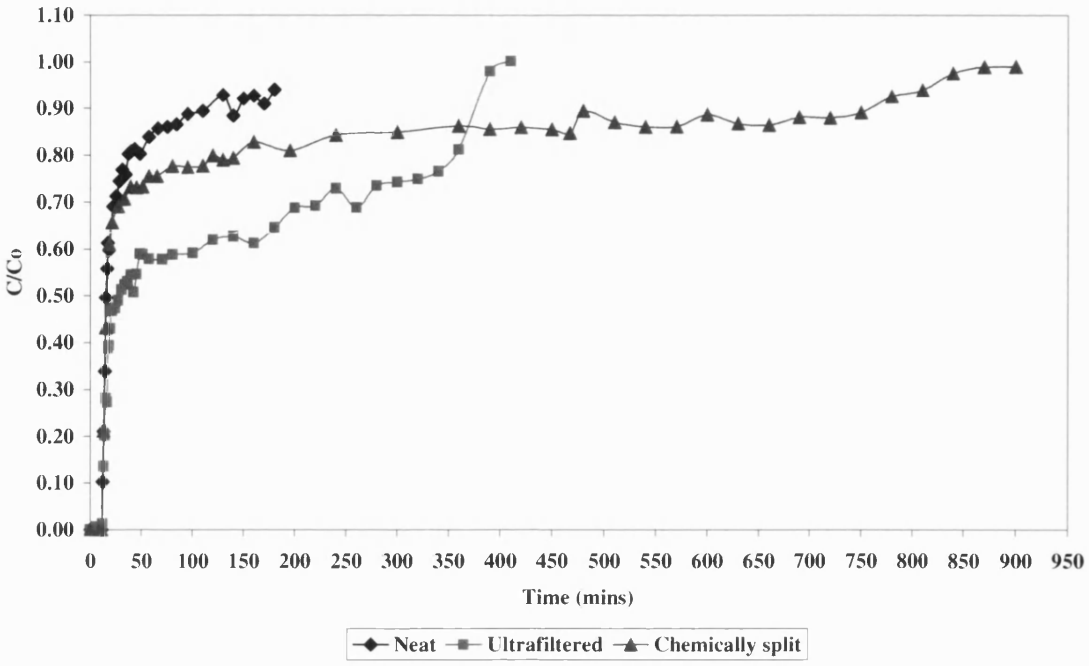

Figure 7.3 A comparison of dynamic column studies between neat, ultrafiltered and chemically split cutting fluids using SS 607C

Table 7.1 Mass Balances of Dynamic Column Experiments showing a Comparison between Neat and Pre-treated Cutting Fluids using SS 607C

Figure	Cutting fluid	Column length (cm)	Mass dry adsorbent (g)	C_o (mg l^{-1})	Flowrate ($cm^3 hr^{-1}$)	Total mass adsorbed (mg)	% mass adsorbed	Complete loading (mg mg^{-1})
7.3	Neat	10	3.41	402.10	301.24	57.45	15.81	0.017
7.3	Ultrafiltered	10	3.25	127.65	294.36	79.62	31.01	0.025
7.3	Chemically split	10	2.41	169.60	295.87	111.56	14.82	0.046

The total mass adsorbed was calculated by integrating the curve to determine the amount of adsorbate leaving the column and subtracting this value and the amount of adsorbate remaining in the pipework from the total throughput. The percentage mass adsorbed is calculated by dividing the total mass adsorbed by the total throughput and multiplying the resulting value by 100.

The batch equilibrium loadings for the ultrafiltered and chemically split solutions, using SS 607C, at similar equilibrium concentrations of 130 and 170 mg l^{-1} were 0.0067 and 0.0027 mg mg^{-1}, respectively (Chapter 6). Comparisons of these batch loadings with the dynamic loadings, given in Table 7.1, show that whilst an instantaneous breakthrough occurred in the column studies, the complete equilibrium loadings by far exceeded the batch equilibrium loadings. The differences in these two loadings (discussed in greater detail later in this Section), suggest that the adsorbent alone is not the cause of the early breakthrough.

7.4.2 The effect of carbon activation on the adsorption system

One of the aims of this thesis was to find a carbon best suited for this system. Therefore a comparison of many other carbons (such as MAST carbons with various activation levels, and various pore sizes) was required. In the case of the dynamic column studies, using an approximate flowrate and feed concentration of 150 ml hr^{-1} and 1050 mg l^{-1}, respectively. Figure 7.4 shows a comparison of dynamic column studies for three carbons with activation levels of 50% (MAST E-15-50-C), 40% (MAST E-15-40-C) and 80% (SS 607C). As can be seen, carbon activation appeared to have little effect on the breakthrough time, although the adsorption profile decreases slightly as carbon activation level decreases.

This was as expected as the ASAP studies (Chapter 5) showed the higher activated carbon to have a larger micropore surface area, which would suggest a higher adsorption capacity. Table 7.2 shows the conditions, amounts adsorbed and loadings for each of the experiments in Figure 7.4. It can be seen that, whilst the 80% activated carbon adsorbed the most amount of adsorbate overall, it had the lowest loading. This low loading value is probably due to the novel manufacturing process of the MAST carbon, and its novel macropore structure, which the SS 607C is shown not to have (Chapter 5), rather than the activation level.

Early breakthrough of a component may be attributable to the mesoporous nature of carbon. If the carbon pores are too small for non-adsorbable compounds, or non-adsorbable molecules are too large, then the mesopores might become blocked. This would inhibit the diffusion of other adsorbable molecules into the micropore structure of

the carbon, hence preventing adsorption from taking place. Therefore experiments using various pore size carbons were required to examine this theory.

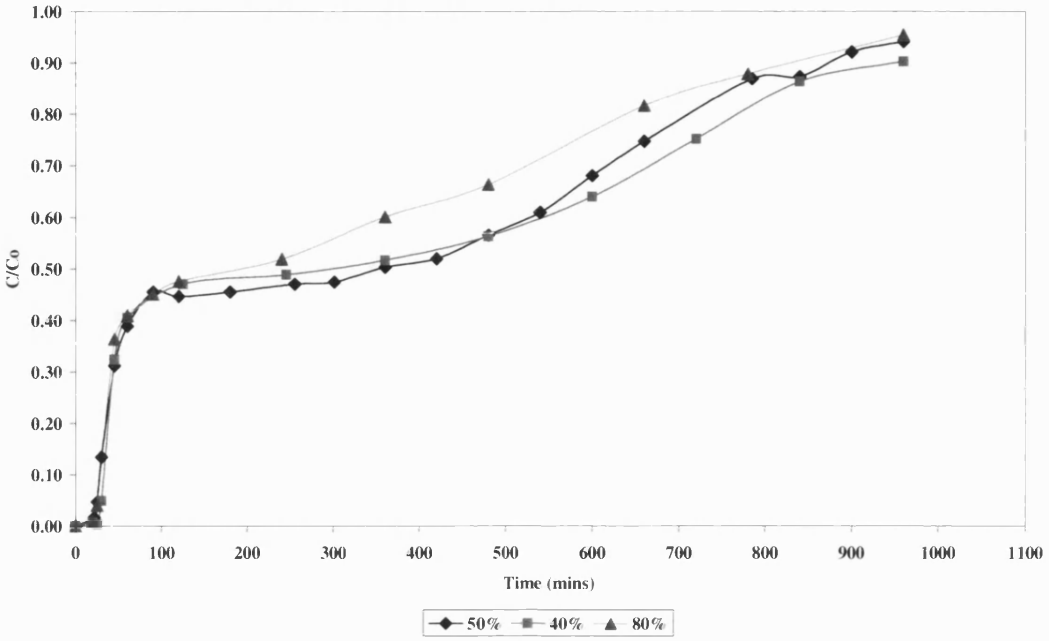

Figure 7.4 A comparison of dynamic column studies between 50%, 40% and 80% activated carbon using chemically split cutting fluids

Table 7.2 Mass Balances of Dynamic Column Experiments showing a Comparison between Carbons with Various Activation Levels

Figure	Adsorbent	Column length (cm)	Mass dry adsorbent (g)	C_o (mg l^{-1})	Flowrate (cm^3 hr^{-1})	Total mass adsorbed (mg)	% mass adsorbed	Complete loading (mg mg^{-1})
7.4	MAST (50%)	20	4.70	1050.00	150.00	57.45	36.84	0.198
7.4	MAST (40%)	20	5.10	1049.50	150.00	79.62	37.87	0.187
7.4	SS 607C (80%)	20	6.50	1073.50	150.00	111.56	31.57	0.125

These experiments again produced an immediate breakthrough with the ultrafiltered and chemically split cutting fluids, suggesting that the pore size was also not the cause of early breakthrough. This confirmed the conclusion made earlier that the adsorbent was not the

underlying cause of the early breakthrough, leading to the thought that the problem concerned either the system design or the adsorbate. To gain a better insight into this idea, experiments were conducted using simpler, single compound fluids such as butyl glycol and propionic acid, compounds known to adsorb onto activated carbon (Ford, 1978; Tennison, 1998), as benchmarks.

7.4.3 The effect of single compound fluids on the adsorption system

The experiments with butyl glycol and propionic acid used a column length of 20 cm, a residence time of approximately 17 minutes, an EBCT of around 4.7 minutes, a flowrate of approximately 300 cm^3 hr^{-1} and an approximate feed concentration of 1000 mg l^{-1} for each solution (apart from the ultrafiltered solution which had an initial concentration of 168.60 mg l^{-1}). Figures 7.5 and 7.6 show a comparison of breakthrough experiments for ultrafiltered cutting fluid, butyl glycol and propionic acid (Figure 7.6 is a close up of the first 500 minutes in Figure 7.5).

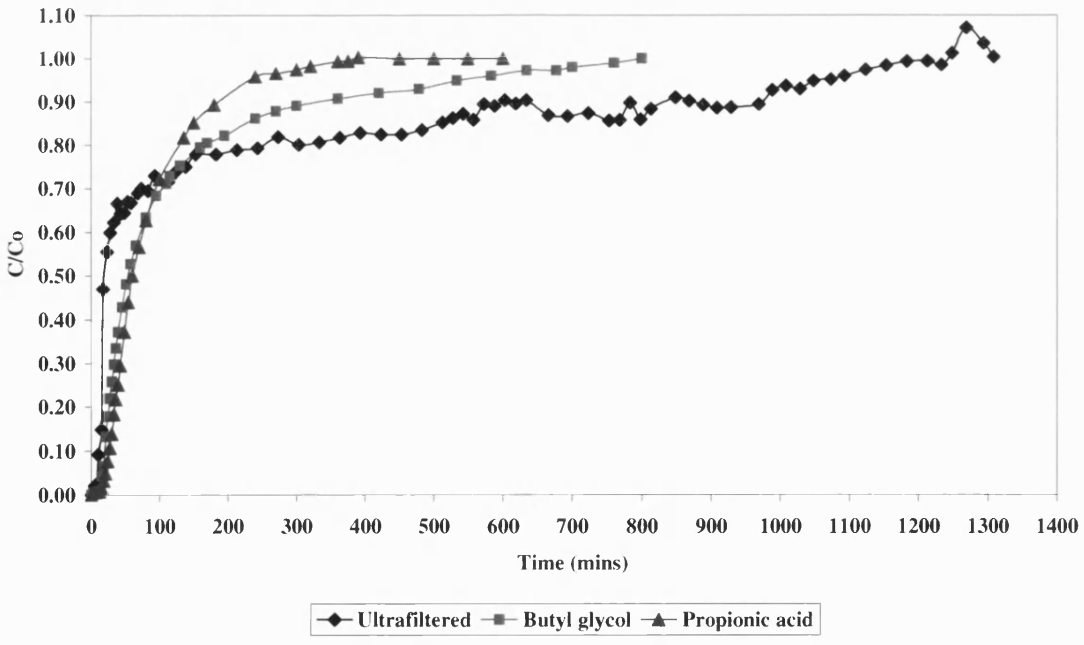

Figure 7.5 Dynamic column studies showing a comparison of ultrafiltered cutting fluid, butyl glycol and propionic acid using E-15-35-C carbon

The butyl glycol and propionic acid breakthrough graphs shown in Figure 7.6 appear to have the desired, smooth s-shape curve, demonstrating a stable mass transfer zone and

perhaps a viable system. The graph for the ultrafiltered cutting fluid solution, on the other hand, shows a steeper, less smooth breakthrough curve. This uneven breakthrough curve suggests that although the ultrafiltered cutting fluid is considered to be a homogeneous single component solution, it is in fact a multicomponent solution where the various components are probably adsorbing at different rates and times.

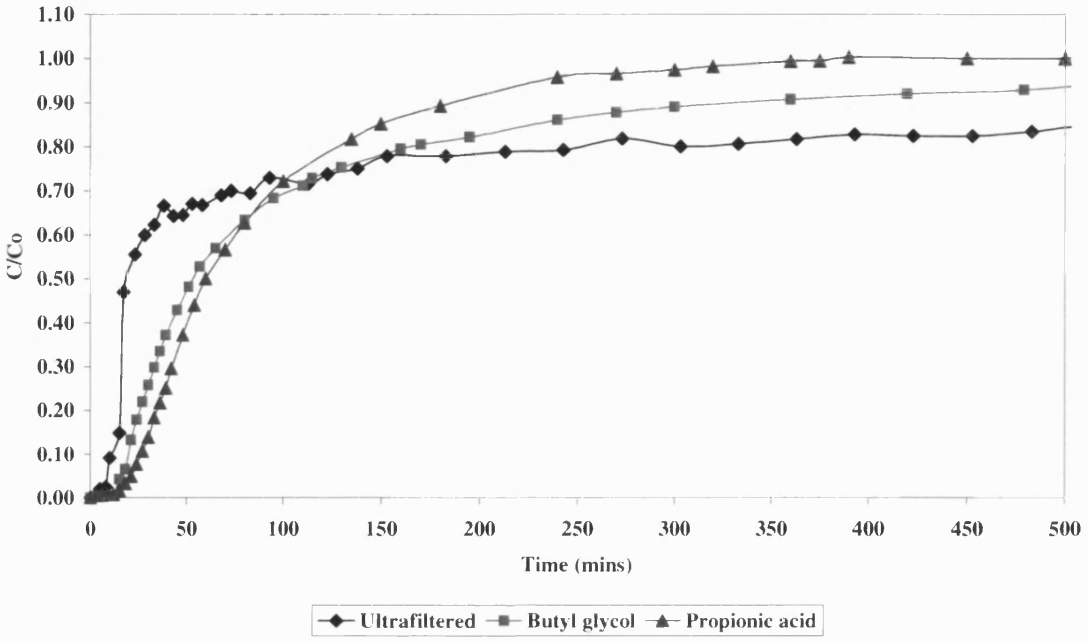

Figure 7.6 A close up of dynamic column studies showing a comparison of ultrafiltered cutting fluid, butyl glycol and propionic acid using E-15-35-C carbon

In addition, the breakthrough of the ultrafiltered solution is immediate, at a time roughly equal to that of the residence time (around 17 minutes) in the system, whereas the butyl glycol and propioinc acid have breakthrough times of 20 and 24 minutes respectively. However, even though the breakthroughs for the propionic acid and butyl glycol were not immediate, the difference in breakthrough times is small. Therefore breakthrough is still believed to be premature. The mass balances shown in Table 7.3 relate to the experiments in Figures 7.5 and 7.6.

A comparison of the total mass adsorbed between the two ultrafiltered experiments shown in Tables 7.1 and 7.3, reveals the mass adsorbed to have increased by approximately 60% in the latter, although the dynamic loadings are similar. This can be explained by

comparing the system conditions for both experiments. Although the flowrates were similar, the feed concentration was slightly higher in the latter experiment (resulting in a small increase in throughput) and the column length was doubled from 10 cm to 20 cm (thereby also doubling the mass of adsorbent and the EBCT). The increase in column length would therefore explain the increase in total mass adsorbed onto the carbon and the similar loadings.

Table 7.3 Mass Balances of Dynamic Column Experiments showing a Comparison between Ultrafiltered Cutting Fluid, Butyl Glycol and Propionic Acid using E-15-35-C Carbon

Figure	Feed	C_o (mg l^{-1})	Flowrate (cm^3 hr^{-1})	Column length (cm)	Total mass adsorbed (mg)	% mass adsorbed	Complete loading (mg mg^{-1})
7.5/7.6	Ultrafiltered	168.60	291.05	20	124.85	16.78	0.024
7.5/7.6	Butyl glycol	1151.67	282.66	20	533.56	22.61	0.102
7.5/7.6	Propionic acid	991.60	289.94	20	371.87	19.90	0.071

The complete equilibrium loadings for butyl glycol and propionic acid (Table 7.3) are somewhat much greater than for the ultrafiltered solution, because they are simple compounds known to adsorb onto activated carbon. These findings demonstrate that carbon has the ability to adsorb organic compounds and therefore it would seem that the carbon is not the cause of the immediate breakthrough, but rather the system design or the adsorbate. Hence the following sections investigate the effect of various system conditions and designs.

7.4.4 The effect of EBCT on the adsorption system

Figure 7.6 has shown butyl glycol and propionic acid to produce a smooth s-shaped mass transfer zone. Nevertheless a sharper, steeper, breakthrough curve with a higher breakthrough time would be preferable. The steepness of the breakthrough curve is affected by the contact time (flowrate), equilibrium relationship and the overall rate of adsorption. Even though lowering the flowrate increases the EBCT, which in turn provides more time for the molecules to adsorb onto the carbon, if the flowrate is too low

then there is minimal mixing, if at all, in the system. This may cause liquid films to form around the particles creating a resistance and hindering the diffusion of molecules into the carbon pores, thus decreasing the mass transfer and system kinetics. However, at higher flowrates any external film resistances are reduced, increasing the mass transfer through the pores of the carbon, but the contact time is also reduced which may bring the breakthrough time forward. Another aspect to consider is the column length *i.e.* if the amount of adsorbate put through the system is the same and the amount of adsorbent is changed by altering the column length then this varies the amount of adsorbent to adsorbate. Hence, if the column length is too short the amount of adsorbent to adsorbate may also be low and therefore a complete mass transfer zone may not be achieved. Increasing the column length increases the EBCT, but decreases the length of unused bed and mass transfer zone for any given breakthrough level (Perry and Green, 1984). In addition, the influent concentration needs to be studied. For example if the concentration is too high, the amount of adsorbate to adsorbent may also be high and an immediate breakthrough obtained.

Generally, a certain EBCT is required for the mass transfer zone to be developed fully within the GAC bed. In practice the EBCT should have a minimum value of 15 minutes (Horner, 1999). If the EBCT is too short (*i.e.* the hydraulic loading rate is too large), the length of the mass transfer zone will be greater than the GAC bed depth and the adsorbable contaminant will not be completely adsorbed by the carbon. Therefore to sharpen the breakthrough curve and to increase the EBCT, the flowrate needs to be optimised such that the best system conditions may be achieved. Therefore in order to investigate the packed bed system the main factors to consider were column length, flowrate and influent concentration.

7.4.5 The effect of flowrate on the adsorption system

As mentioned, one method of increasing the EBCT is to lower the influent flowrate. Using propionic acid as a benchmark, an experiment was conducted reducing the flowrate to half of that used in the experiments shown in Figure 7.5. Figure 7.7 shows a comparison of breakthrough curves for propionic acid with MAST carbon, using a 20 cm column, with flowrates of around 300 cm^3 hr^{-1} and 150 cm^3 hr^{-1}, residence times of 17 and 31 minutes and EBCTs of 4.6 and 8.7 minutes, respectively. It is clear from Figure 7.7 that the higher

flowrate produced an earlier breakthrough. This is more than likely due to the fact that a higher flowrate reduces the EBCT which consequently brings the breakthrough time forward. Halving the flowrate to 150 cm^3 hr^{-1}, almost doubled the residence time and the EBCT. Keeping the column length and hence the mass of adsorbent more or less constant in both experiments, kept the total mass adsorbed and the loading more or less the same as shown in Table 7.4. Figure 7.7 also shows that the width of the mass transfer zone varies with flowrate. The lower flowrate produces a broader mass transfer zone with a shallower mass transfer front. This is because dispersion, diffusion and channelling in a granular medium are directly related to the flowrate.

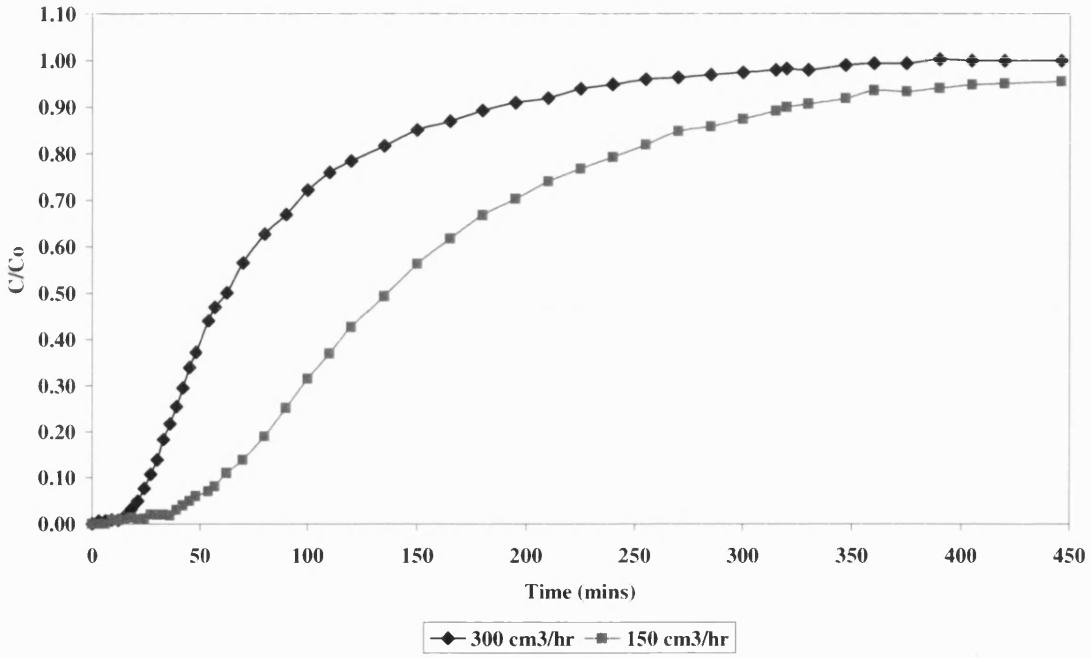

Figure 7.7 A comparison of dynamic column studies for propionic acid using E-15-35-C carbon with various flowrates

Table 7.4 Mass Balances of Dynamic Column Experiments for Propionic Acid using E-15-35-C Carbon and Various Flowrates

Figure	C_o (mg l^{-1})	Flowrate (cm^3 hr^{-1})	Total mass adsorbed (mg)	% mass adsorbed	Complete loading (mg mg^{-1})	k_f (m s^{-1})
7.7	991.60	300	371.87	19.90	0.071	1.20×10^{-4}
7.7	985.75	150	378.57	33.42	0.072	1.18×10^{-4}

Chapter 6 discussed the system kinetics of batch experiments through the assessment of the external mass transfer coefficient (k_f) and *Bi* number. This evaluation identified whether the diffusion of the adsorbate molecules was film or pore controlled. The external mass transfer coefficient for packed beds (with *Re* numbers in the range of 3-10,000) were calculated using the Wakao and Funazkri (1978) correlation (Equation 7.1), which takes the effect of axial dispersion into account and is applicable to favourable adsorption isotherms:

$$Sh = 2.0 + 1.1 Sc^{0.33} Re^{0.6} \qquad 7.1$$

Assuming the viscosity and density of water at 20°C (298K) to be 0.001 kg m^{-1} s^{-1} and 1000 kg m^{-3} respectively, and the diffusivity coefficient of ethanol in water $1x10^{-9}$ m s^{-1}, (Perry and Green, 1984) *Sh*, *Sc* and *Re* were calculated using the relationships defined in Chapter 4 (page 72). The low k_f values shown in Table 7.4 verify that the rate of diffusion is film controlled.

7.4.6 The effect of column length on the adsorption system

The adsorption of propionic acid onto MAST carbon using a 20 cm column and a flowrate of around 150 cm^3 hr^{-1} gave an EBCT of 8.7 minutes (Figure 7.7), which according to Horner (1999), is just over half of the minimum required to fully develop the mass transfer zone within the carbon column. Unfortunately due to pump restrictions the flowrate could not be decreased any further. Another method of increasing the EBCT is to increase the bed length. If the bed length is too short then a full mass transfer zone is not contained within the bed, and hence the equilibrium loading is not obtained. An increase in the column length increases the mass of the carbon, which leads to an increase in the number of adsorptive sites. This in turn increases the adsorption capacity of the bed, which should, theoretically, therefore also improve the kinetic characteristics of the system which are represented by the sharpness and steepness of the isotherm. If halving the flowrate (to 150 cm^3 hr^{-1}) and doubling the column length (to 20 cm) increased the EBCT by 4 fold, then doubling the column length further (to 40 cm) should double the EBCT further. Therefore a column length of 40 cm should produce an EBCT of approximately 18 minutes, which is above the minimum to obtain a fully developed mass transfer zone. However, to be certain a 100 cm column was tried. Figure 7.8 shows the column length to have a marked effect

on adsorption breakthrough. The increase in column length raised the residence time from approximately 31 to 68 minutes, and the EBCT from 8.7 to 44.8 minutes, which is plenty of time for good adsorption to occur. Consequently the breakthrough time was also increased from 39 minutes to 631 minutes, which is almost 9 times greater than the residence time, suggesting that the early breakthrough problem had been solved. It must be noted that the 20 cm column used MAST E-15-35-C carbon whilst the 100 cm column used SS 607C, although from previous experiments it has been shown that whilst there is a slight difference in breakthrough curves between the two carbons, this is not the reason for the change in breakthrough times, shown in Figure 7.8.

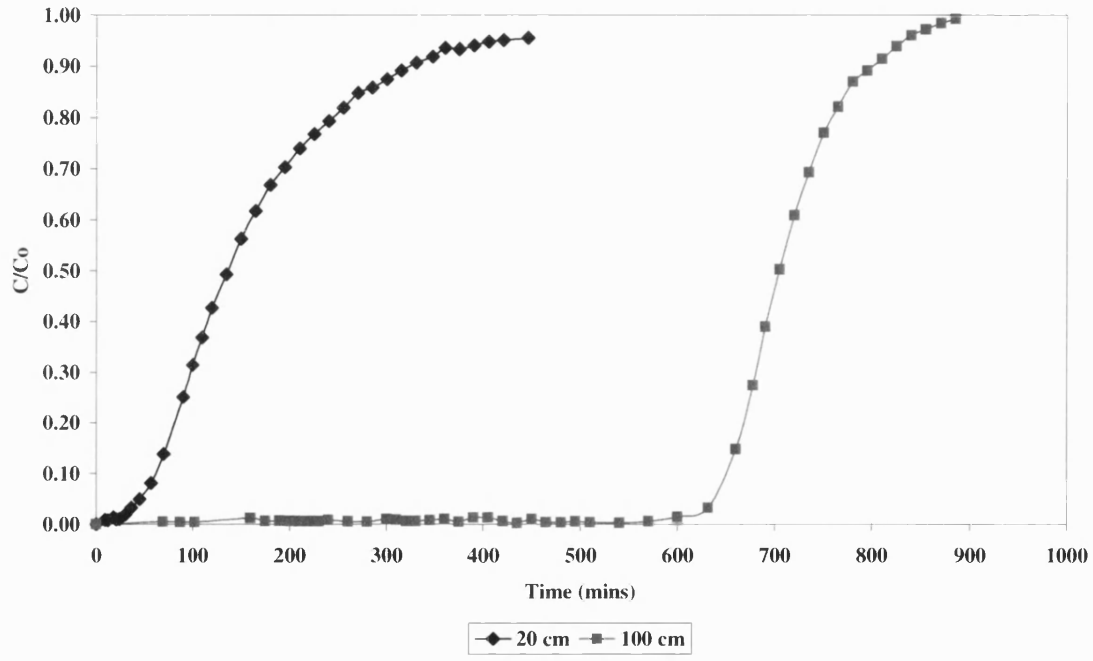

Figure 7.8 Comparison of dynamic column experiments for propionic acid with varying column lengths

The mass balances provided in Table 7.5 shows the loading until breakthrough and complete loading corresponding to the experiments shown in Figure 7.8. As previously explained, the complete loading is also called the equilibrium loading, because it is at this stage in the process where the concentration of adsorbate in the effluent stream is equal to the concentration of adsorbate in the feed (*i.e.* $C/C_0=1$). The loading until breakthrough is the dynamic loading of adsorbate on to the carbon, calculated when adsorbate is first detected in the effluent stream.

Table 7.5 Mass Balances of Dynamic Column Experiments for Propionic Acid showing a Comparison between 20 cm and 100 cm Columns

Figure	Feed	C_o (mg l^{-1})	Flowrate (cm^3 hr^{-1})	Column length (cm)	Total mass adsorbed (mg)	% mass adsorbed	Breakthrough loading (mg mg^{-1})	Complete loading (mg mg^{-1})
7.8	Propionic acid	985.75	154.60	20	378.57	33.42	0.0037	0.072
7.8	Propionic acid	749.10	150.00	100	1312.87	79.21	0.0375	0.045

Table 7.5 shows the complete loading is lower for the 100 cm column (0.045 mg mg^{-1}) than the 20 cm column (0.072 mg mg^{-1}). However, if considering the loading until breakthrough the 100 cm column has a greater loading of ten fold (0.0375 mg mg^{-1}) than the 20 cm column (0.0037 mg mg^{-1}). In practice, the loading at breakthrough is more important for design considerations, as it is at this time when the adsorption bed is either regenerated or replaced to produce an efficient process. From the breakthrough point to the end of the experiment (mass transfer zone) the 20 cm column produced a shallower, broader breakthrough curve (422 minutes), whereas the 100 cm column gave a much steeper, narrower curve (285 minutes). This suggests that most of the adsorption for the 20 cm column took place after breakthrough had commenced. Whereas the greater part of adsorption for the 100 cm column took place before breakthrough had commenced. In addition, the influent concentration was also lower for the 100 cm column (as shown in Table 7.5), decreasing the total mass throughput for the 100 cm column for the same period of time. Another possible reason for the difference in loadings is due to the integral calculation of the area beneath the curve. This calculation for the 100 cm column was conducted noting that the final flat plateau at the end of the run is not present. This is because the run was stopped before the flat plateau was obtained.

Figure 7.9 shows the results of adsorption breakthrough studies of butyl glycol with varying column lengths (10 cm, 20 cm, and 100 cm), an approximate feed concentration of 1000 mg l^{-1}, flowrates of 300 cm^3 hr^{-1} and 150 cm^3 hr^{-1}. Similar to propionic acid, the 100 cm column gave a steep, sharp mass transfer front profile, with a narrow mass transfer zone, suggesting excellent kinetics, in comparison to the 10 cm and 20 cm columns, which clearly show early breakthrough times. As with the experiment in Figure 7.8, the 10 cm

and 20 cm columns used MAST E-15-35-C as the adsorbent, whilst the 100 cm column used SS 607C, but this again was not the reason for the change in breakthrough times, shown in Figure 7.9.

The mass balances in Table 7.6, as expected, show the 100 cm column to produce the highest and the 10 cm column to produce the lowest percentage mass adsorbed and equilibrium (complete) loadings.

The mass balance values are as expected, such that the 100 cm column gave the highest equilibrium loading and the 20 cm column gave the lowest equilibrium loading. There are no discrepancies between the values as the all the experiments were stopped at the top of the curve (without the flat plateau at the end of the curve) and hence the conditions for the integration for all the experiments were the same. However, if the inlet concentrations had been exactly the same, all the columns should give the same equilibrium loading after complete breakthrough.

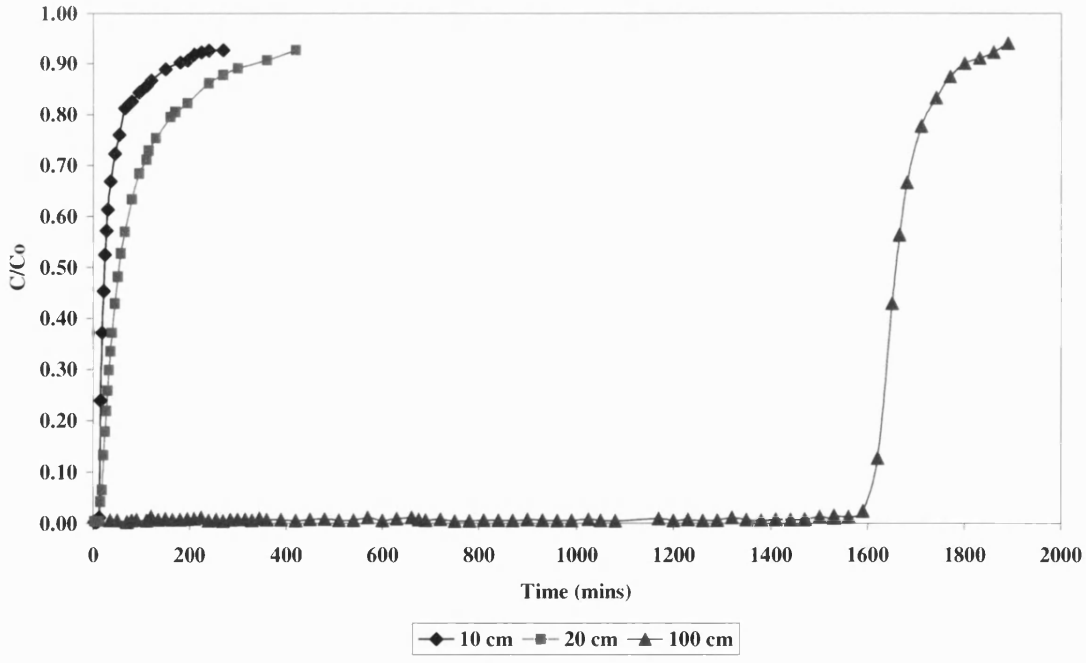

Figure 7.9 A comparison of dynamic column experiments for butyl glycol with various column lengths

Table 7.6 Mass Balances of Dynamic Column Experiments for Butyl Glycol with Various Column Lengths

Figure	Feed	C_o (mg l^{-1})	Flowrate (cm^3 hr^{-1})	Column length (cm)	Total mass adsorbed (mg)	% mass adsorbed	Complete loading (mg mg^{-1})
7.9	Butyl glycol	1117.00	286.95	10	166.74	17.34	0.074
7.9	Butyl glycol	1151.67	282.66	20	533.56	22.61	0.102
7.9	Butyl glycol	868.00	150.00	100	3784.46	92.27	0.112

7.4.7 The effect of various fluids using the 100 cm column on the adsorption system

In contrast to the single compound results fluids shown in Figures 7.8 and 7.9, when the adsorption of chemically split cutting fluid onto carbon was tested using the 100 cm column, a feed flowrate of 150 cm^3 hr^{-1} and concentration of 1380 mg l^{-1} (similar conditions as the butyl glycol and propionic acid), an immediate breakthrough of almost 55% of its feed concentration was produced (Figure 7.10).

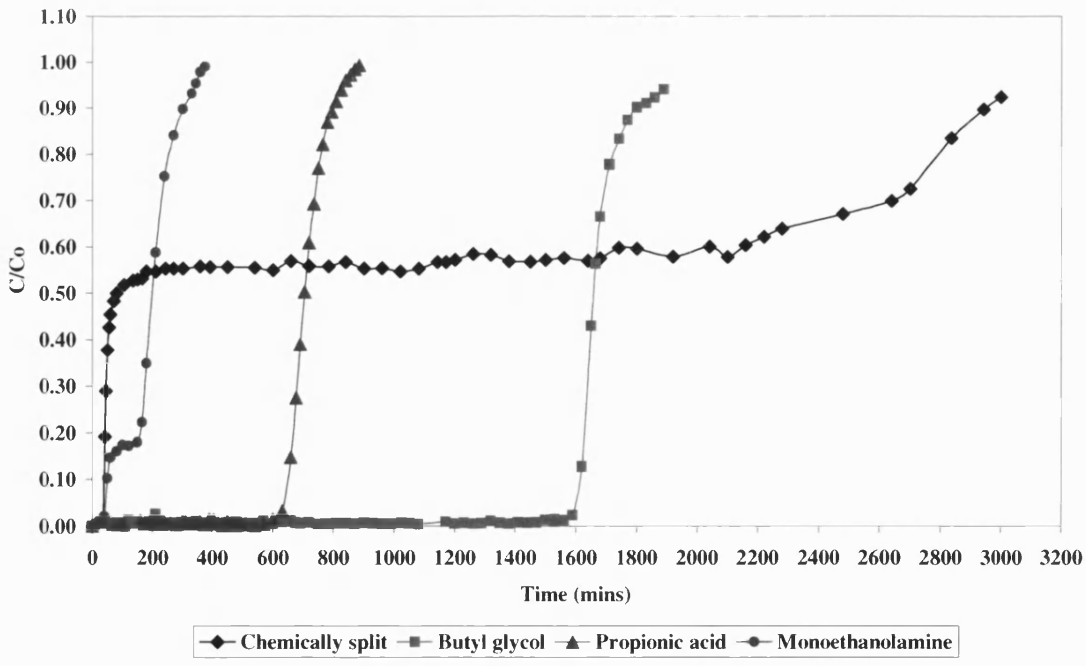

Figure 7.10 A comparison of dynamic column experiments for chemically split cutting fluid, butyl glycol, propionic acid and MEA using a 100 cm column and SS 607C

This suggests that there is at least one component, which is not adsorbing onto the carbon, thereby hindering the complete adsorption of all the organic components in the cutting fluid. The remaining 45% or so (adsorbing portion) of the chemically split cutting fluid, produced a somewhat jagged breakthrough curve, implying it contains more than one component, each of which is adsorbing at different rates. Chapter 6 showed that the cutting fluid could be considered to be a pseudo binary mixture consisting of an "amine" fraction, which was not adsorbable by carbon and an "organic" fraction which was adsorbable by carbon. This might help explain the immediate breakthrough of 55% (the "amine" fraction) and the long drawn out mass transfer zone of the "organic" fraction (45%).

Another dynamic column experiment was conducted using the 100 cm column, monoethanolamine (MEA) as the feed solution with a flowrate of around 150 cm^3 hr^{-1} and feed concentration of around 660 ml hr^{-1} to see the exact effect of the "amine" fraction on the carbon (Figure 7.10). Like the chemically split cutting fluid profile an immediate breakthrough is also produced with the MEA. This implies that the "amine" does not completely adsorb onto activated carbon. The chemically split system produces a broad mass transfer zone and a shallow breakthrough curve following the immediate breakthrough, which indicates an unsuitable system with poor kinetics. The MEA profile shows a step in the adsorption curve after the immediate breakthrough. This feature is similar to that for the chemically split fluid profile, although the latter is much more drawn out. This step with MEA is more than likely due to two components or two sets of components (*e.g.* "ethanol" and "amine" fractions) adsorbing at different rates and therefore breaking through at different times.

This confirms research carried out by Giusti *et al.* (1974), Ford (1978), Calgon Carbon Corporation (1986) and Childers *et al.* (1990), who proposed compounds such as alcohol amines (monoethanolamine (MEA) and diethanolamine (DEA)), which are present in cutting fluids as corrosion inhibitors, do not adsorb onto carbon. Giusti *et al.* presented experimental data on the adsorption of various organic compounds (such as alcohols, aldehydes, amines, aromatics, esters, ethers, glycols, ketones and organic acids) onto activated carbon. Their findings showed that MEA, methanol, ethanol, formaldehyde, and ethylene glycol only gave concentration reductions of 7.2, 3.6, 10.0, 9.2, 6.8 percent, respectively, from the influent solution. In contrast the aromatic compounds such as

benzene, nitrobenzene, benzaldehyde and benzoic acid all gave percentage reductions greater than 90%. The factor differentiating the non-adsorbable compounds from the relatively adsorbable compounds was their aqueous solubility. Non-adsorbable compounds were completely soluble in water, and the adsorbable compounds were less than 0.33% soluble. Ford (1978) independently conducted adsorbability experiments on many of the same compounds and achieved almost identical results. Childers *et al.* (1990) conducted adsorbability tests on compounds from each of the groups shown in Table 2.1 (Chapter 2), and again showed similar results to Giusti *et al.* (1974) and Ford (1978). Calgon Carbon Corporation, on the other hand, used granular activated carbon to primarily purify ethanolamines from acid gas constituents such as carbon dioxide and hydrogen sulphide, where the carbon did not adsorb the "amines" but adsorbed all the other compounds that were present.

A comparison of the mass balances for the corresponding breakthrough graphs in Figure 7.10 is given in Table 7.7.

Table 7.7 Mass Balances of Dynamic Column Experiments for Chemically Split Cutting Fluid, Butyl Glycol, Propionic Acid and MEA using a 100 cm Column

Figure	Feed	C_o (mg l^{-1})	Flowrate (cm^3 hr^{-1})	Column length (cm)	Total mass adsorbed (mg)	% mass adsorbed	Complete loading (mg mg^{-1})
7.10	Chemically split	1380.05	150.00	100	4070.10	39.32	0.141
7.10	Butyl glycol	868.00	150.00	100	3784.46	92.28	0.112
7.10	Propionic acid	749.10	150.00	100	1312.87	79.21	0.045
7.10	MEA	658.90	150.00	100	294.58	47.69	0.010

The chemically split cutting fluid is shown to produce the highest equilibrium loading of 0.141 mg mg^{-1}, but a greater percentage of butyl glycol (92%) and propionic acid (79%) is adsorbed by the carbon. MEA, on the other hand, has a low loading and percentage mass adsorbed values, indicating that MEA does not adsorb onto activated carbon. Despite the early breakthrough, the mass balances in Table 7.7 show the chemically split cutting fluid to have a higher equilibrium loading than the butyl glycol and propionic acid systems.

This is more than likely due to the period of adsorption of the "organic" fraction, which is shown as the long plateau after the immediate breakthrough. However, the breakthrough graphs of the butyl glycol and propionic acid are both illustrated with steep, narrowing mass transfer zones therefore showing the system to be stable and viable with good kinetics.

Equivalent experiments to the chemically split cutting fluid were conducted with the ultrafiltered cutting fluid. Similar trends were observed. It is now obvious from the batch studies and the dynamic column studies shown in Figure 7.10 that it is the "amine" fraction, present in the cutting fluid which does not adsorb onto the carbon. However, other factors such as the effect of pH, carbon pore size and the effect of concentration were considered in case these were also hindering the adsorption process.

7.4.8 The effect of pH on the adsorption system

The cutting fluid solution had a pH of 9.4 (alkaline) and the carbon had a pH of 7.5 (slightly alkaline). Therefore it was thought that acidifying either the cutting fluid solution or the carbon may assist the "amine" fraction of the cutting fluid to adsorb onto the carbon. The carbon pH was lowered by two methods: (i) air oxidation at 400°C and (ii) refluxing in nitric acid. During air oxidation the carbon reacts with oxygen to produce carbon dioxide hence removing all the carboxyl and hydroxyl groups from the carbon, but this slightly increased the pH to 8.3. Refluxing, on the other hand, involved heating the carbon in nitric acid, resulting in a reduction of the carbon pH to 3.5. The pH of the cutting fluid was lowered by the addition of acetic acid and hydrochloric acid. This produced pH values of 2.8 and 2.2, respectively. Dynamic column experiments were then conducted using the modified carbons and cutting fluid. Despite all of these approaches, all the results from these experiments produced instantaneous breakthroughs, indicating that a change in pH through carbon or feed acidification would not resolve the breakthrough problem.

7.4.9 The effect of amines on the adsorption system

Each grade of cutting fluid contains a different amine or amine derivative. Therefore to verify that MEA is not the only amine derivative which fails to adsorb onto carbon, and to show it is not only this particular grade of cutting fluid which fails to adsorb onto carbon

completely, dynamic column experiments were conducted using diethanolamine (DEA) and Polartech (a boric acid/MEA additive). Again, similar results to MEA were obtained, where immediate breakthrough and very little adsorption took place. These findings suggest that every grade of cutting fluid containing an amine compound or an amine derivative will cause an immediate breakthrough when passed through a carbon column. Accordingly, an alternative method to carbon adsorption was required to remove the "amine" fraction from the cutting fluid.

7.4.10 The effect of ion exchange on the adsorption system

Chapter 6 (batch studies), refers to ion exchange as being a simple, cost effective method, similar to that of adsorption, such that no extra equipment is required for its use. As explained in Chapter 4, ion exchange works on the basis of the exchange of ions from the resin and the influent solution. These ions are either cations or anions depending on the solution/matrix configuration. For example, in this case, the "amine" fraction of the cutting fluid is an alkaline solution which contains cations, therefore a cationic resin is required for its removal. Many ion exchange resins were studied and as discussed earlier in the batch studies the outcome was to use a strong acid cationic exchanger (*e.g.* Purolite C150H), which is macroporous with excellent resistance to attrition and osmotic shock.

Figure 7.11 shows the effect of ion exchange on the chemically split solution, using a flowrate of 150 cm^3 hr^{-1} and an approximate feed concentration of 1100 mg l^{-1}. In addition to analysing the effluent sample using the Dohrmann DC180 analyser, which monitors the TOC of the solution ("organic" and "amine" fractions), titration with 0.01 N hydrochloric acid was also used to monitor the amine content in the effluent. It is clear from the titration graph (Figure 7.11) that the ion exchange resin has removed the "amine" fraction, as breakthrough of "amine" does not occur until approximately 270 minutes. The TOC graph, on the other hand, again shows an early breakthrough. This breakthrough is shown to occur in two steps. The first step now corresponds to the "organic" fraction breaking through from an ion exchange resin (43%), while the second step corresponds to the "amine" fraction breaking through. The first breakthrough step more or less corresponds to the breakthrough of the "organic" fraction (45%) from the chemically split cutting fluid as shown in Figure 7.10. This suggests the remainder 57% or so (from Figure 7.11) is almost the entire "amine" fraction.

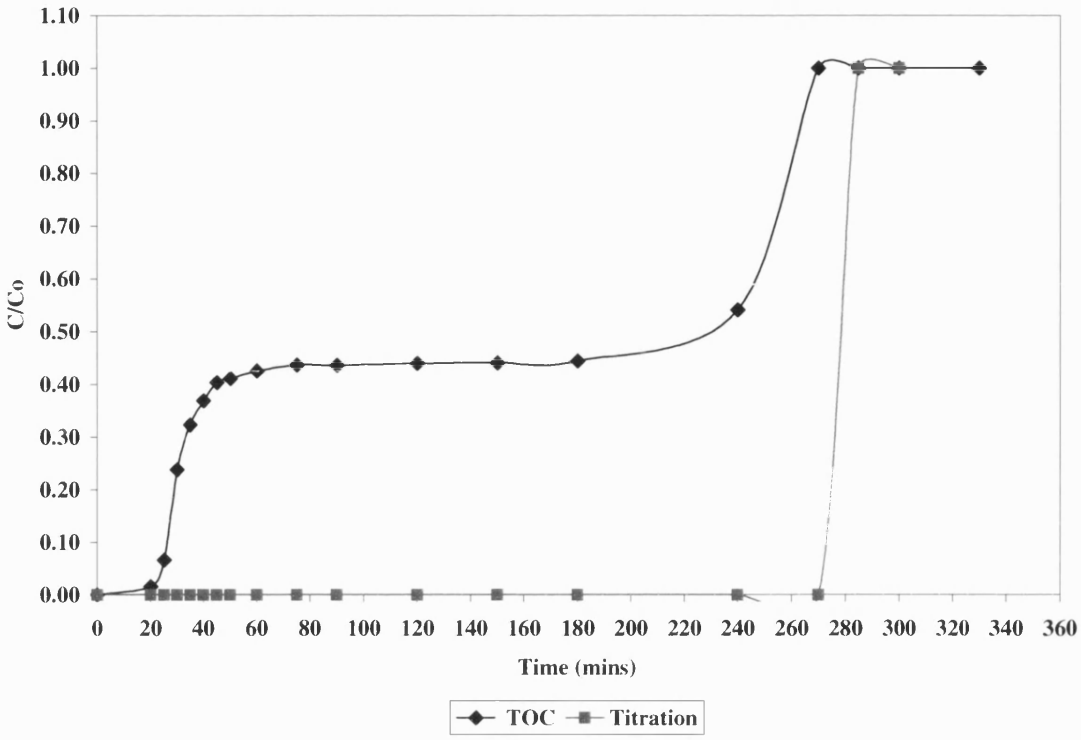

Figure 7.11 A comparison of analysis methods for a dynamic column experiment using chemically split cutting fluid with Purolite C150H

7.4.11 The effect of a mixed ion exchange and carbon on the adsorption system

To show that the non-adsorbable compound is almost all "amine", in the chemically split cutting fluid, a breakthrough study was conducted using a 50:50 mixture (by mass) of both activated carbon and ion exchange resin, using a flowrate of 150 cm^3 hr^{-1} and an approximate feed concentration of 1100 mg l^{-1}, the results of which are shown in Figure 7.12. Even though the TOC graph is somewhat jagged and there is a slight initial increase in C/C_o, breakthrough does not occur until approximately 80 minutes (which is more than double the residence time of 32 minutes), and the "amine" fraction (observed from the titration curve) does not breakthrough until almost 200 minutes into the experiment. This shows that the breakthrough is no longer immediate or early and confirms that both the "amine" and "organic" fractions are being adsorbed.

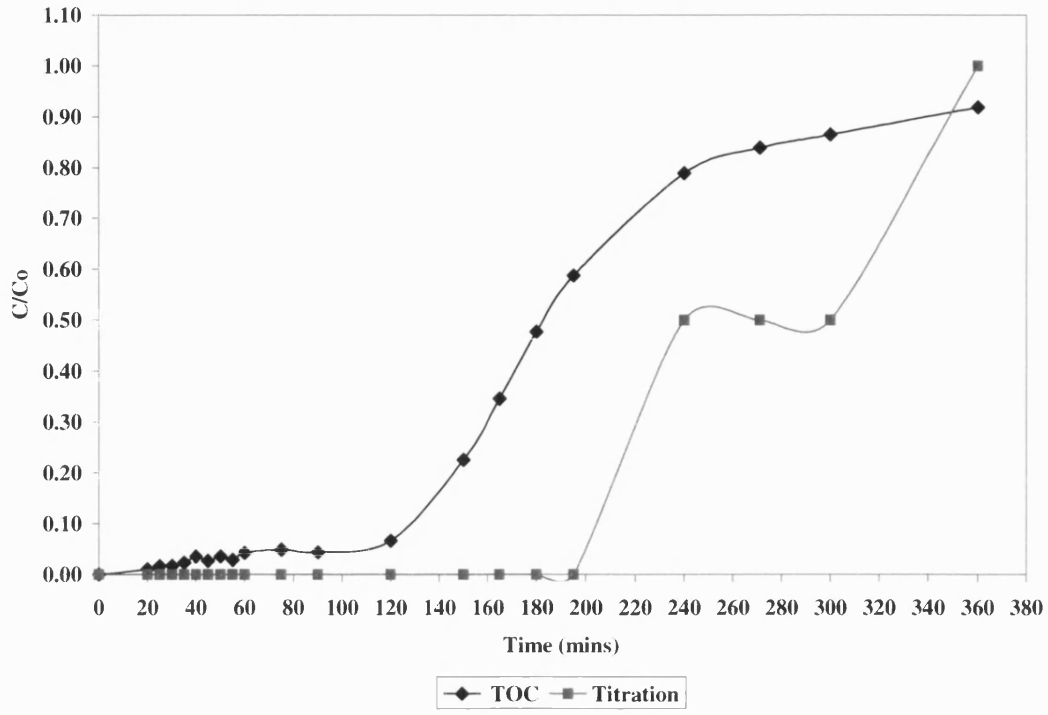

Figure 7.12 A comparison of analysis methods for a dynamic column experiment using chemically split cutting fluid with MAST E-15-50-C and Purolite C150H

Table 7.8 Mass Balances of Dynamic Column Experiments for Chemically Split Cutting Fluid with MAST E-15-50-C and Purolite C150H using a 20 cm Column

Figure	Column	C_o (mg l^{-1})	Flowrate (cm^3 hr^{-1})	Column length (cm)	Total mass adsorbed (mg)	% mass adsorbed	Complete loading (mg mg^{-1})
7.11	Purolite	1102.70	150.00	20	327.20	35.97	0.060
7.12	MAST and Purolite	1124.00	150.00	20	511.15	50.53	0.059

Table 7.8 provides a comparison of mass balances between the two experiments shown in Figures 7.11 and 7.12. Both experiments produced similar TOC loadings, which would suggest that both the Purolite and carbon behave in a similar manner. However, the overall percentage mass adsorbed is higher for the mixed carbon and ion exchange resin matrix, which is expected as more components are being removed from the feed solution.

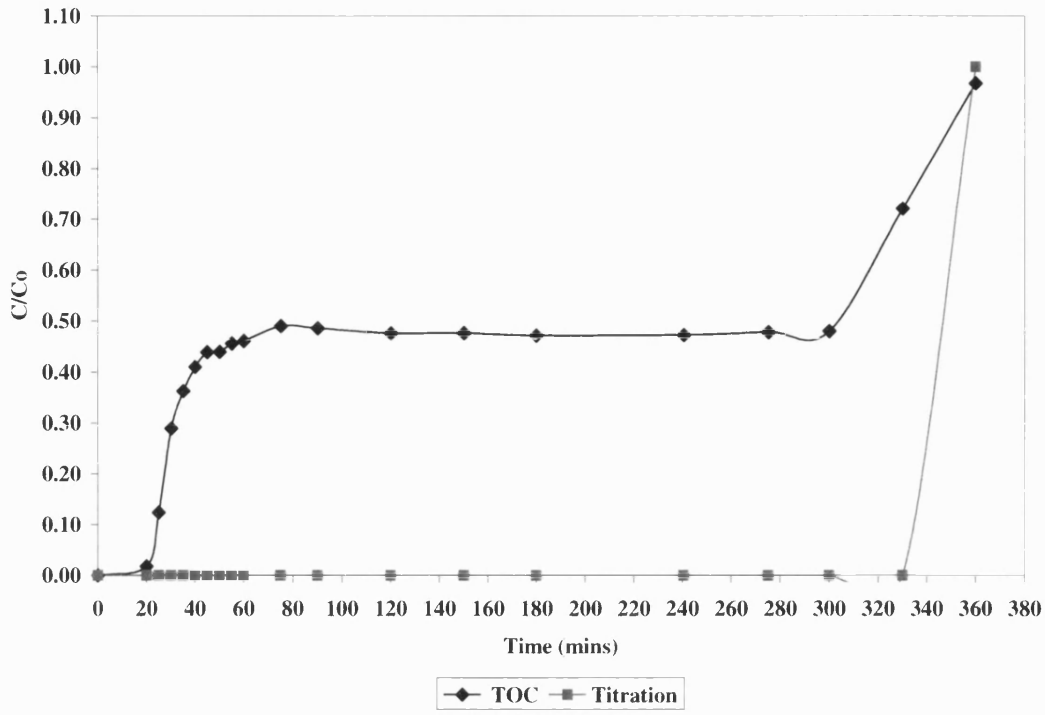

Figure 7.13 A comparison of analysis methods for a dynamic column experiment using ultrafiltered cutting fluid with Purolite C150H

Figures 7.11 and 7.12 refer to the adsorption of "organic" and "amine" fractions from the chemically split cutting fluid solution. Equivalent experiments were conducted using ultrafiltered cutting fluid, using similar initial conditions flowrates of 150 cm^3 hr^{-1} and feed concentrations of approximately 1100 mg l^{-1}, the results of which are shown in Figures 7.13 and 7.14 and their corresponding mass balances in Table 7.9.

As can be seen from the shapes of the graphs (Figures 7.13 and 7.14) the outcome of using the ultrafiltered solution is broadly similar to that of the chemically split solution (Figures 7.11 and 7.12). However, the mass balances in Table 7.9 show the ultrafiltered cutting fluid to give a slightly higher loading than the chemically split solution (Table 7.8). This could be due to experimental error or (as previously explained) it may be due to the fact that there is no horizontal 'flat' period at the end of the curve, which provides an error on integration whilst calculating the amount adsorbed.

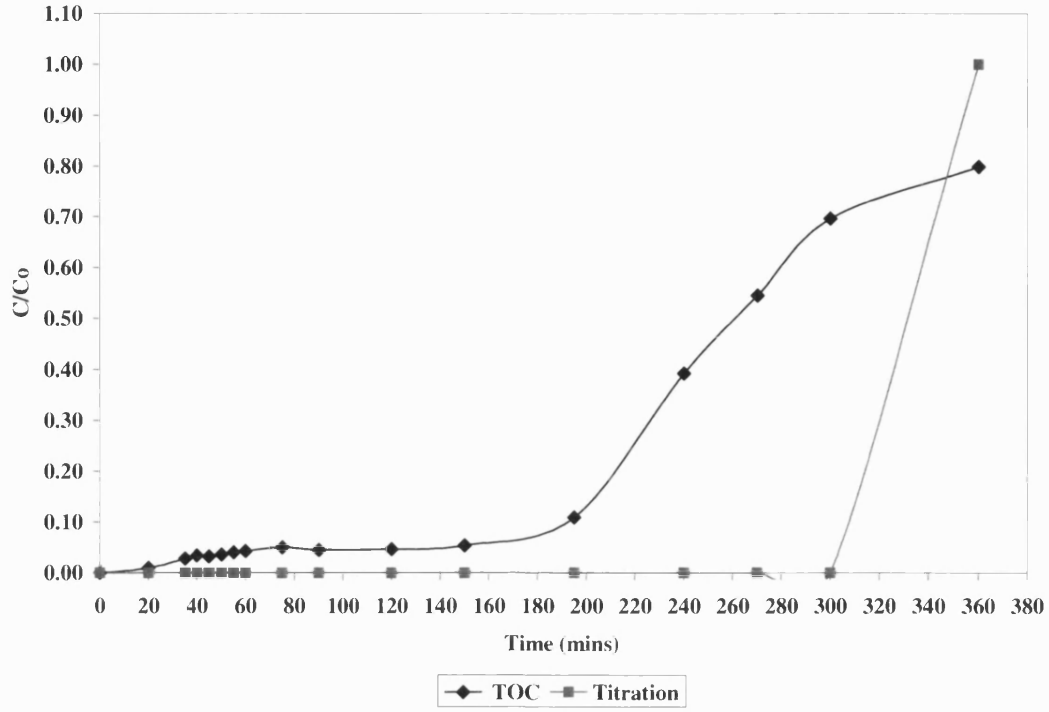

Figure 7.14 A comparison of analysis methods for a dynamic column experiment using ultrafiltered cutting fluid with MAST E-15-50-C and Purolite C150H

Table 7.9 Mass Balances of Dynamic Column Experiments for Ultrafiltered Cutting Fluid with MAST E-15-50-C and Purolite C150H using a 20 cm Column

Figure	Column	C_o (mg l^{-1})	Flowrate (cm^3 hr^{-1})	Column length (cm)	Total mass adsorbed (mg)	% mass adsorbed	Complete loading (mg mg^{-1})
7.13	Purolite	1113.00	150.46	20	480.15	47.83	0.072
7.14	MAST and Purolite	1074.00	150.00	20	658.55	68.13	0.079

Figure 7.15 shows a comparison of the chemically split cutting fluid, "amine" fraction and the "organic" fraction using MAST E-15-50-C carbon and Purolite C150H ion exchange resin. The "amine" and "organic" fractions were obtained by passing the chemically split cutting fluid solution through a carbon and an ion exchange resin bed, respectively, the effluent solution from each producing the individual fraction. The initial conditions for the experiments were a flowrate of 150 cm^3 hr^{-1} and a feed concentration of approximately 1050 mg l^{-1}, 930 mg l^{-1} and 450 mg l^{-1}, for each of the fluids respectively. The analysis

method used was TOC. Even though the 100 cm column had proved to make a marked difference to the complete loading of the carbon, due to a restricted amount of amine solution, Purolite C150H resin, and MAST carbon it was not possible to use the 100 cm column for these adsorption experiments. Therefore the 20 cm column was used.

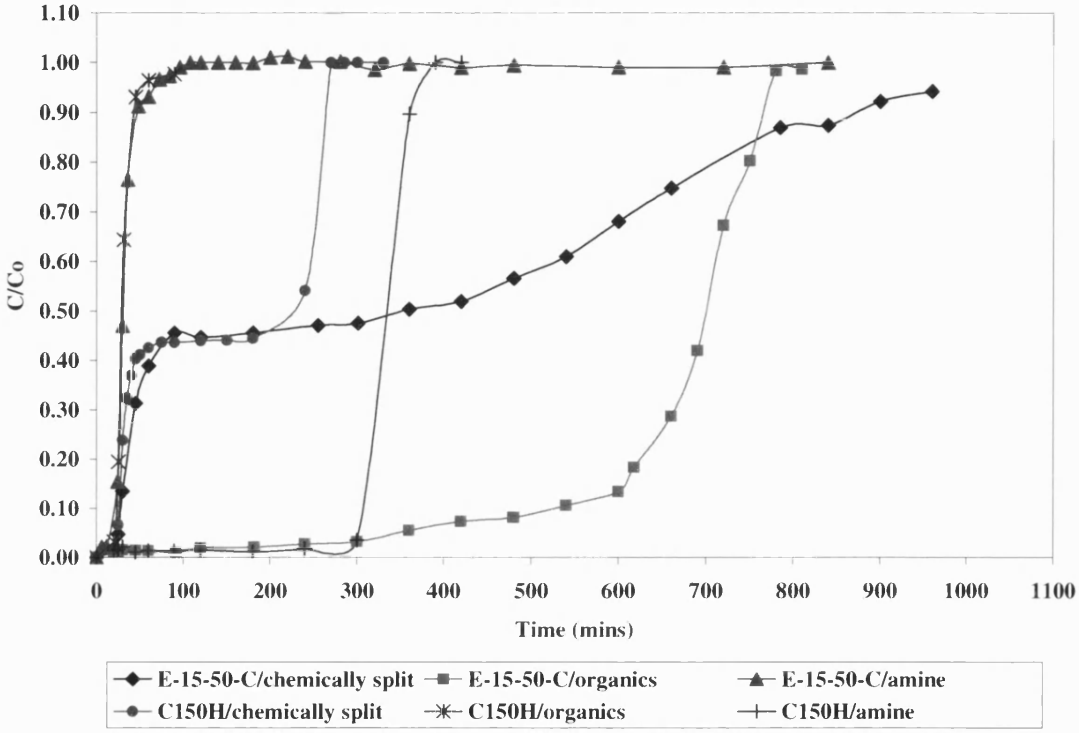

Figure 7.15 A comparison of dynamic column studies for various combinations of MAST E-15-50-C carbon, Purolite C150H ion exchange resin, using chemically split cutting fluid, and the individual "organics" and "amine" fractions

Four of the six graphs in Figure 7.15 show immediate breakthrough. The chemically split solution produced similar graphs for the both the carbon and the ion exchange resin (E-15-50-C/chemically split and C150H/chemically split), such that they both broke through immediately to a C/C_o ratio of approximately 0.45. The "amine" fraction with the carbon (E-15-50-C/amine) and the "organic" fraction with the ion exchange resin (C150H/amine) produced almost identical and immediate breakthrough profiles. The "amine" fraction with the ion exchange resin (C150H/amine), and the "organic" fraction with the carbon (E-15-50-C/organics), on the other hand, produced more reasonable breakthrough times of approximately 300 and 600 minutes, respectively. In addition, the C150H/amine profile

produced a sharp mass transfer front showing good kinetics and good ionic bonding between the resin and the "amine" fraction. This is also shown in the latter section of the C150H/chemically split profile. The mass transfer zone for E-15-50-C/organics is not sharp but rather shallow, indicating poor kinetics. This is probably due to the fact that even though the non-adsorable "amine" fraction has been removed from the chemically split solution, the "organic" fraction still consists of a multi-component mixture, with components adsorbing at different rates.

From Figure 7.15 it might have been expected that the E-15-50-C/organics system would have had the highest loading, the C150H/amine to have the second highest loading, and E-15-50-C/amine and C150H/organics to have the lowest loadings. Table 7.10 shows the mass balances corresponding to the adsorption studies in Figure 7.15.

However, as can be seen from Table 7.10 the latter two predictions are correct, but the first two were not as expected.

Table 7.10 Mass Balances of Dynamic Column Experiments for Chemically Split Cutting Fluid, "Organic" and "Amine" Fractions with MAST E-15-50-C and Purolite C150H using a 20 cm Column

Figure	Column	Feed	C_o (mg l^{-1})	Flowrate (cm^3 hr^{-1})	Total mass adsorbed (mg)	% mass adsorbed	Complete loading (mg mg^{-1})
7.15	MAST	Chemically split	1050.00	150.00	928.34	36.84	0.198
7.15	MAST	Organics	453.55	150.46	734.16	79.94	0.110
7.15	MAST	Amine	931.15	150.00	60.20	12.29	0.025
7.15	Purolite	Chemically split	1102.70	150.00	327.20	35.97	0.060
7.15	Purolite	Organics	474.40	150.00	18.28	17.13	0.003
7.15	Purolite	Amine	673.55	150.00	525.41	74.29	0.081

As before, one of the reasons the amine/C150H loading is not as high as would be expected is that the horizontal portion at the end of the curve is absent and therefore it has not been accounted for in the integral calculation for the mass balances, thereby producing an error. The highest loading was given by the MAST E-15-50-C /chemically split system.

This was probably due to the fact that this run has a broad mass transfer zone and it was carried out for a longer period than any of the other experiments. The reason for the lower than expected loadings of the other studies was probably due the length of the adsorption column being relatively short (20 cm).

If, in the future, an ion exchange unit were to be incorporated into the WOWSEP process, its location to achieve the best results would need to be determined. The ion exchange column could either be placed directly before or directly after the carbon adsorption column.

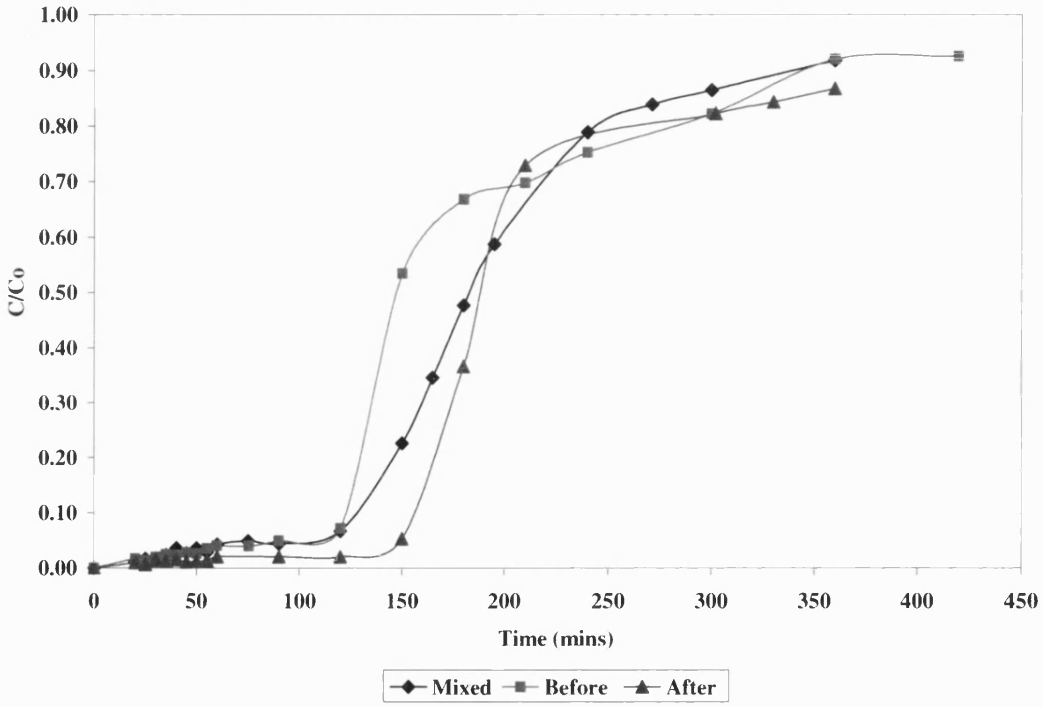

Figure 7.16 A comparison of dynamic column experiments for varying positions of the ion exchange column with regard to the carbon column with chemically split cutting fluid

Figure 7.16 shows a comparison of dynamic column experiments for these two positions of the ion exchange column and a column containing a mixed (50:50, by mass) carbon and resin bed. The feed was a chemically split cutting fluid, with an approximate flowrate of 150 cm^3 hr^{-1} and feed concentration of 1100 mg l^{-1}. As can be seen from the graph all three experiments gave broadly similar breakthrough times (ranging from 120 to 150

minutes), and the shapes of breakthrough curves were moderately steep. The profile for the mixed carbon/resin matrix is relatively shallow and falls in between the "before" and "after" curves, which is reasonable as it can be considered to be an average of the "before" and "after" curves.

The mass balances in Table 7.11 show that all three studies had similar feed flowrates, feed concentrations and loadings. Therefore in general terms the location of the ion exchange unit with regard to the carbon column is not important. For practical reasons and from the industrial point of view, it was decided that ion exchange was not essential and a carbon adsorption column alone was deemed to be sufficient for the WOWSEP process.

Throughout this thesis so far, the pre-treated cutting fluid (whether chemically split or ultrafiltered) has generally been considered to be a single component, homogeneous solution. The experiments have shown this to be untrue however. It has been shown that the solution is, in general terms, a "binary" solution consisting of an "organic" and "amine" fraction. This could help to explain a number of apparent ambiguities in this study. For example, it was mentioned earlier that there is a difference in equilibrium loadings between the batch and dynamic column studies, as summarised in Table 7.12.

Table 7.11 Mass Balances of Dynamic Column Experiments using Chemically Split Cutting Fluid with Purolite C150H Ion Exchange Resin, Before, After and Mixed with MAST Carbon with a 20 cm Column and a Flowrate of 150 cm^3 hr^{-1}

Figure	Position	Feed	C_o (mg l^{-1})	Flowrate (cm^3 hr^{-1})	Total mass adsorbed (mg)	% mass adsorbed	Complete loading (mg mg^{-1})
7.16	Mixed	Chemically split	1124.00	150.00	511.15	50.53	0.059
7.16	Before	Chemically split	1066.00	150.00	465.97	41.63	0.054
7.16	After	Chemically split	1096.50	150.46	466.16	51.53	0.057

Table 7.12 Comparison of Equilibrium Batch and Column Loadings for Various Adsorbents and Adsorbates

Adsorbent	Adsorbate	C_o (mg l^{-1})	Batch loading (mg mg^{-1})	Column loading (mg mg^{-1})
MAST	Propionic acid	991.60	0.065	0.071
MAST	Chemically split	1050.00	0.025	0.198
Purolite	Chemically split	1102.70	0.012	0.060
MAST+Purolite	Chemically split	1124.00	0.065	0.059
MAST	Ultrafiltered	168.60	0.009	0.024
Purolite	Ultrafiltered	1113.00	0.014	0.072
MAST+Purolite	Ultrafiltered	1074.00	0.067	0.079

Table 7.12 shows, firstly, that the equilibrium batch and column loadings for propionic acid are largely similar. The slight difference in the two loadings is probably due to an error in integrating the dynamic column graphs where there is not always a horizontal period at the end of the curve. In the case of the ultrafiltered and chemically split cutting fluids the batch and column loadings vary considerably, when either the MAST carbon only or the Purolite resin is used alone. The differences in loadings are not only due to the errors explained above, but more so due the fact that the loading calculations were carried out on the assumption that the solution was homogeneous and a single component. However, Table 7.12 shows clearly that the batch and dynamic column loadings are comparable for the chemically split and ultrafiltered cutting fluid solutions when the MAST carbon is mixed with the Purolite resin. It is therefore necessary to review some of the loading calculations, by calculating the independent loadings of the "organic" and "amine" fractions on the carbon and ion exchange resin.

7.4.12 Modelling of the adsorption system

Experimental data (such as loading, initial concentration, mass of adsorbent, *etc.*) from the batch and column studies were used to model the "binary" system. As previously explained the pre-treated cutting fluid was assumed to contain a 50:50 ratio of an "organic" and "amine" fraction, each of which only adsorbs onto the carbon and ion exchange resin respectively.

Chapter 4 discussed the theory of Henry's Law, and provided the relationship

$$q = Kc \qquad 4.12$$

Here K is Henry's constant for the desired range of interest, c is the total organic concentration (mg l^{-1}) and q is the loading (mg mg^{-1}) of the respective adsorbate.

Firstly the "organic"/carbon and "amine"/carbon processes were considered. For example, for the "organic" fraction (subscript *org*), from the chemically split cutting fluid solution on a MAST carbon column matrix, it is assumed that the isotherm is linear in the range of interest. Rearranging Equation 4.12 for the "organic" fraction gives Equation 7.2.

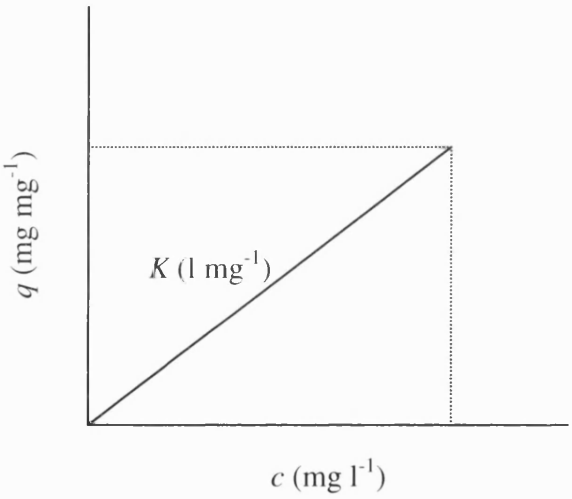

$$K_{org} = \frac{q_{org}}{c_{org_i}} \qquad 7.2$$

The value of K (l mg^{-1}) was calculated (Equation 7.2) using information, such as the initial concentration (c_i) and complete equilibrium loading, obtained from the column studies (Table 7.10 and Figure 7.15). For example the value of K_{org} was calculated to be:

$$K_{org} = \frac{0.110}{453.55} = 0.000242 \text{ (l mg}^{-1}\text{)}$$

Chapter 4 also explained the mass balance for a batch system for a single solute at equilibrium (where V is the volume of adsorbate in litres and M is the mass of adsorbent in mg), subscripts i and f refer to the initial and final concentrations respectively.

$$q = \frac{V(c_i - c_f)}{M} \qquad 4.28$$

Rewriting Equation 4.28 for the "organic" fraction gives Equation 7.3.

$$q_{org} = \frac{V}{M}\left(C_{org_i} - C_{org_f}\right) \qquad 7.3$$

Assuming the adsorbent loading and hence the value of K is the same for both the batch and equilibrium dynamic column studies, Equation 7.1 can be made equal to Equation 7.3.

$$K_{org} c_{org_f} = \frac{V}{M}\left(c_{org_i} - c_{org_f}\right) \qquad 7.4$$

Hence Equation 7.4 can be used to calculate the final (equilibrium) "organic" concentration (c_{orgf}, mg l^{-1}) in the solution, after adsorption has taken place. This equilibrium concentration could then be substituted back in to Equation 7.2 used to calculate the new loading.

This computation was repeated using various initial concentrations in Equation 7.4, and the respective loadings calculated from Equation 7.3. The new calculated loadings were then plotted against the equilibrium concentration to produce an isotherm.

Equation 7.4 can similarly be written for the "amine" fraction (subscript *amine*) as shown in Equation 7.5.

$$K_{amine} c_{amine_f} = \frac{V}{M}\left(c_{amine_i} - c_{amine_f}\right) \qquad 7.5$$

Therefore these calculations were then repeated for the "amine" fraction from the chemically split solution on the carbon and the respective isotherms produced, as shown in Figure 7.17. As expected the "organic" loading on the carbon is much higher than the "amine" loading.

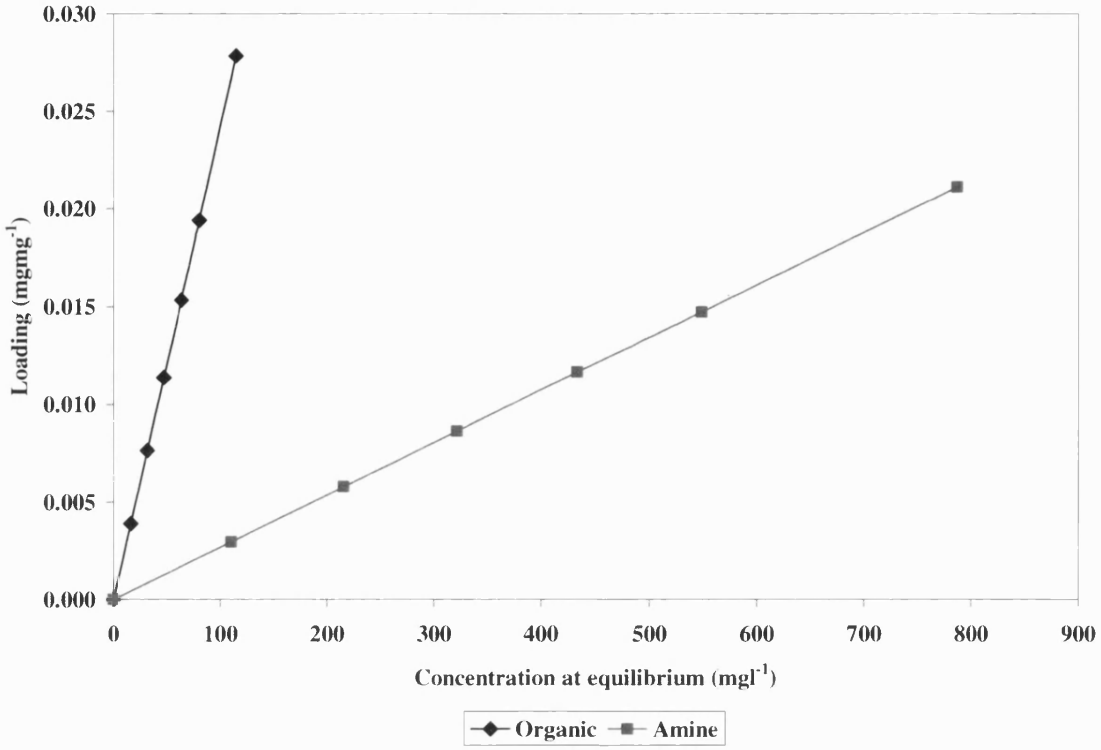

Figure 7.17 A graph showing the individual batch loading obtained from the model of the "organic" and "amine" fractions from chemically split cutting fluid on MAST carbon

Assuming there is no interaction between the "organic" and "amine" fractions, the total loading of the chemically split cutting fluid (q_{cs}) is equal to the summation of the individual loadings (Equation 7.6).

$$q_{cs} = q_{org} + q_{amine} \qquad 7.6$$

This produces a third isotherm for the adsorption of chemically split cutting fluid onto carbon. Figure 7.18 shows a comparison of the batch isotherms obtained experimentally and from the model, using chemically split cutting fluid and MAST carbon. As can be seen both isotherms vary greatly.

Rearranging Equation 7.4, in order to find the final equilibrium concentration gives

$$c_{org_f} = \frac{c_{org_i}}{\left(\frac{K_{org}M}{V} + 1\right)} \qquad 7.7$$

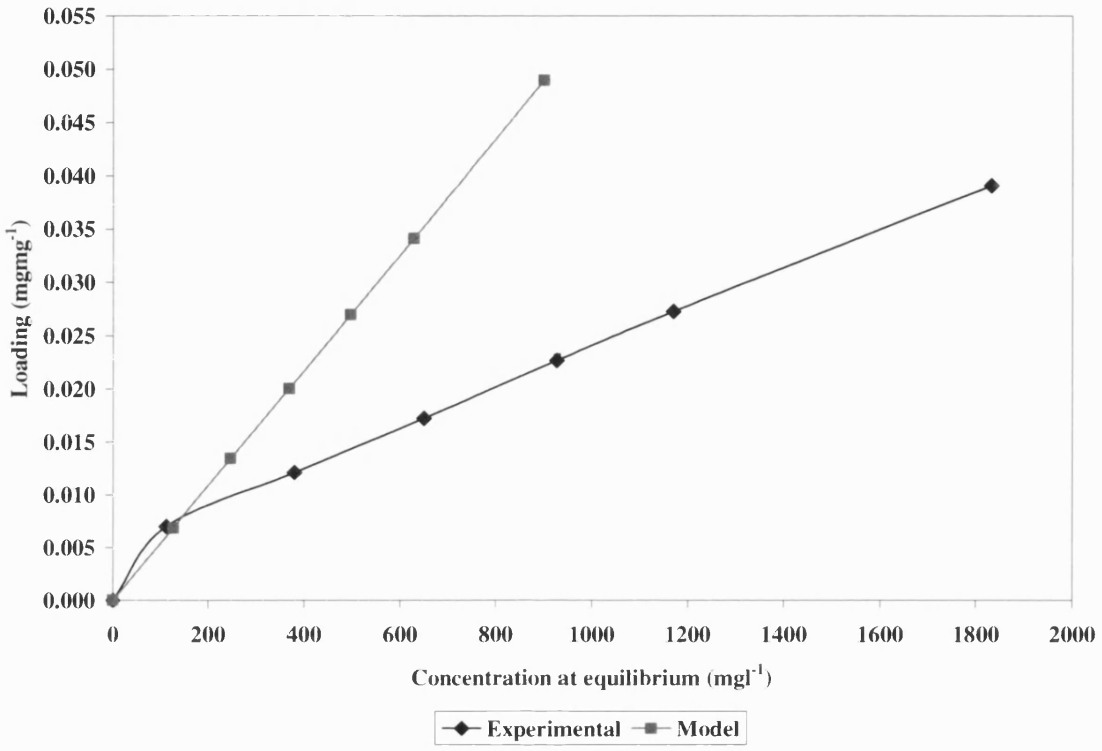

Figure 7.18 A comparison of equilibrium batch loadings obtained experimentally and from a model for chemically split cutting fluid on MAST carbon

In order to verify whether the experimental or model data isotherms represent the true isotherm of the carbon, the model calculations (Equations 4.12 and 4.28) had to be reiterated, until the new isotherms produced converged. The new value of K obtained from the gradient of the model isotherm (Figure 7.18) was then re-introduced into Equation 7.7 (although the subscripts would read *cs*, for the chemically split cutting fluid, rather than *org* for the organics.

For batch studies the initial concentration of feed varies but the values of K, M and V are constant. Hence substituting various values of c_i into Equation 7.7 produces various values of c_f. These values of c_f can then be substituted into Equation 4.12 to find the respective values of the loading, q. The calculated values of q were then plotted against the equilibrium concentration in order to produce a new isotherm. From the gradient of this

isotherm a new value of K was obtained, and these calculations repeated, to produce a new isotherm. This process is repeated until the resultant isotherms converged, as shown in Figure 7.19, where "Series" is the number of reiterations. From this graph it can be seen that Series 3 has the same gradient and profile as Series 2, and if Series 3 was extrapolated to an equilibrium concentration of 1050 mg l^{-1} the total loading of the chemically split cutting fluid on MAST carbon would be 0.198, which is equal to the equilibrium loading obtained from the dynamic column studies (Figure 7.15) for the same concentration (Table 7.12).

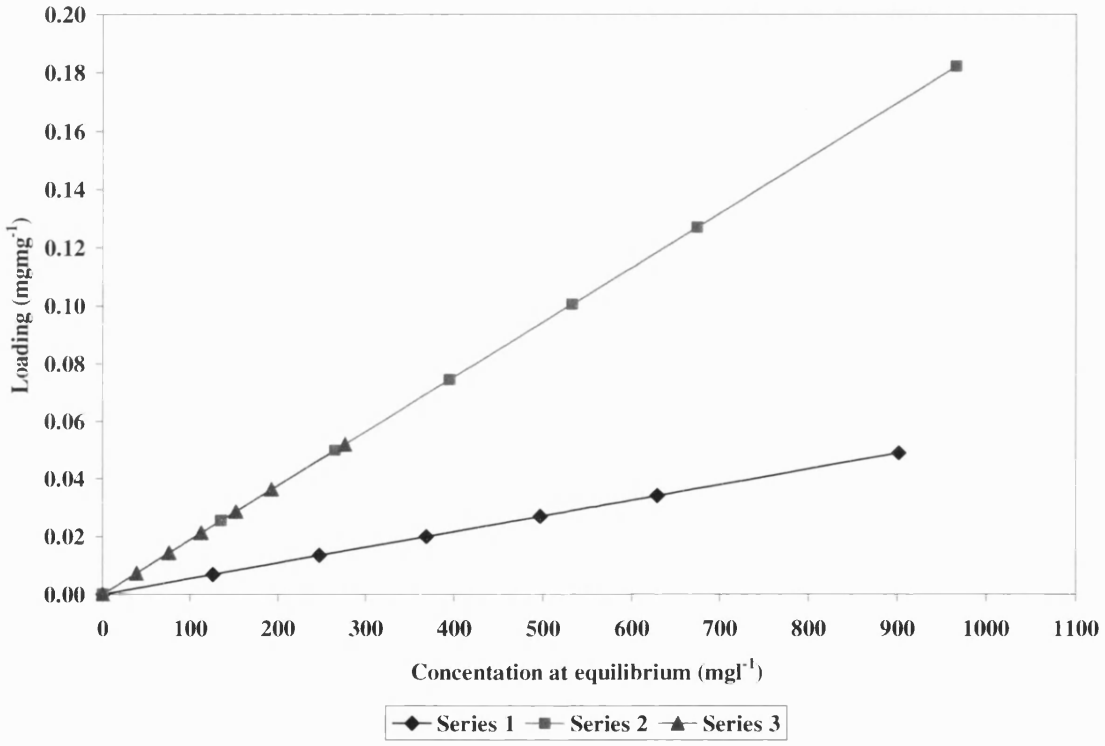

Figure 7.19 Reiteration graphs showing the loading of chemically split cutting fluid on MAST carbon

The loadings of the "organic" and "amine" fractions on the ion exchange resin were similarly calculated using the model. These results are shown in Figures 7.20 to 7.22. Figure 7.20 compares the "organic" and "amine" fraction loadings on the ion exchange resin, and, as expected, the "amine" loading is shown to be higher than the "organic" loading.

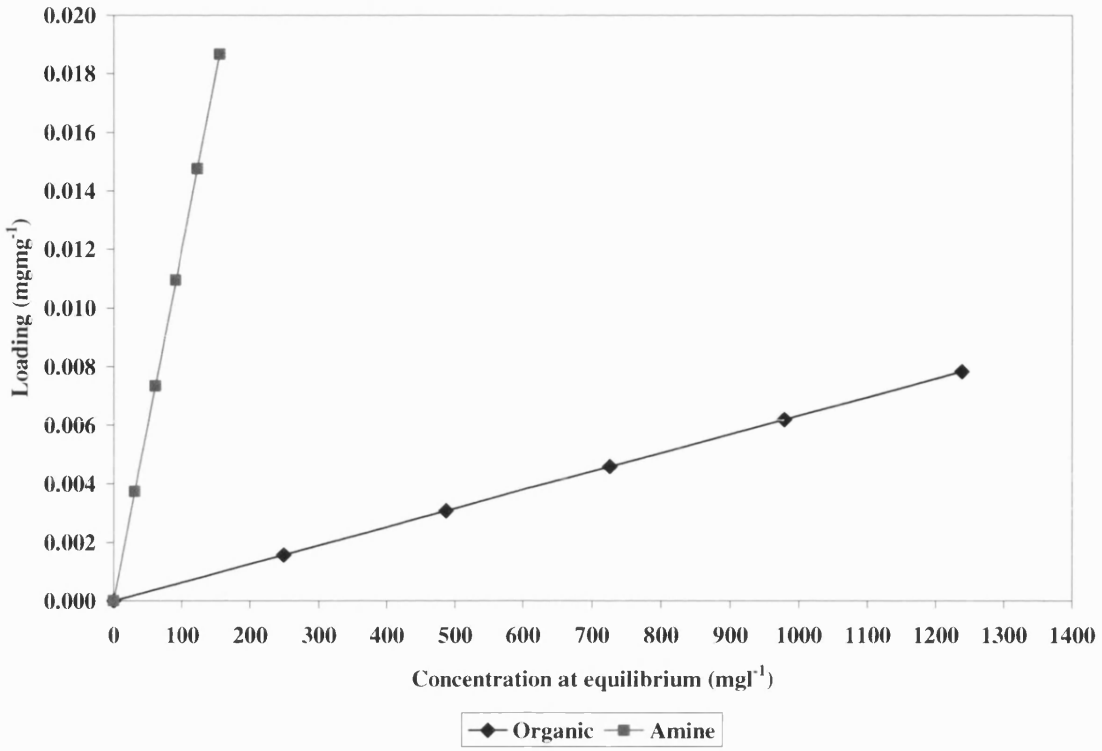

Figure 7.20 A graph showing the individual batch loading obtained from the model of the "organic" and "amine" fractions on Purolite C150H ion exchange resin

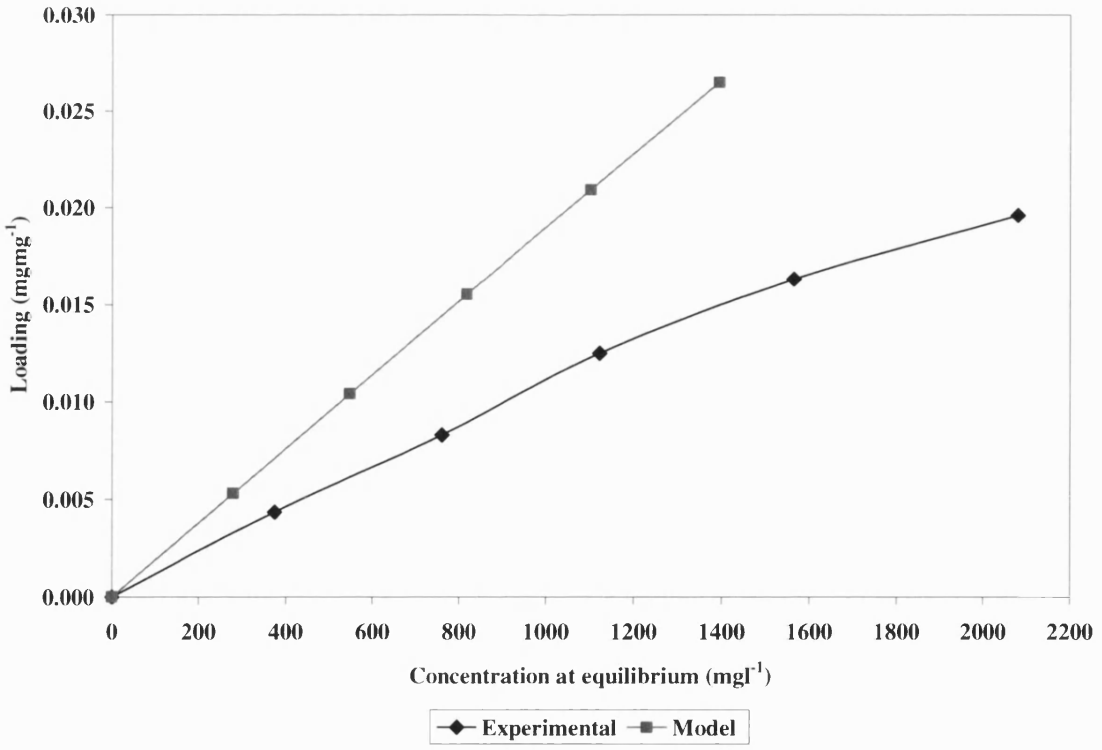

Figure 7.21 A comparison of equilibrium batch loadings obtained experimentally and from the model for chemically split cutting fluid on Purolite C150H resin

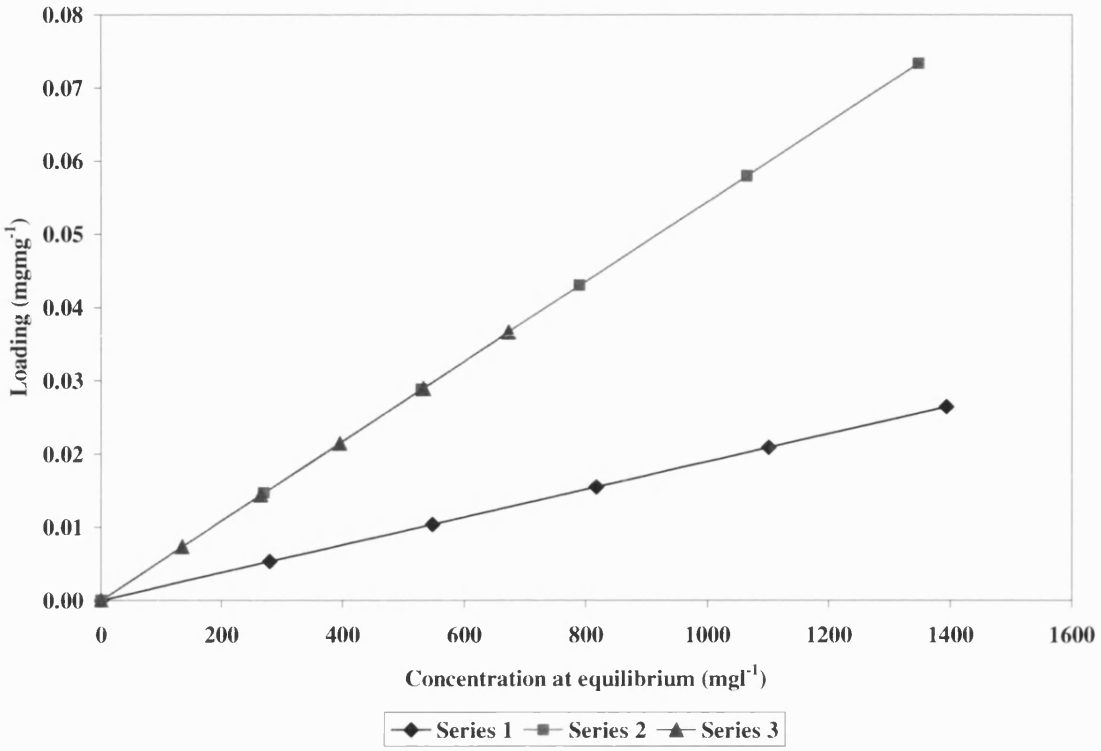

Figure 7.22 Reiteration graphs showing the loading of chemically split cutting fluid on Purolite C150H ion exchange resin

As in Figure 7.18, Figure 7.21 also shows there is a difference between the model and experimental isotherms. This suggests that the reiteration process had to be carried out in order to find the true loading as shown in Figure 7.22. Similar to Figure 7.19, Series 3 (in Figure 7.22) again shows that if it was extrapolated to an equilibrium concentration of 1102.7 mg l^{-1} the total loading of the chemically split cutting fluid on Purolite C150H would be 0.06, which is equal to that obtained from the dynamic column studies (Figure 7.15) for the same concentration (Table 7.12). This would suggest that the complete loading from the column studies is the true loading in both cases of the adsorption of chemically split cutting fluid on carbon and ion exchange resin.

7.4.13 Reproducibility studies

The final factor that needed to be considered in order to test the viability of the adsorption system was the study of reproducibility. This study shows the effectiveness of a system and whether identical results could be reproducibly obtained under the same conditions.

Figure 7.23 shows the results of five reproducibility experiments which were each conducted using fresh MAST E-15-40-C carbon, under almost identical conditions using the 20 cm column, chemically split cutting fluid, and a flowrate of 150 cm^3 hr^{-1}. Even though ion exchange was not used in these experiments (due to time constraints) and the shorter column was used, all of the experiments are clearly very similar. This shows excellent reproducibility and confirms the viability of the system.

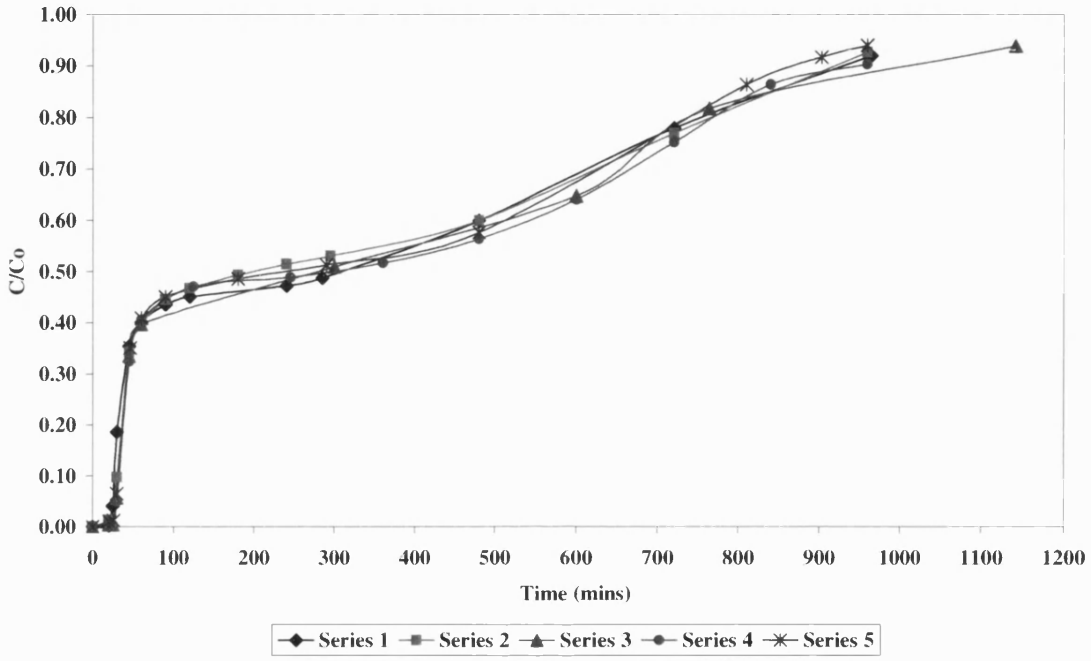

Figure 7.23 A graph showing adsorption reproducibility using MAST E-15-40-C and chemically split cutting fluid

Table 7.13 Mass Balances of a Series of Five Breakthrough Experiments using MAST E-15-40-C Carbon and Chemically Split Cutting Fluid

Figure	Series	Flowrate (cm^3 hr^{-1})	Column (cm)	C_o (mg l^{-1})	Total mass adsorbed (mg)	% mass adsorbed	Complete loading (mg mg^{-1})
7.15	Series 1	150	20	1054.75	938.62	36.89	0.196
7.15	Series 2	150	20	1056.25	913.38	36.03	0.183
7.15	Series 3	150	20	1042.68	1021.26	34.31	0.196
7.15	Series 4	150	20	1037.50	901.34	36.20	0.180
7.15	Series 5	150	20	1049.50	953.89	37.87	0.187

The corresponding mass balances (Table 7.13) are also shown to be very similar (a maximum difference in loading of 7%).

Repeatability studies were also conducted to verify the durability of the carbon and to see how many continuous adsorption/regeneration cycles can be conducted without a loss in carbon capacity. These repeatability studies are discussed in greater detail in the next Chapter.

7.5 Conclusions

Whilst there have been many theoretical models to predict the mass transfer zones and concentration profiles in a fixed bed, uncertainties of flow patterns and correlations to predict diffusion and mass transfer often make them inaccurate. Therefore laboratory-scale experiments were essential in order to scale-up the process for industrial use.

Even though pre-treatment processes like ultrafiltration and chemical splitting reduced the total TOC content of the neat cutting fluid, they did not assist in the complete adsorption of the "organic" content onto activated carbon. It was found that this might have been due to a number of reasons such as pH, influent flowrate, influent concentration, column length, carbon activation and carbon pore size. The pH of the influent and of the carbon were altered and tested with the dynamic column system. Various carbons with different pore sizes and activation levels were used. Unfortunately, these did not solve the immediate breakthrough problem. The flowrate, influent concentration and column length, on the other hand, did affect the breakthrough studies marginally, but not to such an extent that the premature breakthrough problem was resolved. It was found that for a flowrate of 150 $cm^3\ hr^{-1}$, a 1.27 cm (½") diameter column and a minimum EBCT of 15 minutes, a column length of at least 40 cm was required to achieve an ideal breakthrough graph with a fully developed mass transfer zone. Column length was not the underlying cause of the immediate breakthrough however. The immediate breakthrough was found to be due to the presence of non-adsorbable alcoholamine (*e.g.* MEA), which is present in cutting fluids in the form of corrosion inhibitors. Although, whilst fluid reformulation was an option, these compounds play an important role in the fluid formulations and so they cannot simply be omitted from the cutting fluid. Experiments using DEA, Polartech, MEA *etc.* showed that any solution containing an amine derivative will not be wholly adsorbable by

carbon. Therefore the amine compound would have to be removed from the cutting fluid solution before it could be treated using a carbon adsorption process. The most appropriate method to remove the "amine" fraction from the wastewater was found to be ion exchange, as it is a simple efficient step which does not require any complicated equipment.

The experimental batch and dynamic equilibrium loadings were found to be different due to an initial assumption of the cutting fluid being a single component homogenous solution. It was found that the cutting fluid solution could be assumed to be made up of two components consisting of an "organic" and "amine" fraction. A model was developed to take into account the fact that the cutting fluid was a binary mixture. From this model it was found that the equilibrium (complete) loading was the more accurate loading of the adsorbent.

The reproducibility of the process was tested through a set of five reproducibility experiments in series, using fresh carbon after each experiment. The results gave almost identical graphs.

To make the WOWSEP process economically viable it should be possible to reuse the carbon. Therefore the next Chapter studies the effect of carbon regeneration.

8.0 Regeneration Studies

Activated carbon has been used for many years in adsorption processes as a very effective adsorbent for the removal of organic pollutants and toxic substances and for the recovery of valuable substances from waste streams. Initially, activated carbon was used on a 'throwaway' basis and was usually sent to landfill. However, it was soon realised that not only was the disposal and replacement of the spent carbon making this process uneconomical (Gronvaldt and Dietrich, 1987), but a renewable resource was being wasted. In addition, this was contributing to an already increasing national waste disposal dilemma (Parmele *et al.*, 1986). Consequently, activated carbon has recently been developed with sufficient mechanical stability to withstand repeated regeneration, restoring the carbon's original adsorptive power for reuse and recovering the valuable components from the adsorbed phase (Lombana and Halaby, 1991, Waer *et al.,* 1992). Therefore regeneration of carbon makes the adsorption process a more economical, energy efficient and environmentally sound option (Cannon *et al.,* 1994; Hashimoto *et al.*, 1985; Jankowska *et al.*, 1991b).

Generally carbon is the core expense of an adsorption process. However, when considering a system which includes both carbon adsorption and regeneration the major part of the total operating costs is associated with regeneration (Liu *et al.*, 1995). These operating costs stem from capital costs, transportation, equipment, operations, maintenance and the cost of makeup carbon (Waer *et al.,* 1992). Therefore, regeneration becomes economically worthwhile when the carbon exhaustion rate is high, making savings from purchasing replacement carbon and the ability to recycle the recovered product offsets the amount invested in the regeneration system. Additional savings may be made if regeneration is conducted *in-situ*, rather than having to pay extra for the expenses associated with off-site regeneration and/or waste disposal (*e.g.* transportation, makeup carbon *etc.*). Hence, both the product and carbon from the regeneration process must be valuable enough, restored in a usable form, easily purified, or alternative treatment more costly in order for the recovery process to be feasible.

Regeneration occurs when a change in system conditions (*e.g.* temperature, pressure, pH, solubility, polarity, molecular shape, size and weight) reverses the equilibrium of the process. This change is usually aided by using a regenerating medium (regenerant) such as

steam, chemical or biological reagents or solvents. The change in system conditions decreases the strength of the adsorbent-adsorbate forces and increases the regenerant-adsorbate forces, resulting in regeneration of the spent carbon and recovery of the adsorbate (Fox and Kennedy, 1985). Over the years many regeneration techniques (chemical, biological, oxidation, and thermal) have been developed to regenerate adsorbent materials, such as carbon, and to recover adsorbed materials.

Chemical regeneration involves the addition of chemical reagents to the adsorber. A chemical reaction takes place which alters the pH of the system and changes the affinity between the adsorbate and adsorbent. This is similar to the elution process in ion exchange (Kittredge, 1980). There are two types of chemical regeneration: acidic or basic (alkaline). Acidic regeneration is used if the major organic component is basic and the adsorber is under basic conditions, vice versa for basic regeneration (Lyman, 1978).

Biochemical or chemical oxidation desorbs the adsorbate from the carbon as a result of the reversible nature of an equilibrium process. The driving force, for further desorption, is provided by the addition of an oxidising agent which consumes molecules that have diffused out into a less concentrated solution surrounding the carbon particles (Kittredge, 1980).

Biological regeneration is dependent on the biodegradability of the adsorbed organics. If carbon is incorporated into a biological treatment system, it is then recovered with activated sludge in a clarifier and regenerated by aeration of the carbon/sludge mixture.

Chemical regeneration, oxidation, and biological regeneration are non-destructive (to the adsorbent or adsorbates) processes, but they are extremely slow and usually inefficient in achieving complete regeneration (Parmele *et al.*, 1986), so much so that often thermal regeneration is also periodically required (Lyman, 1978).

Thermal regeneration is a logical extension of the carbon activation process and so is often called reactivation (Fox and Kennedy, 1985). It involves heating the carbonaceous material in controlled gas atmospheres at temperatures up to 1000°C (George *et al.*, 1995). This heating process is usually characterised in four-stages (Waer *et al.*, 1992):

1. Drying: Heating the wet, spent carbon to temperatures up to 150°C eliminates approximately 50% of the water (by weight) and highly volatile adsorbates. However, the chemically bound and higher boiling point organics remain on the carbon.
2. Vaporisation: Increasing the temperature up to 500°C decomposes the less volatile and chemically bound adsorbates to form volatile fragments, removes the remaining water and dries the carbon. This usually takes place in an inert gas atmosphere to minimise oxidation. Residual polymers, tars and very high boiling point organics still remain in the micropores on the dry, spent carbon.
3. Pyrolysis: Increasing the temperature further to 700°C exposes the non-volatile adsorbates to an inert gas environment forming a carbonaceous char on the surface of the activated carbon.
4. Oxidation: The introduction of oxidising agents (such as steam or carbon dioxide) to temperatures above 700°C gasifies the carbonised char, drives off the residues and tars as well as other high boiling point adsorbates from the internal surface of the carbon. This process also slightly widens the GAC pores.

Thermal regeneration is generally considered to be the most successful means of restoring the adsorptive capabilities of spent carbon (Parmele *et al.*, 1986; Kittredge, 1980). However, even though it is popular it also has many disadvantages:

(i) Excessively high temperatures mean *in-situ* regeneration is not a viable option therefore the carbon needs to be transferred from the adsorber to special furnaces. During transportation, carbon fines may be lost and so require replacing with virgin carbon. In addition, maintenance and operating costs of furnaces can be high.

(ii) Oxidation and mechanical attrition results in carbon pores being destroyed or enlarged. In many cases, high temperatures of thermal regeneration destroy up to 15% capacity of the carbon (Stenzel and Merz, 1989; Metcalf and Eddy, 1991), which would need replacing with fresh carbon. However, regeneration is only regarded as successful if it does not significantly alter the physical and chemical properties of the carbon (McGinnis and Horwitz, 1981).

(iii) The presence of inorganic salts and ash cannot be removed by thermal regeneration thereby causing a loss in adsorption capacity, although a preliminary acid wash may help to avoid this problem (Lyman, 1978; Pilard *et al.*, 1996). In addition, if the spent carbon contains corrosive materials (*e.g.* amines which could result in high

NO_x emissions), explosive materials (*e.g.* TNT) or radioactive materials, then thermal regeneration could be extremely hazardous.

Steam regeneration (which is a variation of thermal regeneration), uses steam to displace the liquid in the adsorber bed, heat the adsorbent and strip the organics off the carbon (Hashimoto *et al.*, 1985; Fox and Kennedy, 1985). Whilst steam regeneration is similar to thermal regeneration using a non-condensable purge gas, steam regeneration is qualitatively different. For example when using a non-condensable gas the velocity of the gas entering the bed is roughly the same as the effluent leaving the bed, and a temperature drop manifests itself as heat losses from the vessel. When using steam the temperature is not significantly affected during regeneration and its velocity changes as it adsorbs and condenses within the vessel at the walls and in the bed (Schweiger and Le Van, 1993).

The choice of regeneration process depends on the degree of saturation of the carbon, the type of adsorbate, the regeneration equipment available and the quality of regeneration required (Kittredge, 1980; Parmele *et al.*, 1986; Liu *et al.*, 1995). Of these regeneration methods, steam regeneration has recently become more reputable than thermal regeneration. This is mainly because it has no emissions into the atmosphere; it is relatively low in cost, has good effluent quality and can be applied without causing any damage to the porous structure or activity of the carbon (Hashimoto *et al.*, 1985; Parmele *et al.*, 1986; Schork and Fair, 1988; Fox and Kennedy, 1985; Liu *et al.*, 1995). Therefore steam regeneration has become popular as the most effective way to regenerate an adsorbent.

In this project, both the carbon and the cutting fluid were relatively costly and hence single use followed by disposal was definitely uneconomical. As a result, the aims and objectives of this project were to develop a carbon adsorption system capable of being regenerated *in-situ.* It was therefore essential to develop the WOWSEP process so as to restore the carbon's original porous structure and activity, with as little damage to the carbon as possible, and to facilitate the recycling of purified water on-site as well as possibly recycling all or of part of the organic compounds. Generally, high steam pressures and resulting high temperatures are not recommended as the organics could react with the steam to produce higher boiling materials. This is especially so in the presence of granular activated carbon which can also act as a catalyst (Fox and Kennedy, 1985). The novelty of

the WOWSEP regeneration process was that it used relatively low temperature superheated steam to drive off the soluble contaminants *in-situ* from the internal structure of the novel synthetic carbon (Crittenden *et al.*, 2001).

8.1 Design of the regeneration system

One of the aims of the WOWSEP process was to have an *in-situ* regeneration process such that it was incorporated with the adsorption system as a single bed operation; there would be no liquid/solid separation at the column inlet or outlet. In general, *in-situ* regeneration minimises the amount of attrition and abrasion between particles as the adsorbent does not require transportation via pumps *etc.* However, in order for an *in-situ* process to be successful, the direction of the regenerant flow with respect to the adsorbate flow through the carbon column must be considered carefully. Co-current flow (where the adsorbate and regenerate flow in the same direction) is relatively low in capital cost, simple to operate, does not require complex controls and is generally low maintenance. A major limitation of the co-current process, however, is that if adsorption takes place in the downward direction, the upper part of the adsorption bed becomes saturated a great deal more than the lower part of the bed. In this case, if regeneration takes place with flow in the same direction, the lightly saturated lower part of the adsorption bed is exposed to a high concentration of solute, possibly resulting in an unfavourable equilibrium during subsequent loading cycles. Counter-current regeneration (where the adsorbate and regenerate flow in opposite directions), gives a highly cleansed lower bed, which is never exposed to a high solute concentration. Overall, counter-current flow reduces regeneration costs and regenerant volume, increasing the effluent quality and generally producing a sharper, more efficient regeneration. Therefore the WOWSEP process was designed with counter-current flow.

The use of superheat means that relatively low steam temperatures and pressures could be used to regenerate the activated carbon. In order to regenerate activated carbon economically and effectively it is vital to determine the thermal behaviour of the adsorbates (Liu *et al.*, 1986), since this influences the amount of char formed in the adsorbent bed. Unfortunately, very little information was available on the characteristics of the adsorbates present in the cutting fluid. Therefore the thermal behaviour of the

adsorbates was unknown and the steam temperature required for regeneration of the activated carbon in the WOWSEP process was determined by trial and error.

A laboratory-scale process was designed to produce relatively low temperature superheated steam at atmospheric pressure. This was achieved by pumping water through a heat exchanger coil which was immersed in a heated and fluidised sand bath. The heat exchanger coil was calculated to be long enough to convert water at approximately 10°C to superheated steam at 200°C and atmospheric pressure.

Generally, during steam regeneration most of the energy provided by the steam goes towards heating the adsorbent vessel the carbon in the bed together with any residues of solvent and water (Schweiger and LeVan, 1993). In the laboratory-scale rig, this problem was overcome by immersing the column in the fluidised sand bath, such that the steam, column *etc.* were all at the same temperature. This ensured the steam was only being utilised to desorb the contaminants from the carbon bed and not to heat the bed. There were two thermocouples, one at the exit of the heat exchanger coil and the other in the adsorption bed to monitor the temperature of the steam. Although the laboratory-scale rig was designed with a heat exchanger coil to produce superheated steam, the pilot scale rig in the WOWSEP process was designed with an in-line electrical steam generator, so that it could be used independently as a standalone process or as an 'add-on' to an existing treatment process.

In addition, to ensure there was no condensation on the inside of pipes and to keep the system at constant temperature, the 'hot' regenerant pipes in the laboratory-scale rig were insulated with Cooper-Knit 500 (a knitted silica thermal insulation blanket able to withstand temperatures of up to 950°C). In order to collect the regenerated product at the exit, the hot vapour product had to be cooled and condensed. The simplest and most cost effective condenser that would fit in well with the WOWSEP process was a double pipe heat exchanger. This condenser was therefore used to reduce the temperature of the hot regenerant vapour product from a maximum of 300°C to minimum of 50°C.

The steam flowed in the inside pipe and water (the cooling fluid) on the outside. The temperature reduction in the superheated steam means that the steam would have to go

through three stages (desuperheating, condensation and sub cooling) before achieving the final state.

One objective of the regeneration studies was to investigate the effect of steam temperature. There were two ways of altering the temperature of the steam in the laboratory-scale process: (i) to vary the length of the heat exchanger coil or (ii) to vary the fluidised sand bath temperature. However, it was not practical to change the length of the heat exchanger coil and so the steam temperature in the laboratory-scale process was varied by changing the temperature of the sand bath.

Figure 8.0 shows a schematic diagram of the regeneration side of the laboratory-scale rig, and Figure 8.1 is a schematic diagram of the complete *in-situ* adsorption/regeneration process.

8.2 Experimental procedure

After the adsorption process had taken place and the adsorption bed was saturated with adsorbate, the system was flushed through with ultrapure water, which was supplied from a Millipore Ultrapure Water Purification System. The sand bath was then supplied with air, at a flowrate of 57 l min^{-1} and a pressure of 3 psi, via a distribution plate, such that the sand was fluidised. The sand bath temperature was set according to the final steam temperature required using a digital temperature controller (*e.g.* a sand bath temperature of 300°C produced superheated steam at 200°C). In the fluidised state, the electric heater switches itself on providing heat to the system. The cooling water to the double pipe condenser was turned on. The fluidised sand bath was then raised using a hydraulic pump ensuring the heat exchanger coil and the adsorbent bed were completely immersed into the hot sand. Ultrapure water was pumped into the heat exchanger coil at the desired flowrate (*e.g.* 50 ml hr^{-1}). This water flowrate varies the amount and flowrate of steam produced in the heat exchanger coil. This steam then flows counter-currently downwards through the column, where it is contacted with the spent carbon. The vapour product was condensed to a concentrated liquid and samples collected for periodic TOC analysis. The regeneration experiments were repeated with various water flowrates and superheated steam temperatures ranging between 25-115 ml hr^{-1} and 180°C-225°C, respectively.

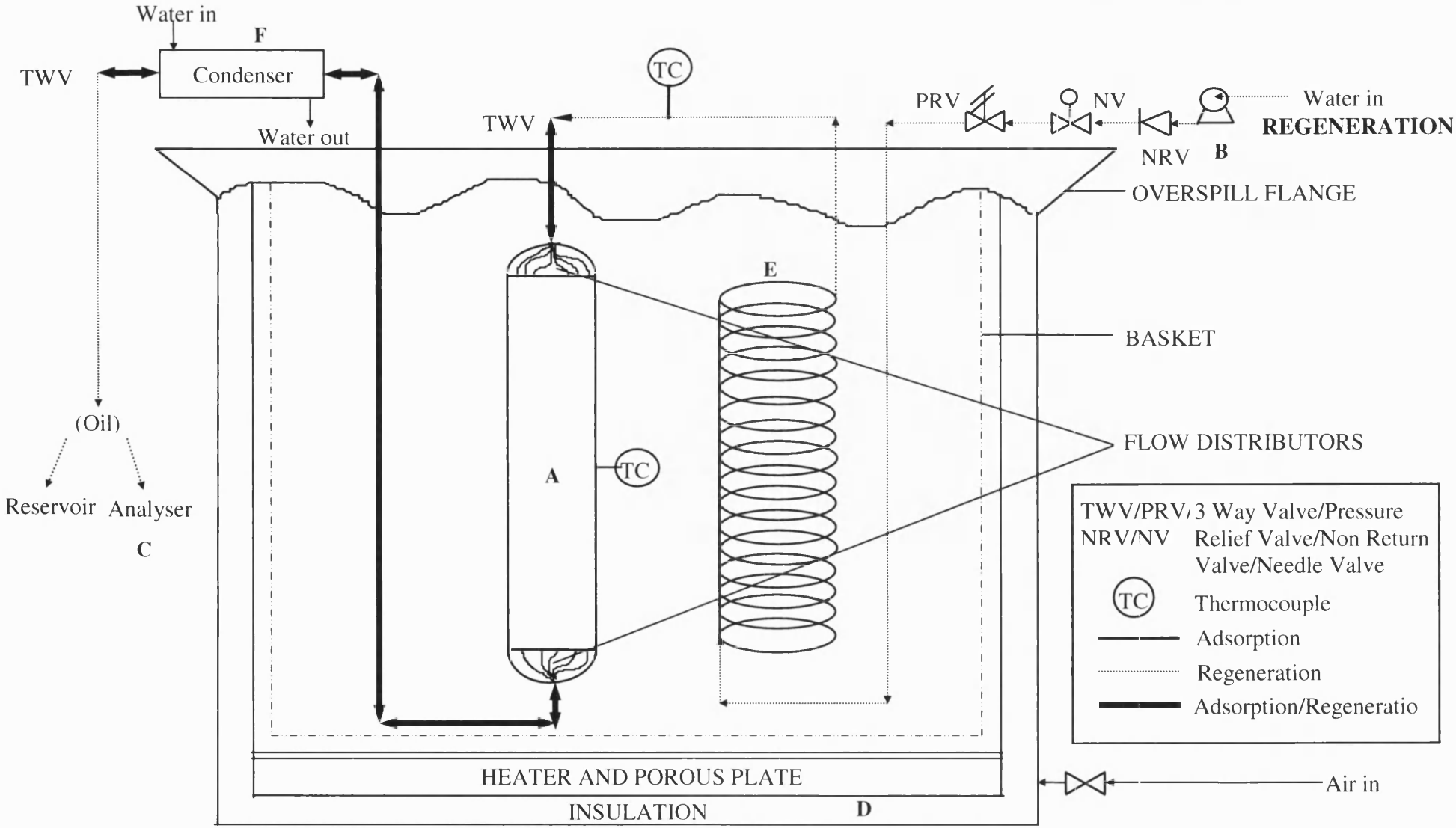

Figure 8.0 Schematic diagram of the regeneration side laboratory-scale rig

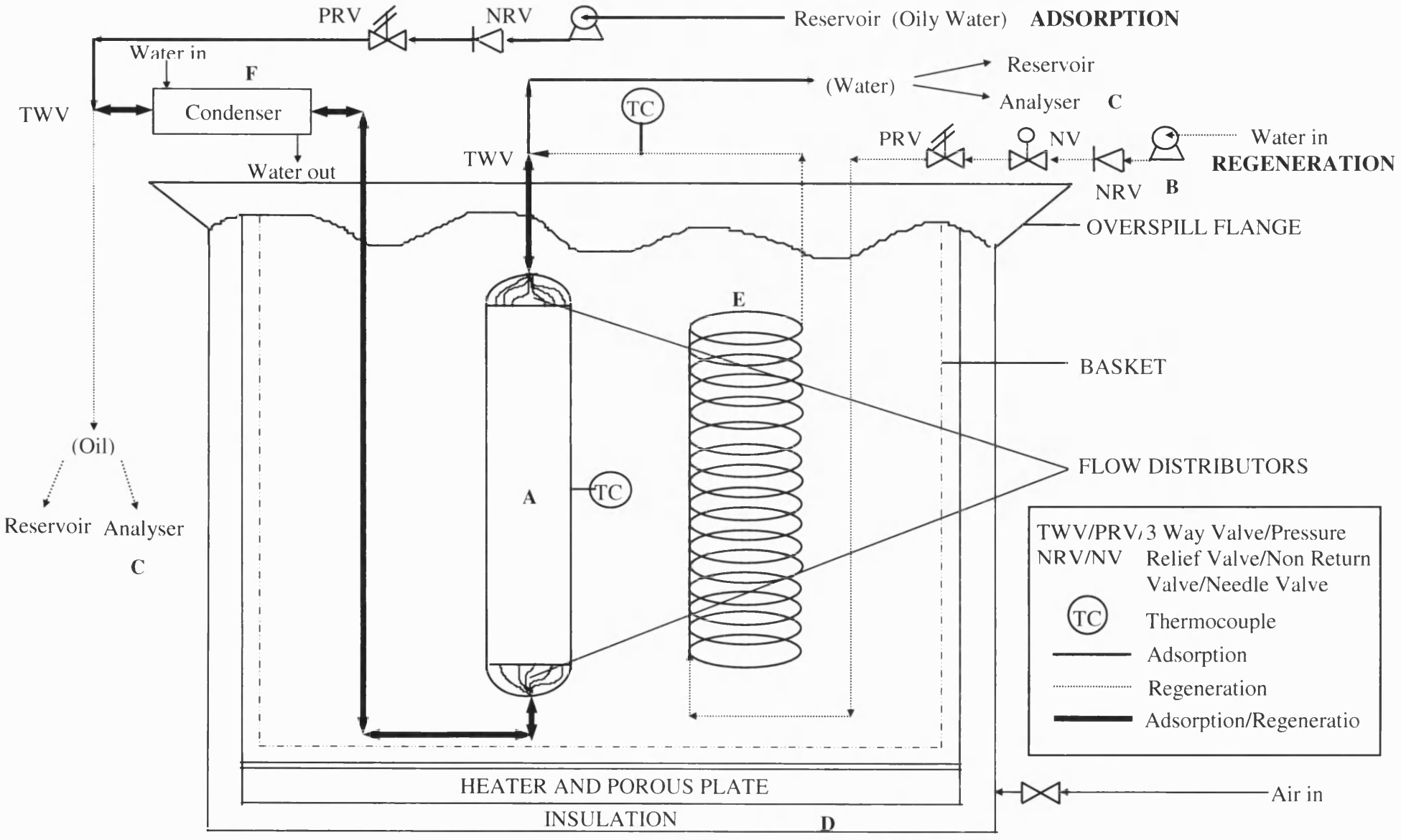

Figure 8.1 Schematic diagram of the complete laboratory-scale rig

8.3 Results and discussions

In order to find the ideal conditions for the prototype WOWSEP process, many experiments had to be conducted in the laboratory. This section discusses the effects of various conditions (such as carbon type, cutting fluid type, water/steam flowrate, temperature *etc.*) in order to determine the best conditions for the regeneration process.

As well as considering the regeneration process conditions, reproducibility and repeatability tests also have to be carried out (Fox and Kennedy, 1985). In addition, a comparison of the amount adsorbed onto the carbon (loading) with the amount desorbed off the carbon (offloading) can be made. The difference between the two figures is related to the efficiency of the system. If the discrepancy between the two amounts is small, then the process may still be considered viable. If, on the other hand, the discrepancy is large, the system would be deemed inefficient. Generally, there are two scenarios which may arise from the comparison between the loading and the recovery on regeneration:

1. The adsorbed amount equals the desorbed amount. This is the ideal situation and would prove the system was extremely efficient and therefore viable.
2. The adsorbed amount is much greater than the desorbed amount. This situation would suggest the regeneration process to be inefficient, wherein complete regeneration was not taking place and the process was unable to desorb all of the adsorbed components.

The following sections study various system conditions and their impact on the regeneration process. Table 8.0 shows a summary of all the regeneration experiments and their respective adsorption experiments, which are discussed in this Chapter.

Table 8.0 Summary of Conditions for Adsorption and Respective Regeneration Experiments

Figure	Adsorbent	Feed solution	Column length (cm)	Mass dry adsorbent (g)	C_o (mg l^{-1})	Water flowrate (cm^3 hr^{-1})	Temperature (°C)	Complete adsorption (mg mg^{-1})	Complete regeneration (mg mg^{-1})	Discrepancy (mg mg^{-1})
-	MAST E-15-35-C	Ultrafiltered	10	2.46	155.80	288.31	20	0.062		
8.2	MAST E-15-35-C	Steam	10	2.46	3.90	108.61	200		0.062	0.000
-	MAST E-15-50-C	Chemically split	20	4.10	1087.75	150.00	20	0.163		
8.2	MAST E-15-50-C	Steam	20	4.10	13.38	100.00	205		0.179	-0.016
-	MAST E-15-35-C	Ultrafiltered	10	2.46	155.80	288.31	20	0.062		
8.3	MAST E-15-35-C	Steam	10	2.46	3.90	108.61	200		0.062	0.000
7.3	SS 607C	Ultrafiltered	10	3.25	127.65	294.36	20	0.025		
8.3	SS 607C	Steam	10	3.25	15.00	108.61	200		0.035	-0.010
-	Untreated MAST E-15-35-C	Ultrafiltered	10	2.46	155.80	288.31	20	0.062		
8.4	Untreated MAST E-15-35-C	Steam	10	2.46	3.90	108.61	200		0.062	0.000
-	Air oxidised MAST E-15-35-C	Ultrafiltered	10	2.46	172.68	291.60	20	0.061		
8.4	Air oxidised MAST E-15-35-C	Steam	10	2.46	4.20	107.30	200		0.046	0.015
7.16	MAST E-15-50-C	Chemically split	20	4.70	1050.00	150.00	20	0.198		
8.5	MAST E-15-50-C	Steam	20	4.70	14.79	50.00	205		0.250	-0.052
7.4/7.23	MAST E-15-40-C	Chemically split	20	5.10	1049.50	150.00	20	0.187		
8.5	MAST E-15-40-C	Steam	20	5.10	1.38	50.00	205		0.112	0.075
-	MAST E-15-50-C	Chemically split	20	4.10	1062.25	150.00	20	0.207		
8.6	MAST E-15-50-C	Steam	20	4.10	11.56	20.00	205		0.195	0.012

Table 8.0 Summary of Conditions for Adsorption and Respective Regeneration Experiments (continued)

Figure	Adsorbent	Feed solution	Column length (cm)	Mass dry adsorbent (g)	Co (mg l^{-1})	Water flowrate (cm^3 hr^{-1})	Temperature (°C)	Complete adsorption (mg mg^{-1})	Complete regeneration (mg mg^{-1})	Discrepancy (mg mg^{-1})
-	MAST E-15-50-C	Chemically split	20	4.30	1060.25	150.00	20	0.214		
8.6	MAST E-15-50-C	Steam	20	4.30	11.34	50.00	205		0.198	0.016
-	MAST E-15-50-C	Chemically split	20	4.10	1087.75	150.00	20	0.163		
8.6	MAST E-15-50-C	Steam	20	4.10	13.38	100.00	205		0.179	-0.016
7.23	MAST E-15-40-C	Chemically split	20	4.80	1054.75	150.00	20	0.196		
8.7	MAST E-15-40-C	Steam	20	4.80	0.80	50.00	180		0.165	0.031
7.4/7.23	MAST E-15-40-C	Chemically split	20	5.10	1049.50	150.00	20	0.187		
8.7	MAST E-15-40-C	Steam	20	5.10	1.38	50.00	205		0.112	0.075
7.23	MAST E-15-40-C	Chemically split	20	5.00	1037.50	150.00	20	0.180		
8.7	MAST E-15-40-C	Steam	20	5.00	3.70	50.00	225		0.109	0.071
-	Series 1 MAST E-15-50-C	Chemically split	20	4.10	1062.25	150.00	20	0.190		
8.8	Series 1 MAST E-15-50-C	Steam	20	4.10	14.06	50.00	205		0.176	0.014
-	Series 2 MAST E-15-50-C	Chemically split	20	4.30	1060.75	150.00	20	0.214		
8.8	Series 2 MAST E-15-50-C	Steam	20	4.30	11.34	50.00	205		0.198	0.016
7.23	Series 3 MAST E-15-40-C	Chemically split	20	5.20	1042.68	150.00	20	0.196		
8.9	Series 3 MAST E-15-40-C	Steam	20	5.20	1.55	50.00	205		0.095	0.101

Table 8.0 Summary of Conditions for Adsorption and Respective Regeneration Experiments (continued)

Figure	Adsorbent	Feed solution	Column length (cm)	Mass dry adsorbent (g)	Co ($mg\ l^{-1}$)	Flowrate ($cm^3\ hr^{-1}$)	Temperature (°C)	Complete adsorption ($mg\ mg^{-1}$)	Complete regeneration ($mg\ mg^{-1}$)	Discrepancy ($mg\ mg^{-1}$)
-	Series 4 MAST E-15-40-C	Chemically split	20	5.10	1049.50	150.00	20	0.187		
8.9	Series 4 MAST E-15-40-C	Steam	20	5.10	1.38	50.00	205		0.112	0.075
8.10	Cycle 1 MAST E-15-50-C	Chemically split	20	4.70	1050.00	150.00	20	0.198		
8.11	Cycle 1 MAST E-15-50-C	Steam	20	4.70	14.79	50.00	205		0.250	-0.052
8.10	Cycle 2 MAST E-15-50-C	Chemically split	20	4.70	1019.65	150.00	20	0.178		
8.11	Cycle 2 MAST E-15-50-C	Steam	20	4.70	3.13	50.00	205		0.149	0.029
8.10	Cycle 3 MAST E-15-50-C	Chemically split	20	4.70	1047.25	150.00	20	0.176		
8.11	Cycle 3 MAST E-15-50-C	Steam	20	4.70	0.94	50.00	205		0.169	0.010
8.10	Cycle 4 MAST E-15-50-C	Chemically split	20	4.70	1034.50	150.00	20	0.159		
8.11	Cycle 4 MAST E-15-50-C	Steam	20	4.70	2.66	50.00	205		0.128	0.031
8.10	Cycle 5 MAST E-15-50-C	Chemically split	20	4.70	1035.75	150.00	20	0.143		
8.11	Cycle 5 MAST E-15-50-C	Steam	20	4.70	2.31	50.00	205		0.169	-0.026

8.3.1 The effect of adsorbed ultrafiltered and chemically split cutting fluid on regeneration

The adsorption studies in Chapter 7 investigated the difference between the adsorption of neat, ultrafiltered and chemically split cutting fluid solutions. Figure 7.4 showed that the neat cutting fluid broke through immediately, with minimal adsorption. The ultrafiltered cutting fluid produced a jagged curve, implying various components were being adsorbed at different rates, but the smoother curve for the chemically split fluid suggested a pseudo-single component may have adsorbed onto the carbon at a constant rate.

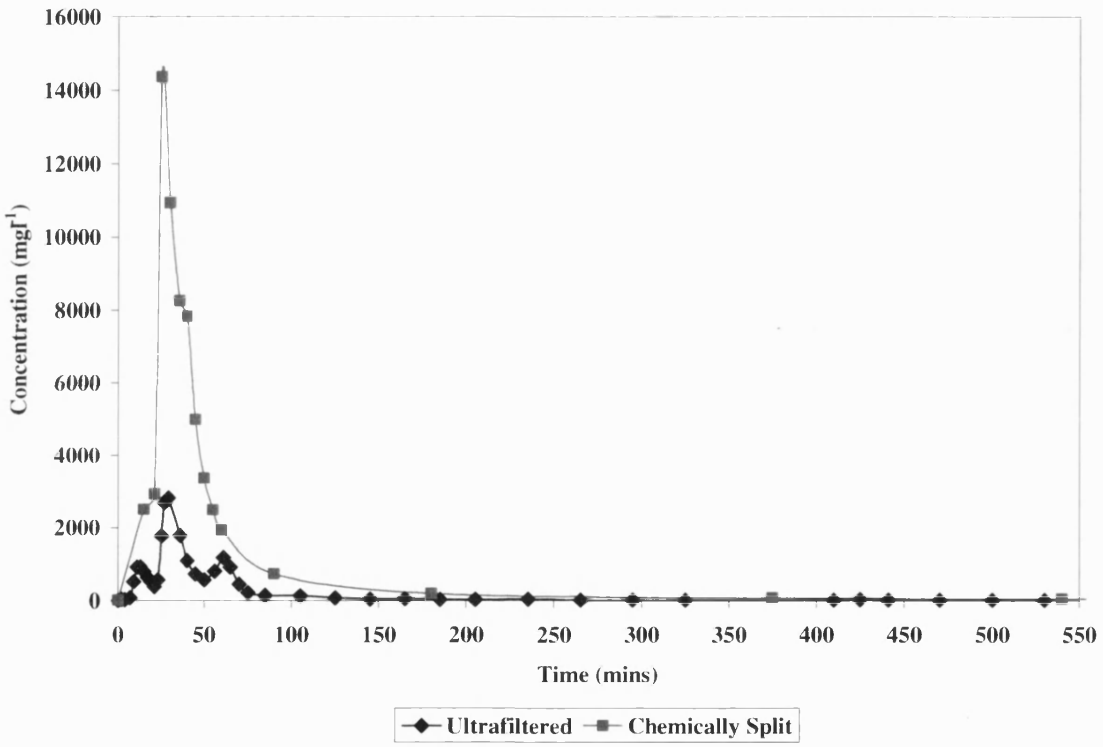

Figure 8.2 A comparison of regeneration profiles for adsorbed ultrafiltered and chemically split cutting fluids

The respective mass balances (in Table 7.1) showed that the activated carbon adsorbed almost twice as much organic carbon from the chemically split cutting fluid than from the ultrafiltered and neat cutting fluid solutions. These results correspond with those in Figure 8.2, which show the desorption profiles of ultrafiltered and chemically split cutting fluid solutions, using superheated steam at 200°C. The graph for the ultrafiltered case shows three distinct peaks, which would suggest three groups of components being desorbed from the carbon at different rates. However, due to the complexity of the cutting fluid from

which unknown compounds were adsorbed, it was impossible to determine the exact desorbed compounds. The single peak shown with the chemically split fluid regeneration case, on the other hand, shows that either a pseudo-single component is desorbing or all the components are desorbed at the same rate.

The regeneration curves show when regeneration is complete (*i.e.* when the concentration of the desorbed product more-or-less equals the concentration of the ultrapure water). Whether the regeneration process was successful in desorbing all of the adsorbed products can only be determined by comparing the total mass desorbed with the total amount adsorbed. For desorption this mass was obtained by integrating the area under the curve.

Table 8.1 compares the mass balances calculated for complete adsorption loading with the corresponding complete regeneration from Figure 8.2.

Table 8.1 A Comparison of the Complete Adsorption and Desorption for the Ultrafiltered and Chemically Split Cutting Fluid Solutions

Figure	Adsorbate	Water flowrate (ml hr^{-1})	Temperature (^{o}C)	Complete adsorption (mg $mg^{-1)}$	Complete desorption (mg mg^{-1})	Discrepancy (mg mg^{-1})
8.2	Ultrafiltered	108.60	200	0.062	0.062	0.000
8.2	Chemically split	100.00	205	0.163	0.179	-0.016

It shows that comparing the amount adsorbed and amount desorbed per mass of adsorbent is excellent for the ultrafiltered fluid. This implies that what is adsorbed onto the carbon is also desorbed from the carbon, suggesting that the WOWSEP system would be efficient for the ultrafiltered cutting fluid with regeneration taking place at 200°C. The mass balances for the chemically split cutting fluid, on the other hand, show a discrepancy between the complete adsorption loading and complete regeneration offloading, the offloading amount being greater than the adsorption loading. This discrepancy suggests that more adsorbate is being desorbed from the carbon than was initially adsorbed onto the carbon. Whilst this situation seems unreasonable and unlikely, it could arise due to a number of reasons (most of them relating to experimental errors). For example errors may have arisen from:

1. Measuring quantities such as flowrates, volumes, mass *etc.*, which were measured using a peristaltic pump, pipettes, and weighing scales. If these pieces of equipment were causing the errors, they would be small and consistent throughout the course of the research.
2. Integration of adsorption. In many cases of the dynamic column studies there was not always a flat plateau to the end of the adsorption curves, and the C/C_0 value did not always equal 1, although there seemed to be a levelling off in the concentrations. This would have produced an inconsistency in the calculation of the complete loadings.
3. Integration of regeneration curves. The peaks shown in the regeneration profiles have been assumed on the basis of a single point. However, this point may not have been the actual peak or the highest concentration of the desorbed product. There may have been errors in the timings *e.g.* the highest concentration may have been seconds/minutes before or after the sample was collected. In addition the samples give an average concentration of the solution collected at that particular time.
4. Small discrepancies are often amplified on a small scale than on larger scale. This is because, for example, the slightest discrepancy in concentration may seem exaggerated relative (in proportion to) initial or equilibrium concentrations used. These discrepancies become more apparent when studying percentages and ratios. So, it would be advantageous to conduct these experiments on a larger scale to see if the same discrepancies are obtained.
5. There is almost a 10% error between the loading and offloading masses. The TOC analyser (Dohrmann DC180) manual states that it has a maximum ±2% marginal error/accuracy. Calibration of the TOC analyser, using potassium hydroxide solution, did indeed prove this level of accuracy. However, this error was found for a standard and simple solution. A more complex solution on the other hand has been shown to produce a much larger error, up to 20% for dissolved organic materials (Aiken *et al.,* 2002). Thus the TOC analyser may not have been able to deal with the high concentrations of such a complex mixture of components.
6. If the recovered solution is in a more concentrated form than the adsorbed solution
7. If extremely high temperatures are used carbonisation of the carbon bed may occur, the product of which may then be detected in the desorbed (recovered) product.

However, in this case, superheated steam at 200°C is relatively low and so carbonisation is highly unlikely and so can be disregarded.

It must be assumed that the TOC analyser is providing accurate results for the adsorption and regeneration experiments, only then will the following results and discussions be valid. However, if the TOC results are not accurate in value but they the discrepancies produced are consistent, then the trends could be compared and general assumptions and discussions could be made accordingly.

In order to ensure that the regeneration process did not affect the carbon capacity and that the carbon was not carbonising, reproducibility and repeatability studies were conducted. The reproducibility studies consisted of carrying out the same adsorption and regeneration experiments using identical conditions and fresh carbon for each cycle. The repeatability studies consisted of conducting continuous adsorption/regeneration cycles using identical conditions but the same carbon. However, before the repeatability studies were carried out, the optimum process conditions were studied.

8.3.2 The effect of various carbons on regeneration

Various carbon types, with different levels of activation *etc.* were studied to find the optimum conditions for the WOWSEP process on the adsorption side. Accordingly, it was necessary to study their regeneration.

The equilibrium studies investigated the loading capability of MAST and Sutcliffe Speakman carbons. It was found that the equilibrium loading was dependent on the adsorbate solution (whether neat, ultrafiltered or chemically split) as well as on the concentration range being examined. The kinetic studies, for the same carbon types showed that the MAST carbon had better kinetic properties than the Sutcliffe Speakman carbon. The dynamic column studies, on the other hand, showed the difference between MAST and Sutcliffe Speakman carbons to be minimal with both chemically split and ultrafiltered cutting fluid solutions. The regeneration profiles for the desorption of the ultrafiltered cutting fluid from MAST and Sutcliffe Speakman carbons with superheated steam at 200°C are now shown in Figure 8.3.

From the graph it can be seen that both carbons produced three peaks. The MAST carbon, however, had three larger and sharper peaks than the Sutcliffe Speakman carbon. This suggests that the MAST carbon has better kinetic properties than the Sutcliffe Speakman carbon, agreeing with the kinetic studies.

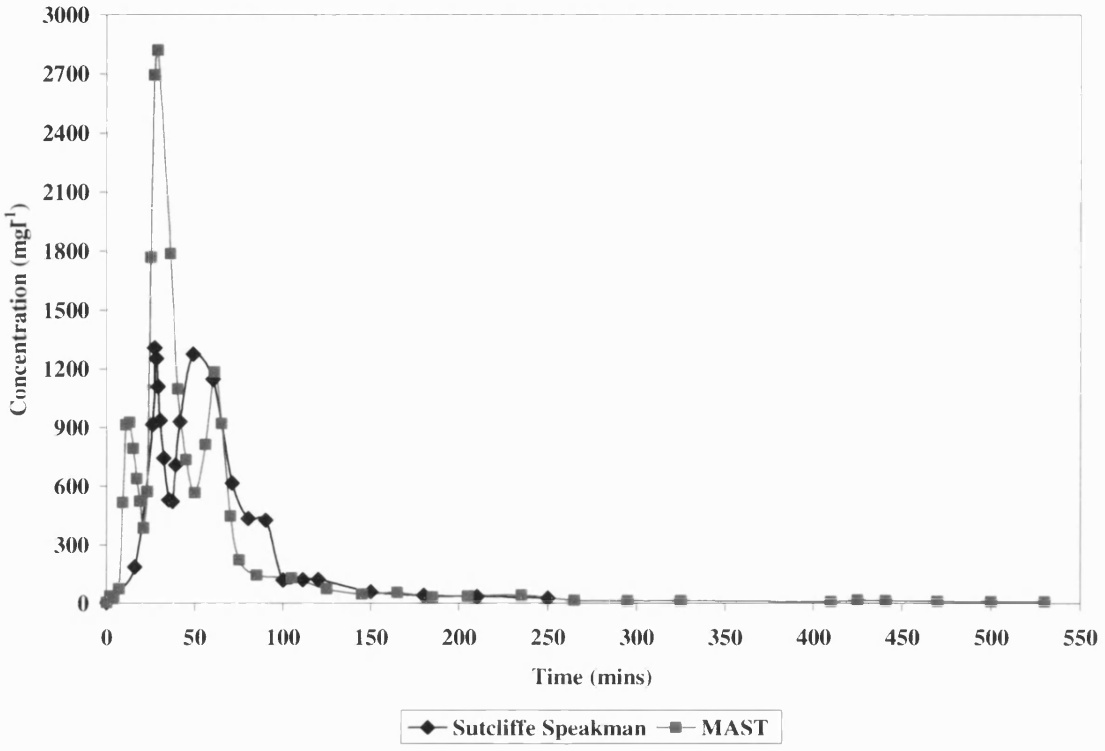

Figure 8.3 A comparison of regeneration studies between Sutcliffe Speakman and MAST carbon after the adsorption of ultrafiltered cutting fluid

The corresponding mass balances in Table 8.2 show that the MAST carbon desorbed all of the adsorbed components. The Sutcliffe Speakman carbon, on the other hand, is shown to apparently desorb more than what was initially adsorbed. This, as explained previously, is more than likely due to experimental error and the higher concentration of the desorbate in comparison to the dilute adsorbate solutions. However, it must be noted that these errors would equally apply to the MAST carbon and that whilst it may seem plausible that the MAST and SS carbons behave differently, and that MAST carbon has a higher loading than the SS carbon as shown by the adsorption studies (Figure 7.4), this cannot be confirmed by the regeneration studies. Overall, it seems acceptable that a general trend may be observed from the regeneration studies but any true conclusions may not be made.

Table 8.2 A Comparison of the Adsorption and Desorption of Ultrafiltered Cutting Fluid Solution using MAST and Sutcliffe Speakman Carbons

Figure	Carbon	Water flowrate (ml hr^{-1})	Temperature (°C)	Complete adsorption (mg mg^{-1})	Complete desorption (mg mg^{-1})	Discrepancy (mg mg^{-1})
8.3	MAST	109	200	0.062	0.062	0.000
8.3	Sutcliffe Speakman	109	200	0.025	0.035	-0.010

Other variations in carbon type which were tested for their effect on adsorption and regeneration, included air oxidised MAST carbon and carbon with various activation levels. Chapter 7 explained how air oxidation slightly increased the pH of the carbon by removing the carboxyl and hydroxyl groups. Adsorption studies showed that air oxidation did not have a marked effect on the adsorption process and the carbon's loading capability. Figure 8.4, provides the respective regeneration data.

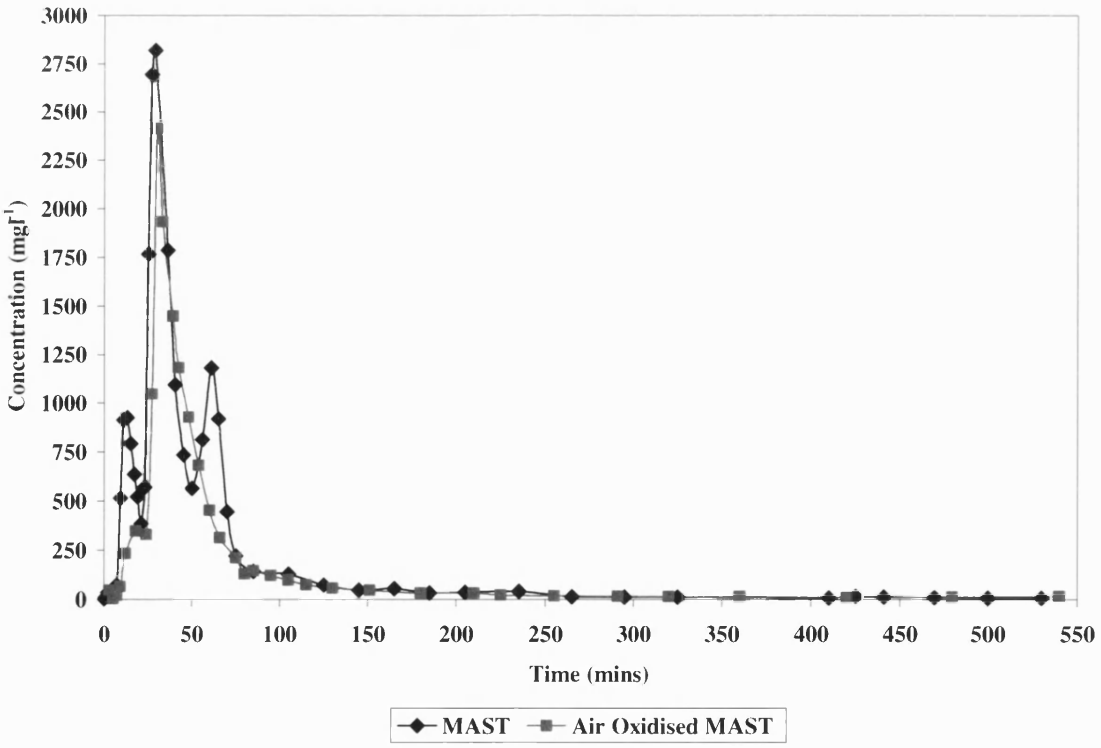

Figure 8.4 A comparison of regeneration studies between untreated MAST carbon and air oxidised MAST carbon after the adsorption of ultrafiltered cutting fluid

The air oxidised MAST carbon shows only one distinct peak, whilst the untreated MAST carbon has three distinct peaks. The early shoulder and the main peak of the air oxidised MAST carbon correspond well with the first and second peaks of the untreated MAST carbon. This would suggest that the untreated MAST carbon was desorbing three groups of compounds at different rates. The single peak of the air oxidised MAST carbon suggests that either the entire adsorbed product was being desorbed or the same group(s) of compounds were being desorbed at the same rate and time, as that of the untreated MAST carbon.

Table 8.3 A Comparison of the Adsorption and Desorption of Ultrafiltered Cutting Fluid from MAST and Air Oxidised MAST Carbons

Figure	Carbon	Water flowrate (ml hr^{-1})	Temperature (°C)	Complete adsorption (mg mg^{-1})	Complete desorption (mg mg^{-1})	Discrepancy (mg mg^{-1})
8.4	Untreated MAST	109	200	0.062	0.062	0.000
8.4	Air oxidised MAST	107	200	0.061	0.046	0.015

Comparing the mass balances (Table 8.3) of the two carbons, it is shown that both the untreated and air oxidised carbons adsorbed similar amounts of carbon (0.062 and 0.061 mg mg^{-1}, respectively). However, whilst the untreated MAST carbon is shown to have had removed the entire adsorbed product (0.062 mg mg^{-1}), the air oxidised MAST carbon had only removed 75% of the adsorbed product (0.046 mg mg^{-1}). This suggests that the air oxidised MAST carbon is not desorbing the entire adsorbed product, but just part of it. Table 8.4 shows the amounts of mass desorbed from the peaks for each carbon.

The cause of the difference in desorption capability of the untreated and air oxidised MAST carbons could be due to the strength of the adsorbent-adsorbate attractive forces. It would seem that the air oxidised MAST carbon might have required more energy to break the adsorbent-adsorbate bonds in order to recover the adsorbed product, suggesting that the adsorbent-adsorbate interactions must be much stronger than the untreated MAST carbon. It can be concluded that whilst air oxidation does not have a significant effect on the loading capability of the carbon, it does affect the regeneration process adversely.

Table 8.4 A Comparison of Desorption Amounts of Ultrafiltered Cutting Fluid from MAST and Air Oxidised MAST Carbons for each Peak

Carbon type (from Figure 8.4)	Desorption (mg mg^{-1})			
	Peak 1	**Peak 2**	**Peak 3**	**Total**
Untreated MAST	0.0068	0.0316	0.0235	0.0619
Air oxidised MAST carbon	0.0032	0.0431		0.0463

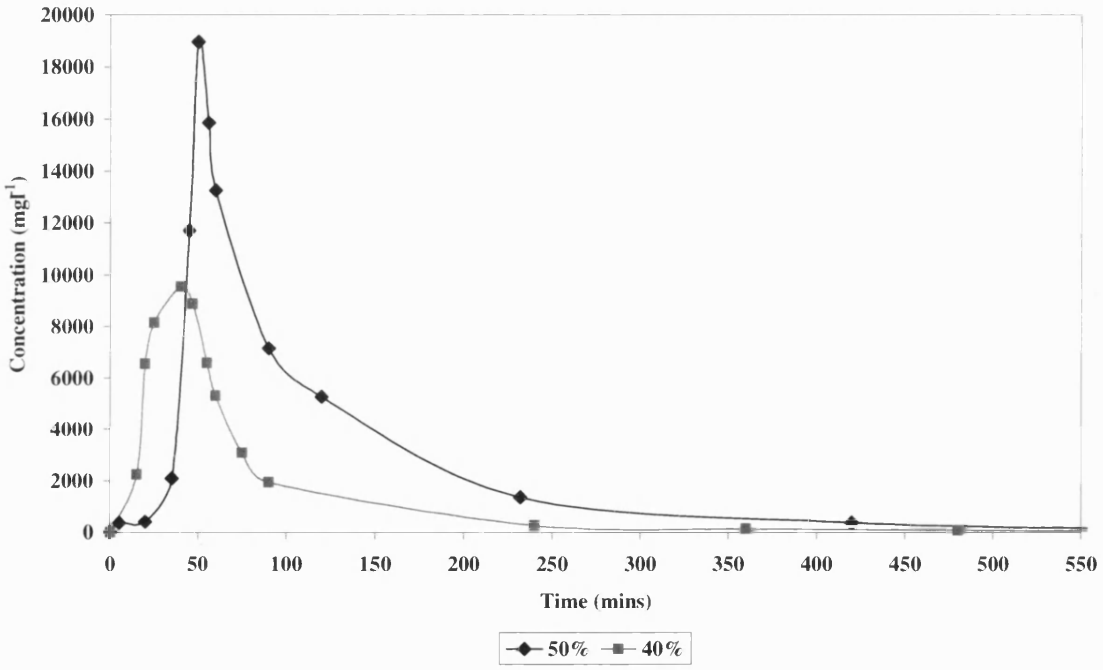

Figure 8.5 A comparison of regeneration studies using MAST carbons with different activation levels after the adsorption of ultrafiltered cutting fluid

Thermal regeneration is often associated with reactivation. Therefore it was important to study the effect of carbon activation on the regeneration process. Figure 8.5 shows the regeneration profiles for 50% and 40% activated MAST carbons.

The 50% activated carbon has a much taller and narrower peak than the 40% activated carbon. The height of the 50% activated carbon peak is approximately twice as large and the base is almost twice as wide as the 40 % activated carbon. This information is

conveyed in the mass balances shown in Table 8.5, where the amount desorbed from the 50% activated carbon was approximately twice as much as from the 40% activated carbon.

Table 8.5 A Comparison of the Adsorption and Desorption of Chemically Split Cutting Fluid using 50% and 40% Activated MAST Carbons

Figure	Carbon activation (%)	Water flowrate (ml hr^{-1})	Temperature (°C)	Complete adsorption (mg mg^{-1})	Complete desorption (mg mg^{-1})	Discrepancy (mg mg^{-1})
8.5	50	50	205	0.198	0.250	-0.052
8.5	40	50	205	0.187	0.112	0.075

From Table 8.5 it can be seen that the discrepancy between the adsorption and regeneration for the 50% activated carbon was very large whilst the 40% activated carbon appeared to desorb less than that adsorbed. However, as discussed earlier these results are likely to be due to experimental error rather than to any other factor.

8.3.3 The effect of steam flowrate on regeneration

The flowrate of steam is dependent on the water flowrate passed to the heat exchanger coil. The influence of steam flowrate on regeneration was therefore studied by varying the water flowrate. Figure 8.6 shows the results for three water flowrates, 20 ml hr^{-1}, 50 ml hr^{-1} and 100 ml hr^{-1}.

All three curves show that the regeneration peak (during which period the majority of regeneration occurs) occurred within the first 100 minutes or so. However, whilst the height of the peak was very similar in all three cases the width of the peak varied, with the highest flowrate giving the narrowest peak and the lowest flowrate giving the broadest peak, which indicates that the highest flowrate has better system kinetics.

The mass balances in Table 8.6 show that the adsorption loading is more or less equal to the desorption. In the case of the 100 ml hr^{-1} water feed flowrate, a negative discrepancy was produced, which suggests that more was desorbed than was adsorbed. The most likely explanation for this is again experimental error, especially since the discrepancies shown in Table 8.6 are all within the same range ± 0.016 mg mg^{-1}.

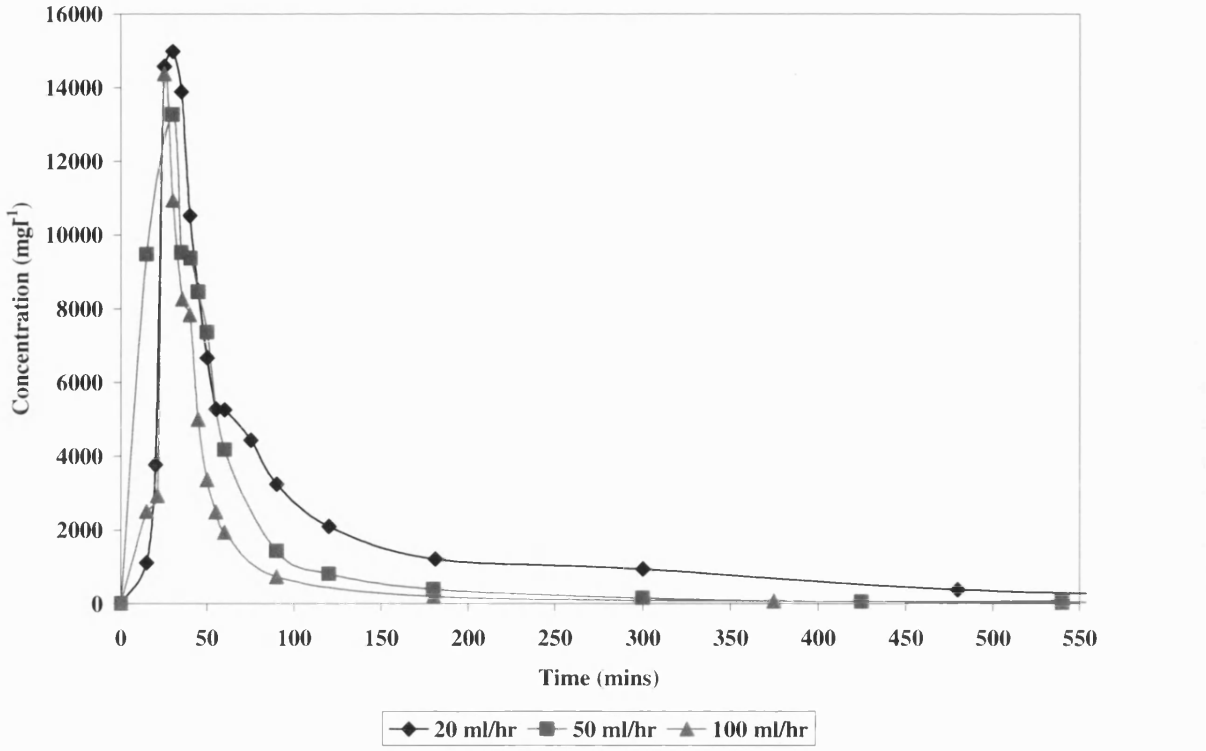

Figure 8.6 A comparison of the regeneration studies of MAST E-15-50-C carbon using various water flowrates after the adsorption of chemically split cutting fluid

Table 8.6 A Comparison of the Adsorption and Desorption of Chemically Split Cutting Fluid using Various Water Flowrates

Figure	MAST carbon	Water flowrate (ml hr^{-1})	Temperature (°C)	Complete adsorption (mg mg^{-1})	Complete desorption (mg mg^{-1})	Discrepancy (mg mg^{-1})
8.6	E-15-50-C	20	205	0.207	0.195	0.012
8.6	E-15-50-C	50	205	0.214	0.198	0.016
8.6	E-15-50-C	100	205	0.163	0.179	-0.016

8.3.4 Effect of steam temperature on regeneration

In addition to the optimum amount of steam required for regeneration to occur, the optimum temperature of steam also needs to be found. The effect of steam temperature was studied by altering the fluidised sand bath temperature. Figure 8.7 shows a

comparison of regeneration profiles with steam at temperatures of 180°C, 205°C and 225°C.

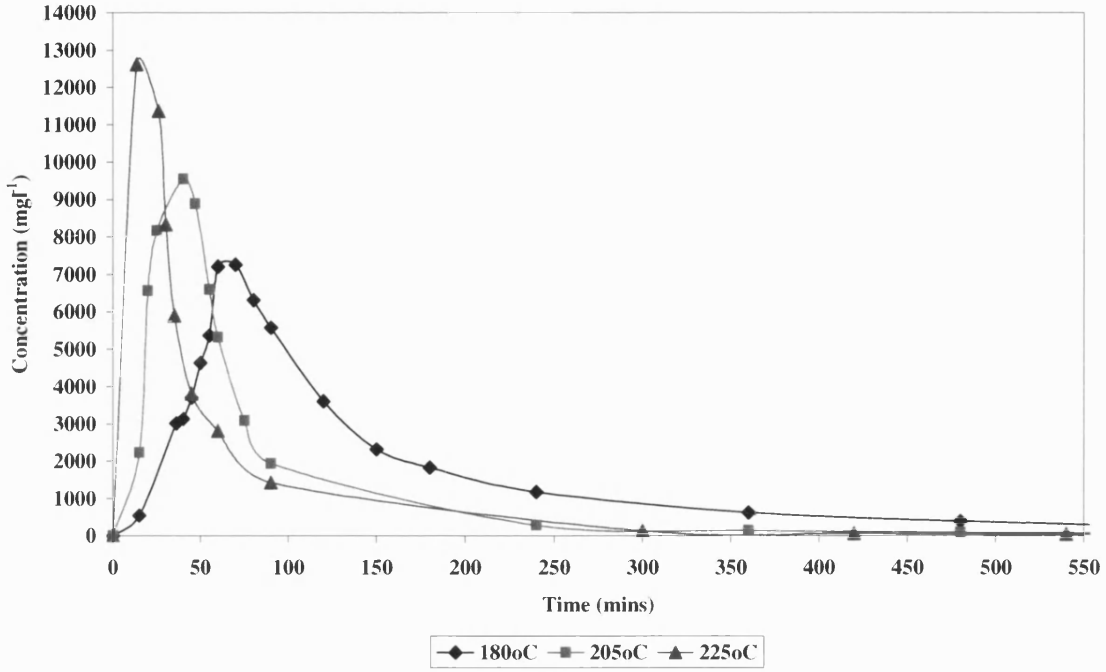

Figure 8.7 The effect of various steam temperatures on the regeneration of MAST E-15-40-C carbon after the adsorption of chemically split cutting fluid

It can be seen that as the temperature is decreased the regeneration peak becomes shorter and wider. As explained before, the shape of the peak represents the kinetic properties, where a sharper, narrower peak is indicative of better kinetics. From this information it would suffice to say that the lower the steam temperature, the worse the system kinetics. In addition, Figure 8.7 also shows that as the steam temperature is decreased the peak shifts to the right, confirming that as the temperature is lowered it takes longer for the regeneration to be completed.

It might be supposed that as lower regeneration temperatures lead to lower desorption amounts, this could mean that thermal regeneration should be conducted at very high temperatures (up to 1000°C for best efficiency). However, the results in Figure 8.7 show that this is not necessarily the case. The mass balances in Table 8.7 show that the lower the temperature gives the lowest discrepancy between adsorption and desorption.

Table 8.7 A Comparison of the Adsorption and Desorption of Chemically Split Cutting Fluid using Various Steam Temperatures

Figure	MAST carbon	Water flowrate (ml hr^{-1})	Temperature (°C)	Complete adsorption (mg mg^{-1})	Complete desorption (mg mg^{-1})	Discrepancy (mg mg^{-1})
8.7	E-15-40-C	50	180	0.196	0.165	0.031
8.7	E-15-40-C	50	205	0.187	0.112	0.075
8.7	E-15-40-C	50	225	0.180	0.109	0.071

In summary the most suitable conditions for the regeneration side of the WOWSEP process were:

- Chemically split cutting fluid
- Untreated MAST PRC carbon (50% activated)
- Higher steam flowrate (better kinetics)
- Higher steam temperature (better kinetics)

It was important now to be sure that good results were reproducible.

8.3.5 Reproducibility of regeneration experiments

Reproducibility experiments require conducting exactly the same experiment twice (or more) and seeing whether or not there is good agreement in the results. Chapter 7 explained the dynamic adsorption column reproducibility studies, which showed the adsorption system to be effective and reliable with regard to being capable of reproducing the same results. Figures 8.8 and 8.9 show 2 regeneration profiles conducted for MAST E-15-50-C and MAST E-15-40-C, respectively, and the mass balances in Table 8.8.

The adsorption studies were conducted using MAST carbon, 20 cm column, approximately 5 g of dry adsorbent, an initial concentration of approximately 1050 mg l^{-1} of chemically split cutting fluid, and a feed flowrate of 150 cm^3 hr^{-1}. Fresh carbon was used for each adsorption run, after which regeneration was conducted at a temperature of 205°C and a feed water flowrate of 50 ml hr^{-1}.

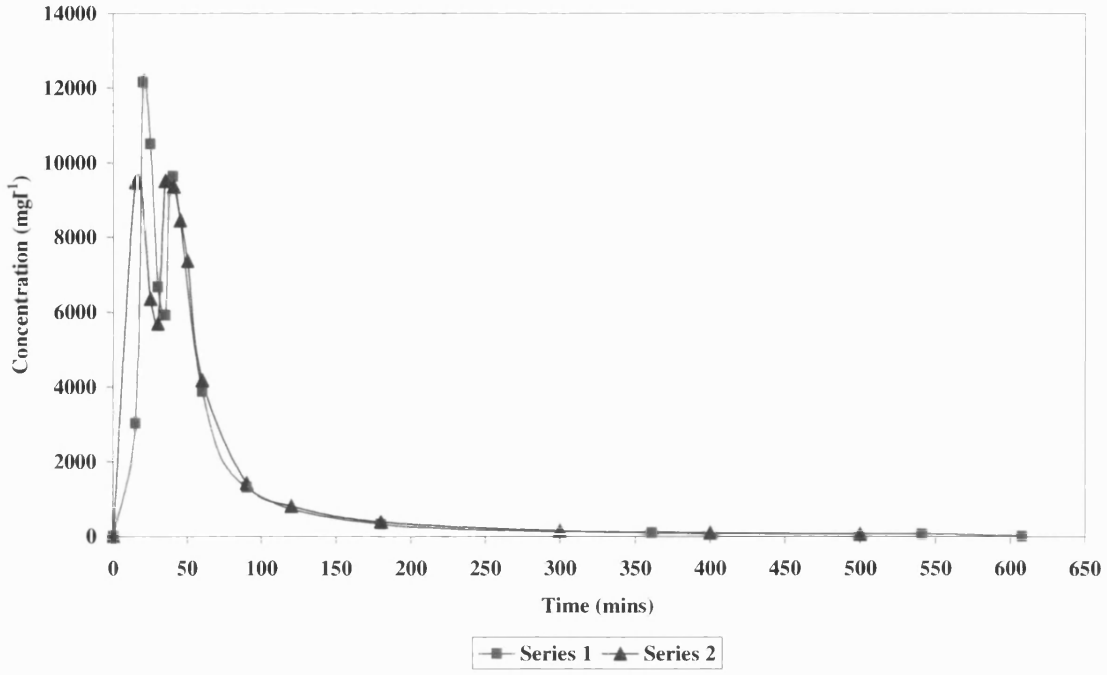

Figure 8.8 A comparison of two regeneration profiles conducted using the same adsorption and regeneration conditions and fresh MAST E-15-50-C carbon for each experiment to show the reproducibility capability of the system

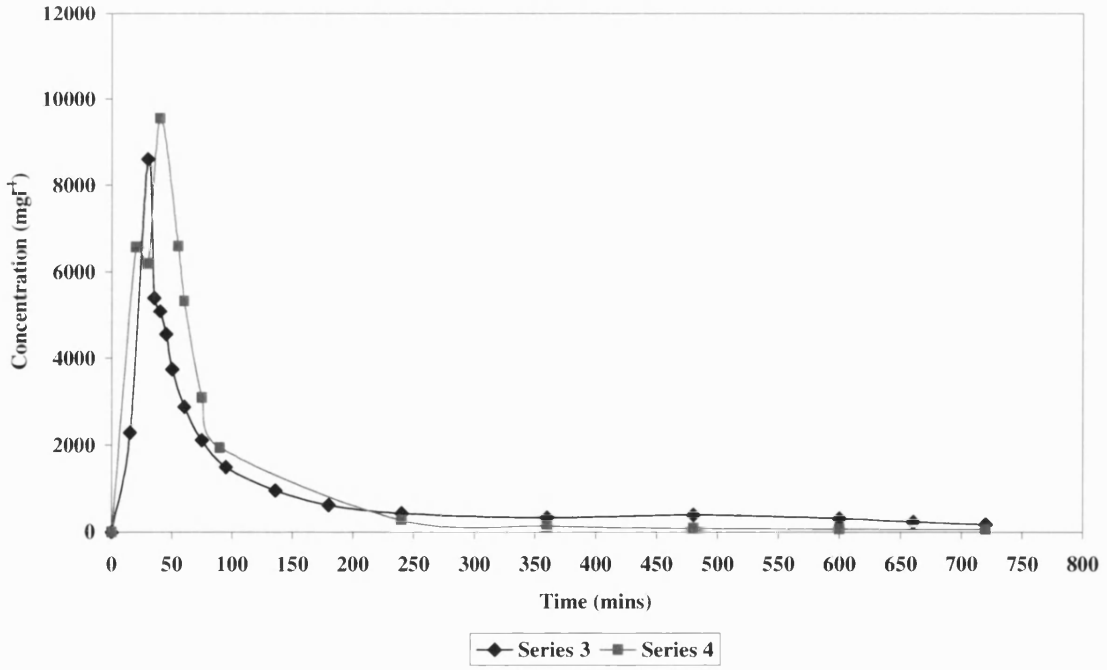

Figure 8.9 A comparison of four regeneration profiles conducted using the same adsorption and regeneration conditions and fresh MAST E-15-40-C carbon for each experiment to show the reproducibility capability of the system

Overall the graphs in both Figures 8.8 and 8.9 are broadly similar, with the peak being detected at the same place. The width of the peaks is very similar, the majority of regeneration is shown to take place within the first 150 minutes or so, but height of the peak varies slightly. MAST E-15-50-C is shown to produce show two peaks, whilst MAST E-15-40-C only produces one. The respective mass balances in Table 8.8 show that The mass balances of MAST E-15-50-C (Series 1 and 2) showed very similar adsorption and desorption amounts, whereas those for MAST E-15-40-C (Series 3 and 4) show the largest discrepancies.

Table 8.8 A Comparison of the Adsorption and Desorption of Chemically Split Cutting Fluid for Four Regeneration Experiments in Series

Figure	Series	Water flowrate (ml hr^{-1})	Temperature (°C)	Complete adsorption (mg mg^{-1})	Complete desorption (mg mg^{-1})	Discrepancy (mg mg^{-1})
8.8	Series 1	50	205	0.190	0.176	0.014
8.8	Series 2	50	205	0.214	0.198	0.016
8.9	Series 3	50	205	0.196	0.095	0.101
8.9	Series 4	50	205	0.187	0.112	0.075

8.3.6 Repeatability of regeneration experiments

Repeatability experiments involve conducting successive adsorption/regeneration cycles repeatedly using the same spent and regenerated carbon for each experiment. The adsorption/regeneration profiles produced are then studied to investigate the carbon performance in relation to the number of cycles conducted. Therefore, generally, the main factor which influences the lifespan of the process is the ability to regenerate the carbon repeatably over a number of adsorption and desorption cycles. In addition, repeatability studies help examine the carbon's life expectancy. In this case, five repeated adsorption and steam regeneration cycles were conducted, as shown in Figures 8.10 and 8.11, respectively. The adsorption experiment conditions for all the experiments were: MAST E-15-50-C carbon and chemically split cutting fluid with an approximate initial feed concentration and flowrate of 1000 mg l^{-1} and 150 ml hr^{-1}, respectively, using a 20 cm column. The corresponding regeneration conditions were: an approximate water flowrate of 50 ml hr^{-1} and a temperature of 205°C.

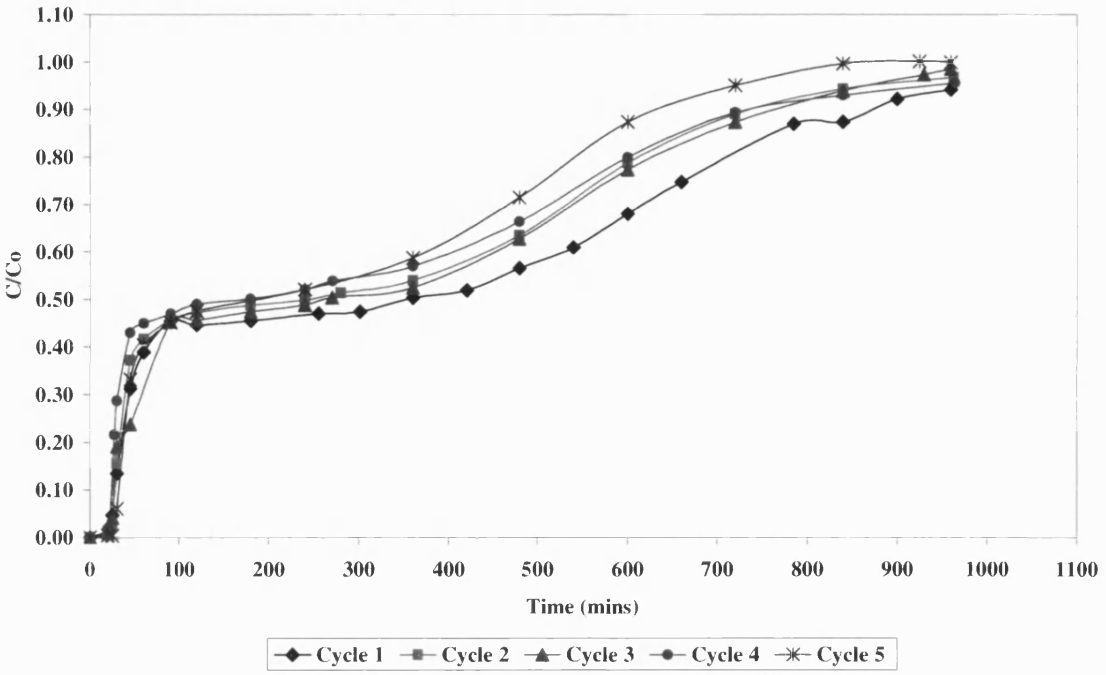

Figure 8.10 A comparison of breakthrough curves for consecutive adsorption cycles following regeneration using chemically split cutting fluid and MAST E-15-50-C carbon

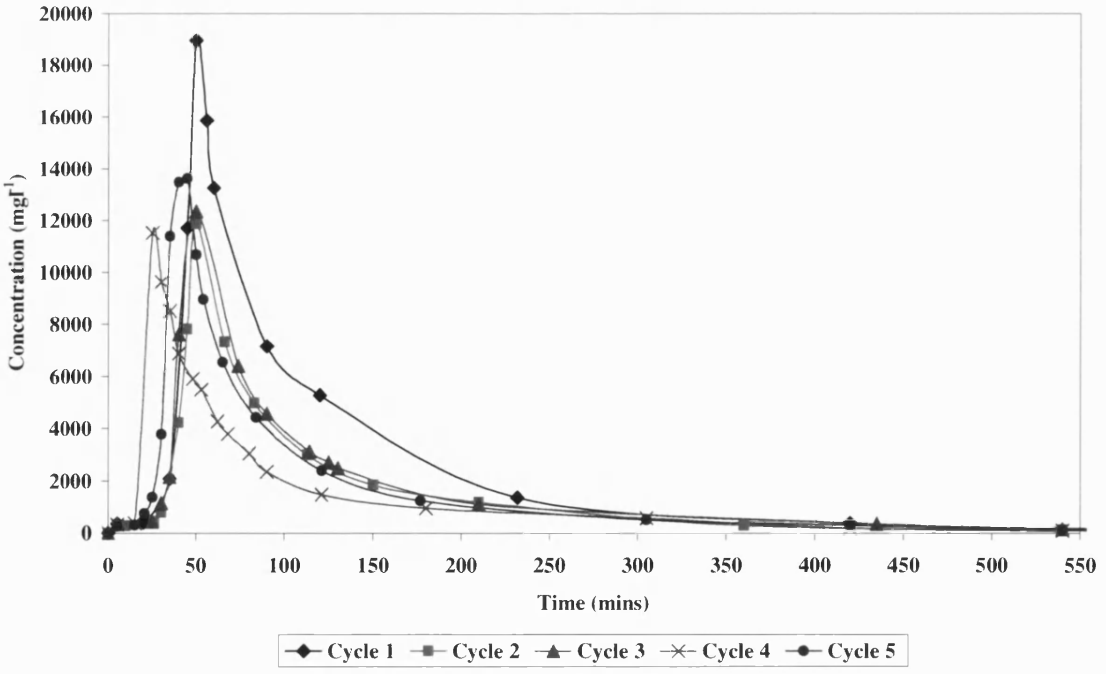

Figure 8.11 A comparison of five consecutive regeneration cycles using MAST carbon

Figure 8.11 shows the regeneration results of five consecutive adsorption/regeneration cycles for MAST E-15-50-C carbon, using superheated steam at 205°C. As can be seen, the first cycle gives the tallest regeneration peak and all the subsequent cycles produced smaller peaks, implying there is a decrease in adsorption capacity after each cycle.

Moore *et al.* (2001) studied the changes in pore structure of granular activated carbon during full-scale water treatment. A comparison between the pore volume distributions of the virgin and thermally reactivated carbons (after six cycles of water treatment and thermal reactivation), showed that the virgin carbon was mostly microporous comprising generally of pore size changes of less than 5 nm (50 Å) in diameter. The reactivated carbon was found to be mainly mesoporous with pore size changes between 10 nm and 50 nm in diameter. However, it must be noted that Moore *et al.'s* reactivation study was taken at a much higher temperature of 800°C, which is sufficiently high enough to allow for carbonisation to occur. The WOWSEP system, on the other hand, utilises a lower temperature of 205°C, which is unlikely to alter the porous structure of the carbon. Therefore there must be an alternative reason for the reduction in capacity of the carbon. It follows that the decrease in adsorption capacity could be due to the retention of adsorbed contaminants after regeneration in the smaller carbon pores.

Table 8.9 A Comparison of the Adsorption and Desorption of Chemically Split Cutting Fluid for Five Adsorption/Regeneration Cycles

Figure	Cycle	Water flowrate (ml hr^{-1})	Temperature (°C)	Complete adsorption (mg mg^{-1})	Complete desorption (mg mg^{-1})	Discrepancy (mg mg^{-1})
8.9/10	Cycle 1	150/50	20/205	0.198	0.250	-0.052
8.9/10	Cycle 2	150/50	20/205	0.178	0.149	0.029
8.9/10	Cycle 3	150/50	20/205	0.176	0.169	0.010
8.9/10	Cycle 4	150/50	20/205	0.159	0.128	0.031
8.9/10	Cycle 5	150/50	20/205	0.143	0.169	-0.026

A comparison of the mass balances (Table 8.9) shows the gradual loss in adsorptive capacity of the carbon following regeneration. (Figure 8.10) shows that after the first cycle, all subsequent cycles give a lower loading than the last. This information could be used to predict the carbon's working life. After the first cycle, the carbon lost 10% of its

working capacity and then 11%, 20%, and 28% for all subsequent cycles. This information ultimately identifies whether it is environmentally and economically viable to regenerate the carbon or whether replacement of all or part of the spent carbon after each cycle would be financially feasible and practical.

Table 8.9 shows that during the five cycles the loading decreases as the number of cycles increases. However, with regeneration, the desorption generally decreases with the exception of Cycle 3, but it does not, as expected, lead to regeneration of all of the adsorbed products. The desorption is sometimes shown to be greater than the loading (Cycles 1 and 5 as well as in previous experiments). This would suggest that the regeneration performance cannot be easily predicted or calculated. Nevertheless, regardless of the regeneration process, if the adsorption process suffers from less error than the regeneration process, then a 28% decrease in adsorption capacity after five adsorption cycles is probable and might make this process viable.

8.3.7 The effect of water ratio on regeneration

In order to demonstrate the effectiveness of the adsorption/regeneration process the amount of water required to complete the regeneration relative to the amount of feed water used is calculated. This is known as the water ratio.

$$\text{Water Ratio} = \frac{\text{Water Required For Regeneration}}{\text{Water Required In Adsorption}}$$

The lower the water ratio the more effective becomes the overall process. An added bonus arises if the regeneration effluent is reusable. Figures 8.7 and 8.11 show comparisons of regeneration profiles for various regeneration temperatures and the five consecutive adsorption/regeneration cycles, respectively, Tables 8.10 and 8.11 provide the water ratios corresponding to these figures.

Table 8.10 shows that while the times for complete adsorption are the same for all three experiments, the regeneration time decreases as the superheated steam temperature is increased. As a result the water ratio is lowered with increasing steam temperature. Whilst this suggests that if the temperature was increased even further, say to 1000°C (as in

thermal regeneration), this would make regeneration more efficient and effective. However, this would also make the process extremely energy intensive. This would complicate the process design especially with regard to safety. Consequently, a balance between temperature, cost and efficiency is required to make the process viable.

Table 8.10 A Comparison of Adsorption/Regeneration Water Ratios for Various Superheated Steam Temperatures

Temperature (°C)	**180**		**205**		**225**	
	Time (hrs)	Flow (ml hr^{-1})	Time (hrs)	Flow (ml hr^{-1})	Time (hrs)	Flow (ml hr^{-1})
Adsorption of E-15-40-C @ 20°C, 1050 mg l^{-1}, 150 ml hr^{-1}	16	150	16	150	16	150
Regeneration	12	50	6	50	5	50
Water Ratio (%)	25.0		12.5		10.4	

The water ratios in Table 8.11 show that for the five consecutive adsorption/regeneration cycles at 205°C, the water ratio was highest for the first cycle at 20.8% and thereafter remained constant for the next four cycles at 18.8%. This would suggest that the regeneration process is more effective after it has been primed by the first cycle.

A comparison between Tables 8.10 and 8.11 shows that at a temperature of 205°C there is a difference in water ratios of 8.3% and a time of three hours. The experiments in Table 8.10 used 40% activated MAST carbon, whilst those in Table 8.11 used 50% activated MAST carbon. This would suggest that the 40% activated carbon is more efficient in regeneration than the 50% activated carbon as it takes less time to regenerate. This agrees with the results in Figure 8.5, which shows the 40% carbon to complete regeneration faster than the 50% carbon. Nevertheless the 50% activated carbon produces a much larger, narrower peak, implying better kinetics.

Table 8.11 A Comparison of Water Ratios for Five Consecutive Adsorption/Regeneration Cycles

Cycle	1		2		3		4		5	
	Time (hr)	Flow (ml hr^{-1})	Time (hr)	Flow (ml hr^{-1})	Time (hr)	Flow (ml hr^{-1})	Time (hr)	Flow (ml hr^{-1})	Time (hr)	Flow (ml hr^{-1})
Adsorption of E-15-50-C @ 20°C, 1050 mg l^{-1}, 150 ml hr^{-1}	16	150	16	150	16	150	16	150	16	150
Regeneration @ 205 °C	10	50	9	50	9	50	9	50	9	50
Water Ratio (%)	20.8		18.8		18.8		18.8		18.8	

The water ratio confirms that a compromise of kinetics, carbon type, carbon activation, temperature has to be made along with the environmental and economical issues of the company at which this process is to be considered for recovery factory oil wastes.

8.4 Modelling of the regeneration system

Modelling provides an opportunity to predict results without having to conduct experiments. A model was created to study the effect of temperature on the regeneration of MAST E-15-40-C carbon.

Figure 8.7 showed that a decrease in steam temperature shifted the regeneration curve to the right, decreasing the peak height (concentration) and increasing the peak width (time). The concentration time profiles after the peaks given in Figure 8.7 are shown again in Figure 8.12. The equations of the curves were obtained from Microsoft Excel, based on exponential decay curves. They are given on the graph and summarised in Table 8.12. Here c is the concentration (mg l^{-1} TOC) and t is the time (mins).

As the cutting fluid was assumed to be a single pseudo compound, a first order decay was assumed. Equation 8.1 gives the general equation for a first order rate of regeneration, where $(dc/dt)_r$ is the rate of regeneration (mg l^{-1} $mins^{-1}$) and k is the rate constant ($mins^{-1}$).

$$-\left(\frac{dc}{dt}\right)_r = kc \qquad 8.8$$

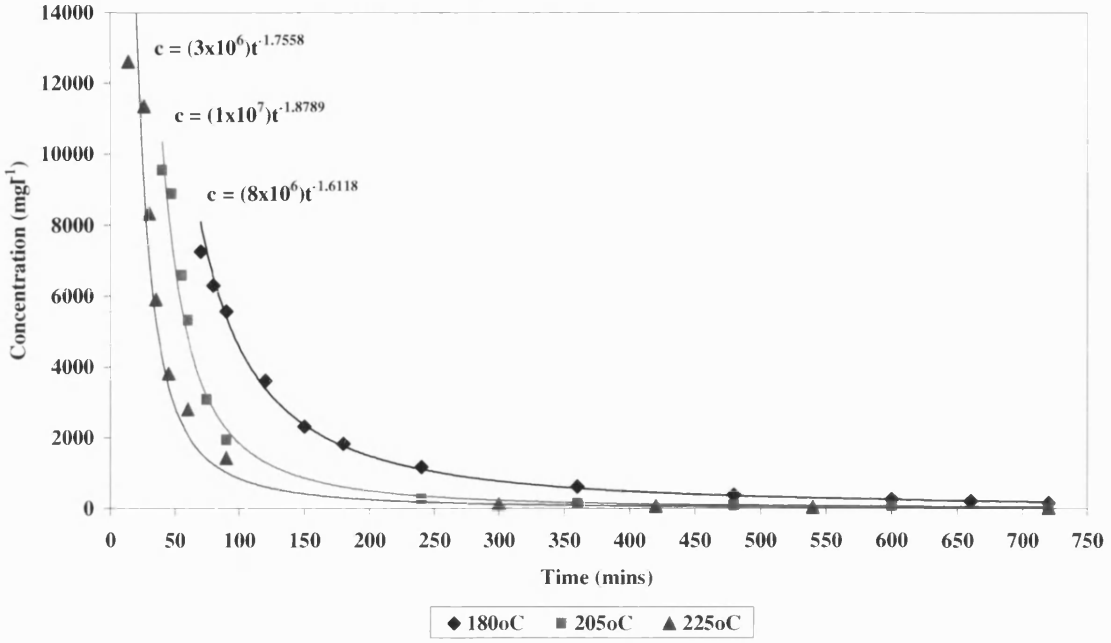

Figure 8.12 A graph showing the decreasing slopes of the regeneration curves from Figure 8.7

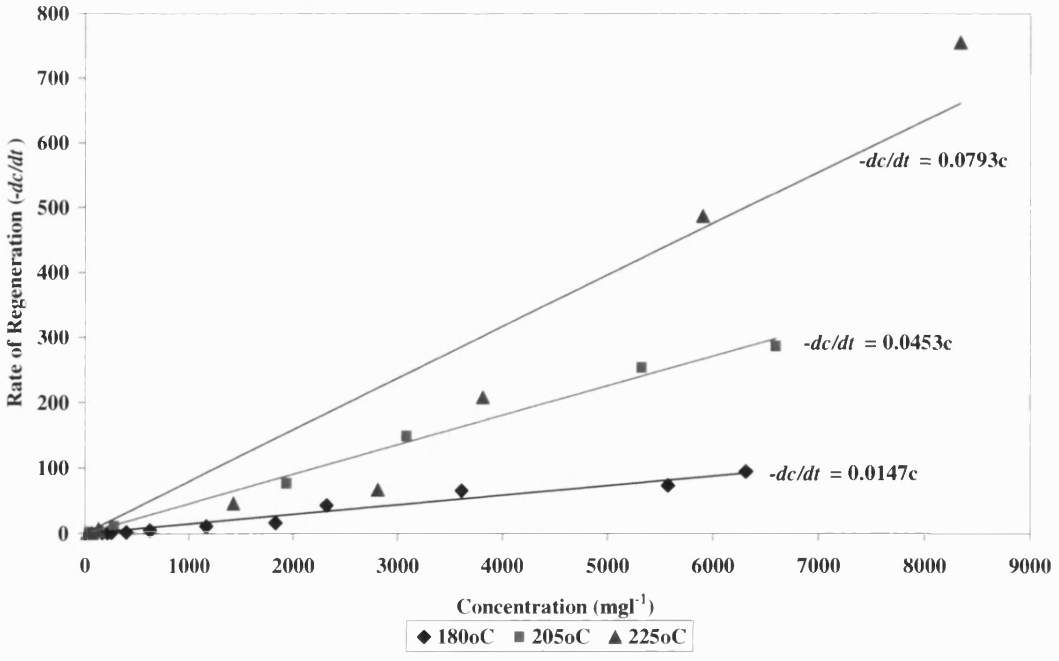

Figure 8.13 A graph of the rate of desorption $(-dc/dt)_r$ against concentration at various temperatures

Differentiating the equations shown in Figure 8.12, gives the rate equations for each temperature, from which the rate constants can be calculated. These are shown graphically in Figure 8.13, which shows a plot of $(-dc/dt)_r$ against c and from which k can be obtained. Table 8.12 gives a summary of the power equations, with their respective rate equations and rate constants.

Table 8.12 Summary of Power Equations, Rate Equations and the Rate Constants for Various Superheated Steam Temperatures

Temperature (°C)	**180**	**205**	**225**
Power equation	$c = (8x10^6)t^{-1.6118}$	$c = (1x10^7)t^{-1.8789}$	$c = (3x10^6)t^{-1.7558}$
Rate equation	$(-dc/dt)_r = 0.0147c$	$(-dc/dt)_r = 0.0453c$	$(-dc/dt)_r = 0.0793c$
Rate constant (k, mins^{-1})	0.0147	0.0453	0.0793

Figure 8.13 shows that as the temperature increases the gradient of the linear graph increases confirming that the rate of regeneration also increases. The rate constants provide the means to calculate the activation energy (ΔH, kJ kmol^{-1}) required for regeneration to take place using the Arrhenius equation (Equation 8.2).

$$k = k_o * e^{(-\Delta H/RT)} \qquad 8.2$$

where: R is the molar universal gas constant (8.314 kJ kmol^{-1} K^{-1})

k_o is the Arrhenius constant or the frequency factor (mins^{-1})

T is the absolute temperature (K)

Linearising the Arrhenius equation gives rise to Equation 8.3

$$lnk = lnk_o - \Delta H/RT \qquad 8.3$$

A plot of the log of the rate constant (lnk) against the reciprocal of the absolute temperature ($1/T$) as shown in Figure 8.14. The point at which the linear graph crosses the y axis, at $1/T$=0, provides the value of lnk_o. The gradient is equal to activation energy divided by the universal gas constant ($\Delta H/R$). The values of k_o and ΔH were found to be 2.29x10^6 mins^{-1} and 7.10x10^4 kJ kmol^{-1} respectively.

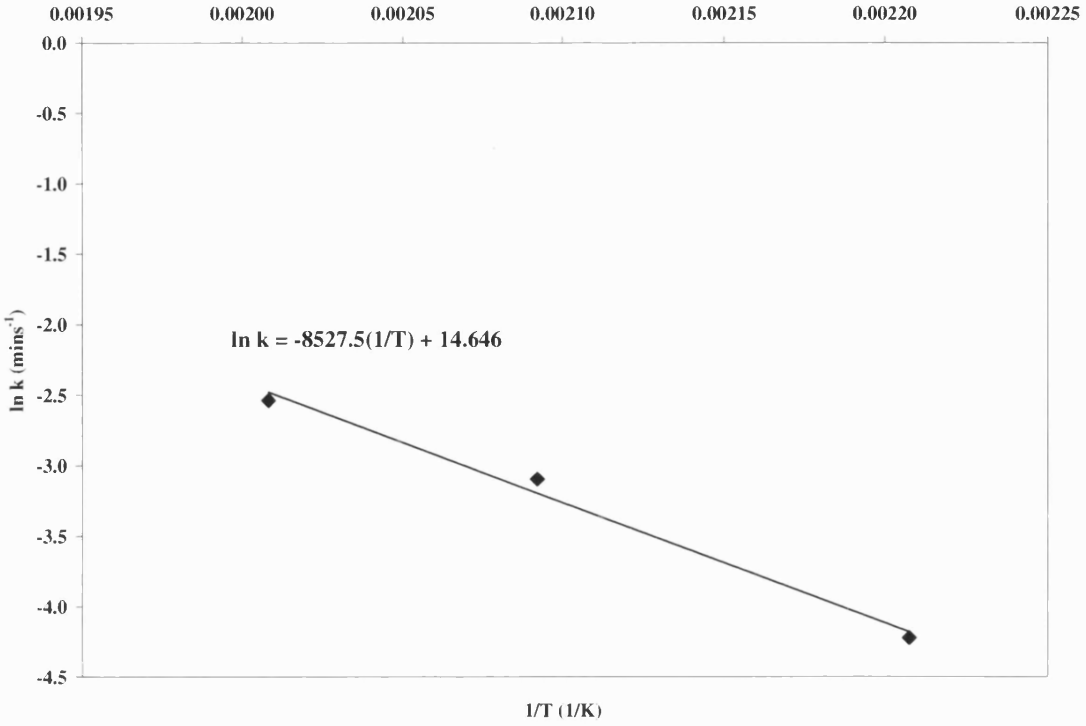

Figure 8.14 A graph of the log of the rate constant against the reciprocal of the absolute temperature

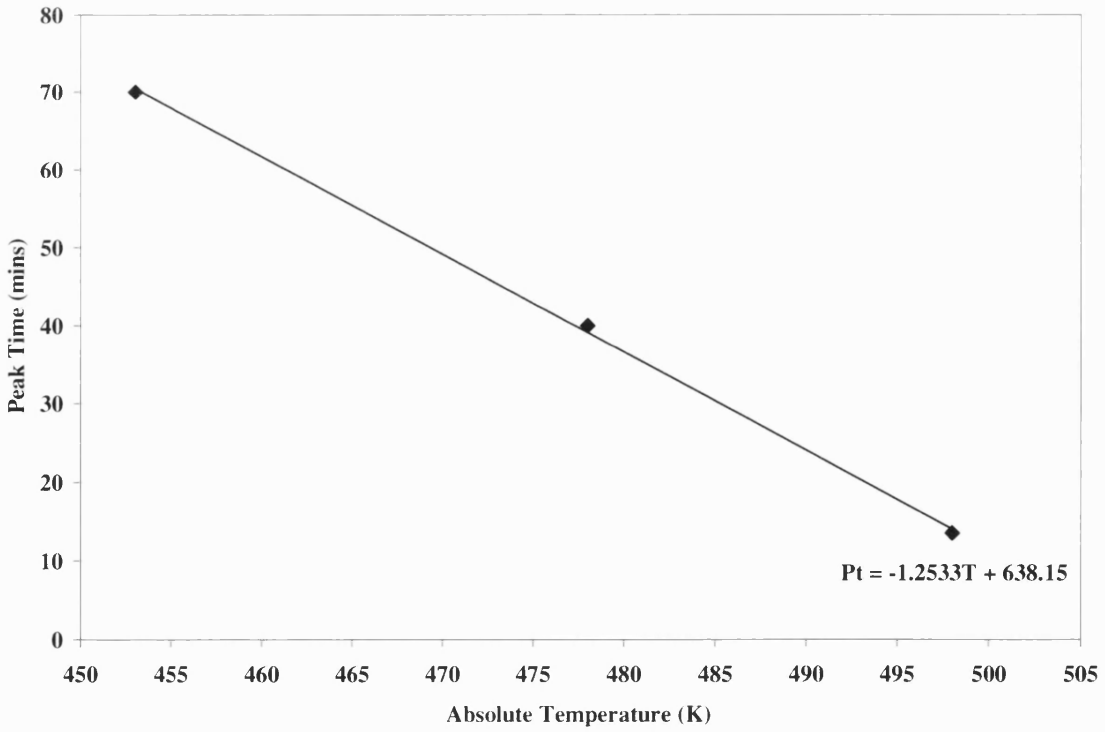

Figure 8.15 A graph showing the peak time against absolute temperature

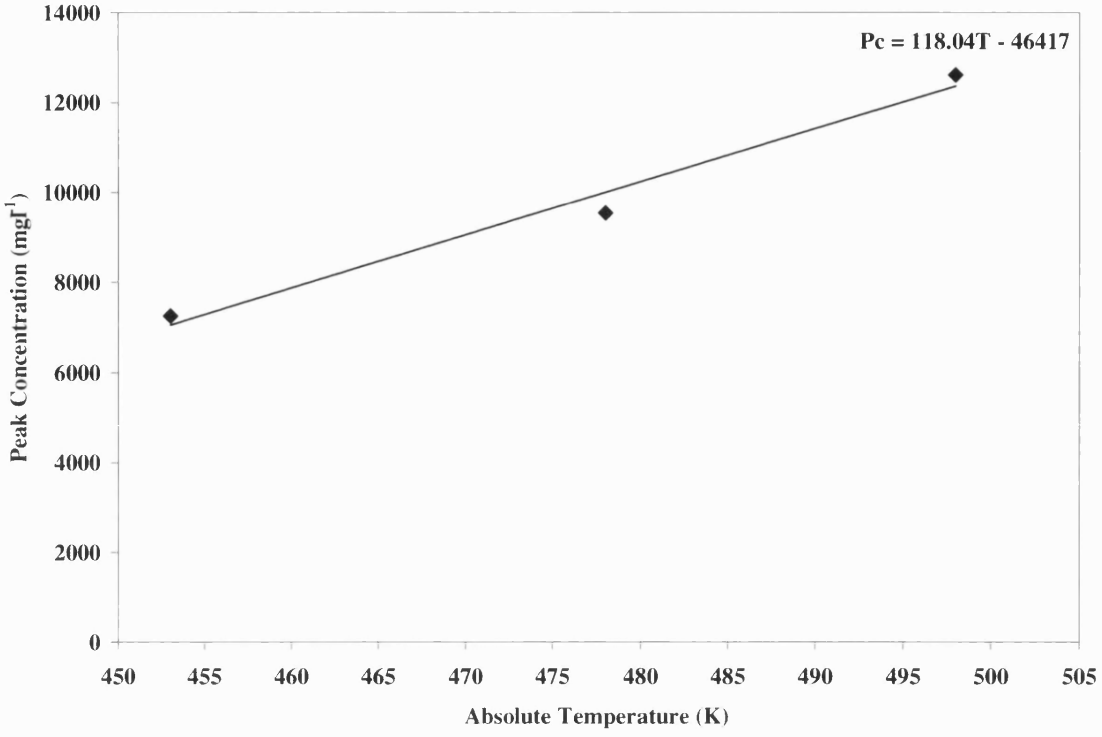

Figure 8.16 A graph to show the peak concentration against absolute temperature

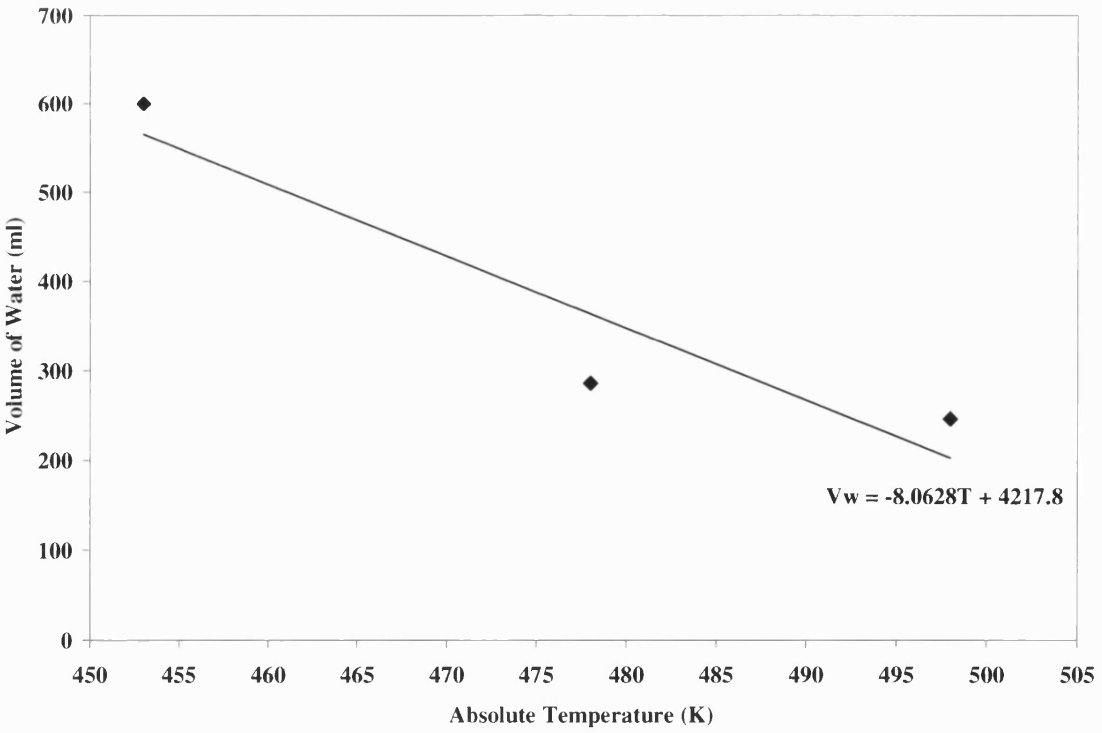

Figure 8.17 A graph showing a plot of the volume of water required for regeneration against absolute temperature

Figures 8.15, 8.16 and 8.17 show the effect of steam temperature on the peak time, peak concentration and the volume of water required to achieve complete regeneration, respectively. All three trends follow a linear pattern, with the three points being close to the line of best fit.

Figure 8.15 shows that the time to the regeneration peak decreases as the absolute temperature increases. Figure 8.16 shows that as the temperature increases so does the concentration of the peak. Figure 8.17 shows that as the temperature increases the volume of water required for regeneration decreases. Taken together it is clear that the regeneration process is favoured by a higher steam temperature.

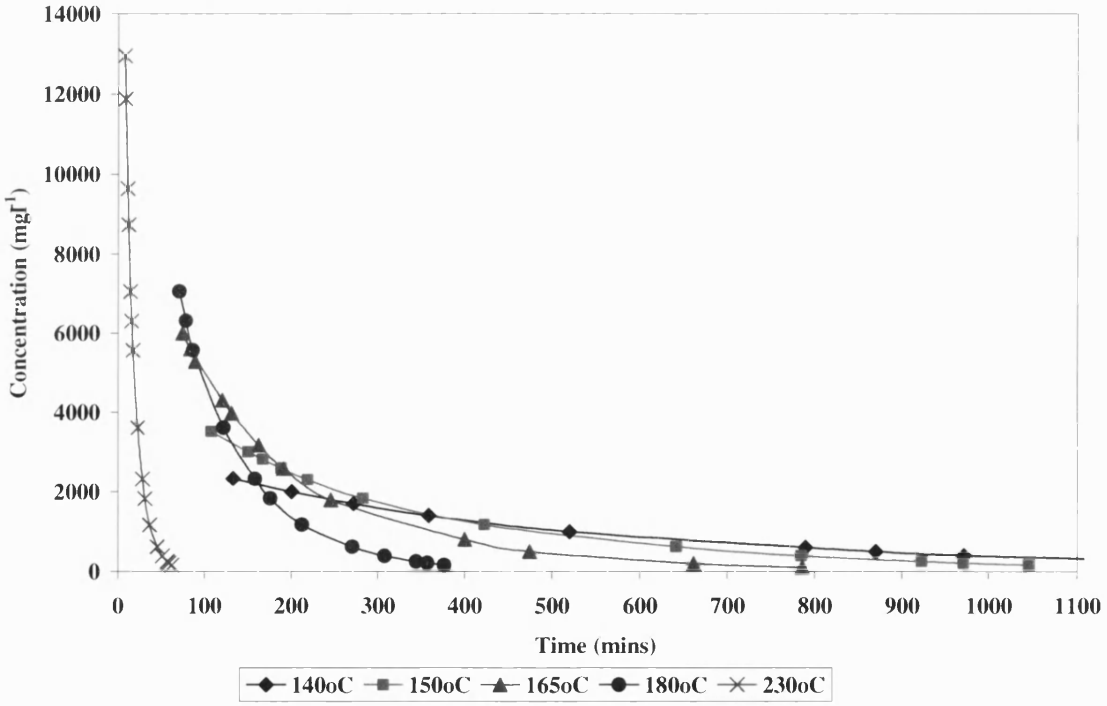

Figure 8.18 A comparison of regeneration graphs produced using the model at a range of temperatures

Figure 8.18 shows the trends in regeneration are predicted by the first order model. The graphs, as expected, are similar to those of Figure 8.7. It can be seen from Figure 8.18 that the regeneration curve produced by the model for a temperature of 230°C is almost vertical, whilst the regeneration curve for a temperature of 140°C is almost horizontal. This might suggest that the model has strict limitations in its applications which do not extend to an upper limit of 230°C and a lower limit of 140°C.

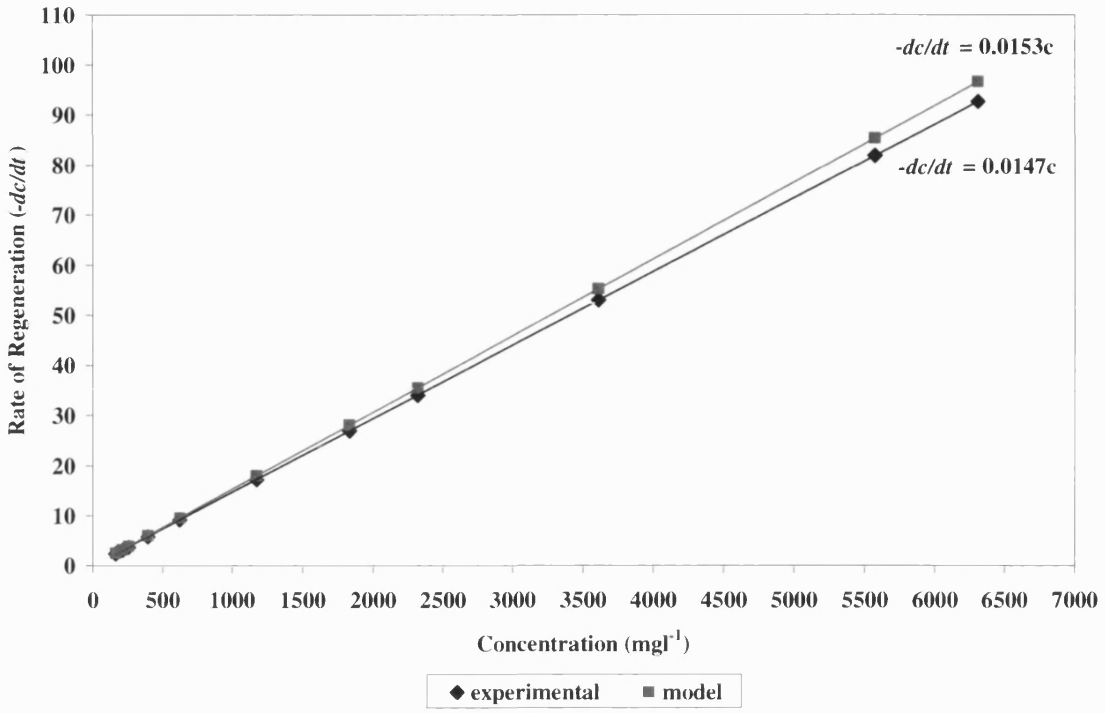

Figure 8.19 A comparison of experimental and model regeneration data at 180°C

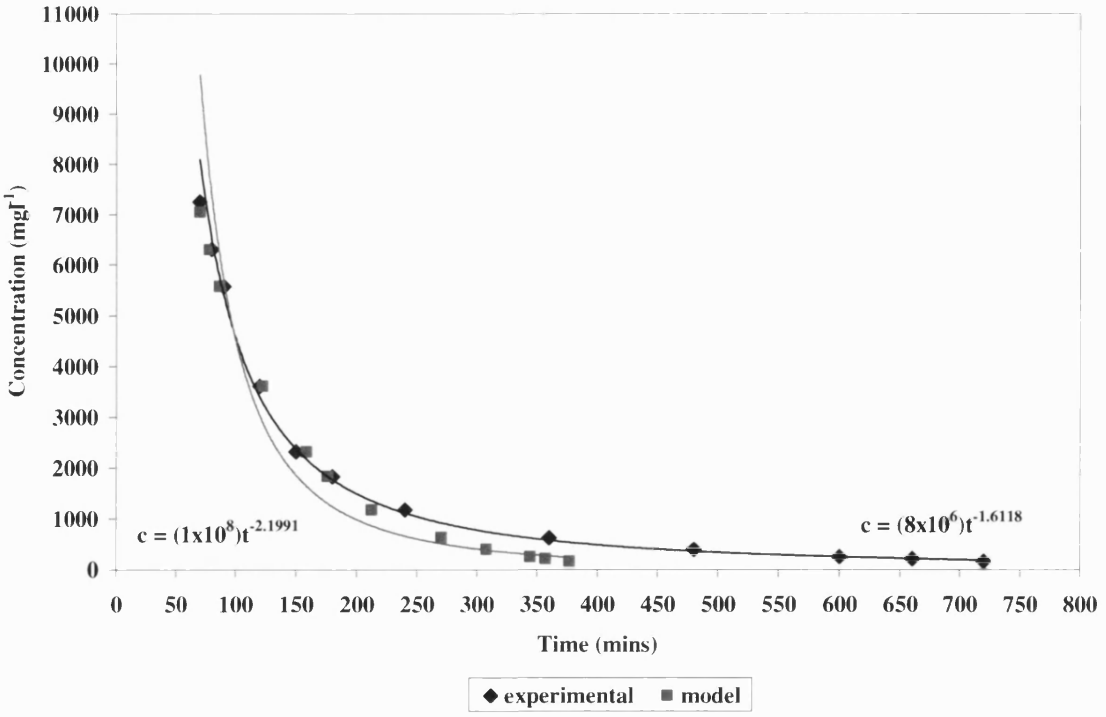

Figure 8.20 A comparison of experimental and model regeneration curves at 180°C

Figures 8.19 and 8.20 show a comparison between the model and experimental data for a superheated steam temperature of 180°C. The comparisons between model predictions and experimental results are quite good. This is expected because 180°C lies within the range of experimental data used in determining the model parameters.

8.5 Conclusions

The regeneration profiles shown in this chapter provide information with respect to whether regeneration is possible and how long it will take. The regeneration profiles represent the kinetics of the system; the larger, narrower peaks illustrate better regeneration kinetics than shorter, wider peaks. The regeneration profiles have shown the system kinetics to be affected by the type of adsorbate, the type of activated carbon, carbon activation, water flowrate and superheated steam temperature. Better system kinetics are provided, as expected, by a higher steam flowrate and a higher steam temperature. It has been shown that the kinetics of the system can be changed by the type of adsorbate, carbon and steam flowrate.

Mass balances showed that the lower activated carbons recovered less adsorbate, whilst higher steam temperatures the less the amount desorbed.

Generally, the reproducibility studies, which uses fresh carbon for each run and show whether the system is able to reproduce the same results over and over again, have been shown to be fairly good. The repeatability studies, which uses the same carbon over a number of adsorption/regeneration cycles, showed a decrease in adsorption capacity by approximately 28% after five cycles. This would suggest that after the five cycles the spent carbon should be replaced with fresh carbon for the next set of experiments.

The water balances showed the regeneration process to have a 10-25% water ratio, which implies that the initial waste water was decreased in volume by 75-90% and the recovered organics are in a more concentrated form than the adsorption feed water. It was also shown that as the superheated steam temperature was decreased more water was required to complete regeneration.

A model was created to predict experiments for various temperatures of superheated steam. Therefore while the practical experiments showed the regeneration concept to be successful at temperatures as low as 180°C, the theoretical model showed that this particular system would be valid for steam temperatures ranging from 140-230°C.

Overall, it was proven that the regeneration process did not produce as accurate results as the adsorption process. I believe this was generally because the TOC was not able to analyse the extremely high concentrations of the complex regenerant samples accurately. The general regeneration profile trends have shown regeneration at temperatures of approximately 200°C to be fairly reproducible and consistent. However, studies of the mass balances have often shown that there are many errors or inconsistencies in the results, mainly showing that more adsorbate is being desorbed from the carbon than was initially adsorbed. As explained previously, this could be due to many experimental errors such as measuring volumes, masses, flowrates and concentrations. Of these quantities the volume, mass and flowrate were measured using, pipettes, weighing scales and a peristaltic pump, respectively. Each of which would more than likely produce a consistent error, regardless of the solution or solid. The concentration, on the other hand, was analysed using the TOC analyser, which was calibrated using a known concentration of potassium hydroxide. However, this was a simple fluid and when analysing other simple fluid such as propionic acid and butyl glycol consistent results (±1 mg l^{-1} maximum) were also obtained. The cutting fluid, on the other hand, was a much more complex fluid, the exact contents of which were unknown, and analysis of this fluid using the TOC analyser was not as consistent (±1250 mg l^{-1} maximum) as with the simpler fluids. It must be noted that the higher end of these discrepancies generally occurred at larger concentrations and mainly with the desorbed regenerant rather than the initial ultrafiltered or chemically split cutting fluid. In addition, it must also be noted that this discrepancy of ±1250 mg l^{-1} is equivalent to a ±7% discrepancy. The TOC manual suggested that a maximum of ±2% error may occur in analysis, but this 7% is more than three times that. An explanation for this may be that the desorbed solution is either unstable, or even more complex than the original cutting fluid that the TOC analyser was unable to manage this complicated solution.

Other errors could have originated in calculating the mass adsorbed and desorbed, by integration of the area under the adsorption and regeneration curves. In many instances the adsorption curve had not achieved its flat plateau, the point at which the system reaches

equilibrium, and the run had been stopped at the end of the mass transfer zone. During the regeneration studies, there may have been errors in evaluating the peak(s). The peak was determined from when samples as well as their concentration. However, it may also be possible that the actual peak may have occurred just before or just after a sample had been taken, and as the sample is taken over a period of time (30s or so) the peak concentration may be diluted by lower concentrations within the same sample. These inconsistencies may also have caused errors in calculating the mass balances.

9.0 Overall Conclusions and Future Work

9.1 Overall conclusions

(i) The main aim of this research project was to develop an on site oily wastewater treatment system, in order to achieve a high quality purified water and a recovered organic fraction for reuse. However, a wastewater of this nature would contain particulates, free, emulsified and soluble oils, all of which would be required to be treated in order to achieve the objectives. Generally, most existing treatment systems, in any industry, would have processes already in place to remove the particulates and free oils to comply with regulations set by water authorities. However, the emulsified and soluble oils are generally left untreated. Hence, it was the treatment of these contaminants using carbon adsorption, ion exchange and carbon regeneration; which was investigated. Overall, the outcome of this research showed that these aims and objectives were met, and a system has been successfully designed in order to remove and recover the soluble organic fraction of the feed wastewater.

(ii) As previously explained in Chapter 2, in order to get the best performance from the carbon adsorption unit, the emulsified oils had to be removed from the neat cutting fluid. This was done using ultrafiltration and chemical splitting. Experimental results from batch equilibrium and dynamic column studies showed that the shapes of both curves varied slightly, although the respective mass balances were similar. The chemically split curve was much smoother than the ultrafiltered curve. This would suggest that the chemically split fluid was a pseudo single component solution, whilst the ultrafiltered cutting fluid (with its a jagged curve) was a multicomponent solution. Likewise, the regeneration studies showed that the chemically split cutting fluid produced a single regeneration peak, whilst the ultrafiltered cutting fluid produced three regeneration peaks. Whilst both fluids produced similar results, the pilot scale study used the chemically split cutting fluid as it was a more economical pre-treatment process.

(iii) Chapter 5 detailed the characterisation of many organic and inorganic adsorbents using SEM and ASAP. SEM provided an overview of the internal and external

surfaces of adsorbents. However, they do not give a high enough resolution to detect the micropores. Overall, it was shown that MAST carbons had a homogeneous internal and external structure with irregular shaped pores, whilst the Sutcliffe Speakman carbons showed a heterogeneous surface. This information is advantageous in understanding the mechanisms in the adsorbent-adsorbate relationships. A homogeneous adsorbent would be in favour of specific applications to remove a particular compound or group of compounds with a similar molecular size. A heterogeneous surface, on the other hand, due to the variety of its pore sizes, could adsorb a range of compounds with varying molecular sizes. In this instance as the contents of the cutting fluid were unknown it was impossible to tell which adsorbent would be best suited for the adsorbate, without trial and error testing. Due to the nature of this research project, it was a requirement that MAST carbon was to be studied. However, Sutcliffe Speakman carbon was also studied as it was a standard industrial coconut shell carbon which was readily available.

(iv) Figure 9.0 shows a flow diagram of the optimum conditions developed from the results of the laboratory scale studies for the scale up of the WOWSEP process which was to be used in the pilot scale studies at PERA and Ford Motor Co.

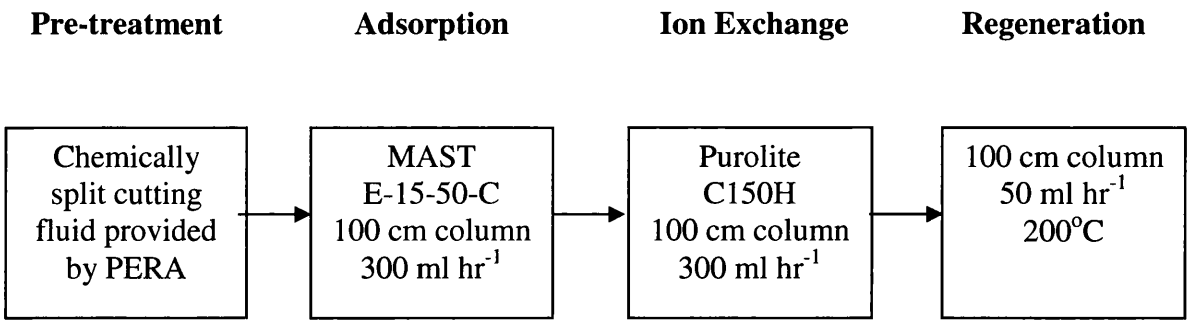

Figure 9.0 A flow diagram to show the optimum conditions obtained from the laboratory scale process for the scaled up pilot scale process

The inclusion of the ion exchange step was necessary to deal with the corrosion inhibitors which were present in the cutting fluid (generally in the form of amines).

(v) Overall, the batch kinetic and equilibrium studies showed that the adsorption process itself is extremely fast and the greatest part of adsorption had taken place within the first 30 minutes or so and that equilibrium could easily be achieved within 24 hours. Equilibrium isotherms showed that in every case the system followed the Freundlich model, which was as expected as the Langmuir model was initially developed for gas phase systems, whilst the Freundlich model was developed for liquid phase systems.

(vi) The laboratory scale rig was initially designed with a 10 cm column, 300 cm^3 hr^{-1} influent flowrate, an EBCT of 2.2 minutes and a residence time of 13.8 minutes. However, dynamic column experiments using this configuration gave an immediate breakthrough using ultrafiltered, chemically split cutting fluids and simpler organic fluids. This suggested that the system was incapable of adsorbing adsorbates satisfactorily under these conditions. It was found that this instantaneous breakthrough was due to two reasons:

1. the system design
2. the presence of an amine type compound (or compounds) which does not adsorb onto carbon.

(vii) The optimum system design was found using propionic acid and butyl glycol, which are two simple organic fluids known to adsorb onto carbon. Adjusting the system design using propionic acid, it was found that the optimum for laboratory study to produce a good breakthrough curve was a 100 cm long column operated with a feed flow rate of 150 ml hr^{-1}. These conditions increased the EBCT from 8.7 minutes to 44.8 minutes, the residence time from 32 minutes to 68 minutes and the breakthrough time from 39 minutes to 631 minutes, thereby producing much better system kinetics. This system produced acceptable results for the laboratory scale with a sharp s-shaped breakthrough curve for the simpler propionic and butyl glycol solutions. However, with the cutting fluid solutions (whether chemically split or ultrafiltered) an immediate breakthrough was still observed. It could now be concluded that this was mainly due to a non adsorbable "amine" fraction. Accordingly, the ion exchange resin (Purolite C150H) was introduced to remove the "amine" fraction and hence when both carbon and Purolite C150H were used

the immediate breakthrough problem was resolved. In this way, the sequence of steps shown in Figure 9.0 was developed.

(viii) In some cases, a complete equilibrium isotherm could not be achieved; this could have been due to the fact that there were limitations to the maximum initial concentration of the ultrafiltered and chemically split solutions. Another reason for the maximum loading not being achieved was the presence of a component(s) in the cutting fluid which did not adsorb onto the carbon. The majority of the non-adsorbable fraction was found to be an "amine" component which is present in cutting fluids as a corrosion inhibitor. The use of a strongly acidic cationic exchange resin was required for the removal of this "amine" fraction. Many ion exchange resins (Purolite C150H, Amberlite XAD-4, Dowex 50, Duolite, Dowex M and MN500) were studied using the ultrafiltered cutting fluid to determine whether they would be able to remove this "amine" fraction. MN500 was found to be best suited to carry out this separation, as it behaved most like the carbons (due to its macro and microporous structure) and as it gave the highest loadings from all the ion exchange resins tested. Of the ion exchange resins MN500 was also found to have the lowest $1/n$ and highest K_f values (strongest interaction and highest adsorption capacity) in the Freundlich isotherm. Nevertheless, due to a limited supply of the MN500 being available, the majority of the ion exchange experiments were conducted using Purolite C150H, which was the second best ion exchange resin.

(ix) Regeneration was conducted such that the carbon could be reused repeatedly. The regeneration graphs show the amount of adsorbate being desorbed from the carbon against time. Generally, the mass balances showed that the organics adsorbed on to the carbon could be subsequently removed using relatively low temperature superheated steam. Occasionally, the mass balances seemed to show that more organics were desorbed from the carbon than was initially adsorbed. However the main explanation for this was experimental error as discussed in Section 8.5. Overall, regeneration was found to be successful at a temperature of 205°C, using superheated steam, with the greater part of regeneration occurring in the first 100 minutes or so.

(x) The graphs obtained from the reproducibility studies, for both the adsorption and regeneration experiments were fairly consistent in shape, which established that the system design was viable. From the repeatability experiments, the adsorption profiles showed a decrease in adsorption capacity after the first cycle and thereafter to the fifth cycle. The adsorption profiles for the second, third and fourth cycles were very similar. The overall loss in adsorption capacity, after the first five cycles was 28%. The regeneration profiles of the repeatability studies showed that the first cycle produced the tallest peak, whilst all subsequent cycles produced smaller peaks, which implies that the amount being desorbed from the carbon was decreasing. This, however, is as expected as the adsorption capacity is decreasing after each cycle and hence, as the mass balances revealed, the amount adsorbed is also decreasing. These results indicated that the carbon had a life expectancy of at least five cycles (i.e. the carbon would not need replacing for at least 5 cycles).

(xi) A theoretical model was created to predict the temperature ranges for regeneration. Graphs of the tail end of the regeneration (after the initial peak in concentration) obtained from the model (Figure 8.18) showed that at a temperature of 140°C a horizontal line was produced, whilst at a temperature of 230°C a vertical line was produced. This would suggest that if using superheated steam at atmospheric pressure, regeneration would only be successful between temperatures of 140°C – 230°C.

(xii) The prototype unit constructed at PERA consisted of pre-treatment stages to remove the particulates, free and emulsified oils from the cutting fluid waste, a purification stage to remove the soluble organic contaminants and a final innovative stage to recover the soluble contaminants. The prototype unit was able to treat up to 1000 litres of feedstock at up to 300 l hr^{-1} and was used to measure performance parameters including water quality *e.g.* COD, volume reduction, treatability and recycling of by-products, the costs of treatment, and the payback period of full-size units. The package steam generator provided superheated steam at temperatures up to 220°C.

(xiii) An economic model developed to demonstrate the technical and economic promise of the WOWSEP process showed that even if the "amine" fraction was not removed

from the feedstock, the substantial financial savings on disposal costs (according to the Mogden formula) and/or the fresh water costs which could be gained from the pre-treatment stages followed by the adsorption column made the WOWSEP process viable and worthwhile. Therefore an ion exchange unit was not incorporated into the design of the prototype rig at PERA. If however, at a later date, further purification were to be required, an additional step to carbon adsorption would be necessary to remove this "amine" fraction. The most suitable method for this extra step would be ion exchange, as it could easily be incorporated to the WOWSEP system.

(xiv) PERA found the overall benefits of the WOWSEP process to be:

1. A reduction in waste volume by 90%.
2. Recovery of 95% of water for reuse.
3. Recycle of a minimum 50% waste, recovered oil and organics.
4. A minimum of 50% savings in disposal costs for typical users of the technology.
5. Carbon with a lifetime of greater than 1 year, with 100% regenerable capability, on site.
6. Design versatility, such that the system may be used in conjunction with almost any pre-existing treatment facility.
7. Increase in water softness, therefore increase in feasibility of recycling.

Overall, the investigations presented in this thesis have shown that a combination of carbon adsorption and ion exchange provides excellent results in the purification of cutting fluid wastes. The regeneration results showed that what was adsorbed onto the carbon was more or less desorbed from the carbon, thereby demonstrating that the regeneration process could be efficient and effective, with little or no damage to original porous structure and activity. Therefore on the whole, the objectives of this DTI/EPSRC LINK project were met.

9.2 Future work

This study has provided an insight into the problems caused with the clean up of cutting fluid waste, which is produced by many industries. Whilst the prototype for the WOWSEP

process was commissioned and applied to a motor industry site it has since been made redundant, due to the lack of understanding of the process. Therefore from an industrial and academic point of view, further research would be beneficial in improving the existing system further.

(a) Disclosure of the exact nature and contents of the cutting fluid would have been advantageous in the development of the system. Adsorption and regeneration experiments could then have been carried out using the individual components. This would have provided a thorough analysis and understanding of what was happening during the experiments. It would also have helped determine what components were being adsorbed and desorbed at the different stages within the process. However due to commercial confidentiality, the exact components were not revealed and due to the cutting fluid being such a complex multicomponent solution, the time and effort required to uncover and analyse each of these components would be immense, and maybe worthy of another PhD study.

(b) Further batch kinetic batch experiments using various impeller speeds would be advantageous in order to examine the kinetic properties of the system further and to investigate the rate limiting diffusion process.

(c) Most of the equilibrium isotherms, apart from those for the carbon ion exchange resin mixture, did not reach their maximum loading potential. The unavailability of the pre-treated cutting fluid solution at high enough concentrations and the lack of time prevented these experiments from being carried out. Further equilibrium studies using higher concentrations should be conducted to gain a more thorough insight of the equilibrium phenomena.

(d) Generally, all of the characterisation, batch kinetic and equilibrium, dynamic column, and regeneration/elution experiments conducted with carbon should have been repeated with the ion exchange resin, to provide a fuller understanding and insight into the process. It would be interesting to see what effect MN500 (a macronet with the properties of an adsorbent and ion exchange resin) would have on the system performance. Hence batch kinetic and equilibrium, dynamic column adsorption and steam regeneration experiments need to be conducted with MN500.

(e) Ideally all of the dynamic column (adsorption and regeneration) experiments should be repeated using the 100 cm column as this length resolved the premature breakthrough problem and hence would have provided a better idea of the system kinetics and true loadings. Figure 9.0 show that the optimum column length for adsorption and regeneration would be 100 cm. Unfortunately, regeneration was not possible with the 100 cm column as it was too long to fit inside the fluidised sand bath. Accordingly, further regeneration studies with a longer column are recommended.

Finally, the issue of discrepancies in the mass balances needs to be addressed further. It may be advantageous to find an alternative analytical method (*e.g.* COD) with which results from the TOC analyser could be compared. Nevertheless, it must be noted, that even with the limitations discussed above in (a)-(e), the general trends and results collected from the adsorbent characterisation, batch kinetic and equilibrium studies, dynamic column and regeneration experiments were still important in aiding in the scale up of the laboratory scale rig and in the successful build of an integrated prototype rig which was constructed at PERA where it underwent thorough testing.

APPENDIX I

envirowise
Practical Environmental Advice for Business

Cost-effective treatment of waste oily water

A development project to demonstrate the benefits of a system to treat oily wastewaters

Spent metalworking fluids contain a mixture of free and emulsified oils together with a cocktail of toxic, water-soluble organic compounds. Free and emulsified oils can be recovered using existing treatment techniques, but the water-soluble components are unaffected and remain in the water phase. A prototype system to remove soluble organic compounds from oily wastewater was developed and tested at a site belonging to one of the project partners. The system uses a novel synthetic carbon adsorbent and low-temperature, in-situ carbon regeneration. Trials showed that the prototype system significantly reduced the chemical oxygen demand (COD) of wastewater that had been pretreated to remove free and emulsified oils. The polished water is potentially suitable for re-use on-site. The benefits of this novel treatment system include:

- **Up to 90% reduction in wastewater COD**
- **Reduced waste disposal charges**
- **Significant reduction in water consumption**
- **Potential application to oily wastewaters from other industries**

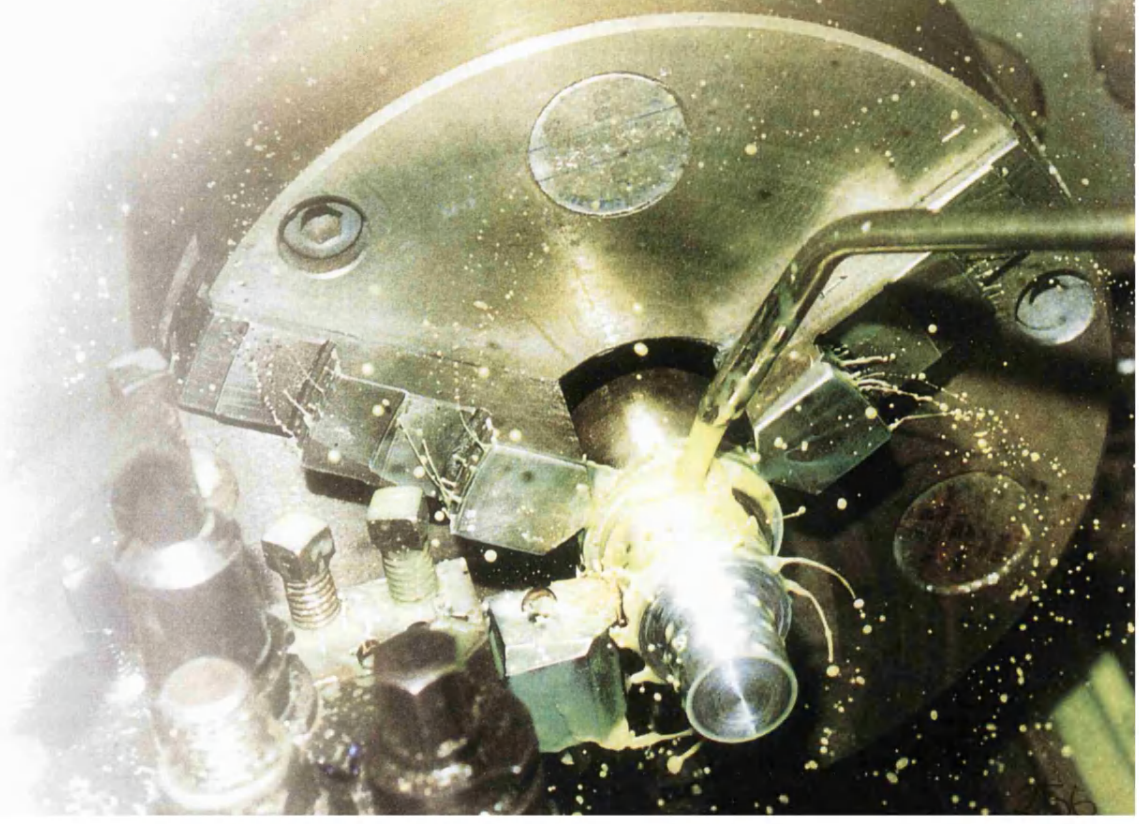

Background

Engineering workshops use large quantities of water-based metalworking fluids to remove heat and swarf from the cutting surfaces, and reduce friction between the tools and the workpiece. Careful management of these fluids[1] helps to extend their useful life, but ultimately they have to be disposed of. Engineering companies generate an estimated 400 000 tonnes/year of spent fluids, which represents a significant cost.

Spent metalworking fluids contain a layer of free/separated oil (5 - 10%), a soluble phase including emulsified oil (80 - 90%) and a small amount of solid material (<0.5%). A mixture of toxic organic compounds, eg biocides and surfactants, is dissolved in the water phase. These compounds are unsuitable for discharge to sewer without treatment. Established processes, such as oleophilic mops, can remove the free/separated oil, while emulsified oil can be separated into organic and aqueous phases, eg by ultrafiltration. The water soluble components, however, remain unaffected by these processes and may find their way into the environment and cause harm.

Project Description

The aim of the project was to develop a prototype system for the cost-effective, on-site treatment of oily wastewater to remove oils and soluble organic compounds. A novel regenerative carbon adsorption technology was selected. Activated carbon adsorption is a proven technique for the removal of soluble oils from wastewater, but it has not previously been found to be cost-effective for the treatment of spent metalworking fluids. This is mainly due to the need for daily regeneration of the activated carbon at high temperatures. The new technology developed in this project uses superheated steam to drive off the organic contaminants in situ from the novel macrostructure synthetic carbon.

The first stage was to construct a laboratory-scale adsorption/regeneration rig at the University of Bath for rapid testing of multiple samples. This allowed a wide matrix of carbon samples and types of waste stream to be assessed. Optimum conditions were identified, paving the way for the design and construction of a prototype rig (see Fig 1).

Fig 1 Prototype treatment system

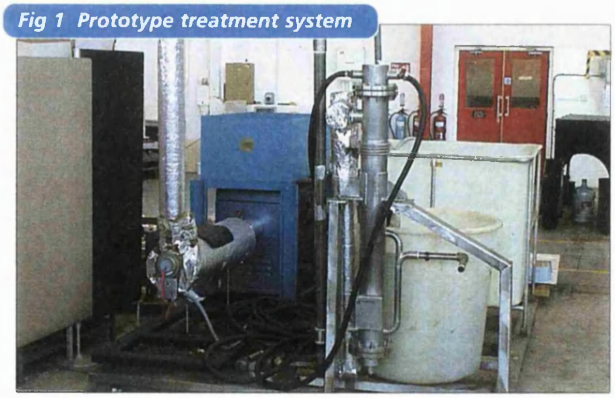

One result to emerge from the laboratory tests was the inability of the carbon adsorbent to successfully treat samples containing emulsified oil. Unless it is removed, the emulsified oil soon saturates the carbon adsorbent. The project partners, therefore, decided to focus on using the prototype to remove soluble hydrocarbons from wastewaters, from which free and emulsified oils had been removed using common pretreatment processes.

[1] See Good Practice Guide (GG199) *Optimising the Use of Metalworking Fluids*, available free of charge through the Environment and Energy Helpline on freephone 0800 585794.

Studies with the polished water obtained from the laboratory-scale rig showed that it was potentially suitable for making up fresh metalworking fluids, for general cleaning or use as cooling water.

Development of the Prototype System

The prototype was designed to prove that the integrated adsorption/regeneration system was both technically and economically feasible and was built to a specification determined through laboratory tests.

Other important design considerations included:

- low-cost manufacture;
- appropriate for most small and medium-sized enterprises (SMEs);
- flexibility of controlled parameters.

Pretreated water is pumped at up to 300 litres/hour from a 1 000-litre feed tank, up through a vertically-mounted stainless steel column of carbon adsorbent. Most of the organic compounds dissolved in the aqueous phase are adsorbed onto the carbon particles. The polished water is collected in a 220-litre receiving tank for subsequent on-site recycling or disposal to sewer. Because it has a much lower COD content, trade effluent charges are significantly reduced. Recycling the recovered water also saves on water supply costs.

As the carbon approaches saturation, it is regenerated using superheated steam at 230°C flowing down through the column. The steam leaving the carbon column is cooled in a condenser and the small volume of condensate is collected in a tank.

Trial of Prototype Performance

Trials using the prototype rig (see Fig 2) were carried out at a site that uses a wide range of water-soluble metalworking fluids (macro, semi-synthetic and synthetic fluid products) during the manufacture of automotive components. The wastewater used in the trials came from the site's existing chemical pretreatment plant.

The prototype's ability to remove water-soluble organic compounds from the wastewater was monitored by measuring the COD of the polished water and comparing it with the COD of the wastewater feed. A typical

Fig 2 Schematic diagram of the prototype integrated treatment system

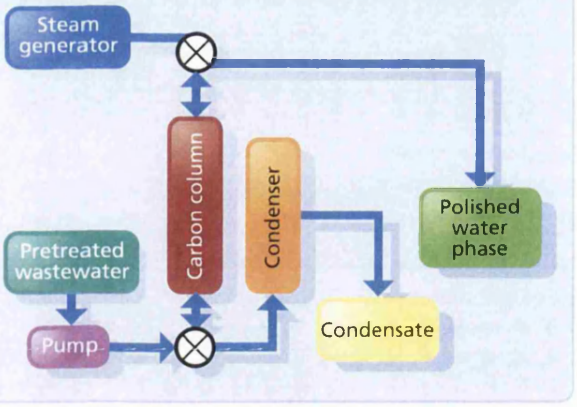

adsorption profile is shown in Fig 3. The cut-off point is dictated by the user, based on experience with the system's use, but should not be allowed to exceed 60 - 70% breakthrough.

COD was also used to assess the efficiency of the regeneration process (see Fig 4). Several regeneration cycles can be carried out without a significant reduction in carbon performance.

Data from a typical trial with the prototype rig are summarised in Table 1, showing that, with a typical pretreated wastewater, it is possible to reduce COD levels by up to 90%. Future work is planned to optimise the performance of the carbon adsorbent.

Cost and Environmental Benefits

The fully developed technology will provide users with an effective treatment system for oily wastewater. Benefits include:

- a reduction of up to 90% in wastewater COD;
- reduced cost of disposal to sewer or removal by tanker;
- potential re-use of water on-site;
- savings in the purchase of mains water;
- reduced carbon disposal/reprocessing costs;
- compliance with current and future legislation.

Fig 3 Typical adsorption profile

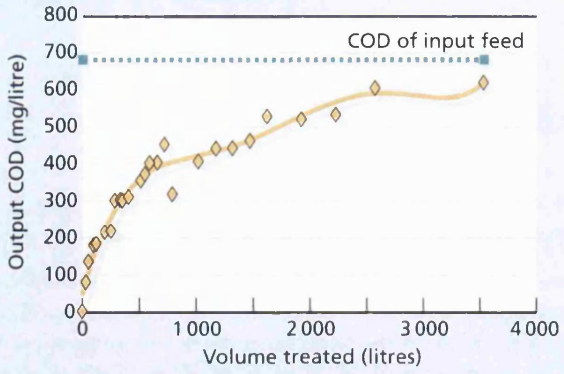

Fig 4 Typical regeneration profile

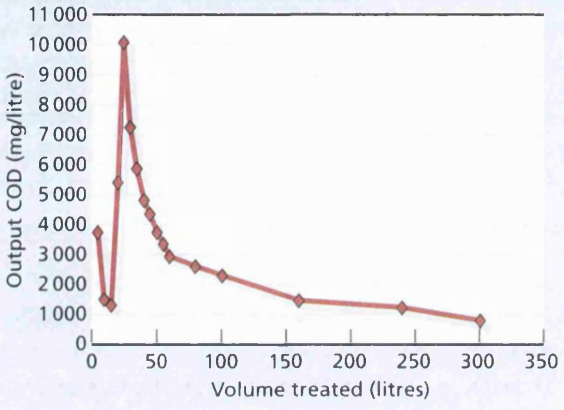

A computer spreadsheet has been developed to help potential users estimate their cost savings from pretreatment and carbon polishing.

For example, an engineering company producing 1 000 m^3/year of oily wastewater could achieve net cost savings of £29 455/year if the recovered water was re-used and £27 340/year if it was not re-used (1999 prices). Without treatment, the oily wastewater would have cost £40 000/year to tanker off-site for disposal. Net treatment costs amount to £10 545/year if the recovered water (around 950 m^3/year) is re-used and £12 660/year if it is not[2].

[2] The calculation assumes that the COD of the final aqueous phase after polishing is 4 500 mg/litre, the initial COD of the oily wastewater is 100 000 mg/litre and the aqueous phase after pretreatment contains 15 000 mg/litre of COD.

Table 1 Typical results using the prototype rig to polish pretreated wastewater

Parameter	Amount
Volume of pretreated wastewater entering the carbon column	4 000 litres (4 m^3)
Average flow rate	220 litres/hour
Average COD of input feed to carbon column	680 mg/litre
Volume of carbon adsorbent	16 litres
Volume of condensate	600 litres (0.6 m^3)
Concentration factor	6.6
Lowest COD of output	79 mg/litre
Final COD of output	660 mg/litre

Re-using water produces cost savings from lower mains water consumption (£700/year) and reduced trade effluent charges (£1 415/year). Running costs (eg utilities and labour) are partially offset by the sale of recovered tramp oil worth £2 250/year. The cost of tankering the 1.9 m^3/year of condensate off-site for disposal is around £100/year. Significant cost savings are also possible with smaller volumes of oily wastewater.

Potential Applications

Carbon adsorption is an established technology. The novelty and innovation of this research lies in the use of an in-situ regenerative system using superheated steam. This saves on costs such as storage and transportation of the spent adsorbent.

Market research suggests that there are 30 000 - 50 000 users of water-soluble metalworking fluids in the UK. The exploitation potential of the technology will increase as they strive to meet the requirement under the Integrated Pollution Prevention and Control (IPPC) Directive for BAT (best available technique) rather than BATNEEC (best available technology not entailing excessive cost).

The developed technology could be applicable to a range of industry sectors, including textile manufacturers, dyers, chemical works, water companies and any industrial site producing a wastewater stream containing soluble organic compounds.

Further Information

For more details about this novel technology and how it can benefit your business, contact the project partner:

OPEC Ltd,
1 Nab Lane,
Batley,
West Yorkshire WF17 9NG

Mr P Ilsley,
Tel: 01924 442701,
Fax: 01924 471925,
E-mail: ilsley@opec.co.uk

Project partners

Lead Organisation:

Pera, Technology Centre,
Melton Mowbray,
Leicestershire LE13 0PB

Tel: 01664 501501
Fax: 01664 501556
Mr A Lesowiec

Lead Investigator:

School of Chemical Engineering,
University of Bath,
Claverton Down,
Bath BA2 7AY

Tel: 01225 826501
Fax: 01225 826894
Professor B Crittenden

Consortium Members:

Alpha Construction Ltd,
Hilton, Derbyshire

BTR Environmental,
Henley Park, Guildford

D A Stuart Oil Co Ltd,
Wolverhampton

Ford Motor Company,
Basildon

MAST International,
Henley Park, Guildford

Useful publications from Envirowise

(GG199) - ***Optimising the Use of Metalworking Fluids***

(EG179) - ***Benchmarking the Consumption of Metal Cutting Fluids***

(GC197) - ***Automatic Recycling of Metalworking Fluid***

envirowise
Practical Environmental Advice for Business

Harwell International Business Centre | 156 Curie Avenue | Didcot | Oxfordshire | OX11 0QJ
E-mail: helpline@envirowise.gov.uk Internet: www.envirowise.gov.uk

Envirowise - Practical Environmental Advice for Business - is a Government programme that offers free, independent and practical advice to UK businesses on saving money and increasing profits by minimising waste. It is managed by AEA Technology Environment and NPL Management Limited.

For further information please contact the

Environment and Energy Helpline
0800 585794

Treatment of Factory Waste Oily Water

by *B D Crittenden, S P Perera and R Mehta*
Department of Chemical Engineering, University of Bath

Abstract

An on-site waste treatment process for factory oily waste-water has been developed in order to facilitate the recycling of purified water on-site as well as the possible recycling of part, or all, of the organic components. Known as "WOWSEP", the process has been applied at the pilot-scale for the treatment of spent metalworking fluids. The novelty of the "WOWSEP" process is that it includes an adsorption technology that uses superheated steam to drive off the soluble contaminants *in situ* from the internal structure of a novel synthetic carbon. The carbon is manufactured from a phenolic resin precursor which is carbonised and then activated, giving it properties that allow it to be regenerated with moderately superheated steam. Free oils are removed upstream of the carbon unit using established processes such as oleophilic mops or coalescers, and emulsified oils are treated by ultrafiltration or chemical separation. Whilst the carbon adsorption technology is unable to remove all the dissolved components from waste metalworking fluids, the reduction in COD of up to 90% in a typical cycle is substantial enough to make the process economic.

Laboratory-scale studies were carried out to determine the optimum combinations of carbon type and processing conditions, including those for regeneration. Trials using a prototype rig containing 16 litres of carbon have been carried out at a site that uses a wide range of water-soluble metalworking fluids during the manufacture of automotive components. A typical flow rate was 220 litres/h. The ability of the prototype to remove water-soluble organic compounds was monitored by measuring the COD of the polished water (starting from 80 mg/litre) and comparing it with the COD of the wastewater feed (680 mg/litre). The process was allowed to continue until around 60-70% of breakthrough had occurred, at which point regeneration was started. Most of the regeneration occurred within the first 300 minutes and several regeneration cycles were carried out without loss of performance. The paper will describe (i) the performance of the carbon adsorption technology at laboratory and prototype scales, and (ii) the case study involving the prototype in order to demonstrate the potential economic advantages.

Keywords: metalworking fluids; carbon adsorption; sewerage

Introduction

Metalworking fluids are essential components for drilling, milling, tapping and turning operations in manufacturing industry. In the UK there are believed to be around 40,000 engineering workshops that use multifunctional fluids, providing lubrication, cooling, prevention of surface corrosion and removal of metal fines or swarf, as well as prolonging the life of the machine tools. There are two types of fluid formulation. The first type comprises fluids which are mixed with water. Whilst these provide good cooling properties, they require monitoring and maintenance in order to retain their properties. Water-mix fluids

are generally diluted to around 5% and so, although the amount of base fluid used is around 11,000 tonnes/year, the total amount of fluid in use and requiring ultimate disposal is around 220,000 tonnes/year. The second type of metalworking fluid comprises neat oils which have good lubrication and lifetime properties and require limited maintenance. Consumption of these fluids amounts to around 22,000 tonnes/year in the UK. Although the cost of the base fluid (*c* £2.30/litre) in a water-mix metalworking fluid is higher than for a neat oil (*c* £1.30/litre), there are clear economic advantages in using the water-mix formulation because of the dilution factor.

The many functions of a metalworking fluid mean that an aqueous-based fluid must contain corrosion inhibitors, emulsifiers, extreme pressure agents, lubrication agents and biocides. Consequently, the wastes from aqueous-based metalworking fluids contain a mixture of free and emulsified oils, together with a mixture of water-soluble organic compounds. A typical spent aqueous-based metalworking fluid contains 5-10% free oil, 80-90% emulsion and less than 0.5% solids. Current treatment techniques can remove the solids and the free and emulsified oils on-site. Processes such as ultrafiltration and chemical treatment can be used to break the emulsions. However, the aqueous phase containing the soluble components is usually sent *via* a sewer to a water treatment works. Any business in the UK that discharges a trade effluent to sewer requires a consent from a sewerage undertaker who will make a charge that takes into account three factors: (i) the nature, composition and volume of the effluent, (ii) additional expense that will be incurred in order to deal with the effluent at the sewage treatment works, and (iii) any revenue that is likely to be derived by the sewerage undertaker from the effluent by way, for example, of the sale of residual sludge as a fertiliser. The cost in the UK of disposing an effluent to sewer is determined by application of the Mogden formula (Croner's, 1991) and is discussed later in this paper.

The overall aim of the project was to develop a prototype system for the cost-effective, on-site treatment of oily waste water for removing the soluble components by means of a novel regenerative carbon adsorption technology. Although adsorption of hydrocarbons from water with carbon is an established technology (McGuire and Suffet, 1983; Faust and Aly, 1987; Crittenden and Thomas, 1998), the novelty and innovation of the technology lie in the use of an *in situ* regenerative system that uses superheated steam for regeneration of the carbon. The overall waste oily water separation technology which comprises solids removal, emulsion-breaking and free oil removal, is known as "WOWSEP".

The prototype was constructed to be compatible with any type of pretreatment technology used to remove free oil and to break the emulsion. The prototype, shown schematically in Figure 1, receives recovered water from the pretreatment process in a collection vessel and is then pumped upwards through a column containing the carbon adsorbent. The purified water is recovered in a separate vessel either for reuse on site or for disposal at low cost since the level of dissolved oil is low. At any appropriate point, the adsorption process is stopped and the carbon is regenerated using steam superheated to 230°C. The steam is produced by an electrically heated boiler at 1 bar and its temperature is raised using an electrical in-line heater. The steam from regeneration is cooled in a condenser to produce a small volume of condensate. The overall technology therefore is essentially a concentrating device. A photograph of the prototype is shown in Figure 2. The overall performance of the

"WOWSEP" process is determined, in part, by the performance of the carbon adsorption unit, the optimisation of which was determined from a series of laboratory-based experiments carried out at the University of Bath.

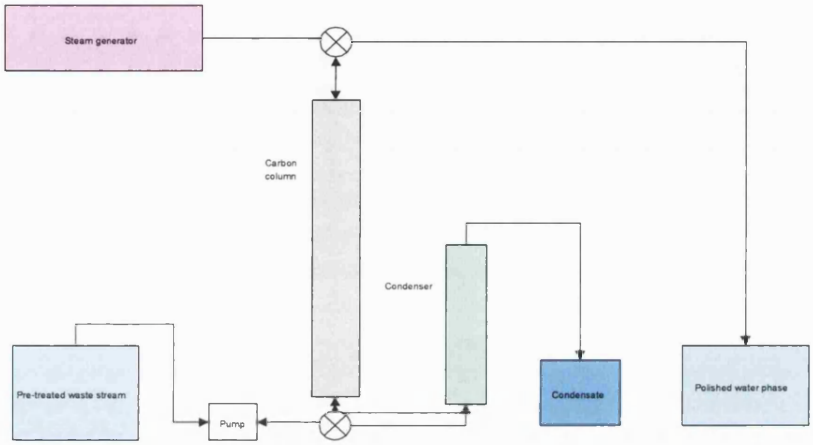

Figure 1 Schematic of prototype carbon adsorption unit

Figure 2 Photograph of prototype carbon adsorption unit

Laboratory-Scale Experiments

Dynamic adsorption and desorption experiments were carried out on the bench-scale using a 1/2" stainless steel column packed with activated carbon in granular form. Before initial use, the system and carbon were primed with ultra-pure water. The feed, at a known concentration was then pumped upwards through the column at the desired flow rate and breakthrough curves were constructed from the total organic carbon (TOC) analyses of samples taken periodically from the effluent. Implicit in this approach was the initial assumption (later to prove invalid from a scientific point of view, although not from an industrial point of view) that the total organic fraction of the feed water could be considered to be a pseudo-single component. Adsorption experiments were carried out at ambient temperature (approx. 20°C) in order to represent typical industrial conditions. Dynamic adsorption column lengths were in the range 10-100 cm, feed flowrates were in the range 150-600 ml/hr and feed concentrations were in the range 120-11,000 mg/l TOC. Feedwaters (containing no free oil) were pretreated either by chemical splitting or by ultrafiltration. Cutting fluids and fractional components were supplied by D A Stuart Oil Ltd.

Following the adsorption step, the adsorbed components were desorbed, and the carbon regenerated, by passing superheated steam in the downwards direction through the column. The steam was generated *in situ* in the laboratory by passing water at the desired flow rate through a preheating coil. The coil and the column were both located within a sand-air fluidised bed that could be heated to 300°C. The vapour product from the column was condensed and samples were collected for periodic TOC analysis, again making the initial pseudo-single component assumption. *In situ* desorption experiments were carried out with water flowrates (for steam generation) in the range 25-115 ml/hr and with column temperatures in the range 180-225°C.

Supporting batch equilibrium experiments were carried out by agitating a known mass of carbon with a known volume of solution of known TOC. Agitation was carried out for a minimum of 24 hours after which the final solution TOC was measured. In order to prepare the adsorption equilibrium isotherms, it was assumed initially that the total organic fraction of the fluid behaved as a single dilute pseudo-component for the purposes of the mass balance. Other physical analysis techniques were used to support the liquid phase adsorption measurements.

Dynamic adsorption-desorption and batch equilibrium experiments were carried out on a variety of novel carbons supplied by MAST Carbon Ltd (Tennison, 1998), for comparison with naturally-derived carbons supplied by Sutcliffe Speakman. MAST's carbons were manufactured from phenolic resins by the sequential processes of extrusion, drying, carbonisation, and activation to varying degrees. Granules were formed from the extrudates by crushing and grinding. MAST and Sutcliffe Speakman carbons gave broadly similar equilibrium isotherms and breakthrough curves. For adsorption, there appeared to be little effect of the degree of activation of the MAST carbon on the breakthrough curve. Equilibrium loadings at solution concentrations of 1000 mg/l TOC were 0.025 mg/mg for chemically split and ultrafiltered feedstocks, 0.13 mg/mg for pure butyl glycol, 0.06 mg/mg for pure propionic acid, and 0.018 for a pure amine fraction.

On a dimensionless concentration basis (C/C_o), breakthrough of TOC occurred very early with neat and ultrafiltered cutting fluids (Figure 3), progressing up to around 70% for the former and 30% for the latter. This was followed by a plateau region for the ultrafiltered feed and then a further rise to 100% (not shown on Figure 3). The shapes of breakthrough curves for chemically treated and ultrafiltered feedstocks were broadly similar for otherwise identical operating conditions. Breakthrough experiments with single pure compounds or compound groups, such as various organic acids, glycols and ethanolamines revealed qualitatively that the early part of the breakthrough curves was almost certainly due to premature breakthrough of amines which are corrosion inhibitors in cutting fluid formulations. For the pure components such as glycols and organic acids, the effect of changing column length was to show that constant pattern behaviour occurred. This could not be observed when cutting fluids were used because of the premature breakthrough behaviour. For the pure components, increasing the feed flowrate reduced the time to initial breakthrough and sharpened the breakthrough curve. For the cutting fluids however, the premature breakthrough masked the expected normal effect of flowrate.

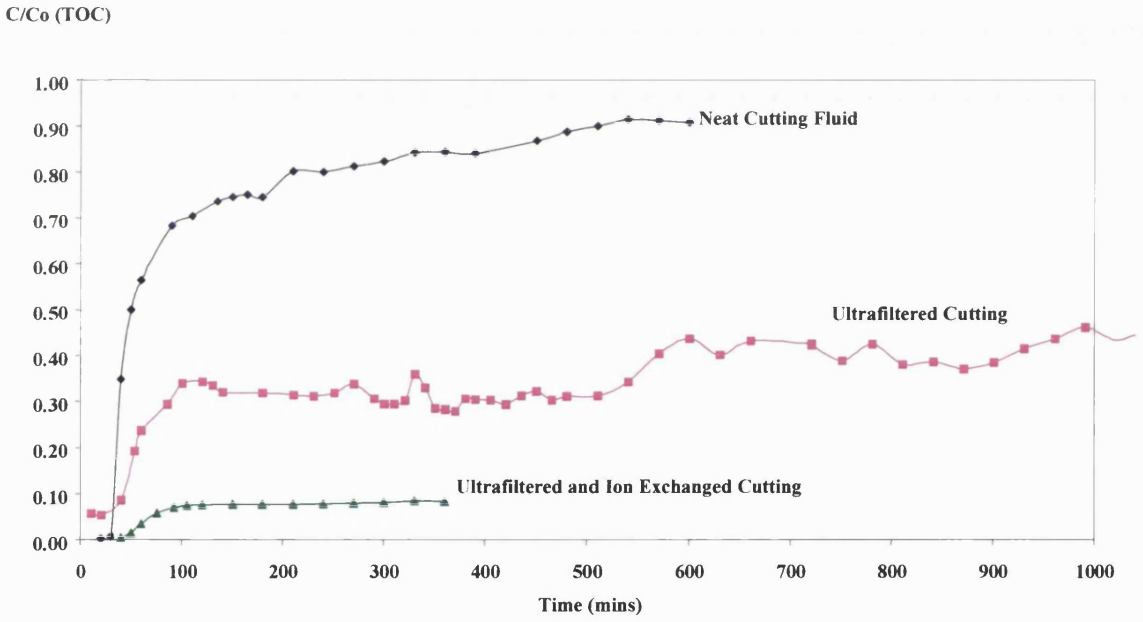

Figure 3 Comparison of breakthrough data for neat cutting fluid, ultrafiltered cutting fluid, and ultrafiltered cutting fluid that has been passed through an ion exchange column (100 cm column length and 150 ml/h feed flow rate).

Two principal approaches were taken to deal with the amine problem. In the first, a MAST carbon was manufactured in a modified form so that it included copper to see whether the amines could be removed on to the carbon by reaction or complexing with the metal. Equilibrium isotherm experiments showed that whilst there was a slight improvement in the

TOC loading with the copper-modified carbon, it was not sufficient an improvement to merit a breakthrough trial. It was found, in any case, that the amines remaining in solution had leached some of the copper from the carbon, and that the pH of the solution in the equilibrium cells had been unaltered.

In the second approach, further pretreatment by incorporating an additional step involving ion exchange was studied. A comparison of results with neat, ultrafiltered and ion exchanged cutting fluids revealed that only by pretreating the fluid by ion exchange could the premature part of the breakthrough curve be removed, as shown in the lowest curve of Figure 3. A matrix of batch equilibrium and dynamic adsorption column experiments involving the mixed feed, the amine fraction, the remaining non-amine fraction, the carbon, the ion exchange resin, and mixed carbon/resin was then carried out to reveal that the amine and non-amine fractions were acting essentially independently of each other. Virtually independent action of the two fractions was ultimately confirmed by dynamic column experiments wherein (i) a carbon bed preceded an ion exchange resin bed, (ii) an ion exchange resin bed preceded a carbon bed, and (iii) the two solid materials were mixed together in a single bed. All these three dynamic column trials provided essentially identical breakthrough curves without premature breakthrough (shown for an ultrafiltered feedstock, for example, as the "middle" three curves in Figure 4).

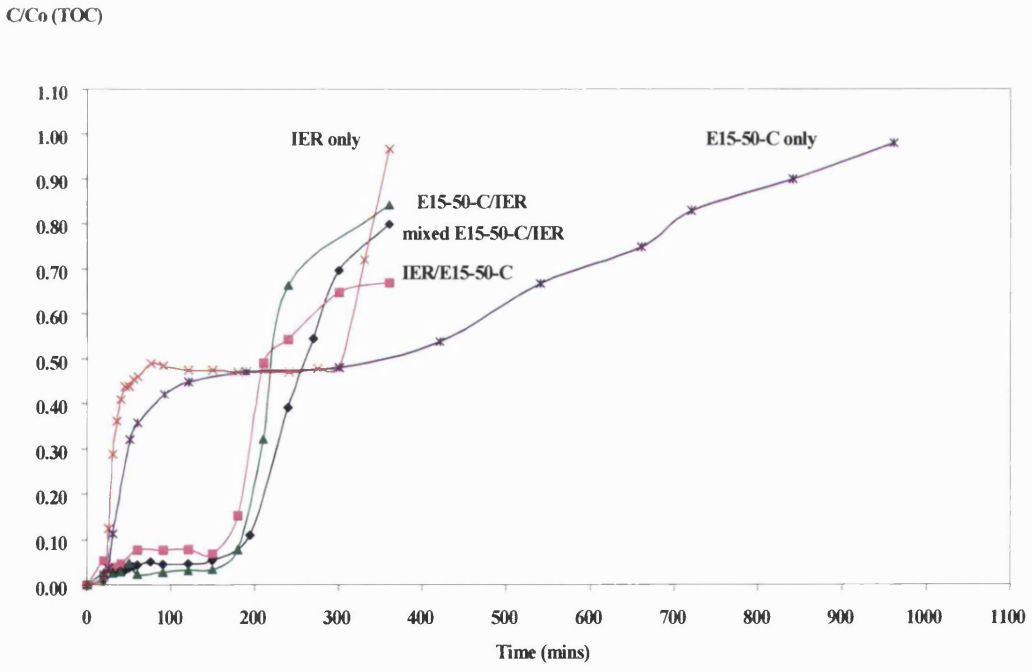

Figure 4 Effect of ion exchange before, after and mixed with the carbon

Further evidence of the independent behaviour of the amine and non-amine fractions was provided by the success in modelling the breakthrough curve of the non-ion exchanged cutting fluid by a simple addition of the breakthrough behaviours of the amine and the non-amine fractions of the pretreated cutting fluid.

Regeneration of both MAST and Sutcliffe Speakman carbons could be accomplished with steam at 1 bar and modest superheat (around 200°C). The mass flowrate of the steam was low compared with the flow rates used in the preceding adsorption step in the cycle. Over the range 25-75 ml/hour, the steam mass flow rate had little effect on the regeneration curves. Additionally, the time for regeneration was substantially lower than the time to reach complete breakthrough on the adsorption step in the cycle. The column effluent TOC rose quickly to a maximum to decline exponentially towards zero (shown as a function of regeneration temperature for chemically split feedstock in Figure 5). The magnitude of the peak TOC concentration increased, whilst the time to this peak and the peak width were reduced, as the steam temperature was increased. These relationships were linear over the range of conditions studied.

Subsequent water mass balances showed that the ratio of regeneration water to feed water varied with regeneration temperature but was in the range 7-23%, thereby providing good concentration factors for the organic fraction adsorbed. The lowest ratio was found with the highest regeneration temperature tested (225°C). Regeneration took longer, and hence more water was required, when the regeneration temperature was lowered. The exponential reduction in effluent TOC concentration on regeneration beyond the peak concentration could be modelled by a first order process with a relatively high apparent activation energy of about 70 kJ/mol. This has facilitated development of a simple model for design purposes. Additionally, although there was no effect on the adsorption breakthrough curve, there was some effect of the MAST carbon activation on the regeneration performance.

Repeated dynamic adsorption experiments, firstly with fresh carbons and secondly with the same batch of carbon over five complete adsorption-desorption cycles revealed good repeatability. The approach to cyclic steady state was fast. Mass balances over a large number of individual adsorption-desorption cycles showed that, within the bounds of experimental error, the mass of material adsorbed was equal to that removed on regeneration, providing further evidence that the carbons could sustain repeated cycles.

The substantial amount of data obtained from the bench-scale apparatus allowed an adsorption column-sizing algorithm to be designed in order to support the commercial development of the "WOWSEP" process. The pre-treatment units of the overall "WOWSEP" process did not require the development of special design algorithms.

Prototype-Scale Experiments

The prototype system shown in Figures 1 and 2 contained 16 litres of carbon and was operated with an average feed flow rate of 220 litres/h. The total volume of feed was 4000 litres having an average COD of 680 mg/l. The results of a breakthrough trial are shown in Figures 6 and 7 for the adsorption and desorption steps, respectively. Figure 6 shows that the

breakthrough occurred immediately to be followed by a gradual increase in effluent COD. This was as expected from the laboratory-scale experiments. The lowest COD was 79 mg/l and the final COD in this trial was 680 mg/l. A typical regeneration profile is shown in Figure 7. As expected from the bench-scale experiments, there was a peak in the effluent COD shortly after the regeneration process was started and most of the regeneration occurred in the first 300 minutes. The volume of condensate was 600 litres and so the volume concentration was 6.67.

Case Study

A computer spreadsheet was developed in order to determine the financial benefits from pretreatment and polishing with the carbon bed. An example case study is provided by Envirowise (2001). The spreadsheet is based not only on the technical capabilities of the "WOWSEP" process but also on the charging structure for disposal of aqueous effluents in the UK. The Mogden formula (named after the sewage treatment works where it was first used) is used in the UK to calculate the charge for the reception, conveyance, treatment and disposal of waste arising from a trade effluent discharge to sewer. The method is aimed at ensuring that a company only pays for the treatment that an effluent receives. The charge is a function of the volume and strength of the effluent and the degree of treatment afforded to it. The formula can vary throughout the UK but a common form is as follows:

$$C = R + [V + Bv] + B[Ot/Os] + S[St/Ss]$$

where the parameters are defined in Table 1. R, V, B and S are the regional average unit costs while B and S are multiplied by factors which relate the strength and solids content of the trade effluent to that of domestic sewage. There is much regional variation in charges. Example values for Anglian Water (extending throughout the Eastern region of England) for 1997/98 are shown in Table 1. It is clear that reductions in cost can be achieved not only by reducing the volume of sewage which can be achieved if water can be recycled within the manufacturing environment, but also by reducing the chemical oxygen demand.

In the following example of the economics of the "WOWSEP" process, it is assumed that the COD of the initial wastewater is 100,000 mg/l and that this value can be reduced to 15,000 mg/l on pretreatment. It is assumed also that the COD of the final aqueous stream after carbon adsorption is 4,500 mg/l. For an engineering company that produces 1000 m^3 per year of oily wastewater, the net annual treatment costs would be £10,500 (at 1999 prices) if the recovered water (*c* 950 m^3) were to be recycled. The net annual treatment costs would be £12,600 if the recovered water could not be recycled. Without treatment, the oily wastewater would have cost £40,000 per year if it were to be tankered off-site for disposal. Thus, net annual cost savings of £29,500 could be realised with the "WOWSEP" process if the recovered water were to be recycled. If recycling of water were not possible, the net annual cost saving would be £27,400.

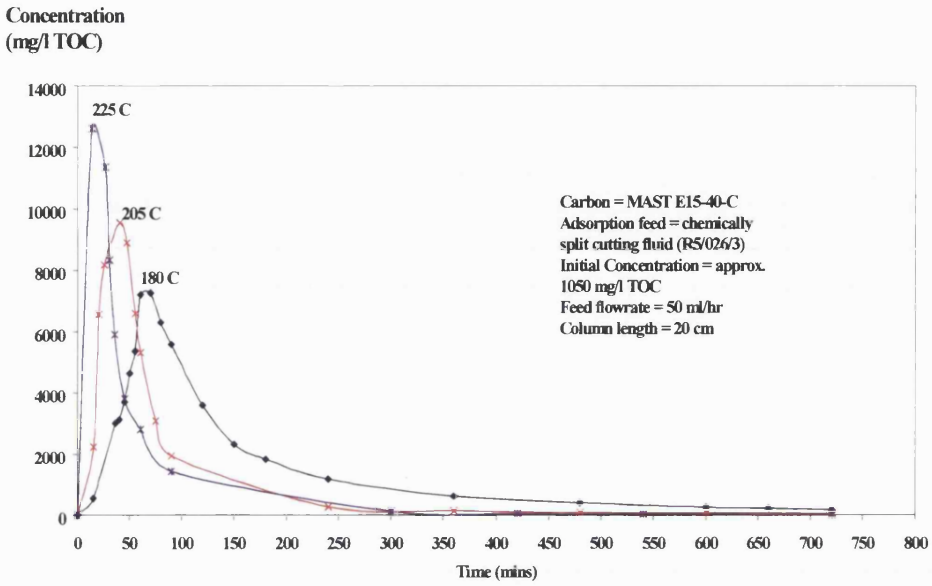

Figure 5 Effect of temperature on the regeneration of a MAST carbon

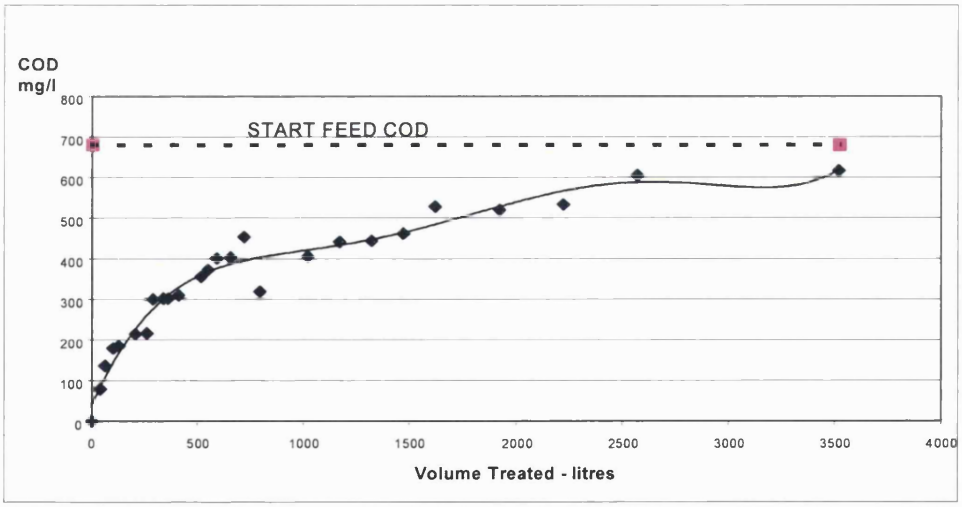

Figure 6 Typical breakthrough profile for prototype

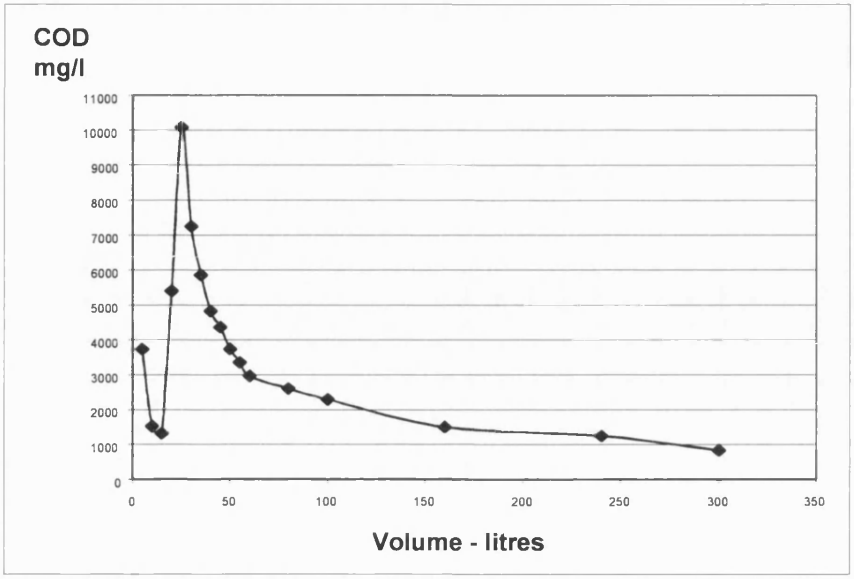

Figure 7 Typical regeneration profile for prototype

Table 1 Parameters in the Mogden formula and some typical values (Croner's, 1991)

Parameter	Definition	1997/98 values (Anglian Water)
B	biological oxidation cost per m^3 of settled sewage, including the cost of secondary sludge disposal	38.66 p/m^3
Bv	additional cost per m^3 where there is biological treatment	3.46 p/m^3
C	total charge in pence/m^3 of trade effluent	
Os	chemical oxygen demand (COD) in mg/l of average strength settled sewage	465 mg/l
Ot	chemical oxygen demand in mg/l of the trade effluent after settlement for a specified period (usually one hour)	
R	reception and conveyance cost/m^3 of sewage	11.42 p/m^3
S	treatment and disposal cost of primary sludges/m^3 of sewage	21.88 p/m^3
Ss	total weight of suspended solids (mg/l) of average strength crude sewage	383 mg/l
St	total weight of suspended solids (mg/l) of the trade effluent	
V	volumetric + primary treatment cost per m^3 of sewage treated	17.88 p/m^3

Conclusions

An integrated process has been developed to facilitate the recycling of water by the treatment of factory waste oily water. Dissolved oils are removed by adsorption onto a novel, synthetic carbon derived from a phenolic resin precursor. The benefits (Envirowise, 2001) include:

- a reduction of up to 95% in wastewater COD;
- reduced cost of disposal to sewer or removal by tanker;
- potential reuse of water onsite;
- savings on the purchase of mains water;
- reduced carbon disposal and reprocessing costs; and
- compliance with current and future legislation.

References

Crittenden, B D and Thomas, (1998), Adsorption Technology and Design, Butterworth-Heinemann, Oxford, 1998.
Croner's Waste Management, (1991), Croner Publications Ltd, Kingston upon Thames, pp 2-389 to 2-390.
Envirowise (2001), Cost Effective Treatment of Waste Oily Water, Case Study CS92, Envirowise, AEA Technology Environment, Harwell.
Faust, S D and Aly, O M, (1987), Adsorption Processes for Water Treatment, Butterworths, Boston, 1987.
McGuire, M J and Suffet, I H, (1983), Treatment of Water by Granular Activated Carbon, American Chemical Society, Advances in Chemistry series, No 202, Washington.
Tennison, S R, (1998), Phenolic-resin-derived activated carbons, *Applied Catalysis*, Vol 173, pp. 289-311.

Acknowledgments

The authors gratefully acknowledge the Department of Trade and Industry, the Engineering and Physical Sciences Research Council, and the Environmental Technology Best Practice Programme (now known as Envirowise) for joint financial sponsorship of this research programme. Use of material provided for the Envirowise case study is acknowledged. The authors are also grateful to their industrial partners which include: Alpha Construction Ltd (Hilton, Derbyshire), BTR Environmental (Guildford, Surrey), Ford Motor Company (Basildon, Essex), MAST Carbon Ltd (Guildford, Surrey), OPEC Ltd (Batley, West Yorkshire), PERA Technology Centre (Melton Mowbray, Leicestershire), and D A Stuart Oil Ltd (Wolverhampton, West Midlands).

Authors:

B D Crittenden, S P Perera and R Mehta
Department of Chemical Engineering
University of Bath, Bath, BA2 7AY, UK
tel: +44 1225 826501
E-mail: B.D.Crittenden@bath.ac.uk

11.0 References

Aiken, G.; Kaplan, L. A. and Weishaar, J. (2002). Assessment of Relative Accuracy in the Determination of Organic Matter Concentration in Aquatic Systems. *Journal of Environmental Monitoring.* **4** pp. 70-74.

Alper, H. (2000). Use of Polymeric Surfactant Infused Substrates in Removal of Emulsions and Aromatic Hydrocarbons from Aqueous Waste Streams. *Naval Engineers Journal*, **112** (4), pp. 177-191.

Alther, G. R. (2001). How to Remove Emulsified Oil from Wastewater with Organoclays. *Water Engineering and Management*, **148** (7), pp. 27-29.

Amarasekera, G., Scarlett, M. J. and Mainwaring, D. E. (1995). Micropore Size Distributions and Specific Interactions in Coals. *Fuel*, **74** (1), pp. 115-118. Butterworth-Heinemann Ltd. Oxford, England.

Anon. (1994). Pinch Cleans Up. *Chemical Engineer* (London), (566), pp. 42-44.

Anon. (1997). Waste Management. Technische Mitteilungen Krupp (English Edition), Special Edition, pp. 20-23.

Archibald, L. C. and Bowes, C. (1990) Who knows the Real Costs of Poor Fluid Management? *Cutting Fluids and Lubricants.* pp. 39-41.

Archibald, L. C. and Bowes, C. (1993). Who knows the Real Costs of Poor Fluid Management? *Cutting Fluids and Lubricants.* pp. 39-41.

Arden, T. V. (1968). Water Purification by Ion Exchange. Butterworth.

Ari, M., Crittenden, J. C. and Lee, M. C. (1981). Preliminary Design of Last Cost Fixed Bed Adsorption Systems using the Homogeneous Surface Diffusion Model. Proceedings - *AWWA Annual Conference*, (2), pp. 1105-1112. AWWA, Denver, Colo, USA.

Aristotle (330BC). *Works.* 7 pp. 933b. Clarendon Press, London.

Arnold, E. (1995). Porosity in Carbons: *Characterisation and Applications.* Editor Patrick. J. W. Edward Arnold, London, UK.

Aukett, P. N., Quirke, N., Riddiford, S. and Tennison. S. R. (1992). Methane Adsorption on Microporous Carbons - A Comparison of Experiment, Theory, and Simulation. *Carbon*, 30 (6), pp. 913-924.

Austin A. E. and Hedden W. A. (1958). *Industrial Engineer Chemical.* 47 1520.

Bansal R. P., Donnet, J. B. and Stoeckli, F. (1988). Active Carbon. Marcel Dekker, New York, USA.

Barrer, R. M., McKenzie, N. and Reay, J. S. S. (1956). *Journal of Colloid Science*, **11** (479).

Belkin, S., Brenner, A., Lebel, A. and Abeliovich, A. (1994). Treatment of High-Strength, Complex and Toxic Chemical Wastewater: End-of pipe `Best Available Technology' vs. an In-Plant Control Program. *Water Science and Technology*, **29** (8), pp. 221-233. Pergamon Press Inc, NY, USA.

Bernal J.D. (1924). Proceedings of the Royal Society (London), A **106**, p.749.

Bernardin, F. E. Jr. (1985). Experimental Design and Testing of Adsorption and Adsorbates. *A Step by Step Approach to Process Evaluation and Application.* Slejko, F. L. (Editor). Adsorption Technology, pp. 37-90. Marcel Dekker, New York, USA.

Bernardin, F. E. Jr. and Bilello, L. J. (1979). Practical System Analysis in Design of Granular Activated Carbon Adsorption. *Proceedings of the Annual Industrial Pollution Conference*, pp. 123-145.

Biscoe J. and Warren B. E. (1942). X-ray Study of Carbon Black. *Journal of Applied Physics.* **13** (6) 364-372.

Blayden H. E. and Westcott D. T. (1963). Proceedings of the 5th Conference. *Carbon.* **2,** p. 97. Pergamon Press, New York, USA.

Bradley, R. H., Clackson, I. L. and Turner, A. (1991). Physical and Chemical Characterisation of Cu/Cr/Ag Impregnated Active Carbons. *Extended Abstracts and Program - Biennial Conference on Carbon*, pp. 90-91. Electrochemical Society Inc. Manchester, NH, USA.

Breach, R. A. (1996). National Report – *UK Water Supply*, 14 (3-4), pp. 248-249.

Brunauer, S., Deming, L. S., Deming, W.E. and Teller, E. (1940). On a Theory of the van der Waals Adsorption of Gases. *Journal of American Chemistry Society*, **62,** pp.1723-1732.

Brunauer, S., Emmett, P. H. and Teller, E. (1938). Adsorption of Gases in Multimolecular Layers. *Journal of American Chemistry Society*, **60 (309)**, pp. 309-319.

Buglass, J. G., Tennison, S. R. and Parkinson, G. M. (1990). Electron Microscopy of Carbon-Supported Catalysts. *Catalysis Today*, **7** (2), pp. 209-217. Elsevier Science, Amsterdam, Netherlands.

Burke, J. M. (1991). Waste Treatment of Metalworking Fluids, A Comparison of Three Common Methods. *Lubrication Engineering*, **47** (4), pp. 238-246.

Cabrera, A. L., Zehner, J. E., Coe, C. G., Gaffney, T. R., Farris, T. S. and Armor, J. N. (1993). *Carbon*, **31**, pp. 969.

Calgon Carbon Corporation (1986). Purification of Amines with Granular Activated Carbon. Granular Activated Carbons for Gas Processing Applications. Calgon Carbon Corporation, Pittsburgh.

Cannon, F. S., Snoeyink, V. L., Lee, R. G. and Dagois, G. (1994). Reaction Mechanism of Calcium-Catalyzed Thermal Regeneration of Spent Granular Activated Carbon. *Carbon*, **32** (7), pp. 1285-1301. Pergamon Press Inc, Tarrytown, NY, USA.

Černý, S. (1970a). Smisek, M and Černý, S (Editors). Methods of Studying the Properties of Active Carbon. *"Active Carbon – Manufacture, Properties and Applications"*. Elsevier Publications, Amsterdam, Netherlands.

Černý, S. (1970b). Smisek, M and Černý, S (Editors). Theory of Adsorption on Activated Carbon. *"Active Carbon – Manufacture, Properties and Applications"*. Elsevier Publications, Amsterdam, Netherlands.

Chang, I.-S., Chung, C. -M., Han, S. -H. (2001). Treatment of Oily Wastewater by Ultrafiltration and Ozone. *Desalination*, **133** (3), pp. 225-232.

Cheremisinoff, N. P. and Cheremisinoff, P. N. (1993). Carbon Adsorption for Pollution Control. PTR Prentice - Hall Inc, Englewood Cliffs, New Jersey, USA.

Cheremisinoff, P. N and Morresi, A.C. (1978). Carbon Adsorption Applications. *Carbon Adsorption Handbook.* pp. 1-53. Ann Arbor Science Publishers, Michigan, USA.

Cheremisinoff, P. N. (1990). Treating Wastewater. *Pollution Engineering.* **22** (9), pp. 60-65.

Cheremisinoff, P. N. (1995). Gravity Separation for Efficient Solids Removal. *National Environmental Journal,* **5** (6), pp. 29-32.

Cheryan, M., Rajagopalan, N. (1998). Membrane Processing of Oily Streams. Wastewater Treatment and Waste Reduction. *Journal of Membrane Science,* **151** (1), pp. 13-28.

Childers, J.C., Huang, S-J and Romba, M. (1990). Metalworking Fluid Additives for Waste Minimization. *Journal of the Society of Tribologists and Lubrication Engineers.* pp. 349-359.

Chow, D. K. and David, M. M. (1978). Activated Carbon Adsorption in Municipal Wastewater Treatment. *American Institute of Chemical Engineers* Symposium Series. **74** (179), pp. 59-70.

Clasen, J. (1998). Efficiency Control of Particle Removal by Rapid Sand Filters in Treatment Plants Fed with Reservoir Water: A Survey of Different Methods. *Water Science and Technology,* **37** (2), pp. 19-26.

Collins, J. J. (1965). The LUB / Equilibrium Section Concept for Fixed Bed Adsorption. *American Institute of Chemical Engineering.* 63 (74). Pp. 31-35.

Conner, W.C., Weist. E. L., Ito, T. and Fraissard, J. (1989). Characterisation of the Porous Structure of Agglomerated Microspheres by ^{129}Xe NMR Spectroscopy. *Journal of Physical Chemistry,* **93**, pp. 4138-4142.

Cookson, J. T. Jnr. (1978). Adsorption Mechanisms: The Chemistry of Organic Adsorption on Activated Carbon. *Carbon Adsorption Handbook.* Cheremisinoff, P. N. (Editor). pp. 241-279. Ann Arbor Science Publishers, Michigan, USA.

Coulson, J. M. and Richardson, J. F. (1991). Particle Technology and Separation Processes. *Chemical Engineering.* 4th Edition. **2.** Pergamon Press, Oxford, England.

Crane, G. A. (1996). Dohrmann DC 180 Total Organic Carbon Brochure.

Crittenden, B. D. and Kolaczkowski, S. (1995). Waste Minimization: A Practical Guide. *Institute of Chemical Engineers*, Rugby, England.

Crittenden, B. D., Perera, S. P. and Mehta, R. (2001). Treatment of Factory Waste Oily Water. *Innovative Technologies in the Water and Waste Industries for the 21st Century.* Proceedings of the 10th Annual Carribean Water and Wastewater Annual (CWWA) Conference and Exhibition, Grand Cayman, Cayman Islands. Edited by Gelia Frederick-van Genderen and Martin B Todd, Water Authority-Cayman, Grand Cayman, Cayman Islands, pp. 239-249.

Crittenden, J. C. and Hand, D. W. (1983). Design Considerations for GAC of Synthetic Organic Chemicals and TOC. *Proceedings of the Am. Water Works Association.* Seminar: Strategies for Controlling Trihalomethanes," 103rd Annual Conference, Las Vegas, Nevada.

Crittenden, J. C. and Hand, D. W. (1984). Modeling of Adsorption, Desorption and Displacement in Fxed Bed Adsorbers. pp. 185-194. *Engineering Foundation*, New York, NY, USA. Available from *American Institute of Chemical Engineering*, New York, NY, USA.

Crittenden, J. C. and Weber, W. J. Jr. (1978a). Model for Design of Multicomponent Adsorption Systems. American Society of Civil Engineers, *Journal of the Environmental Engineering Division*, **104** (6), pp. 1175-1195.

Crittenden, J. C. and Weber, W. J. Jr. (1978b). Predictive Model for Design of Fixed Bed Adsorbers: Parameter Estimation and Model Development. American Society of Civil Engineers, *Journal of the Environmental Engineering Division*, **104** (2), pp. 185-197.

Crittenden, J. C., Luft, P. and Hand, D. W. (1985). Prediction of Multicomponent Adsorption Equilibria in Background Mixtures of Unknown Composition. *Water Research*, **19** (12), pp. 1537-1548.

Croner's Waste Management. (1991). Croner Publications Ltd. Kingston Upon Thames, pp. 2-389 to 2-390.

Davankov, V. A. and Tsyurupa, M. P. (1980). Macronet Isoporous Styrene Copolymers: Unusual Structure and Properties. Die Angewandte Makromolekulare Chemie. **91**, pp. 127-142.

Davankov, V. A., Rogozhin, S. V. and Tsyurupa, M. P. (1969). Patent USSR, 299165.

Davies, G. M., Seaton, N. A. and Vassiliadis, V. S. (1999). Calculation of Pore Size Distributions of Activated Carbons from Adsorption Isotherms. Langmuir, **15** (23), pp. 8235-8245. ACS. Washington DC, USA.

De Boer, H. J. (1958). Everett, D. H. and Stone, F. S. (Editors). The Structure and Properties of Porous Materials. p. 68. Butterworths, London, England.

Dick, R. M. and Foltz, G. (1989). Metalworking Fluids Management. *Carbide and Tool Journal.* **21** (2), pp. 14-17.

Dubinin, M. M. (1966). Structure and Property of Active Carbons. *Chemistry and Physics of Carbon* **2** (251). Marcel Dekker, New York, USA.

Dubinin, M. M. (1975). Progress in Surface and Membrane Science. DA Cadenhead Edition, Acedemic Press, New York, USA.

Dubinin, M. M., Plavnik. G. M. and Zaverina, E. D. (1964). Integrated Study of the Porous Structure of Activated Carbon from Carbonised Sucrose. *Carbon*, **2** (261).

Edwards, H. W., Kostrzewa, M. F., Looby, G. P. (1996). Waste Minimization Assessment for a Manufacturer of Cutting and Welding Equipment. http://es.epa.gov/techinfo/research/reduce/rrel530.html

Eller, J. M. and Gloyna, E. F. (1974). Role of Pre-treatment in the Removal of Organics from Industrial Wastewater. Purdue Univ Eng Bull Eng Ext Ser, (145), pp. 640-647.

Endo, M., Oshida, K., Kogiso, K., Matsubayashi, K., Takeuchi, K., Kobayashi, S. and Dresselhaus, M. S. (1995). Pore Analysis of Activated Carbon Fibers by High Resolution

Transmission Electron Microscope Combined Image Analyser. *Materials Research Society Symposium Proceedings*, **371**, pp. 511-515.

Environmental Agency. www.environment-agency.gov.uk.

Environmental Protection Act. (1990). www.defra.gov.uk.

Envirowise (2000). Effluent Discharges to Sewer (006). www.envirowise.gov.uk.

Envirowise. (2001). Cost Effective Treatment of Waste Oily Water. Case Study CS92, Envirowise, AEA Technology Environment, Harwell.

Evans, C. (1977). Treatment Of Used Cutting Fluids and Swarf. *Tribology International.* **10** (1), pp. 33-37.

Faust, S. D. and Aly, O. M. (1987). Adsorption Processes for Water Treatment. Butterworths, Boston.

Fenelonov, V. B., Okkel', L. G., Slyudkina, N. S. and Malygina, T. M. (1997). Set of the State Standard Samples for Measuring the Specific Surface of Catalysts, Carriers, Adsorbents and other Porous Bodies. *Pribory i Tekhnika Eksperimenta*, n 4, (July-Aug 1997), p 133-136.

Ferreo, M. A., Webb, S.W., Conner, W. C., Bonardet, J. L. and Fraissard, J. (1992). Analysis of the Microporosity of Nascent Polyethylene ^{129}Xe NMR and High Resolution Adsorption. *Langmuir.* **8** (9), pp. 2269-2273.

Ford, D. L. (1977). Advanced Wastewater Treatment of Industrial Wastewaters using Carbon Adsorption. *Proceedings of the Annual Industrial Pollution Conference*, pp. 371-390. Water and Wastewater Equipment Manufacture Association, Inc., McLean, Vancouver.

Ford, D. L. (1978). Carbon Adsorption as an Advanced Wastewater Treatment Process. *Progress in Water Technology*, **10** (5), pp. 1-16.

Foust, A. S., Wenzel, L. A., Clump, C. W., Maus, L. and Andersen, L. B. (1960). Principles of Unit Operations. John Wiley & Sons, Inc. New York.

Fox, C. R. (1985). Industrial Wastewater Control and Recovery of Organic Chemicals by Adsorption. A Step by Step Approach to Process Evaluation and Application. Slejko, F. L. (Editor). *Adsorption Technology*, pp. 167-169. Marcel Dekker, New York, USA.

Fox, C. R. and Kennedy, D. C. (1985). Conceptual Design of Adsorption Systems. A Step by Step Approach to Process Evaluation and Application. Editor Slejko, F. L. *Adsorption Technology*, pp. 91-166. Marcel Dekker, New York.

Franklin R. E. (1950). *Acta Cryst.* **3,** p.107.

Franklin R. E. (1951). *Proceedings of the Royal Society* (London) **209** 196.

FRTR (June 2005). Remediation Technologies Screening Matrix and Reference Guide, Version 4.0. www.frtr.gov/matrix2/section4/4-47.html.

Fugiwara, Y., Nishikawa, K., Ijima, T. and Kaneko, K. (1991). Simulation of Small Angle X-ray Scattering Behaviour of Activated Carbon Fiberss Adsorbing Water. *Journal of the Chemical Society, Faraday Transactions*, **87**, p. 2763.

Gayazov, R. G., Shamanaev, S., Novikov, V. K. and Stikhina, I. L. (1985). Removal of Inorganic Substances from the Surface of Spent Active Carbons. *Soviet Journal of Water Chemistry and Technology* (English Translation of Khimiya i Tekhnologiya Vody), **17** (4), pp. 57-60.

Gean-Koplis, C. J. (1993). Transport Processes and Unit Operations. 3rd Edition. Prentice Hall International Editions Inc. Englewood Cliffs, New Jersey, USA.

George, C. E., Azwell, D. E., Adams, P. A., Rao, G. V. N. and Averett, D. E. (1995). Evaluation of Steam as a Sweep Gas in Low Temperature Thermal Desorption Processes used for Contaminated Soil Clean Up. *Waste Management*, **15** (5-6), pp. 407-416. Pergamon Press Inc, Tarrytown, New York, USA.

Giusti, D. M., Conway, R. A. and Lawson, C. T. (1974). Activated Carbon Adsorption of Petrochemicals. *Journal Water Pollution Control Federation*, **46** (5), pp. 947-965.

Glaves, C. L., Davis, P. J., Gallegos, D. P. and Smith, D. M. (1988). Pore Structure and Analysis of Coals via Low-Field Spin Lattice Relaxation Methods. *Energy and Fuels.* **2** (5), pp. 662-668.

Gomez-Serrano, V., Acedo-Ramos, M. and Lopez-Peinado, A. J. (1997). Study and Characterisation of Activated Carbon Treated with H_2SO_4 Solutions. *Journal of Chemical Technology and Biotechnology*, **68** (1), pp. 82-88. John Wiley & Sons Ltd. Chichester, England.

Greenberg, A. E.; Trussell, R. R.; Clesceri, L. S. and Franson, M. A. H. Editors. (1989a). Standard Methods For the Examination of Water and Wastewater, *American Public Health Association, American Water Works Association, Water Pollution Control Federation*, 17th Edition, Procedure 507, Biological Oxygen Demand.

Greenberg, A. E.; Trussell, R. R.; Clesceri, L. S. and Franson, M. A. H. Editors. (1989b). Standard Methods For the Examination of Water and Wastewater, *American Public Health Association, American Water Works Association, Water Pollution Control Federation,* 17th Edition, Procedure 508, Chemical Oxygen Demand.

Greenberg, A. E.; Trussell, R. R.; Clesceri, L. S. and Franson, M. A. H. Editors. (1989c). Standard Methods For the Examination of Water and Wastewater, *American Public Health Association, American Water Works Association, Water Pollution Control Federation*, 17th Edition, Procedure 509, Chemical Oxygen Demand.

Gregg, S. J. and Sing, K. S. W. (1982). Adsorption, Surface Area and Porosity. Academic Press, London. 2nd Edition.

Gronvaldt, J. and Dietrich, D. (1987). Low - Energy Solvent Recovery from Carbon Adsorption Beds. *American Society of Heating, Refrigeration, Air-Conditioning Engineering Transactions*, **93** (1), pp. 645-650. Atlanta, GA, USA.

Guillot, A., Slasli, A. M., Hugi-Cleary, D. and Stoeckli, F. (2002). The Comparison of Experimental and Calculated Pore Size Distributions of Activated Carbons. *Carbon*, **40** (3), pp. 383-388.

Guo, J. and Lua, A. C. (1999). Textural and Chemical Characterisations of Activated Carbon Prepared from Oil-palm Stone with H_2SO_4 and KOH Impregnation. *Microporous and Mesoporous Materials*, **32** (1-2), pp. 111-117. Elsevier Science, Amsterdam, Netherlands.

Halsey, G. D. (1948). *Journal of Chemical Physics.* **16** (931).

Hashimoto, K., Mura, K. and Kyotani, S. (1985). Regeneration of Activated Carbons used in Waste-Water Treatment by a Moving Bed Regenerator. *American Institute of Chemical Engineers Journal.* **31** (12), pp. 1986-1996.

Hassler, J. W. (1967) "Activated Carbon", Leonard Hill, New York, USA.

Helffrich, F. (1962). Ion Exchange. McGraw Hill, New York, USA.

Hill, E. C. (1977). Microbial Infection Of Cutting Fluids. *Tribology International.* **10** (1), pp. 49-54.

Horner, D. J. (1999). Adsorption of Selected Herbicides from Water using Activated Carbon and Polymeric Adsorbents. PhD Thesis, Loughborough University.

Howard, R. (1996). Types of Cutting Fluids Used on Turning/Machining Centres. ROCOL Ltd, Leeds UK.

Hu, X., Bekassy-Molnar, E. and Vatai, G. (2002). Study of Ultrafiltration Behaviour of Emulsified Metalworking Fluids. *Desalination.* **149** (1-3), pp. 191-197.

Huang, C. P. (1978). Chemical Interactions Between Inorganics and Activated Carbon. *Carbon Adsorption Handbook.* Cheremisinoff, P. N. (Editor). pp. 281-329. Ann Arbor Science Publishers, Michigan, USA.

Huggahalli, M. and Fair, J. R. (1996). Prediction of Equilibrium Adsorption of Water onto Activated Carbon. *Industrial & Engineering Chemistry Research,* **35** (6), pp. 2071-2074.

Hutton, D. G. (1978). Combined Powdered Activated Carbon-Biological Treatment. *Carbon Adsorption Handbook.* Cheremisinoff, P. N. (Editor). pp. 389-447. Ann Arbor Science Publishers, Michigan, USA.

Ingold, N. I. and Stonebridge, N. G. (1987). Trade Effluent Charging - The Mogden Formula. *Water Pollution Control* (Maidstone, England), **86** (1), pp. 172-183.

Innes, R. W., Fryer, J. R. and Stoeckli, H. F. (1989). On the Correlation Between Micropore Distribution Obtained from Molecule Probes and from High Resolution Electron Microscopy. *Carbon.* **27** (1), pp. 71-76.

Ito, T. and Fraissard, J. (1987). ^{129}Xe Nuclear Magnetic Resonance Study of Xenon Adsorbed on Zeolite NaY exchanged with Alkali Metal and Alkaline Earth Cations. *Journal of Chemical Society, Faraday Transactions.* **1** (83), pp. 451-462.

IUPAC, International Committee for Characterisation and Terminology of Carbon. (1985) *Carbon*, **23** (601).

Jankowska H. Swiatkowski A. and Choma J. (1991a). Testing the Porous Structure. *Active Carbon.* Ellis Harwood Publishers, London.

Jankowska, H., Swiatkowski, A. and Choma, J. (1991b). Models of Adsorption and Their Corresponding Isotherms. *Active Carbon.* Ellis Harwood Publishers, London.

Jerebek, K. and Setinek, K. (1989). Structure of Macronet Styrene Polymer as Studied by Inverse Steric Exclusion Chromatography and by Selective Sulfonation. *Journal of Polymer Science*: Part A, Polymer Chemistry. **27**, pp. 1619-1623.

Jüngten, H., Knoblauch, K. and Harder, K. (1981) Carbon Molecular Sieves: Production from Coal and Application in Gas Separation. *Fuel*, **60,** pp. 871.

Kemmer, F. N. ed. (1979). The NALCO Water Handbook, 2nd Edition, pp. 11.1-11.18.

Khalili, N. R., Vyas, J. D., Weangkaew, W., Westfall, S. J., Parulekar, S. J. and Sherwood, R. (2002). Synthesis and Characterization of Activated Carbon and Bioactive Adsorbent Produced from Paper Mill Sludge. *Separation and Purification Technology*, **26** (2-3), pp. 295-304.

Kilbourne, A. and Hodson, C. O. (1996). Guide to Oil/Water Separators. *Pollution Engineering*, **28** (3), p. 55.

Kim, B. R., Rai, D. N., Zemla, J. F., Lipari, F. and Harvath, P. V. (1994). Biological Removal of Organic Nitrogen and Fatty Acids from Metal-Cutting-Fluid Wastewater. *Water Research*, **28** (6), pp. 1453-1461.

Kipling J. J. (1964). *Carbon.* **315** 321.

Kisarov, V. M., Begun, L. B., Kudakova, L. M. and Subbotin, A. I. (1980). Recovery of Naptha Vapor by Adsorption on Carbon. *Chemistry and Technology of Fuels and Oils*, (English translation of Khimiya i Tekhnologiya Topliv i Masel), **16** (1-2), pp. 90-93.

Kittredge, D. (1980). Economics of Carbon Regeneration State of the Art. *Journal of the New England Water Works Association*, **94** (1), pp.1-23.

Knaebel, K. S. (1995). For Your Next Separation Consider Adsorption. *Chemical Engineering*. pp. 92–102.

Kruk, M., Jaroniec, M. and Gadkaree, K. P. (1999). Determination of the Specific Surface Area and the Pore Size of Microporous Carbons from Adsorption Potential Distributions. *Langmuir*, **15** (4) pp. 1442-1448. ACS. Washington DC, USA.

Krupa, N. E. and Cannon, F. S. (1996). GAC: Pore Structure Versus Dye Adsorption. *Journal of American Water Works Association*, **88** (6), pp. 94-108.

Kuennen, R. W., Van Dyke, K., Crittenden, J. C. and Hand, D. W. (1989). Predicting the Multicomponent Removal of Surrogate Compounds by a Fixed-Bed Adsorber. *Journal of the American Water Works Association*, **81** (12), pp. 46-58.

Laing, I. G. (1992). Waste Minimisation. The Role of Process Development. *Chemistry and Industry* (London), (18), pp. 682-686.

Lee, E. W (1989). Treatment and Disposal Options. National Water Conference: Proceedings of the Specialty Conference.

Lee, M. C., Crittenden, J. C., Ari, M. and Snoeyink, V. L. (1983). Design of Carbon Beds to Removing MIC Substances. *Journal of Environmental Engineering*, **109** (3), pp. 631-645.

Lemberg, J. (1870). Ueber Einige Umwandlungen Fundländischer Fedspathe. *Z. deut. Geol. Ges.* **22** pp.355. Ueber Silictumwandlungen.

Lin, C. L. and Miller, J. D. (2000). Pore Structure and Network Analysis of Filter Cake. *Chemical Engineering Journal*, **80** (1-3), pp. 221-231.

Liu, J., Crittenden, J. C., Hand, D. W. and Perram, D. L. (1995). Regeneration of Adsorbents using Heterogeneous Photocatalytic Oxidation. *Journal of Environmental Engineering*, **122** (8), pp. 707-713. ASCE, New York, USA.

Liu, P. K. T., Feltch, S. M. and Wagner, N. J. (1986). Thermal Regeneration of Activated Carbon: Desorption Behaviours of Selected Organic Compounds and Impacts on Pore Size Distribution. *American Institute of Chemical Engineers*, National Meeting, p. 31. American Institute of Chemical Engineers, New York, USA.

Lo, I. M. C. and Alok, P. A. (1996). Computer Simulation of Activated Carbon Adsorption for Multi-Component Systems. *Environment International*, **22** (2), pp. 239-252. Pergamon Press Inc, Tarrytown, NY, USA.

Lombana, L. A. and Halaby, D. (1991). Carbon Regeneration Systems. *Carbon Adsorption Handbook.* Cheremisinoff, P. N. (Editor). pp. 905-922. Ann Arbor Science, Ann Arbor, Michigan.

Lopez, F. (1999). Ion-Exchange and Carbon Adsorption Processes in the Food Industry. *Environmental Protection Engineering*, **25** (1), pp. 103-110.

Lu, G. Q. and Lau, D. D. (1995). Characterisation of Sewage Sludge-Derived Adsorbents for H_2S Removal. Part 2: Surface and Pore Structural Evolution in Chemical Activation. *Gas Separation & Purification*, **10** (2), pp. 103-111. Butterworth-Heinemann Ltd. Oxford, England.

Lu, G. Q., Low, J. C. F., Liu, C. Y. and Lua, A. C. (1996). Surface Area Development of Sewage Sludge during Pyrolysis. *Fuel*, **74** (3), pp. 344-348. Butterworth-Heinemann Ltd. Oxford, England.

Lucas, R. S. (1975) Separation and Monitoring of Oily Bilge Water. *Bundesministerium fuer Forschung und Technologie, Forschungsbericht, Technologische Forschung und Entwicklung.* pp. 557-562. Offshore Technology Conference, 7th Annual, Procedure. OTC 2200.

Lyman, W. J. (1978). Applicability of Carbon Adsorption to the Treatment of Hazardous Industrial Wastes. *Carbon Adsorption Handbook.* Cheremisinoff, P. N. (Editor). pp. 131-165. Ann Arbor Science Publishers, Michigan.

Manes, M. and Greenbank, M. (1981). Adsorption of Multicomponent Liquids From Water onto Activated Carbon: Convenient Estimation Methods. *American Chemical Society*. pp. 5-6.

MAST Carbon Ltd. (1997). Oral Communication. WOWSEP Progress Meeting.

MAST Carbon Ltd. (1998). http://www.mast-int.demon.co.uk.

Mathews, A. and Weber, W. J. (1975). Mathematical Modelling of Multicomponent Adsorption Kinetics. Presented at the 68th Annual Meeting, *American Institute of Chemical Engineers*, Los Angeles, California.

Mattson J. S. and Mark H.B. (1971) Activated Carbon: Surface Chemistry and Adsorption from Solution. Marcel and Dekker Inc. New York.

McCoy, J. S. (1994). Cutting Fluid Conservation Through Chemical Control Programs. Illinois Institute of Technology, Chicago.

McGinnis, F. K. and Horwitz, G. (1981). Effects of Thermal Regeneration on Activated Carbon Properties – A Critical Review of Traditional Physical and Chemical Tests. *American Chemical Society*. pp. 53-55.

McGuire, M.J. and Suffet, I. H. (1983). Treatment of Water by Granular Activated Carbon. *American Chemical Society, Advances in Chemistry Series*, (202), Washington.

McKay, G. (1984). The Adsorption of Dyestuffs from Aqueous Solutions using the Activated Carbon Adsorption Model to Determine Breakthrough Curves. *Chemical Engineering Journal and the Biochemical Engineering Journal.* **28** (2), pp. 95-104. ASCE, New York, USA.

Metcalf, and Eddy. (1991). Chemical Unit Processes-Adsorption. *Wastewater Engineering. Treatment, Disposal, Reuse.* Third Edition. pp. 314-324. Revised by Tchobanoglous, G. / Franklin, L. B. McGraw Hill Series in Water Resources and Environmental Engineering. London, England.

Miller, R. and Anderson, J. (1993). Methods of Reducing Chemical Oxygen Demand of Metalworking Fluids after Pre-treatment by Membrane Separation. SME Technical Paper (Series) MR, pp. 1-16.

Misra, S. K. and Skold, R. O. (1999). Membrane Filtration Studies of Inversely Soluble Model Metalworking Fluids. *Separation Science and Technology*, **34** (1), pp. 53-67.

Mizsey, P. (1994). Waste Reduction in the Chemical Industry: A Two Level Problem. Journal *of Hazardous Materials*, **37** (1), pp. 1-13.

Molina-Sabio, M., Gonzalez, M. T., Rodriguez-Reinoso, F, and Sepulveda Escribano, A. (1996). Effect of Steam and Carbon Dioxide Activation in the Micropore Size Distribution of Activated Carbon. *Carbon*, **34** (4), pp. 505-509. Pergamon Press Inc, Tarrytown, NY, USA.

Moore, B. C., Cannon, F. S., Westrick, J. A., Metz, D. H., Shrive, C. A., DeMarco, J. and Hartman, D. J. (2001). Changes in GAC Pore Structure during Full-Scale Water Treatment at Cincinnati: A Comparison between Virgin and Thermally Reactivated GAC. *Carbon*, **39** (6), pp. 789-807.

Moore, S. V. and Trimm, D. L. (1977). Preparation of Carbon Molecular Sieves by Pore Blocking. *Carbon*, **15** (3) , pp. 177-180.

Mosely, S. (1994). Cutting Costs. *Engineering* (London), Technical File No. **232** (5), pp. 25-28.

Mosely, S. E. and Brandolese, E. (1993) Improve Process Management, Extend Fluid Life and Reduce Production Costs: The Worlds First Automatic Cutting Fluid Condition Monitor. *Part 1 Economics of Fluid Management and Disposal.* p. 7.20-1 - 7.20-10.

Mosely, S., Archibald, L. C. and Bowes, C. (1994). Strategic Developments and Future Implications for the Metalworking Lubricants Market – A Contract Research Perspective. *PERA International*, Melton Mowbray, GB. pp. 18.2-1-18.2-3.

Moses. Exodus. 15 vv23-25

Mouri, M. and Niwa, C. (1993). Pilot Plant Studies on Filtration of Raw Sewage using Floating Filter Media and Multiple Filter Column Inlets. *Water Science and Technology*, **28** (7), pp. 143-151.

Myers, A. L. and Prausnitz, J. M. (1965). Thermodynamics of Mixed-Gas Adsorption. *American Institute of Chemical Engineering Journal.* **11**, pp. 121–127

Napier, S. and Rich, K. (1984). Waste Treatability of Aqueous-Based Synthetic Metalworking Fluids. *Journal of the American Society of Lubrication Engineers,* **41** (6), pp. 361-365.

Noll, K. E., Vassilios, G. and Wain-Sun, H. (1992). Adsorpiton Technology for Air and Water Pollution Control. Lewis Publishers Inc., Michigan, USA.

Ohsaki, T. and Abe, S. (1984). US Patent 4,458,022. Kuraray Chemical Company.

Oshida, K., Kogiso, K., Matsubayashi, K., Takeuchi, K., Kobayashi, S., Endo, M., Dresselhaus, M. S. and Dresselhaus, G. (1995). Analysis of Pore Structure of Activated Carbon Fibers using High Resolution Transmission Electron Microscopy and Image Processing. *Journal of Materials Research.* **10** (10), pp. 2507-2517.

Ostrejko, R. (1900). British Patents 14224 and 18040.

Parmele, C. S. Allan, R. D. and Mehran, M. (1986). Steam Regenerated Activated Carbon an Emmission-Free, Cost-Effective Ground Water Treatment Process. *Environmental Progress*, **5** (2), pp. 135-139.

Peel, R. G., Benedek, A. and Crowe, C. M. (1981). A Branched Pore Kinetics Model for Activated Carbon Adsorption. *American Institute for Chemical Engineers Journal*, **27** (1), pp. 26-32.

PERA (1996 - 1998) Progress Meeting Reports.

Perry, R. H. and Green, D. Editors. (1984). Perry's Chemical Engineer's Handbook. 6th Edition. McGraw-Hill International Editions. New York.

Peterson, E. A. and Sober, H. A. (1956). Chromatography of Proteins. I. Cellulose Ion Exchange Adsorbents. *Journal of American Chemcial Society.* **78** pp. 751-755.

Pharmacia Biotech. (1996). Ion Exchange Chromatography Principles and Methods. Pharmacia Biotech AB. Uppsala, Sweden.

Pilard, M., Dagois, G., Montagnon, P. and Chesneau, M. (1996). Influence of Minerals on the Regeneration of Activated Carbon used in Drinking Water Treatment. *Water Supply*, **14** (2), pp. 263-270. Blackwell Scientific Publishers, Oxford, England.

Purolite International Ltd. (1998a). Technical Bulletin. Cation Exchangers, Anion Exchangers, Mixed Beds, Nuclear Grade, Special Products.

Purolite International Ltd. (1998b). Technical Bulletin. Hypersol-Macronet Sorbent Resins.

Quinson, J. F., Dumas, J. and Serughetti, J. (1986). Alkoxide Silica Gel: Porous Structure by Thermoporosity. *Journal of Non Crysalline Solids.* **79**, pp.397-404.

Reed, B. E., Carriere, P., Lin, W., Roark, G. and Viadero, R. (1998). Oily Wastewater Treatment by Ultrafiltration: Pilot-Scale Results and Full-Scale Design. *Practice Periodical of Hazardous, Toxic, and Radioactive Waste Management*, **2** (3), pp. 100-107.

Riley H. L. (1947). (Title). Quarterly Reviews **1** 59.

Rodriguez-Reinoso F., Molina-Sabio, M. and Munecas, M. A. (1992). *Journal of Physical Chemistry*, **96** (2707).

Rodriguez-Rienoso, F. (1997). Marsh. H., Heintz. E.A. and Rodriguez-Reinoso. F. (Editors) Activated Carbon: Structure, Characterisation, Preparation and Applications. *Introduction to Carbon Technology.* University of Alicante, Alicante.

Rosene, M. R. (1981). Controlling Mechanisms for Granular Activated Carbon Adsorption Columns in the Liquid Phase. *National Meeting - American Chemical Society, Division of Environmental Chemistry*, **21** (1), pp. 79-82. ACS, Washington, DC, USA.

Roth, R. C. (1982). Generation of High Pressure Steam from Low Temperature Waste Heat Sources. Annual Meeting - Technical Section, Canadian Pulp and Paper Association, **83** (12), pp. 72-77. Preprints, pp. B169 to B173. CPPA, Quebec, Canada.

Rousseau, R. W. (1987). Handbook of Separation Process Technology. pp. 644-697. Wiley-Interscience Publication. New York; New York, USA.

Roy, D., Wang, G. T. and Adrian, D. D. (1992). A Simplified Solution Technique for Carbon Adsorption Model. *Water Research*, **27** (6), pp. 1033-1040.

Roy, D., Wang, G. T. and Adrian, D. D. (1993). Simplified Calculation Procedure for Carbon Adsorption Model. *Water Environment Research*, **65** (6), pp. 781-787.

Ruthven, D. M. (1984). Principles of Adsorption and Adsorption Processes. John Wiley and Sons, Inc, New York, USA.

Sales, W. F., Diniz, A. E. and Machado, A. R. (2001). Application of Cutting Fluids Machining Processes. *Journal of the Brazilian Society of Mechanical Sciences*, **23** (2), pp. 227-240.

Samitz, M. H. (1974). Effect Of Metal Working Fluids On The Skin. *SME Technical Paper*, (MR74-182).

Saunders, A. R. (1990). The Metalworking Lubricants Market: Recent and Future Trends. *Industrial Lubrication and Tribology*. **42,** pp. 3-10.

Schork, J. M. and Fair, J. R. (1988). Steaming of Activated Carbon Beds. *Industrial & Engineering Chemistry Research*, **27** (8), pp. 1545-1547.

Schork, J. M., Srinivaan, R. and Auvil, S. R. (1993). *Industrial Engineering Chemical Research*, **32**, p. 22.

Schuliger, W. G. (1978). Purification of Industrial Liquids with Granular Activated Carbon: Techniques for Obtaining and Interpreting Data and Selecting the Type of Commercial System. *Carbon Adsorption Handbook*. Cheremisinoff, P. N. (Editor). pp. 55-83. Ann Arbor Science, Ann Arbor, Michigan.

Schweiger, T. A. J. and LeVan, M. D. (1993). Steam Regeneration of Solvent Adsorbers. *Industrial & Engineering Chemistry Research*. **32** (10), pp. 2418-2429.

Sheng, P. S. and Oberwalleney, S. (1997). Life-Cycle Planning of Cutting Fluids - A Review. *Journal of Manufacturing Science and Engineering*, Transactions of the ASME, **119** (4(B)), pp. 791-800.

Skold, R. O. (1991) Field Testing of a Model Water Based Metalworking Fluid Designed for Continuous Recycling using Ultrafiltration. *Lubrication Engineering*, **47** (8), pp. 653-659.

Skold, R. O. (1996). Three Novel Physical Methods of Contaminant Control in Aqueous Metalworking Fluids. *Lubrication Engineering*, **52** (5), pp. 393-400.

Slater, M. J. (1991). The Principles of Ion Exchange Technology. Butterworth-Heinemann, Oxford.

Sokolov, V. P. and Kuz'min, V. D. (1979). After Treatment of Refinery Wastewater with Activated Carbon. *Chemistry and Technology of Fuels and Oils*, (English translation of Khimiya i Tekhnologiya Topliv i Masel), **15** (3-4), p 266-268.

Sokolovic, S., Secerov-Sokolovic, R. and Sevic, S. (1992). Two-stage Coalescer for Oil/Water Separation. *Water Science and Technology*, **26** (9-11), pp. 2073-2076.

Steckle, W. P. Jr., Mitchell, M. A. and Apen, P. G. (1996). Tailoring the Pore Size of Hypercrosslinked Polymer Foams. *Materials Research Society Symposium Proceedings*, **431** pp. 481-486.

Stenzel, M. H. (1993). Remove Organics by Activated Carbon Adsorption. *Chemical Engineering Progress*, **89** (4), pp. 36-43.

Stenzel, M. H. and Merz, W. J. (1989). Use of Carbon Adsorption Processes in Groundwater Treatment. *Environmental Progress*, **8** (4), pp. 257-264.

Steriotis, T., Beltsios, K., Mitropoulos, A. C., Kanellopoulos, N., Tennison, S., Wiedenman, A. and Keiderling, U. (1997). On the Structure of an Asymmetric Carbon Membrane with a Novolac Resin Precursor. *Journal of Applied Polymer Science.* **64** (12), pp. 2323-2345. John Wiley & Sons Inc, New York, USA.

Steward E. G. and Davidson H.W. (1958). Industrial Carbon and Graphite Society. *Chemical Industry*, London. pp. 207.

Stoeckli, F., Lopez-Ramon, M. V., Hugi-Cleary, D. and Guillot, A. (2001). Micropore Sizes in Activated Carbons Determined from the Dubinin-Radushkevich Model. *Carbon*, **39**(7), pp. 1115-1116.

Stoeckli, H. Fritz. (1990). Microporous Carbons and their Characterization. The Present State of the Art. *Carbon.* **28** (1), pp. 1-6.

Strelko V. Jr., Malik, D. J. and Streat, M. (2002). Characterisation of the Surface of Oxidised Carbon Adsorbents. *Carbon*, **40** (1), pp. 95-104.

Suzuki, M. (1990). Adsorption Engineering. Elesevier Science Publishers. *Chemical Engineering Monographs*, **25**. Amsterdam, Netherlands.

Sweatman, M. B. and Quirke, N. (2001). Characterization of Porous Materials by Gas Adsorption at Ambient Temperatures and High Pressure. *Journal of Physical Chemistry* B, **105** (7) pp. 1403-1411.

Tchobanoglous, G. and Franklin, L. B. (1991). Chemical Unit Processes-Adsorption. *Wastewater Engineering. Treatment, Disposal, Reuse.* Third Edition. pp. 314-324. Revised by Tchobanoglous, G. / Franklin, L. B. McGraw Hill Series in Water Resources and Environmental Engineering. New York, USA

Tennison, S. R. (1998). Phenolic-Resin-Derived Activated Carbons. Applied Catalysis, **173**, pp. 289-311.

Tennison, S. R., Soria, R., Nicholson, D. and Kanellopoulos, N. (1993). *International Conference on Membranes (ICOM).* Heidleberg.

Thomas, A., Gillham, R. and Brotherton, P. (1990). Current Issues in the Management of Hazardous Wastes. *Chemical Engineering in Australia*, **15** (1), pp. 10-11.

Thompson, H. S. (1850). On the Absorbent Power of Soils. *Journal of the Royal Agricultural Society of Engineering.* **11** pp.68.

Traegner, U. K. and Suidan, M. T. (1989). Parameter Evaluation For Carbon Adsorption. *Journal of Environmental Engineering*, **115** (1), pp. 109-128.

Ultrafiltration Handbook. (1989). Romicon Inc. Woburn, MA.

Upton, D. P. (1996). Assessment of Cutting Fluid Performance and Improvements in Surface Finish. *Transactions of the Institute of Metal Finishing*, **74** (3), pp. 103-105.

Vigneswaran, S. and Dharmappa, H. B. (1992). Industrial Waste Minimisation: Concepts and Technology. National Conference Publication - *Institution of Engineers, Australia*, **92** (5), pp. 103-107.

Waer, M. A., Snoeyink, V. L. and Mallon, K. L. (1992). Carbon Regeneration Dependence on Time and Temperature. *Journal of the American Water Works Association*, **84** (3), pp. 82-91.

Wagle, N. G. (1983). Control Of Bacterial Degradation Of Cutting Oil Emulsions. *Chemical Age of India*, **34** (7), pp. 409-411.

Wakao, N and Funazkri, T. (1978). Chemical Engineer Science, **33**, pp. 1375-1384. Cited in Li, Y. Y., Perera, S. P. and Crittenden, B. D. (1998). *Trans IChemE*, **76** A. pp. 931-941.

Wakeman, Richard J. (ed.). (1979). Progress in Filtration and Separation. Volume 1, Elsevier Science Publications Co., Amsterdam, Netherlands.

Walker, P. L. (1966). *Chemistry and Physics of Carbon*. **2**, pp. 257. Edward Arnold, London.

Walter, J. and Weber, Jr. (1992). Adsorption Theory, Concepts and Models. Ann Arbor Science, Ann Arbor, Michigan.

Wang, K. and Do, D. D. (1999). Sorption Equilibria and Kinetics of Hydrocarbons onto Activated Carbon Samples having Different Micropore Size Distributions. *Adsorption*, **5** (1), pp. 25-37.

Wang, S. C. and Tien, C. (1982). Further Work on Multicomponent Liquid Phase Adsorption in Fixed Beds. *American Institute of Chemical Engineers Journal*, **28** (4), pp. 565-573.

Wang, Z. L. and Kang, Z. C. (1997). Graphitic Structure and Surface Chemical Activity of Nanosize Carbon Spheres. *Carbon*. **35** (3), pp. 419-426.

Way, J. T. (1850). On the Power of Soils to Absorb Manure. *Journal of the Royal Agricultural Society of Engineering*. **11** pp.313.

Way, J. T. (1852). On the Power of Soils to Absorb Manure. *Journal of the Royal Agricultural Society of Engineering*. **13** pp.123.

Weber, W. J. and Chakravorty, R. K. (1974). Pore and Soild Diffusion Models for Fixed Bed Adsorbers. *American Institute of Chemical Engineers Journal.* **20**, pp. 228-238.

Wilson, B. F. (1970). Cutting Fluids Can Cut Costs. *American Machinist.* **114** (25), pp. 62-4.

Wolf, W. F. (1958). The Structure of Gas Phase Carbons. *Journal Physical Chemistry*, **62** (829).